Design and Synthesis of Novel Polymeric Dyes
Incorporating Pyrazolone Units
Innovative Polyester Incorporating Highly Energetic
Gem-Diazide Units

Dissertation

Zur Erlangung des Grades Dr. rer. nat.

Angefertigt an der Fakultät für Mathematik und

Naturwissenschaften

der Bergischen Universität Wuppertal

von Anastasiia Krupka

geboren am 10.07.1996 in Kryvyi Rih, Ukraine

Die vorliegende Arbeit wurde in der Zeit von Februar 2020 bis Mai 2023 am Lehrstuhl für Organische Chemie der Bergischen Universität Wuppertal unter Leitung von Prof. Dr. Stefan F. Kirsch angefertigt.

Parts of this work have been presented at conferences:

- A communication poster titled "Polymeric Dyes with Hydrazono-Pyrazolones Units: Design, Synthesis, and Optical Properties" by A. Krupka, B. Derkowska-Zielinska, and S.F. Kirsch was presented at the Bordeaux Polymer Conference 2022 in Bordeaux, France. The poster was assigned the number 414 and appeared on p. 436.

- An oral presentation titled "Synthesis of Rubazonic Acid Derivatives and Their Polymers" by A. Krupka, B. Derkowska-Zielinska, and S.F. Kirsch was presented at the SCF 2023 Congress in Nantes, France. "Synthesis of rubazonic acid derivatives and their polymers". SCF 2023 Congress, 2023, p. 240.

As part of the physical study of materials, an internship was conducted at Nicolaus Copernicus University in Poland from February 1 to February 21, 2023. This internship was made possible through the PROM program competition by NAWA at Nicolaus Copernicus University, and was supervised by Prof. Dr. B. Derkowska-Zielinska.

An oral presentation was given as an invited talk on February 13, 2023 at Nicolaus Copernicus University. The presentation covered the topic of "Rubazonic Acid as a New Dye for Material Science. Polymeric Dyes with Hydrazone-Pyrazolone Units for Anion Detection."

An oral presentation was given as an invited talk on July 29, 2023 in Photonics Laboratory LPhiA in Angers University. The presentation covered the topic of "Unveiling the Potential of Hydrozone Polymers in Material Science."

Acknowledgements

I am deeply grateful to my PhD supervisor, Prof. Stefan F. Kirsch, for the opportunity to defend my thesis as a member of his esteemed research group. His belief in my abilities has been instrumental in my academic growth, I am honored to have worked on fascinating topics in organic chemistry under his guidance. I want to express my sincere appreciation for his daily support, unwavering interest in my research, and discussions on various topics. His mentorship has inspired me to push the boundaries of my knowledge and pursue excellence in my work. Thank you, Prof. Kirsch, for your guidance, encouragement, and invaluable contributions to my academic journey.

I would like to express my gratitude to Beata Derkowska-Zielińska for her invaluable help and guidance during my internship at Nicolaus Copernicus University.

I would also like to extend my heartfelt gratitude to my colleagues at the Bergische Universität Wuppertal. I want to thank Mrs. Christine Schneidereit for her unwavering enthusiasm and efficiency in addressing our concerns and navigating the complex bureaucratic processes at the university. I also want to express my appreciation to Dr. Hülya Aldemir, Dr. Markus Roggel, Dr. Andreas F. Kothaus, for their guidance and support, and Dr. Adrian Gomez-Suarez for enriching my knowledge through seminars.

Furthermore, I want to acknowledge the invaluable contributions of the permanent staff of the Kirsch group, especially Simona Bettinger, Ilka Polanz, and Andreas Siebert, who cooperated in recording the analytical data that was essential to the completion of my research. Special thanks also go to Dr. Björn Beele and Sylwia Adamczyk for their analytical skills in analyzing new polymers.

I am also grateful to the current and former doctoral students of the Kirsch working group for making my time in the lab a truly special experience. I want to thank Federica Borghi and Frederic Ballaschk for their support during my first few months in the lab. Additionally, I am grateful to Ibrahim Celik, Mohit Chotia, Timo Zschau, Marcel Jaschinski, Yasemin Özkaya, Kevin Kunz, Fabia Mittendorf, Bastian Springer, Athanasios Savvidis, Michael Tapera, Srashti Chaudhary, and all the people from the Gómez-Suárez group and AG Scherkenbeck group for their collaborative spirit and scientific curiosity. Lastly, I extend a special thank you to Irina Kollmorgen for her unwavering support and encouragement throughout my academic journey. I also want

Table of Contents

Part I:

Design and Synthesis of Novel Polymeric Dyes Incorporating Pyrazolone Units

I.1. Synthesis and application of pyrazolones

Pyrazolones are a type of heterocycle consisting of two adjacent nitrogen atoms in a five-membered ring. They are essentially a pyrazole derivative with an additional carbonyl (C=O) group [1]. The first synthesis of pyrazolones dates back to 1883, when Ludwig Knorr synthesized 1-phenyl-3-methyl-5-pyrazolone **I-2** by reacting ethyl acetoacetate and phenylhydrazine (Scheme 1) [2].
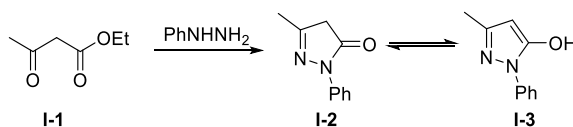
Scheme 1: The synthesis of pyrazolones.

Most pyrazolones and their derivatives are yellow to colorless solids with a melting point above 100 °C. Furthermore, hydrogen bonding strongly influences the predominant tautomeric form of pyrazolones. Specifically, pyrazolone has three tautomeric forms: ketohydrazone **I-4**, phenol **I-5**, and keto-hydrazine **I-6** (as shown in Scheme 2) [3]. In addition to their unique chemical structure, pyrazolones possess both basic and acidic properties, although weakly acidic character generally prevails. They also exhibit good light and solvent stability, making them useful in various applications [2].
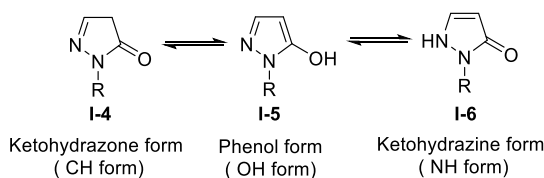
Scheme 2: Tautomeric forms of pyrazolones.

There are several methods for synthesizing pyrazolone derivatives. The most common method involves refluxing aryl hydrazines with acetoacetic esters or acetoacetamide in acetic acid or ethanol to form pyrazolone (Scheme 3) [2].

2
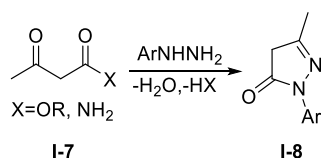
Scheme 3: The synthesis of pyrazolone derivatives from β-ketoesters.

Another method involves condensing an α,β-unsaturated acid, ester or amide **I-9** with hydrazine to synthesis of pyrazolidiones **I-10**, as shown in Scheme 4 [1].
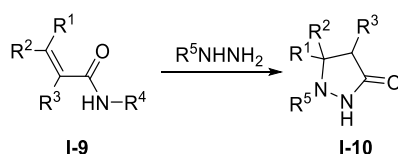
Scheme 4: Synthesis of pyrazolidiones.

Bauer et al. [4] developed an efficient method for synthesizing N-substituted 2-pyrazoline **I-13** from hydrazine addition to chalcones **I-11**, which resulted in unstable pyrazolines **I-12** that were trapped with various electrophiles in the presence of polymer-bound base, as shown in Scheme 5.
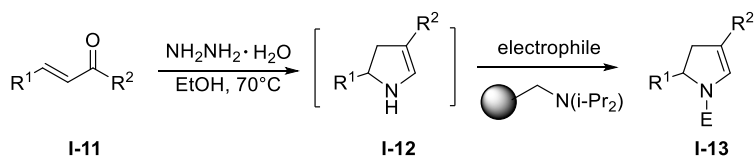
Scheme 5: The solution-phase synthesis of N-substituted 2-pyrazoline.

Robert et al. [5] reported the synthesis of 2,3-pyrazol-1(5H)-ones **I-16** via palladium-catalyzed carbonylation of 1,2-diaza-1,3-butadienes **I-15**, which were generated by thermal extrusion of sulfur dioxide or carbon dioxide from their respective heterocyclic precursors (Scheme 6).
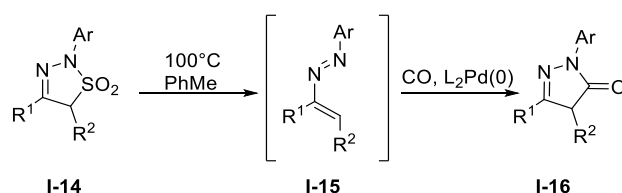
Scheme 6: The synthesis 2,3-pyrazol-1(5H)-ones via palladium-catalyzed.

Pyrazolone derivative **I-19** can also be synthesized via method that were reported Kato method [6], which involves reacting hydrazine derivatives **I-18** and diketene **I-17** in chloroform with triethylamine, as shown in Scheme 7.
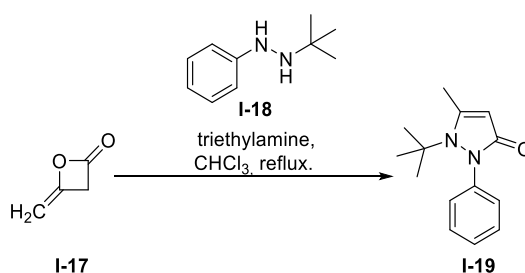
Scheme 7: The synthesis of pyrazolone derivative by method of Kato.

Baciu-Atudosie, L. [7] developed a facile one-pot approach for synthesizing new pyrazolones derivatives containing a phenothiazine unit **I-21** using hydrazine, β-ketoester, and 4Å molecular sieves as a catalyst in dimethylacetamide at 60 °C, as shown in Scheme 8.
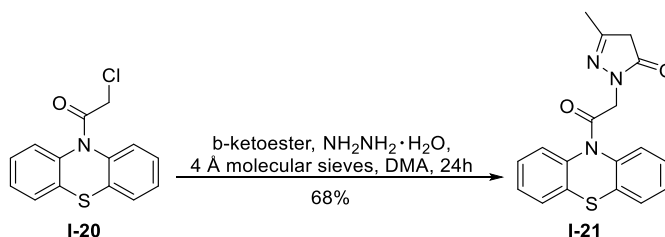
Scheme 8: The synthesis of pyrazolone derivative **I-21**.

Pyrazolones and their derivatives have various applications in fields such as biology, medicine, dyes application, analytical chemistry, and etc. [8] [9].

Overall, pyrazolones and their derivatives have significant potential in many different fields due to their unique chemical properties and biological activities.

Pyrazolones have a wide range of biological properties, including analgesic, antibacterial, antifungal, antagonists, anti-inflammatory, antimicrobial, antidiabetic, antihyperglycemic, and anxiolytic effects [2]. Scheme 9 show a series of biologically important pyrazolones [2].
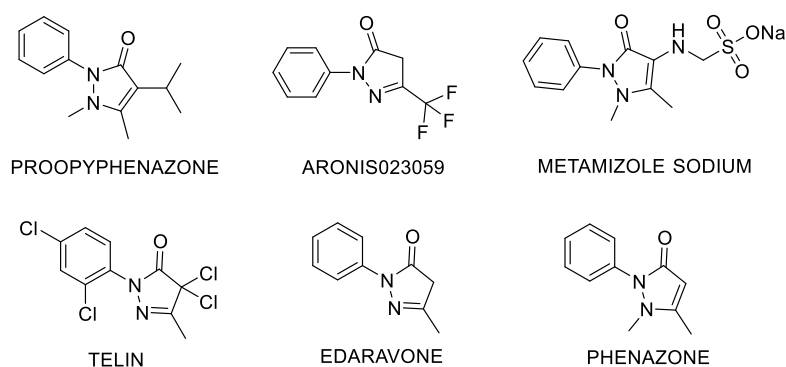
Scheme 9: Biologically active pyrazolones.

Pyrazol-5-one derivatives have been found to possess antitumor properties. For instance, edaravone (as shown in Scheme 9) has been shown to enhance the antitumor effects of CPT-11 (a drug used alone or with other drugs to treat colorectal cancer that has spread to other parts of the body) in murine colon cancer by promoting apoptosis [10]. Additionally, edaravone is used for the treatment of acute brain infarction and subarachnoid hemorrhage during the acute phase [11]. Similarly, telin (Scheme 9) is a potent catalytic blocker of telomerase and is used in medical treatments for cancer and related diseases [12].

Piskarev et al. [13] conducted experiments on the radioprotective effect of pyrazolone derivatives. The results showed that these derivatives significantly increase the resistance to hypoxia in both healthy and irradiated mice during various stages of acute radiation sickness.

In summary, pyrazol-5-one derivatives have promising potential as antitumor agents and have demonstrated radioprotective effects in various experimental settings. The use of compounds such as edaravone and telin in medical treatments highlights the importance of continued research in this field.

The chemistry of pyrazolone dyes dates back to 1884, when Ziegler and Lochner synthesized the first dye of this type, tartrazine, which is still used as a food dye [14]. Pyrazolone dyes are a diverse group of synthetic organic coloring agents that find

wide industrial applications. The pyrazolone molecule couples with diazonium compounds in the 4-position to give pyrazolones based azo compounds (Scheme 10). These dyes are capable of producing bright colors and exhibit superior dyeing properties compared to aniline-based derivatives. Pyrazolones are well-known for their use as cotton dyes, pigments, and dyes for synthetic fibers and plastics [15][19].
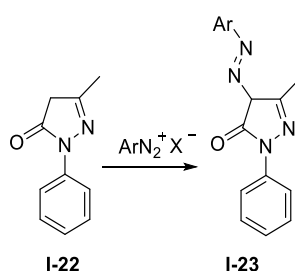
Scheme 10: Method of synthesis for pyrazolones derivatives based on azo compounds.

Seymour first described the pyrazolone azomethine dyes in 1934. These dyes were used as magenta dyes in certain color photographic processes. In addition, pyrazolones and related compounds have proven to be excellent developing agents for black and white photography and polaroid photography. As a result, pyrazolones can be found in almost all types of dyes. [16].

Pyrazolones with fluorine- or trifluoromethyl-substituted aryl groups in the 1-position have been tested and found to be useful as herbicides, fungicides, and insecticides for crop protection [15][17]. Pyrazolones can also be used in analytical chemistry for the extraction and separation of various metal ions, for the determination of phenol, cyanides, and ammonia, and as photographic sensitizers [18].

I.2. Hydrazone derivatives as building block

The hydrazone functional group is characterized by the $R_2C=N-NR_2$ moiety and is considered as a derivative of aldehydes and ketones, where the NNH_2 functional group is replaced by an oxygen atom. The C=N double bond in hydrazones is crucial, as it can be utilized for metal complex formation, organocatalysis, and the synthesis of different organic compounds [19].

The physical and chemical properties of hydrazones are determined by the C=N bond and the terminal nitrogen atom, which contains a single pair of electrons. The C atom in hydrazones exhibits both electrophilic and nucleophilic characteristics,

whereas both N-atoms are nucleophilic, with the nitrogen of the amino type being more reactive. The presence of C=N and N-H groups in monosubstituted and unsubstituted hydrazones gives rise to intermolecular hydrogen bonding [20].

Hydrazones are widely used in organic synthesis and medicinal chemistry, as well as in metal and covalent organic frameworks, supramolecular chemistry, dye chemistry and dynamic combinatorial chemistry, and hole-transporting materials. These properties make hydrazones an attractive choice for a range of industrial applications [21].

I.2.1 Synthesis of hydrazones

The synthesis of hydrazones can be achieved through three main synthetic pathways. The most useful and well-known method is the Japp–Klingemann reaction, which involves the coupling of aryl diazonium salts with β-keto esters or acids (Scheme 11). This reaction has proven to be highly effective and is widely used in the synthesis of hydrazones [22].
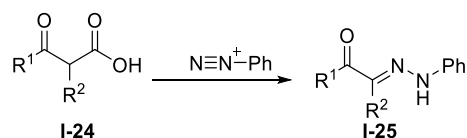
Scheme 11: Synthesis of hydrazone derivatives by Japp–Klingemann reaction.

Another pathway for the synthesis of hydrazones involves coupling between aryl halides and non-substituted hydrazones. Transition metals can catalyze the formation of C-N bonds, making this method a valuable tool for the synthesis of arylamines. Copper or palladium catalysts can be used for the arylation of hydrazine derivatives [23] [24]. This methodology provides a more general approach to a variety of aryl- or heteroarylhydrazine derivatives, avoiding the use of conventional methods such as reduction of diazonium salts or S$_N$Ar reactions using hydrazine derivatives (Scheme 12) [25] [26].
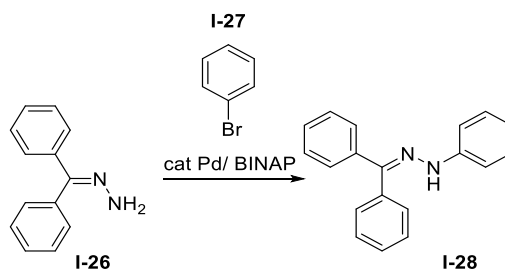
Scheme 12: The synthesis of hydrazones derivatives by or S_NAr reactions.

Emil Fischer, proposed another method for the synthesis of hydrazones in 1894. Fischer described the reaction between phenylhydrazine and reducing sugars, which leads to the formation of hydrazones known as osazones (Scheme 13). This approach has also proven to be useful in the synthesis of hydrazones [27].
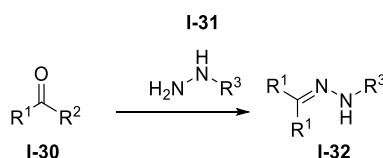
Scheme 13: Synthesis of hydrazones derivatives that was proposed by E.Fischer .

I.2.2 Geometry and isomerism

Crystallographic analysis has shown that the C=N-N group in hydrazones has a planar structure, although coplanarity may be disrupted in some steric hindered molecules. The C=N bond length in hydrazones is dependent on the nature of the substituents R, R', X, and Y and ranges between 1.27 and 1.35 Å. This length is slightly longer than that of aliphatic imines, which have a bond order closer to 2 and bond lengths of 1.24 and 1.25 Å. The presence of a lone pair of electrons on the amine nitrogen atom in hydrazones capable of conjugation with π-electrons reduces the bond order of C=N, resulting in a longer bond length [28].

Hydrazones can exhibit different types of isomerism, such as stereoisomerism and structural isomerism, and in some cases, a tautomeric equilibrium of two or even three forms may be observed [29] [30]. There are three tautomeric forms of hydrazone derivatives, including azo-enol **I-33**, hydrazone **I-34**, and azo-ketone **I-35** (Scheme 14) [31]. The hydrazone tautomeric form is more stable and commonly observed. The hydrazono-azo tautomerism can be characterized by UV–Vis and ^{1}H NMR spectra.
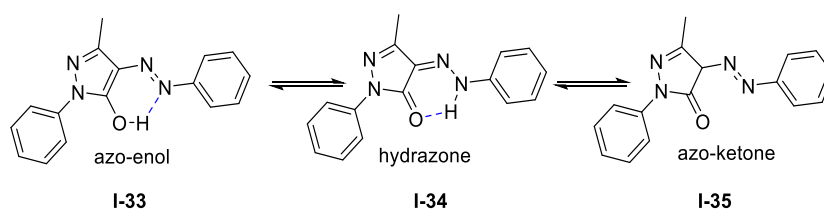
Scheme 14: The tautomeric forms of hydrazone (azo-enol **I-33**, hydrazone **I-34** and azo-ketone **I-35**).

I.2.3 Sensing applications of hydrazones derivatives

Anion recognition has become a subject of significant interest due to its potential applications in medicinal and environmental fields. The N-H hydrazone has acidic nature allows for the detection of anions through H-bond interactions that modify the photophysical properties of the system and can result in color changes that are detectable with the naked eye. Anions such as F^-, AcO^-, and $H_2PO_4^-$ usually form H-bonded adducts with hydrazones. In some cases, the interaction between the anion and the hydrazone N-H proton is so strong that deprotonation occurs [32].

Shuzhen Hu et al. [33] reported a chromogenic anion molecular sensor **I-36** that can detect F^-, AcO^-, $H_2PO_4^-$ and other anions in a competitive mixed acetonitrile-water medium. The association with F^-, AcO^-, and $H_2PO_4^-$ causes a red-shift from 370 nm to 550 nm and an increase in UV-vis absorption, respectively (Figure 1). The imine (C=N) bond in hydrazones can be susceptible to nucleophilic attack, particularly by cyanide (CN^-), making these systems good candidates for reaction-based probing. The addition of CN^- can also be used to turn on the fluorescence resonance energy transfer in hydrazones containing energy donor-acceptor pairs. A similar study about hydrazone derivatives was described in literature [34].
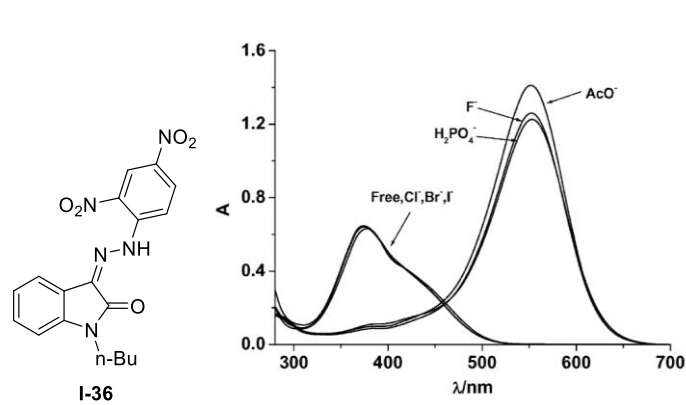
Figure 1: The changes of receptor **I-36** after anions titration in UV-vis absorption spectra [33].

Qian Li et al. [35] proposed a binding mode of hydrazone receptors with fluoride anions (Scheme 15). The deprotonation of hydrazone receptors induced the π-electrons extending from the p-nitrophenyl moiety to the indole moiety. Stable complexes were formed by hydrogen bonding between the indole NH of the receptor and the fluoride anion, enhancing the charge-transfer interactions between the electron-rich and electron-deficient moieties. The increase in π-electrons on the supramolecular system resulted in enhanced fluorescence.
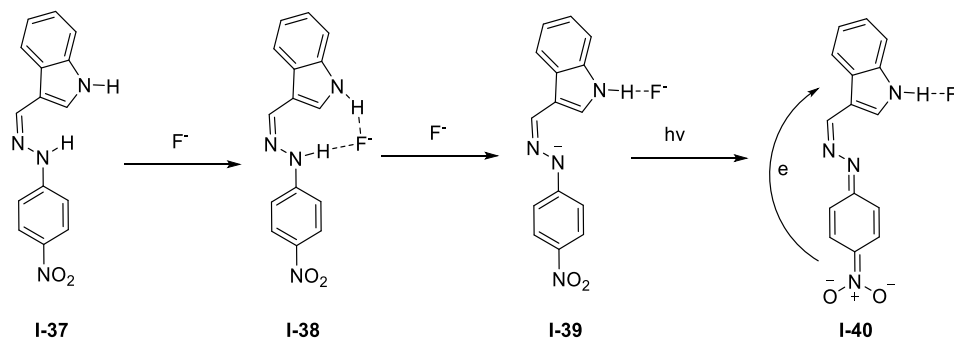
Scheme 15: The hydrazone receptor with fluoride anions [35].

The Yaping Li et al. [36] synthesized two hydrazone compounds based on pyrazalone (Scheme 16) and studied their sensing properties.
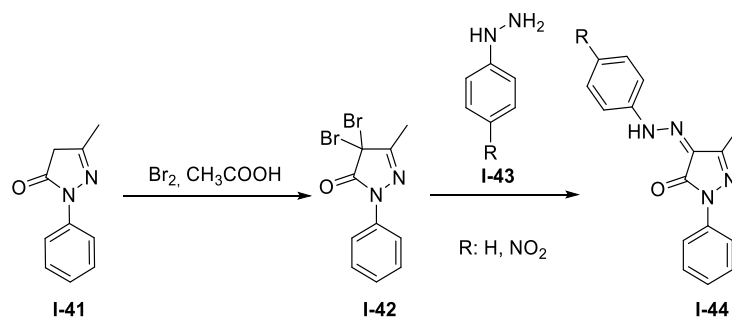
Scheme 16: The synthesis of two hydrazone compounds based on pyrazalone.

Anion complexes were formed for both hydrazone derivatives with F^-, AcO^- and $H_2PO_4^-$ anions, and complexation was monitored by UV-vis and ^1H NMR spectroscopy. The UV-vis spectra during the titration process are shown in Figure 2a and Figure 2b. The receptors exhibited bathochromic shifts and the formation of two new isosbestic points, indicating the formation of anion complexes. Furthermore, the ^1H NMR titration shown in Figure 2c demonstrated the gradual disappearance of H bonds at 13.4 ppm that originated from the NH in the hydrazone moiety. Attempts to form anion complexes with Cl^-, Br^- and I^- anions were made, but as shown in Figure 2d, the complexes were not formed [36].
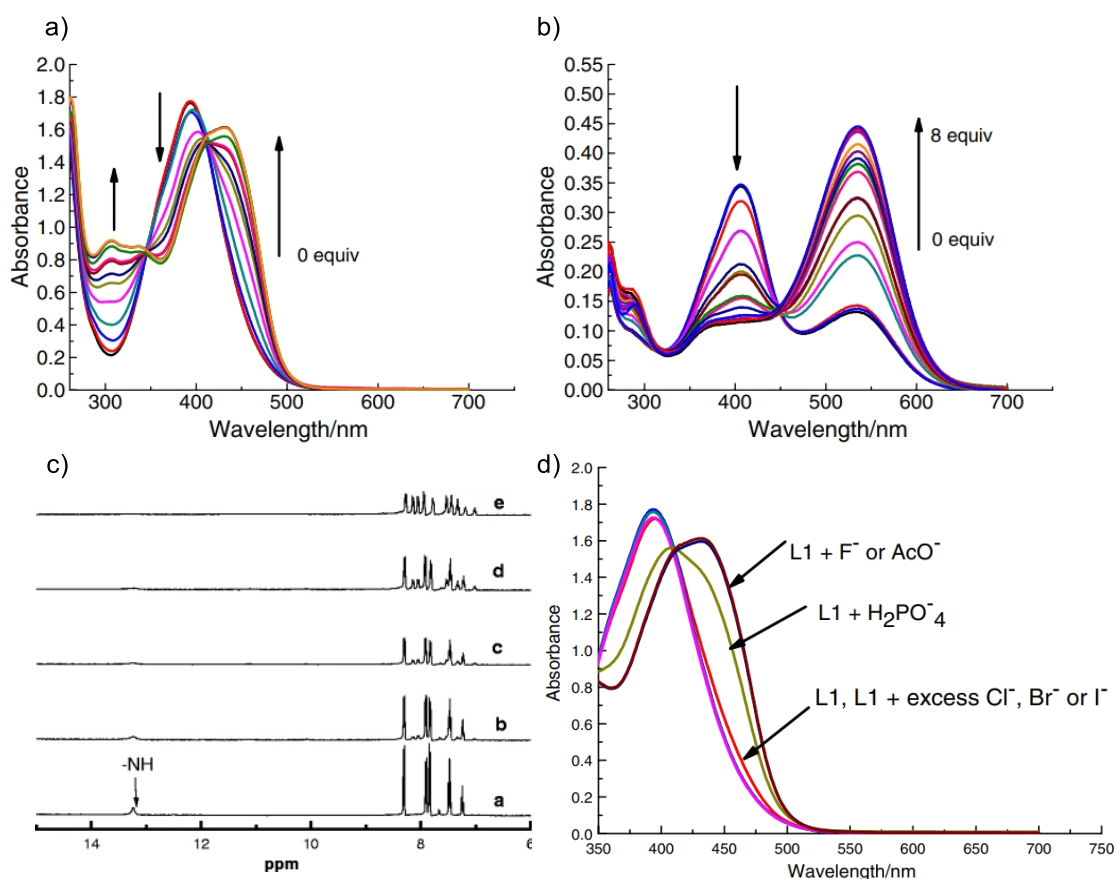
Figure 2: Changes in the UV-vis spectra of **I-44** R=H (a) and **I-44** R=NO$_2$ (b) (1 × 10^{-5} M) in the absence and presence of F$^-$ in DMSO solution; changes in the ^{1}H NMR spectra of **I-44** R=NO$_2$ with gradual addition of F$^-$ in DMSO (c); spectral changes of **I-44** R=H (1 × 10^{-5} M) induced by addition of different anions in DMSO (d)[36].

In addition to their anion sensing properties, hydrazone derivatives also have applications in cation sensing. Hydrazones can bind to metals through their NNN or NNO binding sites. For example, 2-pyridyl hydrazone can form a stable 1:1 complex with Pd^{2+} (Scheme 17a). After binding with Pd^{2+}, a sharp color change from yellow to red can be observed with the naked eye. The pyrene fluorophore hydrazone (Scheme 17b) can bind Zn^{2+} with its NNO binding site. After the formation of cation complexes, the fluorescence is dramatically enhanced because photoinduced electron transfer from the hydrazone nitrogen to pyrene is blocked. Acylhydrazones offer another NNO or ONO binding motif for metals. Hydrazone (Scheme 17c) can be formed into microelectrodes with a polyvinyl chloride support for Er^{3+} sensing. This ion can detect Er^{3+} in the range 1.0 mM-0.3 nM with a limit of detection of 0.2 nM within the pH range 3.0-9.0 by potentiometric methods. The highly selective and sensitive sensors pyrazinyl hydrazone (Scheme 17d) can detect Al^{3+} at the sub-

micromolar level, while quinoxalinyl hydrazone (Scheme 17e) can detect Ni^{2+} [37] [38] [39] [40].
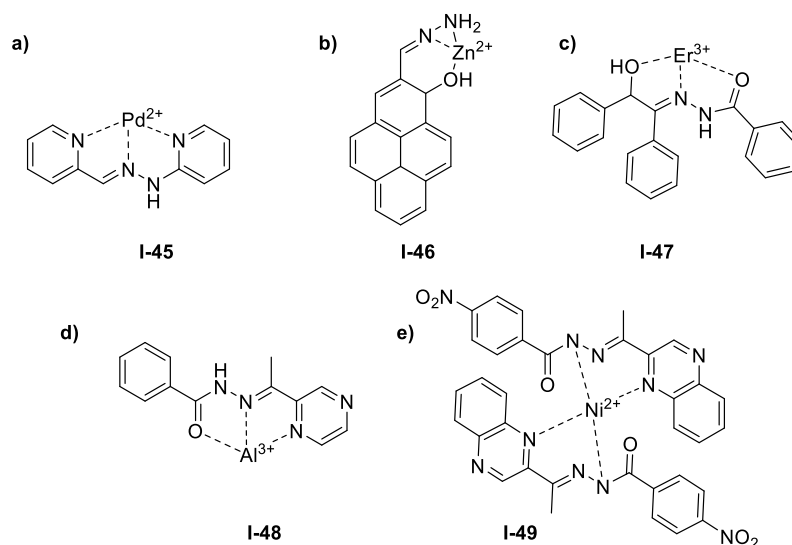
Scheme 17: a) 2-pyridyl hydrazone stable 1:1 complex with Pd^{2+}; b) pyrene fluorophore hydrazone complex with Zn^{2+}; c) *N'*-(2-hydroxy-1,2-diphenylethylidene) benzohydrazide as a highly selective Er(III) membrane sensor; d) pyrazinyl hydrazone Al^{3+} complex; e) quinoxalinyl hydrazone Ni^{2+} complex.

Tong et al. [44] reported an "off-on" fluorescent chemosensor for Cu^{2+} based on a rhodamine B-based hydrazone (Scheme 18). As a spiro lactam, rhodamine B is weakly fluorescent, and upon coordination to Cu^{2+}, the lactam C-N bond is cleaved, and the complex is formed through coordination to the ONO binding site. The ring-opening reaction amplifies the fluorescent emission of the complex, which provides a fluorescent sense of Cu^{2+} at the sub-micromolar level in buffered aqueous solutions [41] [42] [43].
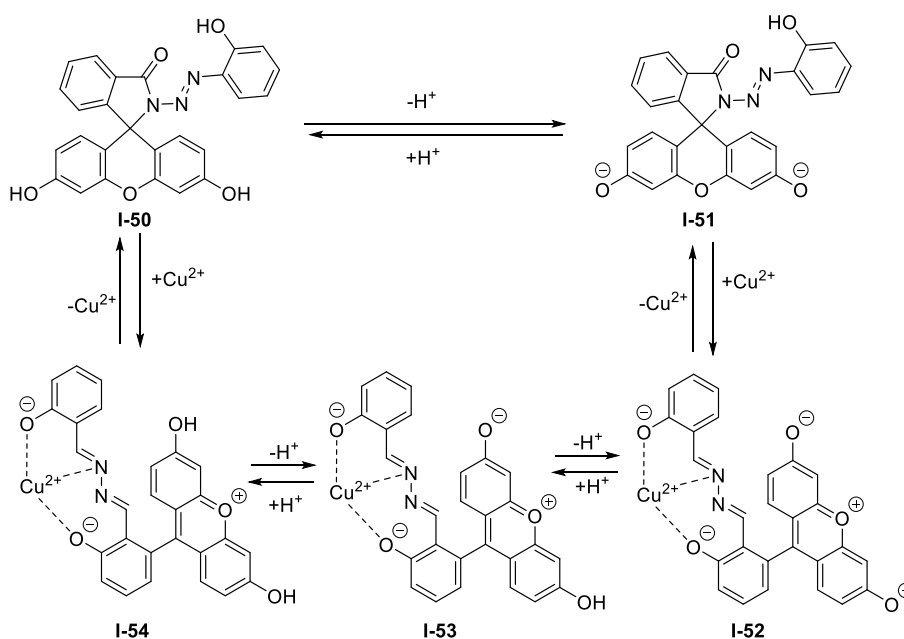
Scheme 18: "off–on" fluorescent chemosensor for Cu^{2+} based on a rhodamine B-based hydrazone.

I.2.4 Photo- and pH-activated switching

The E/Z isomerization of the hydrazone functional group can be activated by both light and chemical inputs. The nature of the C=N bond can lead to configurational isomerism in hydrazone molecules, which can exist in E or Z forms in solution. UV light can provide enough energy for the E-Z isomerization process of the C=N bond, but in most cases, the Z isomers are ephemeral species [44]. Hydrazone photoswitches have potential properties such as high photoconversion, tunable absorption wavelength, fatigue resistance, fluorescence switching, and unsurpassed thermal stability of metastable isomers [45].

Ivan Aprahamian et al. [46] published work about photochromic hydrazone switches. They showed a new family of easily accessible light-activated hydrazone switches. The synthesized hydrazone photo switches derivatives (Scheme 19) find application in various materials, such as liquid crystals, [47] light-switchable nanoparticles for drug release, [48] switchable template for enzymatic synthesis, [49] actuating polymers [50].
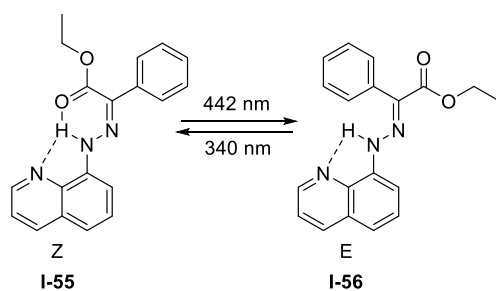
Scheme 19: Photo activated switching in hydrazone derivatives.

Liqiang Yan et al. [51] synthesized a simple photochromic Schiff base from salicylaldehyde and benzoyl hydrazine by condensation and studied its reversible photochromic properties. Compound **I-57** was found to have reversible photochromic properties based on isomerization and excited state intramolecular proton transfer (ESIPT) mechanisms. When irradiated with 365 nm UV light for 2 minutes, the absorption peak of **I-57** at 367 nm showed a significant decrease, while a double absorption peak appeared at 418 nm and 438 nm, and the color of the solution changed from colorless to yellow (**Scheme 20**).
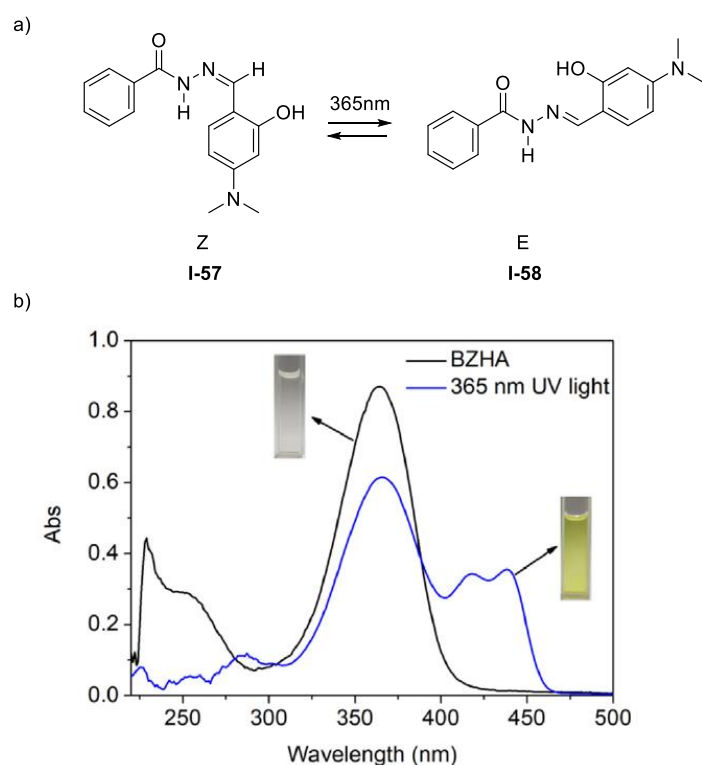
Scheme 20: Photochromism of **I-57** (a) and changes in the UV-vis spectra of I-57 after irradiation [51].

15

Nitro-substituted 2-dicyanomethylene-3-cyano-2,5-dihydrofuran **I-59** hydrazone derivatives could undergo pH-activated switching by sequential addition of base and acid during titration (Scheme 21a). The color of the titrated solution evolved gradually from yellow to purple at pH 7.04, and a new absorption maximum was observed at pH 7, indicating hydrazone-azo tautomerism (Scheme 21b and Scheme 21c) [52].
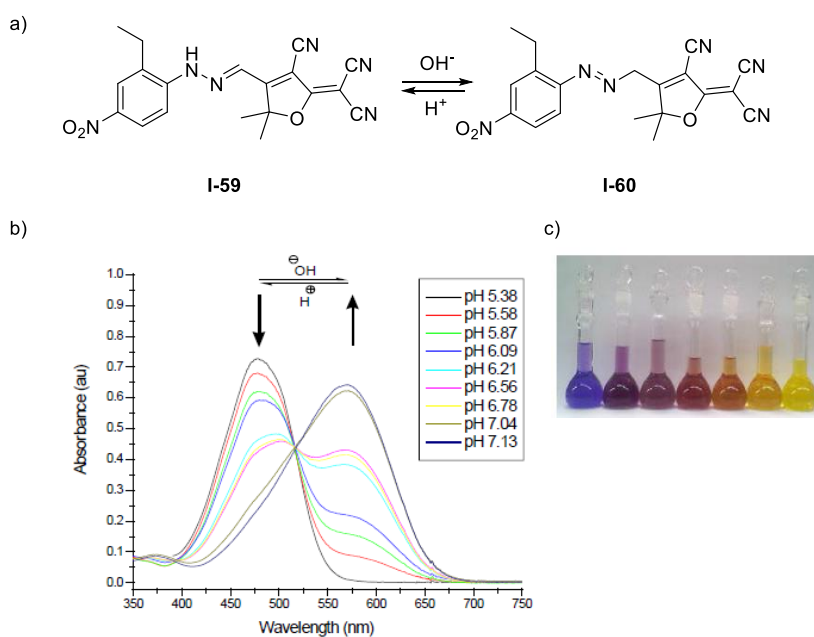
Scheme 21: Hydrazono-azo tautomerism with different pH values (a); the pH dependent absorption spectra of **I-59** in acetonitrile solutions at different pH values at room temperature (b) and color changes during pH titration [52].

Hydrazone derivatives can change their isomer form in solution from hydrazone to azo and vice versa by changing the acid-base equilibrium. Xiao-Lei Zhao et al. [53] reported a study of pH-activated fluorescent probes via transformation of azo and hydrazone forms for lysosomal pH imaging. They tested the photophysical properties of hydrazone **I-61** in Britton-Robinson (BR) buffer solutions with a pH range of 2.02-8.96. The fluorescence of hydrazone **I-61** increased in the pH range from 4.25 to 2.02 (Scheme 22b). The pKa of **I-61** is around 3.97, which is well matched with the lysosome pH in cancer cells (pH = 3.8-4.7). The absolute quantum yield of **I-61** at pH = 2.02 in BR buffer solutions is 9.1%.

a)

I-61   I-62

b)   c)

Intensity (a.u.)

800
600
400
200
0

500 550 600 650 700 750
Wavelength (nm)

2.02
3.27
3.54
3.76
3.94
4.25
4.49
4.86
5.02
7.05
8.96

I_{575}

800
600
400
200
0

2 3 4 5 6 7 8 9
pH values

pKa=3.97
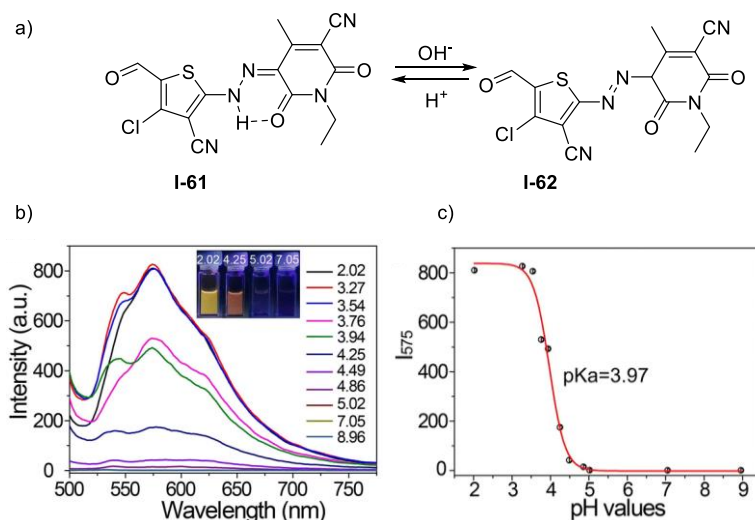
Scheme 22: The pH induced transformation between hydrazone and deprotonated azo forms (a); the fluorescence spectra of **I-61** (20 µM) in Britton-Robinson buffer solutions of pH = 2.02–8.96 and plot of the fluorescence intensity (λ_{em} = 575 nm) versus pH values (b) [53].

I.3 Monomers and polymers based on methacrylate

Poly methyl methacrylate (PMMA) is an important commercial polymer that widely used in various fields due to its optical clarity, hydrolytic stability, and outstanding resistance to air oxidation [54]. PMMA was discovered in the early 1930s by British chemists Rowland Hill and John Crawford, but it was first used by German chemist Otto Rohm in 1934. The first major application of the polymer took place during World War II, when PMMA was used as aircraft windows and bubble canopies for gun turrets [55]. The PMMA belongs to the acrylic polymer family and is known by trademarks Plexiglas and others due to their unique properties. PMMA is more transparent and less brittle than conventional glass with a lighter weight and it is easy to mold to a variety of shapes as well as thin films. PMMA and side-chain polymers based on them shows a wide variety of uses as glass replacement material, urban furnishing, medical applications. The study of PMMA and its derivatives has attracted considerable attention from researchers due to their potential to create new molecules based on dyes, optically active chromophores and nanoparticles etc. [56] [57] [58].

Methacrylate monomers can be synthesized using the Schotten-Baumann reaction, as shown in Scheme 23a [59] [60]. Another method for synthesizing methacrylate monomers is by reacting phenol/amide with methacrylic acid in the presence of 1-

ethyl-3-(3-dimethylaminopropyl) carbodiimide (EDC) and 4-dimethylaminopyridine, as shown in Scheme 23b [61]. Transamidation, as show on Scheme 23c, is another alternative method for synthesizing methacrylic monomers [62].
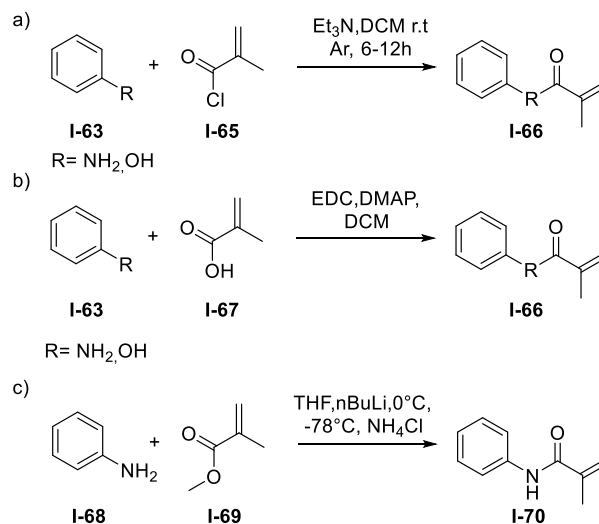
Scheme 23: The methacrylate monomers synthesis by Schotten–Baumann reaction (a), esterification of methacrylic acid (b) and transamidation (c).

Polymethacrylates can be synthesized using free radical polymerization, ionic polymerization, and coordination polymerization techniques [63][64]. Among these, free radical polymerization is the most widely used and important method due to its simplicity and reproducibility. Conventional radical polymerization, atom transfer radical polymerization (ATRP), and reversible addition-fragmentation chain-transfer polymerization (RAFT) are all effective methods for producing high molecular weight PMMA [65] [66] [67].

In conventional free radical polymerization, polymethacrylates can be synthesized via bulk polymerization, solution polymerization, emulsion polymerization, or suspension polymerization techniques [68][69][70]. The most commonly used initiators in conventional radical polymerization are azodiisobutyronitrile (AIBN) and benzoyl peroxide. Scheme 24 illustrates the mechanism of free radical polymerization of polymethacrylates **I-71**.
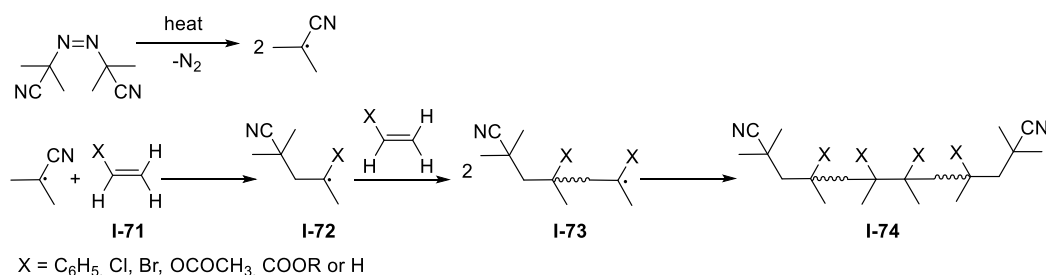
Scheme 24: The mechanism of free radical polymerization of **I-71.**

Atom transfer radical polymerization (ATRP) of MMA has been reported with various catalytic systems, including ruthenium (as shown in Scheme 25) [71], palladium [72], copper [73], nickel [74], iron [75], and rhodium [76]. The initiation step is crucial in ATRP of MMA, and the most effective initiators are sulfonyl chlorides and 2-halopropionitrile due to their large apparent rate constants of initiation (high atom transfer equilibrium constants) [77].
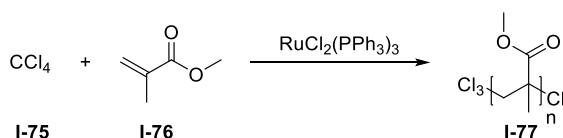
Scheme 25: The ATRP polymerization of MMA with $RuCl_2(PPh_3)_3$.

Reversible addition-fragmentation chain transfer (RAFT) polymerization was developed at CSIRO in the mid-1990s and has since become a reliable and versatile process that can be applied to most monomers subject to radical polymerization (Scheme 26) [78]. RAFT polymerization is known for its compatibility with a wide range of monomers compared to other methods of controlled radical polymerization [79]. The success of RAFT polymerization depends on choosing the right RAFT agent, which varies depending on the specific monomer and reaction conditions.

Z = Phenyl, R = CH(CH₃)Ph
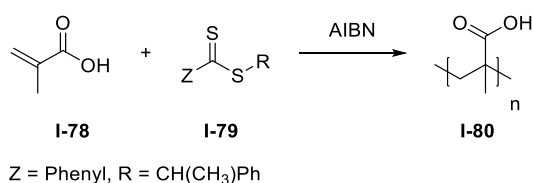
Scheme 26: The RAFT polymerization of MMA.

The Z group in the RAFT agent affects the stability of the S=C bond and the stability of the radical, thus impacting the position and rates of elementary reactions in the

preliminary and main equilibrium (Scheme 26). Meanwhile, the R group stabilizes the radical so that the right-hand side of the previous equilibrium is favorable but remains unstable enough to reinitiate the growth of a new polymer chain [80].

Ionic polymerization, like radical polymerization, follows a chain mechanism where cations or anions are the active centers. During the polymerization process, the solution remains electroneutral, and the number of active centers and their counterions remain constant. The type of substituent on the monomer plays an important role in determining the type of polymerization. For example, monomers with donor-substituents (OR, NR_2, C_6H_4-CH_3) favor cationic polymerization, while those with acceptor-substituents (CN, COOR, $CONR_2$) favor anionic polymerization. The growing chains in ionic polymerization are equally charged, which prevents them from stopping the reaction by combining with each other, and they remain active [81].

Cationic polymerization requires a small amount of a catalyst with strong electron-acceptor capability, such as $AlCl_3$, $AlBr_3$, BF_3, $TiCl_4$, $SnCl_4$ or strong protonic acids like H_2SO_4, $HClO_4$ or H_3PO_4. A co-catalyst, such as water, alcohol, or acetic acid, is also required to form a complex with the catalyst and stabilize the counterion, preventing recombination. The presence of these catalysts allows cationic polymerization to proceed at high rates, both at high and low temperatures [82][83][84]. Boron trifluoride (BF_3) is an example of a useful Lewis acid that can react with trace amounts of water to form an electrophile that initiates chain growth.

Similar to free radical polymerization, an initiator is added to a monomer to form the propagating chain growth center. For example, in a Lewis acid-proton donor complex like boron trifluoride monohydride, a proton is transferred from the complex to the double bond of the vinyl monomer, producing a reactive carbocation. In the propagation step, each carbocation reacts with a vinyl monomer to form a new carbocation, repeating until all the monomers have been used or until the polymerization process has reached termination (as shown in Scheme 27) [85] [86].
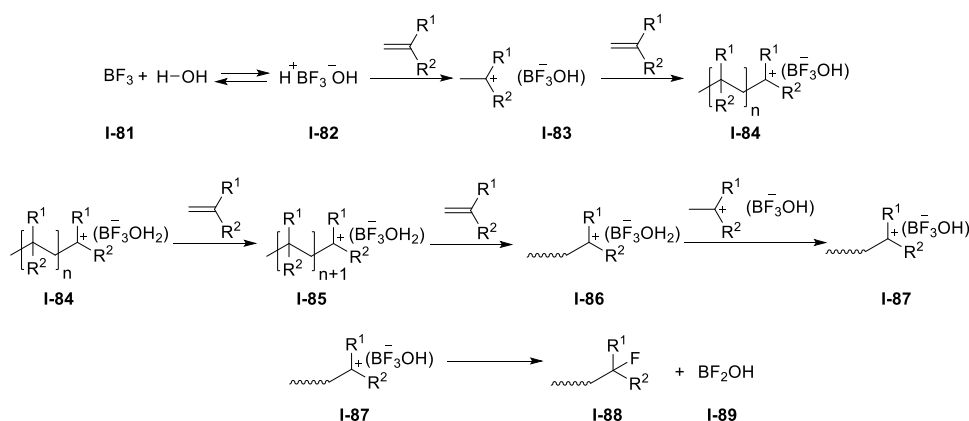
Scheme 27: Mechanism of cationic polymerization.

Anionic polymerization is a chain-growth polymerization that is commonly used for vinyl monomers with strong electronegative groups [87]. Polymerization occurs through the formation of carbanions at the ends of the polymer chain, with the carbanion formed during initiation involving a nucleophilic attack on the monomer. Anionic polymerization has three important steps: initiation, propagation, and termination (with chain transfer occurring to a negligible extent), allowing for precise control over important parameters such as molecular weight, polydispersity, and polymer architecture. Unlike free-radical polymerization, anionic polymerization does not involve cross-coupling between two polymer radicals or transferring an atom from one polymer radical to another due to unfavorable electrostatic interactions. Termination typically occurs when active chain ends react with trace impurities such as oxygen, carbon dioxide, or water. In some cases, termination may be intentionally accomplished by quenching the system with water, alcohol, dry ice, or other proton reagents [88].

Kitayama and coworkers [89] reported highly isotactic-specific anionic polymerization of methacrylate using a combined anionic initiator comprising **I-90** alpha-lithiumisobutyrate (Li-iPrIB) and a large excess of **I-91** lithium trimethylsilanolate (Me$_3$SiOLi), as shown in Scheme 28. They were able to isolate polymethacrylate with a high molecular weight (Mn = 8.25x10^5 Da) and low polydispersity index (Đ = 1.16) using a molar ratio of [methacrylate]:[initiator] = 3000:1.
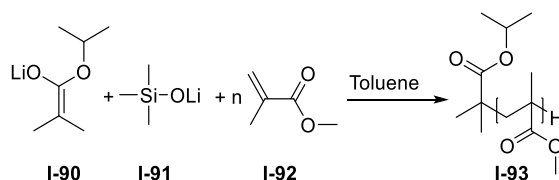
Scheme 28: Anionic polymerization of methacrylate.

Coordination polymerization is an effective method of obtaining PMMA with a high molecular weight (as illustrated in Scheme 29). The catalytic activity and molecular weight of the polymer are significantly influenced by the metal, ligand, temperature, co-catalyst, and the monomer-to-catalyst molar ratio during coordination polymerization. The steric hindrance in the ligand around the metal center has an obvious effect on the catalytic activity. For instance, in pyrazole-based ligands, if the pyrazole moiety has a substituent, the catalytic activity will be enhanced in MMA polymerization. The catalytic activity increases with the voluminous nature of the substituents of the pyrazole fragment, leading to higher catalytic activity for the polymerization of MMA. This method allows for precise control over the molecular weight and polydispersity of the final product [90] [91].
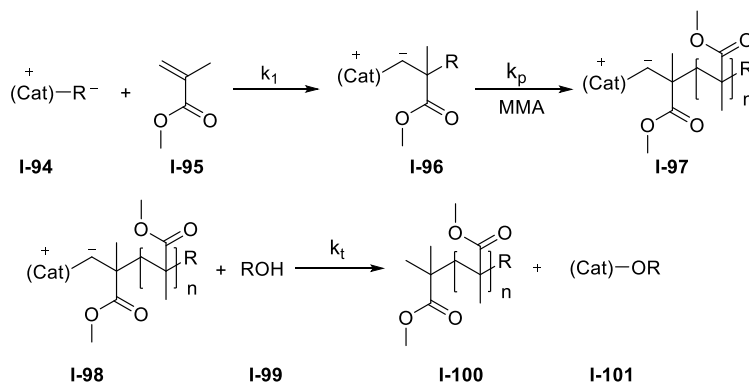
Scheme 29: Mechanism of coordination polymerization of MMA.

22

I.4 Results and discussion

I.4.1 New pyrazolone-hydrazono methacrylic polymer

One of the objectives of this work was to synthesize innovative methacrylic polymeric dyes that incorporate a hydrazone-pyrazolone moiety with chromogenic properties suitable for pH switching and anion detection. These dyes have the potential to be used as highly effective sensors or detectors in various materials. In order to advance this research, the next step involved characterizing the dyes and the polymer based on them by conducting optical studies. This approach was pursued to gain a deeper understanding of their unique properties and explore their potential applications.

The synthesis and characterization of methacrylic polymers containing a hydrazone-pyrazolone fragment were carried out. The synthesis of the polymer dyes initiated with the Japp-Klingemann transformation, which followed a two-step route. In the first step, diazotization of 4-aminophenol **I-102** was achieved using a mixture of sodium nitrite and concentrated HCl at 0-5 °C to form the diazonium salt. The diazotization process was confirmed using β-naphthol solution as an indicator of diazonium salt. In the second step, the freshly prepared diazonium salt reacted with ice-cold active methylene compound **I-103** in the presence of 10% NaOH in ethanol solution at 0 °C with stirring for 1 hour. The resulting in the formation of compound **I-104** as a yellow solid with a yield of 78% over two steps (as shown in Scheme 30).
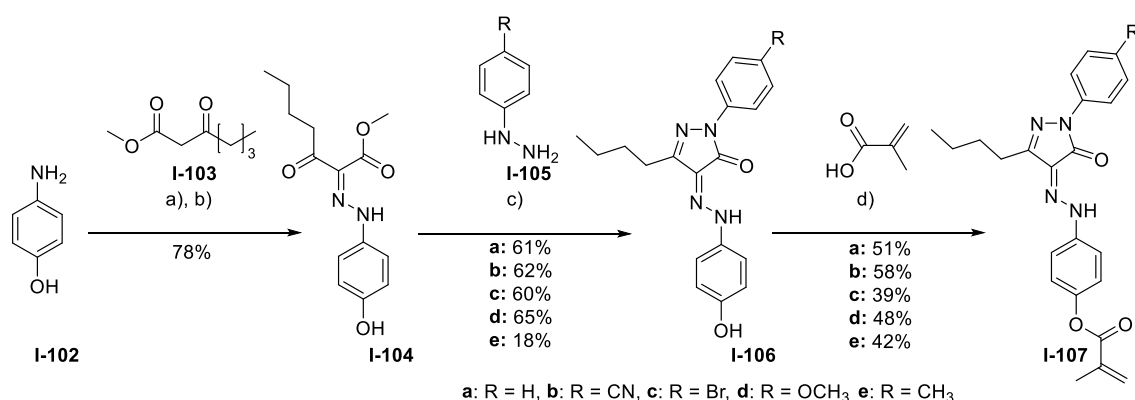
Scheme 30: Synthesis of hydrazone-pyrazolone derivatives a) HCl con, 0°C, NaNO$_2$, H$_2$O, 1h; b) **I-103**, EtOH, 0°C, 10% NaOH, rt, 3h; c) **I-105**, EtOH/H$_2$O, NaOAc, reflux; d) methacrylic acid, DCM, Et$_3$N, EDCl, rt, 48h.

The hydrazone **I-104** was then cyclized with hydrazine derivatives **I-105a-e** by heating at 75 °C in a mixture of ethanol/water (3:1), yielding the hydrazone-pyrazolone products **I-106a-e** as a red solid with yields ranging from 48% till 65% (Scheme 30). The chemical structures of the synthesized compounds were characterized using ^{1}H-NMR, ^{13}C-NMR, HRMS, UV, and IR-spectra.

In this study, five monomers were successfully synthesized, **I-107a-e**, via the condensation of hydrazone-pyrazolone derivatives, **I-106a-e**, with methacrylic acid in the presence of 1-ethyl-3-(dimethylaminopropyl)carbodiimide (EDC). The reaction was carried out for 48 hours under argon atmosphere, and the yields of orange solids ranged from 39% till 58% (Scheme 30). Subsequently, these monomers were used to synthesized several side-chain copolymers, **I-108a-e**, and one homopolymer, **I-109a**, via free-radical polymerization. The azobisisobutyronitrile (AIBN) was used as a radical initiator (Scheme 31).

The synthesis of polymers based on methacrylic monomers **I-107a-e** and methyl methacrylate (MMA) (for copolymers synthesis) was conducted in anhydrous N,N-dimethylformamide with 10% of monomers in initial mole ratios of 1(**I-107a-e**):3(MMA) and AIBN (1 wt % of monomers) at 80 °C for 48 hours under an argon atmosphere. The resulting polymers, **I-108a-e** and **I-109**, were obtained with excellent yields of yellow solids ranging from 87% till 99% (Scheme 31).
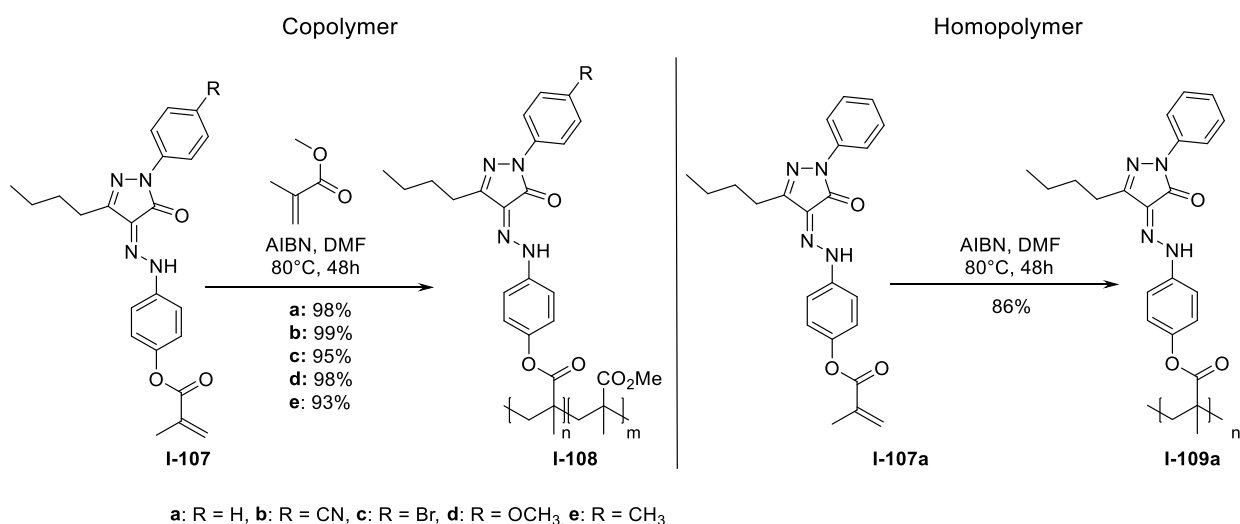
Scheme 31: Synthesis of hydrazone-pyrazolone functionalized methacrylic ester polymers.

The polymer structures were confirmed by ^{1}H-NMR spectra, and the copolymerization ratios of **I-108a-e** were calculated based on the integration ratio of proton signals. The observed n/m values in the polymers (n/m$_{obs}$ $_{(observed\ mole\ ratio\ of}$ $_{monomers\ units\ in\ copolymer)}$) were found to be in reasonable accordance with the initial mole ratios amounts of introduced monomers (n/m). However, due to the less hindered character of the MMA fragments (m values), they were generally present in slight excess in the final composition of the polymers.

The glass transition temperature (T$_g$) and melting endotherm were measured for polymers **I-108a-108e** and **I-109a**, as indicated in Table 1. Polymers **I-108a**, **I-108c**, **I-108d**, and **I-108e** exhibited T$_g$ values ranging from 120-131 °C. However, polymer **I-108b** displayed a significant increase in T$_g$ with a value of 146 °C. This notable difference in T$_g$ can be attributed to the potential hydrogen bonding acceptor characteristics of the nitrile group, as mentioned earlier [92]. The presence of such hydrogen bonding interactions in **I-108b** led to a higher T$_g$ value compared to **I-108a**, **I-108c**, **I-108d**, and **I-108e.** A melting endotherm was observed for the polymers at temperatures between 249 and 263 °C.

The melting endotherm of pyrazolone-hydrazono dyes **I-106a-e** (Table 2) was measured and compared to new polymers **I-108a-e**. It was observed that the polymer molecules displayed an increase in melting endotherm compared to the hydrazone-pyrazolone derivatives **I-106**, which exhibited a melting endotherm range of 204-212 °C and for pure PMMA is 95 °C. These findings suggest that the polymeric dyes possessed a higher melting temperature in comparison to the **I-106** derivatives.

The IR spectra of the polymers show a band of C-H in the region of 2990-3010 cm^{-1}. Additionally, two other bands are visible around 1730 and 1660 cm^{-1}, indicating the presence of two C=O groups. These bands correspond to the ester carbonyl function directly attached to the pyrazolone ring and the ester carbonyl function of the MMA fragments. Notably, there is a clear absence of a broad O-H absorption band around 3400 cm^{-1}. The increased intensity of the C-H sp^3 stretching in the range of 2990-3010 cm^{-1} due to the large number of methyl groups present in the copolymer. Overall, the results of the IR spectroscopic analysis confirm the

successful synthesis of hydrazone-pyrazolone functionalized methacrylic ester polymers.

Table 1: Results of radical polymerization of 10 % methacrylic monomers in DMF at 80 °C.

Polymer	(n/m) [a]	(n/m$_{obs}$) [b]	M_n [c] [g/mol]	Đ [c]	T_g [d] [°C]	T_m [d] [°C]
I-108a	1:3	1:3	47 800	1.7	120	260
I-108b	1:3	1:4	97 100	1.5	146	261
I-108c	1:3	1:4	96 900	1.4	124	263
I-108d	1:3	1:4	100 600	1.6	126	252
I-108e	1:3	1:3	97 100	1.2	131	249
I-109a	-	-	83 200	1.3	142	262

[a] Molar ratio of monomers units in polymer ; [b] n/m stoichiometry in the copolymer as determined from ^{1}H-NMR integration; [c] Measured by GPC with linear poly(methyl methacrylate) standards (M_n 800–2 200 000 g/mol); [d] Measured by DSC.

Table 2: The melting endotherm of **I-106a-e** and **I-108a-e**.

I-106	T_m [a][°C]	I-108	T_m [a][°C]
a	208	**a**	260
b	209	**b**	261
c	212	**c**	263
d	210	**d**	252
e	204	**e**	249

[a] Measured by DSC.

The polymer **I-108a** (powder) was placed on a windowsill in a glass vial and exposed to sunlight for a period of 31 days. UV-vis spectra of the polymer **I-108a** were measured before and after this exposure. Initially, without irradiation, an absorption maximum at 400 nm was observed (Figure 3 (red)). Subsequently, after 31 days of sunlight exposure, a sample of **I-108a** was measured using UV-vis, and no changes were detected (Figure 3 (black)). The absorption maximum remained at 400 nm, and there were no new absorption peaks observed. The concentration of both solutions was 1×10^{-5} M. These findings indicate that the polymer exhibits light

stability, as it did not undergo significant changes or degradation under prolonged sunlight exposure.
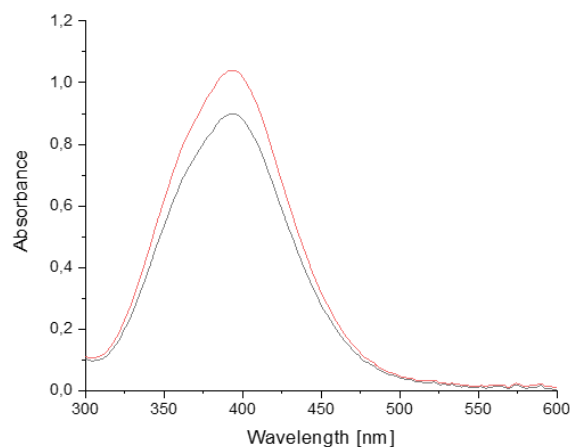
Figure 3: Changes in the UV-Vis spectra during sun irradiation **I-108a** (red) in THF (1×10^{-5} M) without irradiation and **I-108a** in THF (1×10^{-5} M) after 31 days under sunlight irradiation (blacks).

The results of the study demonstrate that the newly synthesized polymeric dyes possess favourable stability properties, including resistance to air, light, and heat. These characteristics are highly desirable for dye materials, as they allow for their reliable use in various applications, from textiles to electronics.

I.4.2 The linear optical studying of polymeric thin films

During the internship at Nicolaus Copernicus University in Poland, a physical study of new polymer materials was conducted under the supervision of Professor Dr. B. Derkowska-Zelinska.

Subsequent optical studies were conducted on thin films of the aforementioned polymers. Specifically, polymer films **I-108a** to **I-108e** were deposited onto a substrate via spin-coating at a speed of 800 rpm for 60 seconds using a 10 wt.% solution of 1,1,2-trichloroethane that had been filtered through a 0.4 μm pore size nylon syringe filter. The resulting thin films were then immediately subjected to vacuum drying at 35 °C for 5 hours to ensure complete removal of any residual solvent (Figure 4).
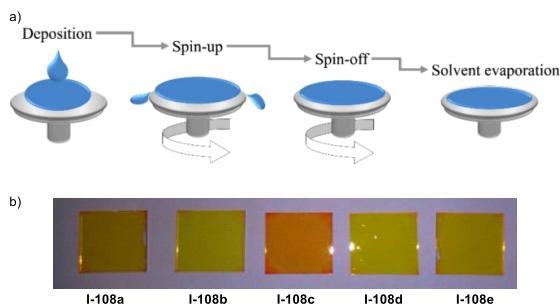
Figure 4: a) Schematic diagram of thin film formation in spin-coating method [93]; b) Polymer thin films **I-108a-e**.

The surface morphology of the thin films was studied using atomic force microscopy (AFM). Figure 5 presents the surface topography of **I-108a-e**. The root-mean-square (RMS) surface roughness was determined for each layer: 0.195 nm (**I-108a**), 0.223 nm (**I-108b**), 0.207 nm (**I-108c**), 0.174 nm (**I-108d**), and 1.36 nm (**I-108e**).
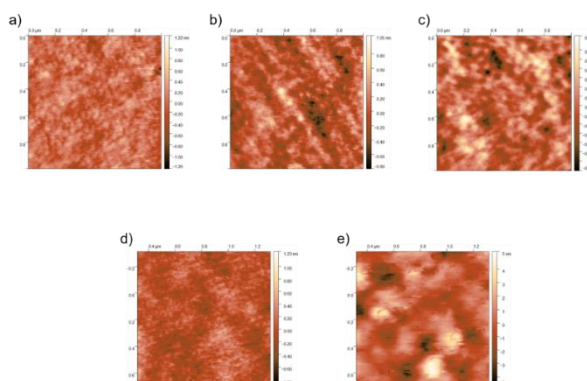
Figure 5: AFM images of the polymeric thin-films **I-108a-e**.

Figure 6 shows the recorded transmission of the prepared thin films of polymeric dyes with hydrazono-pyrazolones fragment. All hydrazone-pyrazolone copolymers have been found to have maximum values of absorption coefficient between 388 nm and 395 nm, indicating π-π* electronic transitions between the aromatic ring. However, the maximum of absorption coefficient can be observed for studied compound with donor substituents (i.e. **I-108e**(CH_3) and **I-108d**(OCH_3)) is redshifted.
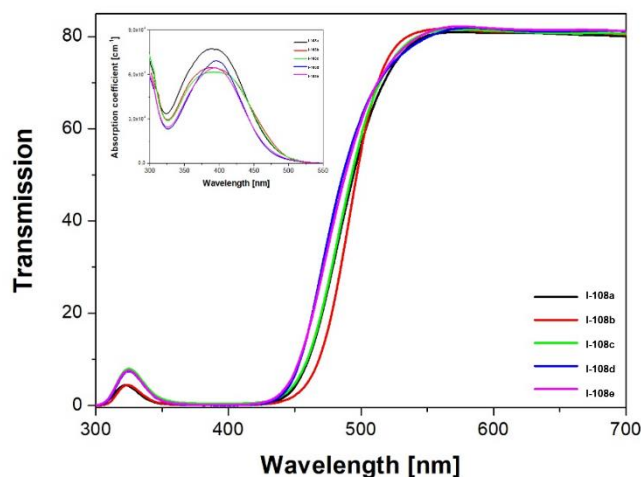
Figure 6: Transmission of the studied polymeric dyes with hydrazono-pyrazolones fragment. Inset: Absorption coefficient of the thin films of the methacrylic polymeric dyes incorporating hydrazono-pyrazolones moiety as a function of wavelength.

In addition, one can see that the full width at half maximum (FWHM) of absorption coefficient of studied compound with donor substituents (i.e. **I-108e**(CH_3) and **I-108d**(OCH_3)) is narrower than for materials with acceptor substituents (**I-108b**(CN) and **I-108c**(Br)) or neutral compound (**I-108a**(H)). The widest value of FWHM is observed for the methacrylic polymeric dyes incorporating hydrazono-pyrazolones moiety with cyano group, which has the highest value of Hammett constant for all studied compounds. In conclusion, the FWHM decreases as the Hammett constant decreases (i.e. $\sigma_{CN} > \sigma_{Br} > \sigma_H > \sigma_{CH3} > \sigma_{OCH3}$).

The experimental ellipsometric azimuths (Ψ and Δ) and the adjustments of the obtained data from the optical model for the methacrylic polymeric dyes incorporating hydrazono-pyrazolones moiety with cyano group (**I-108b**(CN)) thin film are shown in Figure 7. The fit of the model is well suited to the experimental results. Based on these data, the absorption coefficients (α) and the refractive indices (n) of the studied compounds were determined.
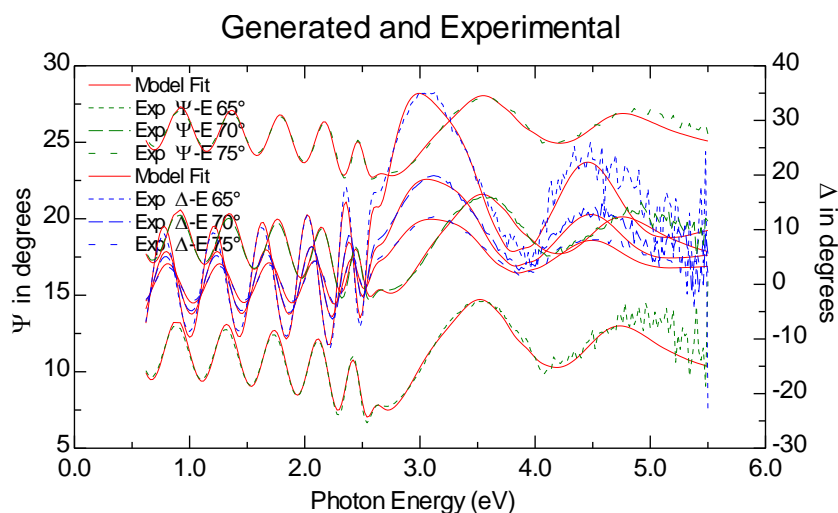
Figure 7: Experimental Ψ and Δ azimuths for three angles of incidence (65°, 70° and 75°) for **I-108b**(CN) thin film.

Figure 8 presents the absorption coefficient (*a*) of the studied polymeric dyes with hydrazono-pyrazolones fragment extracted from SE measurements. The shape of the spectra was parameterized using Gaussian oscillators. We noticed that the maximum absorption coefficient peaks are in the range of 389 nm to 395 nm, such as for the absorption coefficient obtained from the transmission measurements, and agree with those reported for the hydrazone compounds and the pyrazolone-based heterocyclic dyes [94] [95]. The absorption peaks can be ascribed to the C=N double bond n-π* transition and the π-π* electronic transitions between the aromatic rings. One can also see that the values of absorption coefficient of studied compound with donor substituents (i.e. **I-108e**(CH₃) and **I-108d**(OCH₃)) are lower than for materials with acceptor substituents (**I-108b**(CN) and **I-108c**(Br)) or neutral compound (**I-108a**(H)). It was also found that in the case of the methacrylic polymeric dyes incorporating hydrazono-pyrazolones moiety with donor substituents (i.e. **I-108e**(CH₃) and **I-108d**(OCH₃)), the additional shoulder at 352 nm for **I-108e**(CH₃) and 356 nm for **I-108d**(OCH₃) is observed.
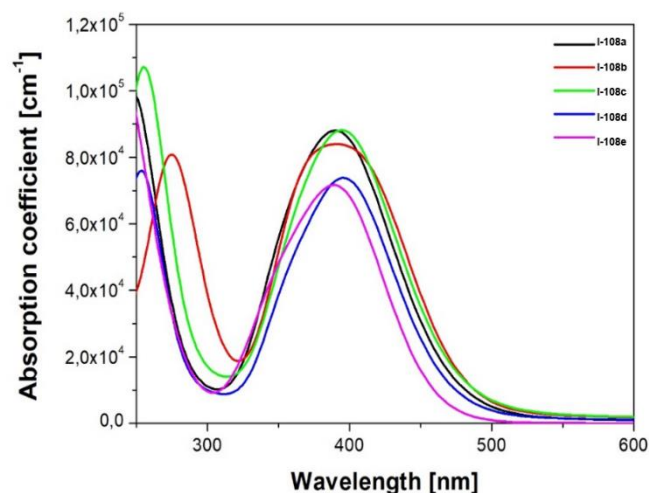
Figure 8: Absorption coefficient of the thin films of the methacrylic polymeric dyes incorporating hydrazono-pyrazolones moiety as a function of wavelength.

Figure 9 shows the refractive indices (*n*) of the methacrylic polymeric dyes incorporating hydrazono-pyrazolones moiety thin layers. One can see that the normal dispersion is visible in the region above 450 nm. We found that the values of refractive indices for the methacrylic polymeric dyes incorporating hydrazono-pyrazolones moiety with acceptor substituents (**I-108b**(CN) and **I-108c**(Br)) and neutral compound (**I-108a**(H)) are close to each other and they are higher than for the compounds with donor substituents (i.e. **I-108e**(CH_3) and **I-108d**(OCH_3)).
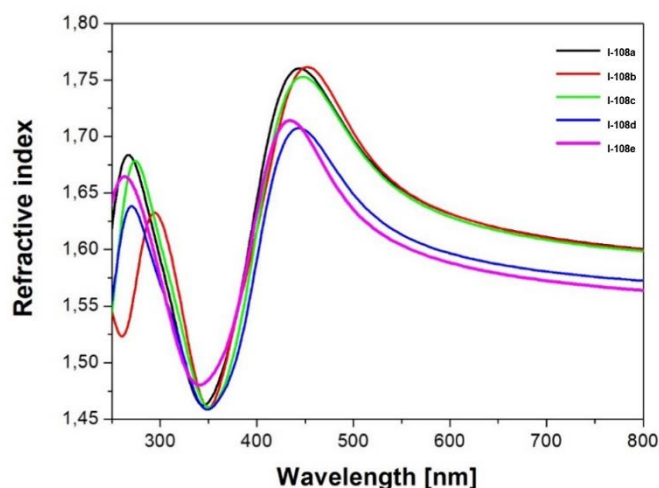
Figure 9: Refractive index of the studied polymeric dyes with hydrazono-pyrazolones fragment.

I.4.3 pH-switching and anion detections studies

According to the literature [29], hydrazone monomers can exist in different tautomeric forms. This has been extensively researched in recent years [31] [96]. Similarly, the novel polymers also exhibit these properties. The hydrazone-azo tautomerism in **I-108a** was discovered and confirmed through Brønsted-Lowry acid-base reactions. The changes in tautomeric forms were monitored using UV-Vis and ^{1}H-NMR.

In DMSO, the hydrazone-pyrazolone methacrylic polymers exhibit a single absorption maximum at 400 nm. This suggests that the polymers predominantly exist in a single tautomeric form at pH=11. When the pH value was increased to 16 by adding 0.01 M CsOH·H_2O solution to **I-108a** in DMSO, a large bathochromic shift occurred, resulting in a color change of the solution from light yellow (1) to dark yellow (2), as shown in Figure 10c. To confirm that the effect was due to pH value rather than Cs cation influence, the **I-108a** was titrated with CsCl solution, and no changes in the spectrum were observed.
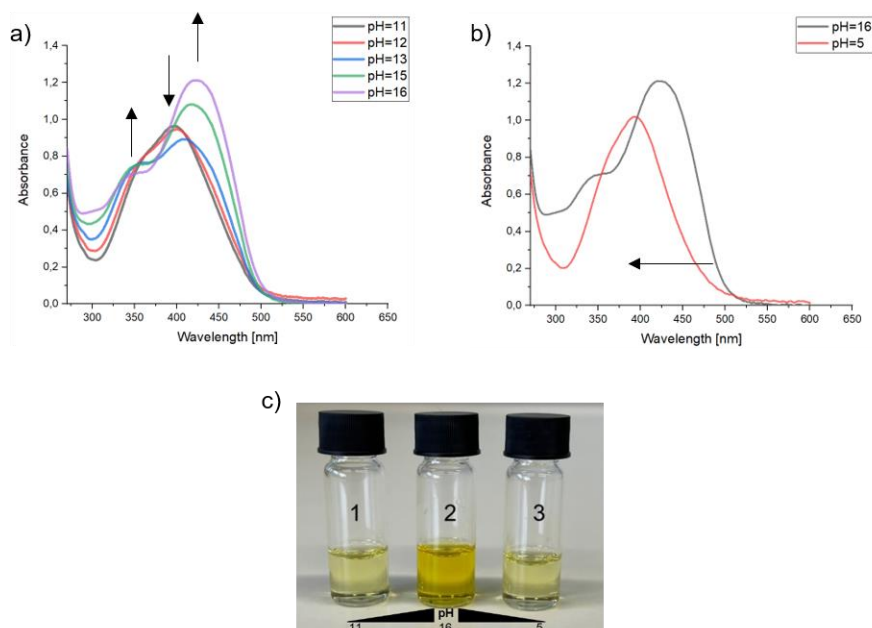
Figure 10: Changes in the UV-Vis spectra and pH value of **I-108a** (1×10^{-5} M) a) during titration by CsOH in DMSO; b) after adding HCl in DMSO; c) color changes of **I-108a** in DMSO before (1) pH=11 and after (2) pH=16 adding CsOH, (3) after adding HCl solution in DMSO, pH=5 (reverse color change).

Upon completion of the titration of **I-108a** with CsOH solution, two new absorption maxima at 352 nm and 425 nm, and two isosbestic points at 356 nm and 395 nm, were observed in the UV-Vis spectra (Figure 10a). When the pH value was decreased from 16 to 5 by adding HCl solution, the absorption peak at 425 nm was reversed back to the initial absorption maximum at 400 nm (Figure 10b). The change in absorption maximum also led to a change in the color intensity of the solution. As shown in the Figure 10c, an increase in pH from 11 to 16 resulted in an increased intensity of the solution from light yellow (1) to a more intense yellow (2), or a decrease in intensity (3) after changing the pH from 16 to 5. These results indicate that the polymer **I-108a** can switch tautomeric forms in solution depending on the pH value. Basic media promotes deprotonation of the polymer from hydrazone to azo form, while acid media promotes the reverse transformation from azo to hydrazone form (Scheme 32).
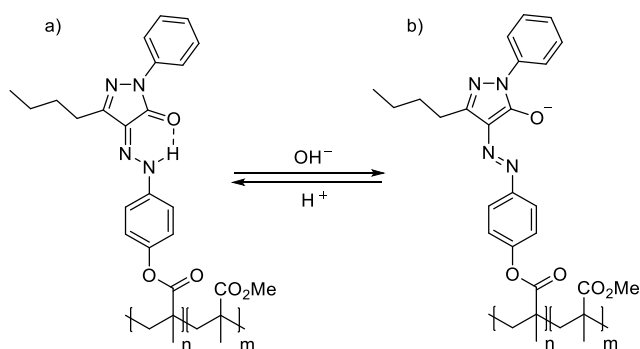
Scheme 32: The two tautomeric form of polymer **I-108a** (a) hydrazo at pH=11 and (b) azo in basic media (pH=16).

The azo-hydrazone tautomerism discussed earlier was further confirmed through ^{1}H-NMR analysis of polymer **I-108a** in CDCl₃. As seen in Figure 11 (1), a large and broad proton signal of N-H at 13.6 ppm indicated that the polymer is in the hydrazone form. However, after the addition of 0.01 M Et₃N, the previous N-H signal at 13.6 ppm disappeared (Figure 11 (2)), confirming the probability of the azo form under alkaline conditions. This result is consistent with the changes observed in the UV-Vis spectra.
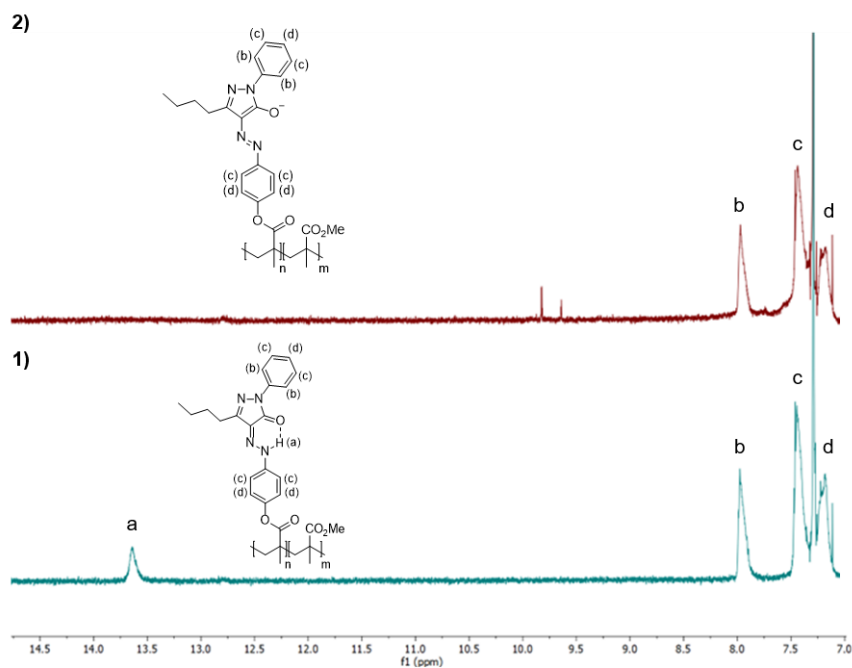
Figure 11: ^{1}H-NMR spectrum of **I-108a** (1) without and (2) with Et₃N in CDCl₃.

The polymers **I-108a-e** were also tested for chromogenic detection of anions by UV-Vis titrations in DMSO solution. The investigated polymers could form a hydrogen bond to an inorganic anion as F^-, $H_2PO_4^-$ (as their tetrabutylammonium salts) in DMSO as well as to CrO_4^-, WO_4^- (sodium salts) (Table 3 and Table 4) and to an organic anion as tetrabutylammonium acetate, sodium ascorbate, adenosine 5'-monophosphate disodium salt (AMP), sodium-L-glutamate-monohydrate, sodium edetate, thymidine 5'-monophosphate disodium salt, L-(+) tartaric acid, disodium salt (Figure 14).

During the titration of **I-108a** receptor with an inorganic anion (F^-, $H_2PO_4^-$, CrO_4^-, WO_4^-) in DMSO solution, the absorption spectrum exhibited a strong absorption band with a maxima at 400 nm. With the addition of F^-, the band at 400 nm progressively decreased, while two new absorption peaks appeared at 341 nm and 436 nm (Figure 12 and Table 3). Similar changes were observed for all investigated polymers, as well as a noticeable color change from light yellow to dark yellow, indicating the formation of a stable complex between the polymer receptor and the anion. The titration of receptor **I-108a** also exhibited two new isosbestic points at 349 nm and 415 nm, as seen in Figure 12. This sensitivity ability is attributed to a tautomeric shift that biases the deprotonated form, similar to basic pH values. Analogous titrations were carried out with F^-, $H_2PO_4^-$ for **I-108b-e** (Table 4) and with CrO_4^-, WO_4^- (Table 3) only for **I-108a**. However, no changes in UV-Vis spectrum and color changes were observed when the polymer was titrated with Br^-, I^- ions (as their tetrabutylammonium salts) (Table 3).

Table 3: Absorption maxima of the polymers **I-108a** in DMSO before and after titration by inorganic anions.

| | | F^- | $H_2PO_4^-$ | CrO_4^- | WO_4^- | Br^- | I^- |
	l_{max} [nm]	l_{max} [nm]	l_{max} [nm]	l_{max} [nm]	l_{max} [nm]	l_{max} [nm]	l_{max} [nm]
108a	400	436	428	430	429	400	400
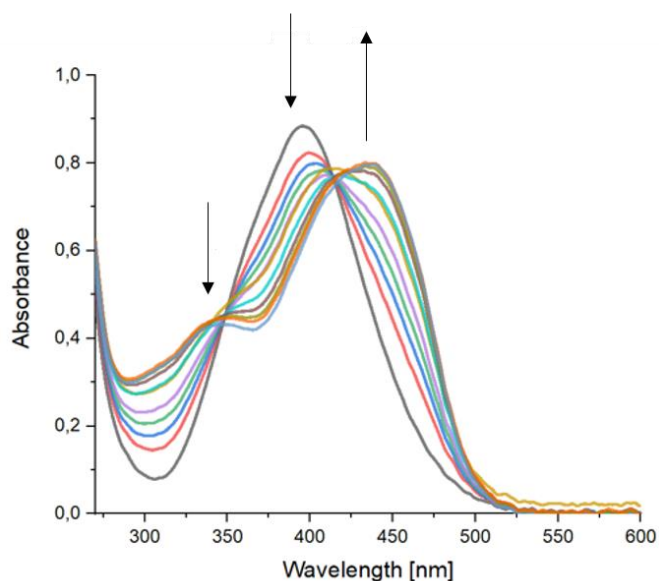
Figure 12: Changes in the UV-Vis spectra for the **I-108a** (1×10^{-5} M) in the absence and presence of fluoride anion in DMSO solution.

Table 4: Absorption maxima of the polymers **108b-e** in DMSO before and after titration by inorganic anions.

		F⁻	H₂PO₄⁻
	I_{max} [nm]	I_{max} [nm]	I_{max} [nm]
108b	402	429	427
108c	405	427	435
108d	401	435	433
108e	400	432	420

The ability of receptor **I-108a** to recognize various organic anions such as tetrabutylammonium acetate, sodium ascorbate (Figure 13), sodium-L-glutamate-monohydrate, sodium edetate (EDTA), thymidine 5'-monophosphate disodium salt, L-(+) tartaric acid, disodium salt, and adenosine monophosphate (AMP) was investigated in DMSO solution. Figure 14 show that the titration of receptor **I-108a** with sodium ascorbate and results for other anions in Figure 14 resulted in similar spectral changes to those observed upon addition of inorganic anions (F^-, $H_2PO_4^-$, CrO_4^-, WO_4^-) to **I-108a** (Table 3 and Table 4). However, no changes were observed

after titration with 2-mercaptopyridine N-oxide and 1,2-dilauroyl-sn-glycero-3-phosphate ions. Notably, the experimental results indicated that **I-108a** exhibited favorable selectivity and sensitivity towards AMP anions compared to adenosine diphosphate (ADP) and adenosine triphosphate (ATP) anions.
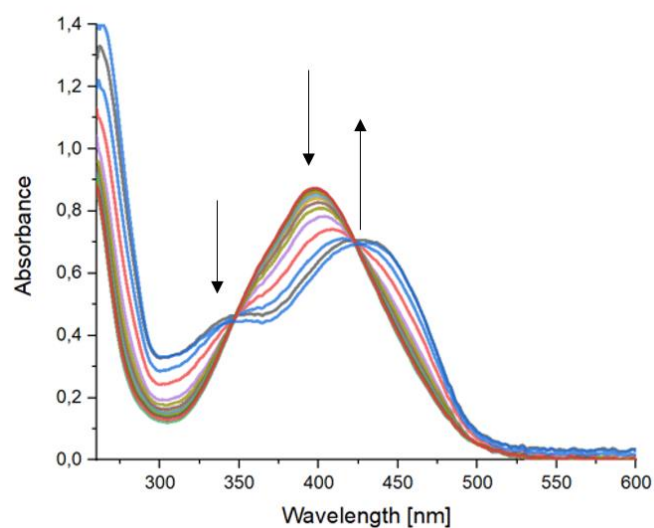
Figure 13: Changes in the UV vis specter of the polymer **I-108a** in DMSO after titration by ascorbate anions.

7a + A⁻ = 7a----A

400 nm   bathochromic shifts

A⁻:

ascorbic acid	tartaric acid ʟ-(+)	ʟ-glutamate	2-mercaptopyridine-n-oxide
absorption max.: 430 nm	431 nm	427 nm	400 nm

A⁻:

EDTA	1,2-dilauroyl-sn-glycero-3-phosphate	acetate	thymidine 5'-monophosphat
absorption max.: 430 nm	400 nm	432 nm	428 nm

A⁻:

AMP	ADP	ATP
absorption max.: 429 nm	400 nm	400 nm
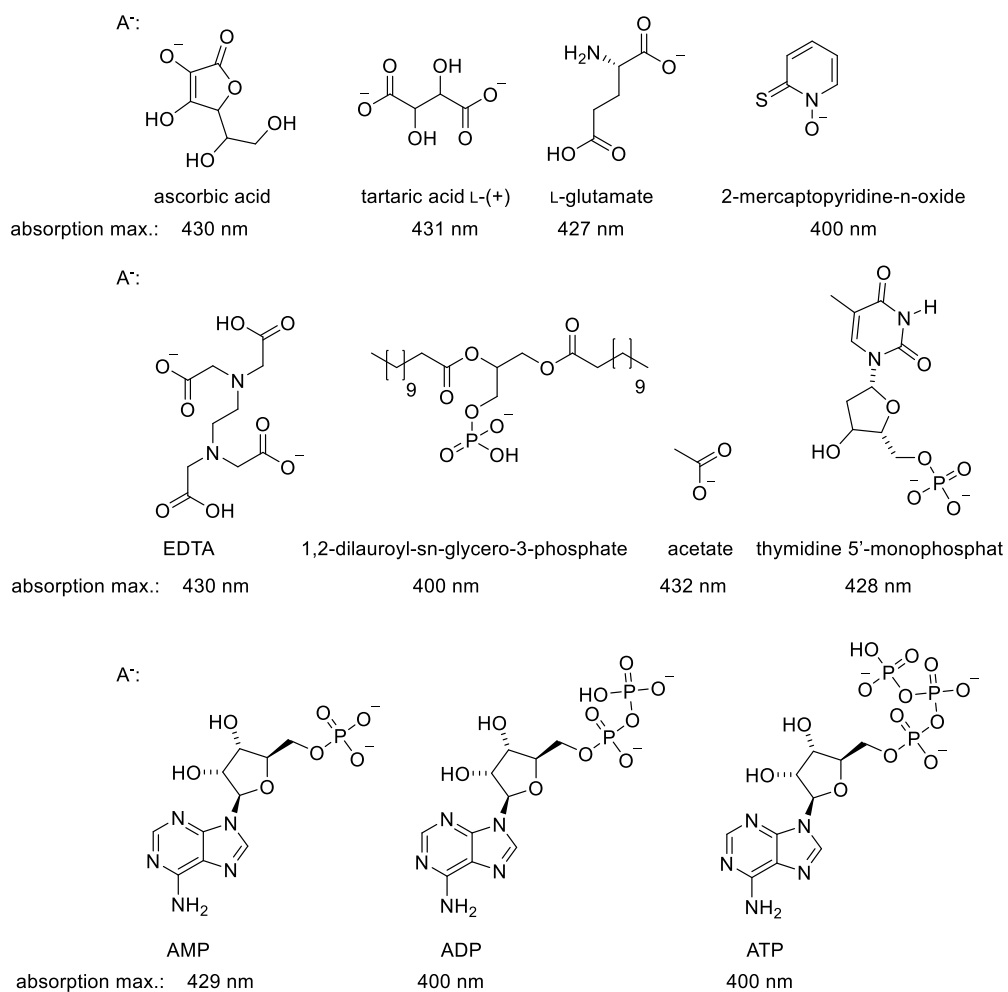
Figure 14: Changes in the UV-Vis spectra of the **I-108a** (1×10⁻⁵ M) in the absence and presence of ascorbate anion in DMSO solution.

38

I.4.4 New hydrazono-pyrazolone methacrylic polymer

Yoshihiko Inukai [97] reported the synthesis of hydrazono-pyrazolones with methacrylic units attached to the pyrazolone moiety via an amino group (Scheme 33).
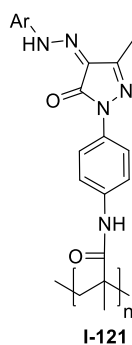
Scheme 33: The hydrazono-pyrazolones homopolymer **I-121** synthesized by Yoshihiko Inukai.

This inspired us to investigate the possibility of synthesizing polymeric derivatives of hydrazono-pyrazolones with methacrylic units attached to the pyrazolone moiety via an ester group. The synthesis route described above was used in this study, and the results were compared with those reported by Yoshihiko Inukai. The main objective was to enhance the yield and polymer lengths for the methacrylic polymer attached to the pyrazolone moiety via an ester group, as compared to the results obtained by Yoshihiko Inukai.

To synthesize the required hydrazono-pyrazolone monomer with a hydroxyl group, 4-phenylhydrazine **I-111** was needed. Unfortunately, this compound was not regularly available and was exceedingly expensive, costing 1,277 euros per gram. As a result, the synthesis of 4-phenylhydrazine was undertaken using various strategies that had been previously described in the literature [98][99]. However, successful results were not obtained. Eventually, the classical route of forming a hydrazine by first forming a diazonium salt from aniline under -10 °C, followed by reduction, was employed and proved to be effective.

The synthesis route employed in this study involved the classic method of generating the diazonium salt by adding a sodium nitrite solution to an acidic water

solution of aniline **I-110** at -10 °C under an argon atmosphere. Reduction was facilitated by tin(II) chloride dihydrate, which was dissolved in 6M HCl. The freshly prepared diazonium salt was then slowly added to the solution of SnCl2, and the reaction mixture was stirred at -10 °C under an argon atmosphere (Scheme 34). It is crucial to control the temperature and maintain an argon atmosphere throughout all steps, there are risk that product can be not formed.

The resulting precipitate was filtered, washed with a small amount of water (since this hydrazine is water-soluble), and dried under high vacuum. Freshly prepared hydrazine **I-111** was utilized for the subsequent step since it is highly sensitive to air. It is recommended to store the compound under argon at -20 °C.
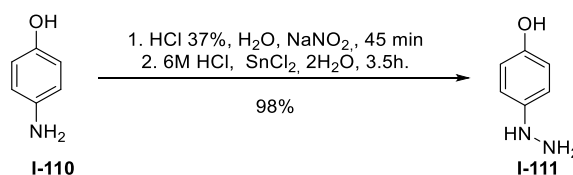
Scheme 34: Synthesis of hydrazine **I-111**.

To synthesize hydrazone derivatives, **I-114**, the Japp-Klingemann transformation was carried out in a two-step process, following the strategy outlined in Scheme 30. The resulting hydrazones were then cyclized with hydrazine **I-111** under reflux in EtOH/H2O with NaOAc under an argon atmosphere, new hydrazono-pyrazolone derivatives **I-115a-d** are form as red solid form with 46%-71% of yields (Scheme 35).

Subsequently, **I-115a-d** was utilized to synthesize the monomers. Methacrylic acid was employed in the presence of 1-ethyl-3-(dimethylaminopropyl)carbodiimide (EDC) under an argon atmosphere for 48 hours, resulting in the formation of product **I-116a-d** as an orange solid with 40%-61% yields (Scheme 35). Overall, this approach offers an efficient and reproducible route for the synthesis of these compounds.
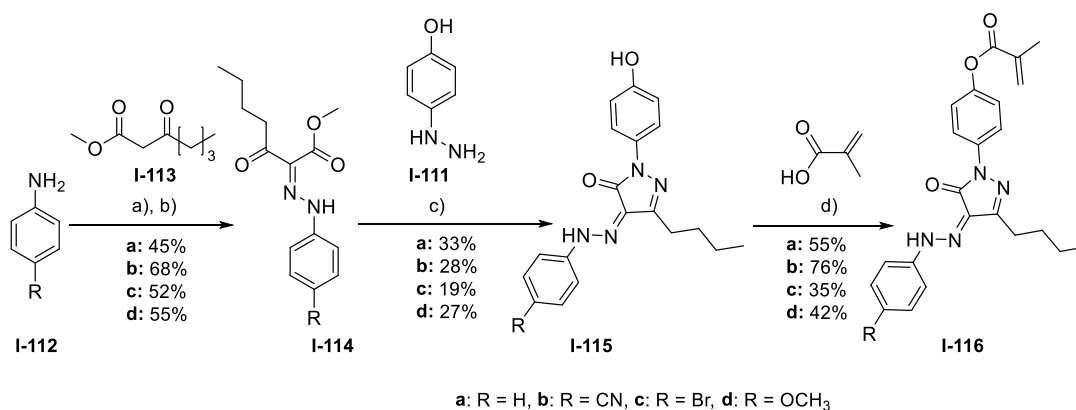
Scheme 35: Synthesis of hydrazone-pyrazolone derivatives a) HCl con, 0°C, NaNO$_2$, H$_2$O, 1h; b) I-113, EtOH, 0°C, 10% NaOH, rt, 3h; c) I-111, EtOH/H$_2$O, NaOAc, reflux; d) methacrylic acid, DCM, Et$_3$N, EDC, rt, 48h.

A comparison of our strategy with that of Yoshihiko Inukai (Scheme 37) reveals a significant difference. Inukai employed amino pyrazolone **I-117**, which is not commercially available and difficult to synthesize. Additionally, they did not describe the synthesis of this pyrazolone. In contrast, our approach utilizes commercially available components or components with a reproducible synthesis (as show on Scheme 30 and Scheme 35).

Inukai employed a method to synthesize methacrylate monomer **I-119** using methacryloyl chloride **I-118** and pyridine in acetonitrile (Scheme 36). However, this approach involves the use of HCl 37%, which can potentially remove the methacrylic group from the amino group, leading to a reduced yield.

The condensation of hydrazono-pyrazolone with methacrylic acid (Scheme 35) was found to be a more effective approach compared to Inukai's method, as it avoided the potential deprotection of the methacrylic moiety that can occur in the presence of HCl.

Inukai proposed to synthesize the polymers **I-121** using free radical homopolymerization (Scheme 36). However, the resulting polymers were in the oligomeric range, with molecular weights ranging from Mn 3 200 – 5 100 g/mol [97]. Although this approach formed polymers, the resulting oligomers had relatively low molecular weight and did not find any practical applications.
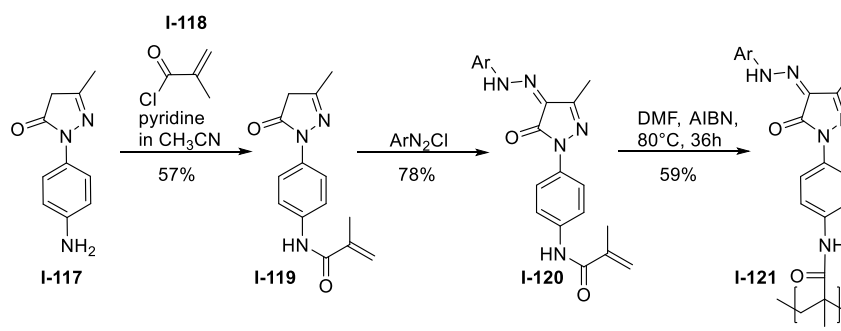
Scheme 36: Synthesis of hydrazone-pyrazolone polymer **I-121**.

Free radical polymerization was utilized for the synthesis of the polymers, similar to Inukai's approach. However, the resulting polymers had higher molecular weights and yields (Table 5), ranging from 87-99% as orange solids. This significant improvement in both yield and molecular weight indicates a promising route for the practical application of these polymers (Scheme 37).
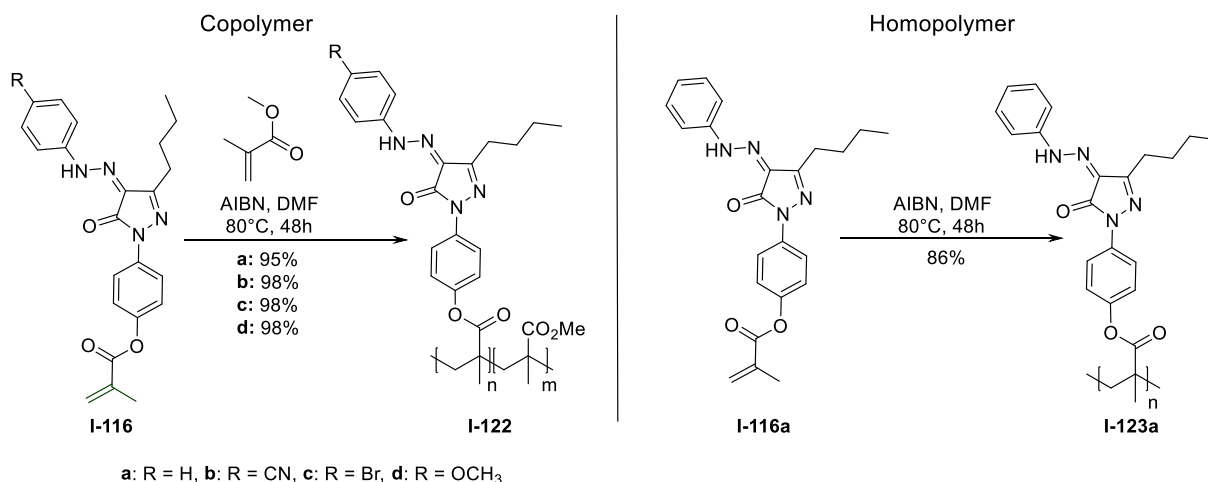
Scheme 37: Synthesis of hydrazone-pyrazolone functionalized methacrylic ester polymers.

The synthesized polymers underwent characterization using various techniques, including ^{1}H NMR, GPC, UV-vis, and IR spectroscopy. The resulting data showed that the molecular weight of polymer **I-122a-d** ranged from 35 000-120 000 g/mol, with a Đ range of 1.2-1.7 (Table 5). The homopolymer **I-123a** had a molecular weight of 41 000 g/mol and a Đ of 1.7. These values are significantly higher compared to the homopolymer **I-121** synthesized by Inukai, which had a molecular weight of only

5 100 g/mol and a Đ of 1.2 (Scheme 36 and Table 5). In conclusion, these results indicate that our approach provides a promising pathway for synthesizing high molecular weight polymers.

Table 5: Results of radical polymerization of 10 % methacrylic monomers in DMF at 80°C.

Polymer	$(n/m)_0$ [a]	$(n/m)_{obs}$ [b]	M_n [c] [g/mol]	Đ [c]	T_g [d] [°C]	T_m [d] [°C]	Yield (%)
I-122a	1:3	1:2	94 000	1.4	151	244	95
I-122b	1:3	1:4	100 000	1.3	142	268	98
I-122c	1:3	1:4	35 000	1.7	133	253	98
\I-122d	1:3	1:3	120 000	1.2	154	238	98
I-123a	-	-	41 000	1.7	80	251	86
I-121	-	-	5 100	1.2	-	-	59

[a] Molar ratio of monomers; [b] n/m stoichiometry in the copolymer as determined from ^{1}H-NMR integration; [c] Measured by GPC with linear poly(methyl methacrylate) standards (M_n 800–2 200 000 g/mol); [d] Measured by DSC.

In previous studies, hydrazono-pyrazolone polymers **I-108a** were investigated for their potential to exhibit anion sensing properties and pH-activated switching. The same investigation for new polymer **I-122a** was performed. The UV-Vis spectra of polymer **I-122a** displayed a single absorption maximum at 400 nm in DMSO at a pH of 8.5. Gradual addition of CsOH·H_2O to the solution resulted in an increase in pH to 14 and a color change from light yellow to dark yellow. This led to a significant bathochromic shift from 400 to 430 nm, as shown in Figure 15a. Additionally, two new isosbestic points at 355 nm and 397 nm were observed in the UV-Vis spectra (Figure 15a). Upon subsequent addition of HCl solution to decrease the pH value from 14 to 3.2, the absorption peak at 430 nm was reversed to the initial absorption maximum at 400 nm (Figure 15a). These results indicate that polymer **I-122a** can switch tautomeric forms in solution depending on the pH value, similar to previous experiments with hydrazone-pyrazolone methacrylic polymers.

Additionally, the anion sensing properties of polymer **I-122a** were investigated, and it was found that the polymer could detect anions. Specifically, when the polymer was titrated with a solution of tetrabutylammoniumfluoride (F⁻), a bathochromic shift from the maximum at 400 nm to 435 nm was observed, along with two new isosbestic points at 350 nm and 402 nm and two new absorption peaks at 345 nm

and 435 nm (Figure 16). The color of the solution also changed from light yellow to dark yellow. Therefore, **I-122a** can detect F⁻ anion, similar to the properties observed in previous polymers **I-108a-e.**
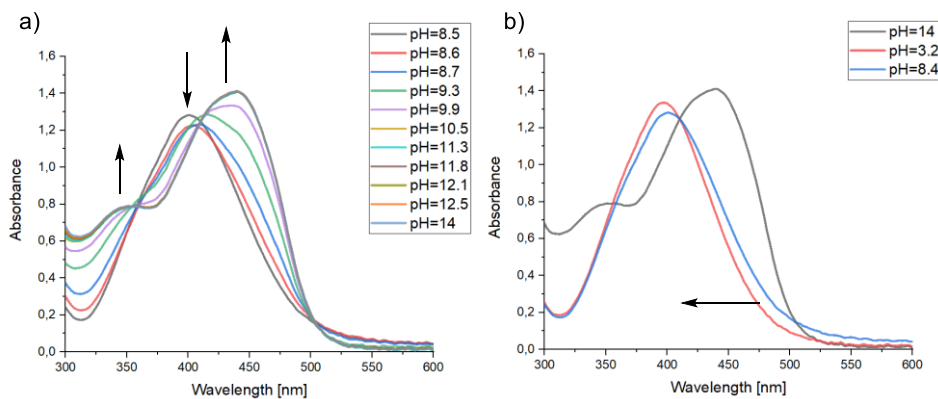
Figure 15: Changes in the UV-Vis spectra and pH value of **I-122a** (1×10^{-5} M) a) during titration by CsOH in DMSO; b) after adding HCl in DMSO.
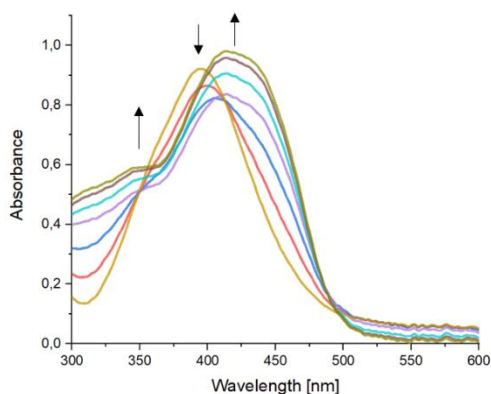
Figure 16: Changes in the UV-Vis spectra for the **I-122a** (1×10^{-5} M) in the absence and presence of fluoride anion in DMSO solution.

I.5 Conclusion

In summary, eleven new polymers containing a hydrazone-pyrazolone moiety were successfully synthesized and characterized with high molecular weight and yield. Thin films of these polymeric dyes were prepared, and their surface morphology was studied using AFM. The RMS roughness of the thin films ranged from 0.174 to 0.223 nm (**108a-108d**) and 1.36 nm (**108e**). Linear optical studies were conducted, including transmission and maximum absorption coefficient (a), which were in the range of 388-395 nm. Refractive index (n) of all samples in the thin films was studied

in the region of 450 nm, confirming the chromogenic nature of these materials. The polymers can exist in two tautomeric forms depending on the pH of the medium, indicating potential applications as acid-base indicators or anion detectors. Various inorganic and organic anions, including F^-, $H_2PO_4^-$, CrO_4^-, WO_4^-, tetrabutylammonium acetate, sodium ascorbate, sodium-L-glutamate-monohydrate, sodium edetate, thymidine 5'-monophosphate disodium salt, L-(+) tartaric acid disodium salt, and adenosine monophosphate (AMP) were detected with favorable selectivity for AMP compared to ADP and ATP anions. Overall, these polymeric dyes are cost-effective and have potential for widespread applications in materials science as detectors of anions and pH-switchers with high thermal, air, and light stability.

I.6 Rubazonic acid as a promising material

Rubazonic acid **I-124** is a symmetrical molecule with strong dyeing properties that were first reported by Ludwig Knorr in the 1880s (**Scheme 38**) [100]. Despite this early discovery, the molecule did not receive much research interest during the 20th century, leaving only a few known synthesis methods and applications for rubazonic acid. This lack of attention presents a challenge for new discoveries in the field of materials science and engineering. The rubazonic acid has great potential as a promising organic dye. Another promising approach is to integrate rubazonic acid into the polymer chain, providing a new potential aspect for their application.

I-124
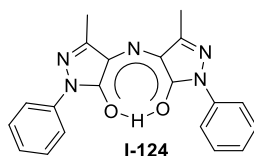
Scheme 38: The structure of rubazonic acid.

It is known that rubazonic acid can exist in three tautomer forms in solution: imine (**I-125**), lactam (**I-126**) or enol (**I-127**) depending on the pH value of the solution (as shown in **Scheme 39a**). These changes can be observed through UV-vis measurements. My Linh Tong and co-workers [101], have conducted a UV-vis titration study of rubazonic acid at different pH values. As shown in **Scheme 39b**, changes in the pH value can shift the absorption maximum. Acidification of rubazonic acid leads to an absorption maximum around 450 nm, resulting in an orange-colored solution. At a pH of 5-6, the absorption maxima shift to 540 and 340 nm, and the color of the solution changes from orange to purple. Furthermore, they studied the effect of solvents on rubazonic acid intermolecular bonding. The dielectric constant and hydrogen bonding capacity of solvents can have the influence on the intramolecular hydrogen bond of rubazonic acid and, consequently, the color of the dye. As shown in **Scheme 39c**, nonpolar and protic solvents result in an absorption maximum at around 450 nm. Whereas in aprotic polar solvents, a solvatochromic effect is observed, resulting in an absorption maximum at around 550 nm.
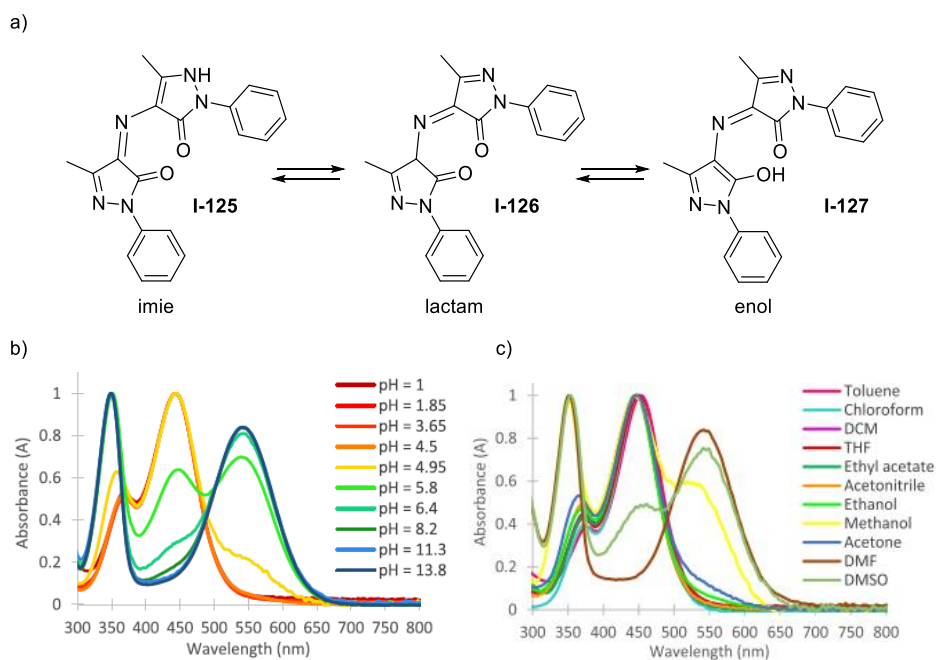
Scheme 39: a) three possible tautomer forms of rubazonic acid, b) UV/vis absorption spectra of rubazonic acid under different pH value, c) UV/vis absorption spectra of rubazonic acid in different solvent [101].

Ludwig Knorr synthesized rubazonic acid while studying pyrazolone derivatives and reported three methods for its synthesis. The first method involves reducing nitrosopyrazolone **I-128** with zinc and acetic acid to aminophenylmethylpyrazolone, and then oxidizing it with iron chloride to form rubazonic acid **I-129** (as shown in Scheme 40a). Additionally, Knorr described another method that involves reacting nitrosopyrazolone **I-128** with sodium methoxide and methyl iodide to synthesize rubazonic acid **I-129** (as shown in Scheme 40b). Rubazonic acid **I-129** can also be synthesized by refluxing pyrazole blue **I-130** in an aqueous solution of ammonia (as shown in Scheme 40c). Hänsel later modified Knorr's synthesis, replacing iron (III) chloride with hydrogen peroxide as the oxidizing agent [102].
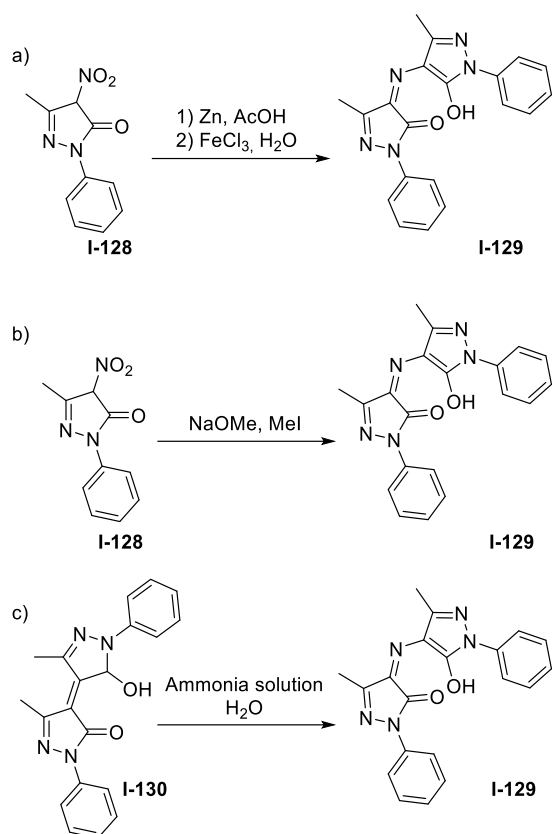
Scheme 40: The rubazonic acid synthesis.

Modern methods for synthesizing rubazonic acid using pyrazolones, with the synthesis methods for pyrazolone being described in the first chapter.

Cerchiaro's group proposed a synthesis method for rubazonic acid **I-132** from 3-methyl-1-phenyl-1H-pyrazole-5(4H)-one **I-131** using methanesulfonyl azide and potassium carbonate in methanol (as shown in Scheme 41). The presence of methanol is crucial for synthesizing rubazonic acid derivatives, as chloroform can result in the formation of diazopyrazolone [103].
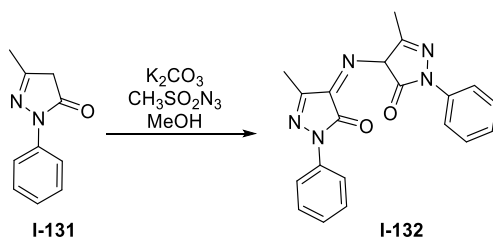
Scheme 41: The synthesis of rubazonic acid from 3-methyl-1-phenyl-1H-pyrazole-5 (4H)-one.

Erkin and Krutikov synthesized rubazonic acid derivatives by reacting 5-hydroxy-3-methyl-1-(6-methyl-2-methylsulfanylpyrimidin-4-yl)pyrazole **I-133** with an aqueous solution of sodium nitrite at 25 °C in diluted acetic acid. They obtained poorly soluble rubazonic acid **II-134** with a yield of 18%, as shown in Scheme 42 [104].
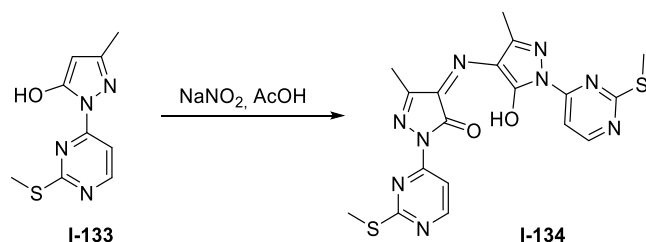
Scheme 42: The synthesis of rubazonic acid derivatives from 5-hydroxy-3-methyl-1-(6-methyl-2-methylsulfanylpyrimidin-4-yl)pyrazole**.**

Recent studies on the synthesis of rubazonic acid derivatives have been conducted by My Linh Tong and co-workers [101]. They proposed a method for preparing rubazonic acid by reacting pyrazolone **I-135** with iodine (2.2 equiv) and sodium azide (6 equiv) in DMSO at room temperature for 1 hour, followed by the addition of a saturated aqueous solution of sodium thiosulfate to form products with yields of 19-88%, as shown in Scheme 43.
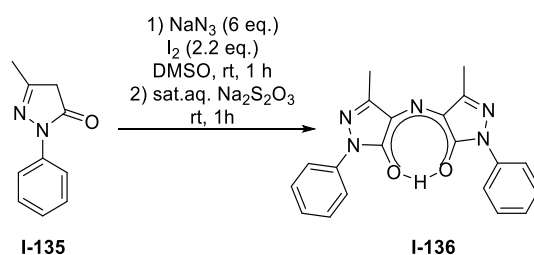
Scheme 43: The synthesis of rubazonic acid derivatives described My Linh Tong. [101]

I.6.1. Applications of rubazonic acid

Rubazonic acid and its derivatives have several different applications. It can be useful as an analytical agent for ammonia determination; this method was first described by Kala [105]. Ballot and co-workers later introduced this method for the

determination of blood ammonia. The great advantage of the proposed method is its high sensitivity and long-term color stability after the determination of ammonia [106]. Additionally, S. E. Sheppard and Wright proposed the use of rubazonic acid in color photography applications [107].

I.6.2 Polymers from alkynes

Conjugated polymers (CPs) from alkenes can be synthesized in various ways (as shown on

Scheme 44). For instance, polymers with repeating units linked by triple bonds can be synthesized through Glaser-Hay and Sonogashira polycoupling. Double-bonded CPs are synthesized through decarbonylative polyaddition, hydrothiolation, hydrosilylation, and polyaromatics generated by polycyclization. Heterocycles, such as polytriazoles from click polymerization and polythiophenes from tandem polymerization, are also possible [108].
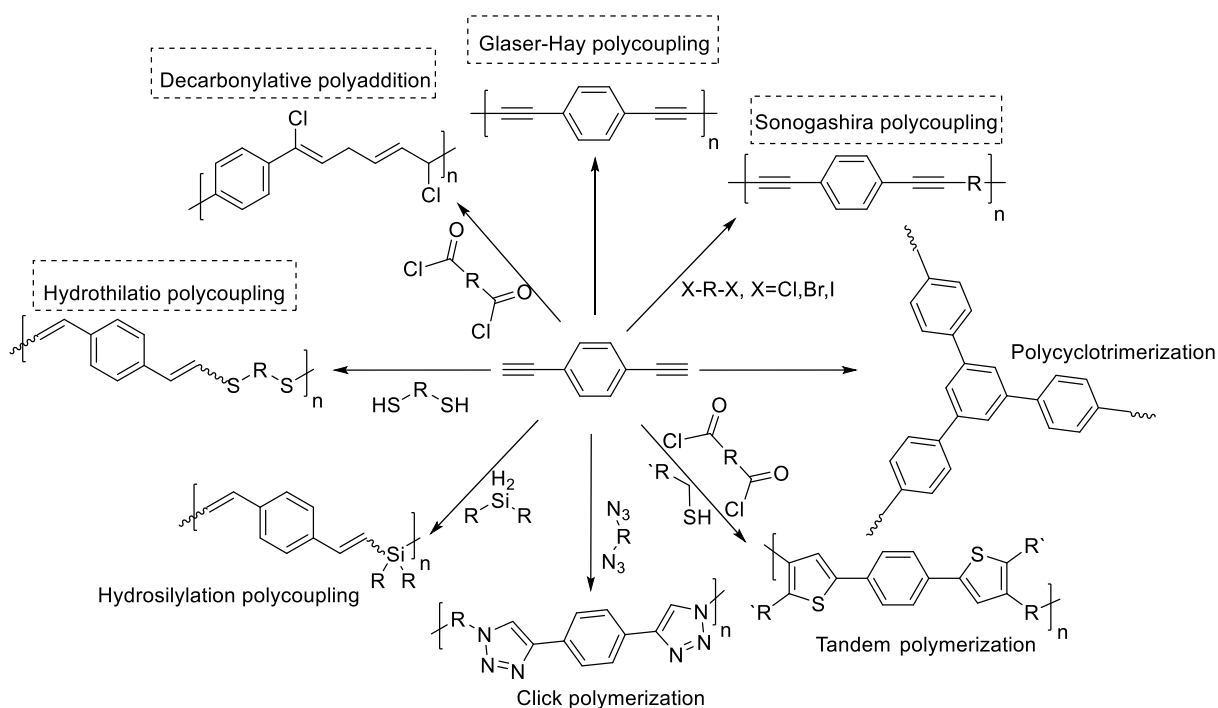
Scheme 44: Synthetic routes to conjugated polymers based on alkynes.

The Sonogashira cross-coupling reaction is a widely used sp^2-sp carbon-carbon bond formation reaction in organic synthesis, involving the coupling of aryl or vinyl

halides with terminal acetylenes catalyzed by palladium and other transition metals [109]. The reaction was first described in 1975 by Sonogashira, Tohda, and Hagihara [110][111]. The reaction conditions are typically mild and conducted at room temperature, and can tolerate various functional groups, such as esters, polypeptides, and even sugars. To carry out the reaction, a palladium source, such as PdCl₂(PPh₃)₂ or Pd(PPh₃)₄, is used as a catalyst, in combination with a co-catalytic amount of CuI and a stoichiometric base to deprotonate the terminal alkyne. Amine bases, such as triethylamine, diisopropylamine, or piperidine, are commonly used, and sometimes serve as the solvent (as shown in **Scheme 45**) [112]. Among the organic solvents, THF is the best solvent for the Sonogashira reaction, as it enhances catalytic activity and reduces sensitivity to oxygen and water. The Sonogashira reaction is also used for the synthesis of polymers [113]. Sonogashira polycoupling is highly efficient in terms of technical simplicity and tolerance to numerous functional groups. However, there are three disadvantages to using this reaction for polymer synthesis: diyne defects cannot be prevented, polymer end groups are poorly defined, and obtaining polymers with high molecular weights is challenging.
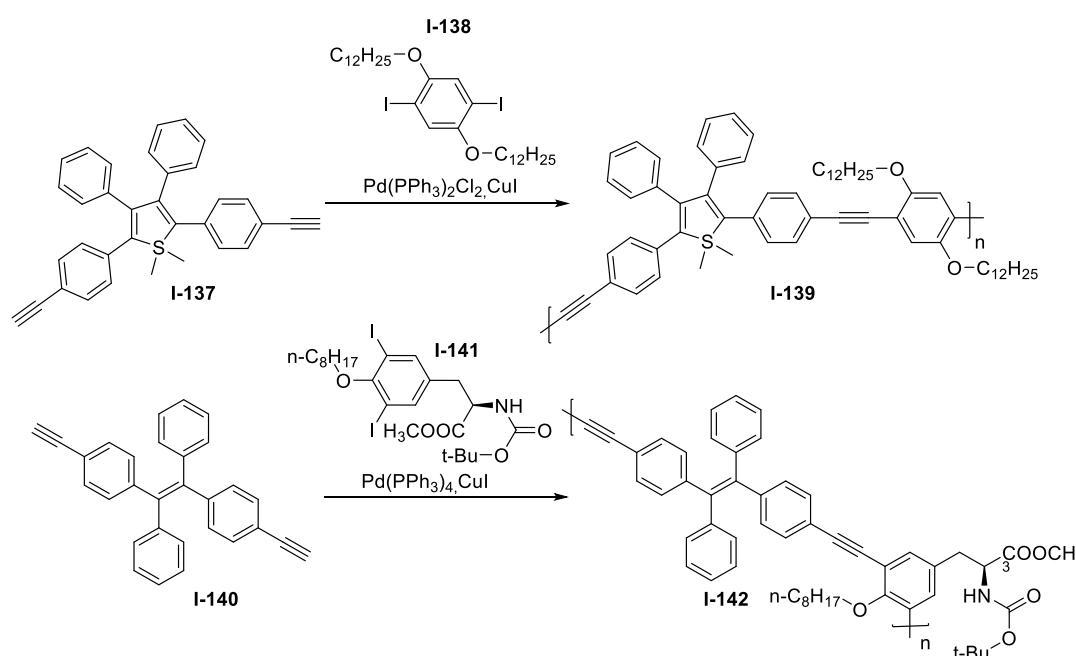
Scheme 45: Sonogashira polycondensation reaction.

Polymerization under Sonogashira conditions has a serious disadvantage: it is competitive oxidative homocoupling, which can occur either from copper-catalyzed

oxidation (Glaser-Hay coupling) or reduction of Pd(II) to Pd(0) by two ethynyls. The problem is that these parallel products end up in the chain. Thus, one must strive for a unique reaction leading to hetero conjugation to obtain well-defined conjugated polymers [114]. However, in some cases, this disadvantage can become an advantage, as will see in the results and discussions of this work.

The first acetylenic coupling was reported by Carl Glaser in 1869 while working at the University of Bonn. He observed that copper(I) phenyl acetylide exposed to air underwent smooth oxidative dimerization to diphenyl diacetylene [115][116]. Scheme 46 shows important dates and reactions for the Glaser couplings, who made a great contribution to the development in this direction.
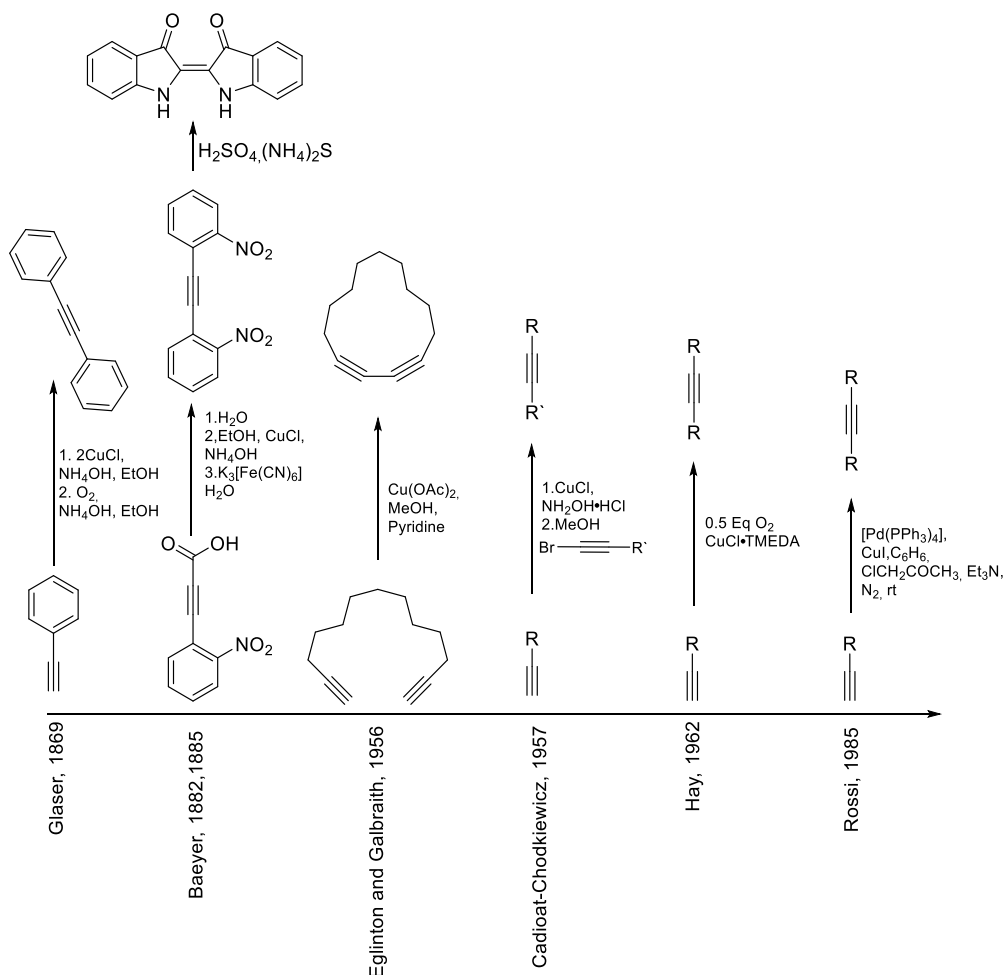
Scheme 46: The timeline for important Glaser reaction.

In 1882, Baeyer demonstrated the synthetic utility of oxidative acetylenic coupling in his synthesis of indigo, using potassium ferricyanide as the oxidizing agent and showing that dioxygen itself is not necessary for the coupling process [117]. Eglinton

and Galbraith introduced the copper(II) salt oxidation in methanolic pyridine in 1956 as a further evolution of oxidative acetylenic coupling [118]. They found that stoichiometric or excess $Cu(OAc)_2$ in methanolic pyridine could accelerate the dimerization of alkynes. In 1962 Hay [119] reported another important modification. He performed oxidative acetylenic couplings with O_2 in the presence of catalytic amounts of the bidentate ligand N,N,N',N'-tetramethylethylenediamine (TMEDA) and copper(I) chloride. Better solubility of the reactive species is one major advantage provided by this reaction.

The discovery of palladium-catalyzed coupling reactions more has initiated explosive growth in the field of organometallic chemistry. Which, of course, did not escape the Glaser coupling. An early observation of palladium-catalyzed coupling reactions was reported in 1975 by K. Sonogashira et al.[120] who described the formation of symmetric diynes via dialkynyl palladium intermediates during couplings between terminal alkynes and aryl or vinyl halides. In a few years, Rossi et al. [121] optimized this process as a homocoupling method for terminal acetylenes. They obtained diaryl- and dialkylbuta-1,3-diynes in moderate to good yields using chloroacetone as the oxidant and a mixture of $Pd(PPh_3)_4$ and CuI as the catalyst together with triethylamine. Additionally, Kim and co-workers [122] reported a 92% yield in the oxidative dimerization of an alkynylpyrrole **I-144** (Scheme 47).
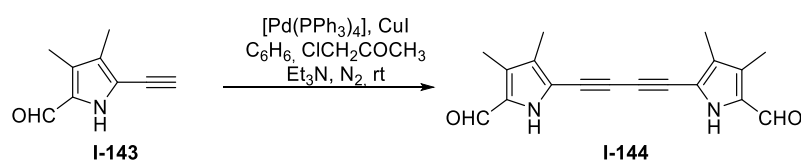
Scheme 47: The oxidative dimerization of an alkynylpyrrole.

The oxidative dimerization of alkynylpyrroles could offer an interesting alternative to the classical Glaser coupling, providing the possibility of controlling reaction conditions and potentially improving selectivity and yield.

Kundu et al.[123] reported the use of a mixture of $PdCl_2(PPh_3)_2$ and CuI as the catalyst in the presence of diisopropylamine, while either 4-iodo-2-nitro-resorcinol or dimethyl sulfoxide served as the oxidant, and found that the reaction proceeded in the absence of CuI, but the absence of the palladium catalyst almost completely suppressed the coupling process.

Kijima and co-workers proposed the use of Pd(PPh3)4, CuI, THF, Et3N, and I2 as the oxidant for the polycondensation of acetylene. In the same year, Burton and Liu reported the synthesis of diynes **I-146** using two different conditions, one involved Pd(PPh3)2Cl2, CuI, and i-Pr2NH, and the other with the addition of I2 to the reaction mixture (Scheme 48). The introduction of I2 improved the yield from 27% till 88%, and the proposed mechanism for the reaction was also discussed [124].
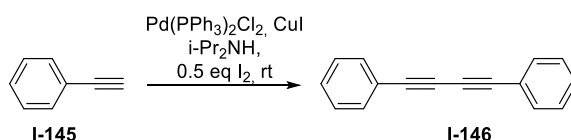
Scheme 48: The synthesis of diynes by Burton and Liu conditions.

They rationalized that the diynes were synthesized via reductive-elimination from bis(triphenylphosphine) dialkynylpalladium, which was derived from 1-alkyne and Pd(PPh3)2Cl2 in the presence of CuI and amine. This reductive-elimination also generates the active palladium(0) species, Pd(PPh3)2. They used I2 to regenerate the Pd(II) catalyst from the Pd(0) formed in the catalytic cycle. The recurrent formation of bis(triphenylphosphine) dialkynylpalladium and subsequent reductive-elimination eventually converts all the 1-alkyne to the corresponding diyne (Scheme 49) [124].
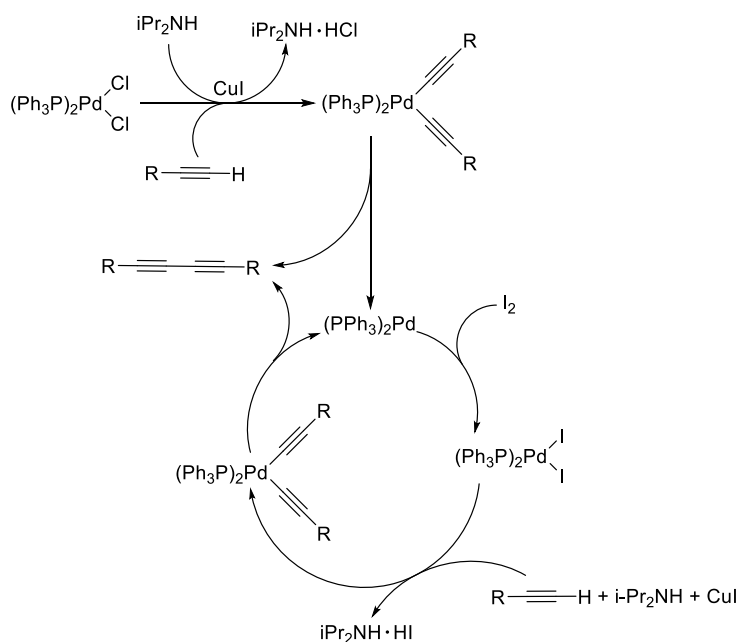
Scheme 49: Mechanism of diynes formation [124].

In addition to I₂ as an oxidative additive, it is possible to use p-benzoquinoline. Williams and Swager described homocoupling and copolymer formation by using Pd(PPh₃)₄, CuI, i-Pr₂NH, benzoquinoline, and toluene (**Scheme 50**). They synthesized two homopolymers **I-148** and a copolymer with Mn ranging from 3 800 till 154 000 g/mol and Đ ranging from 1.9 to 5.2 [125].
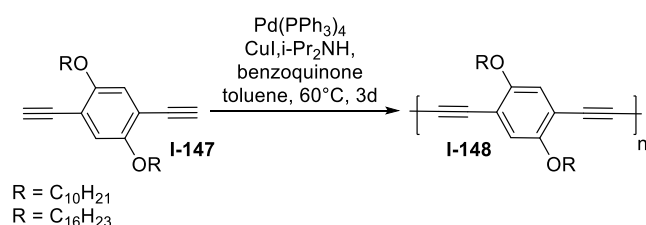
Scheme 50: Synthesis of homopolymers.

This study highlights the potential of using different oxidative additives to improve the yield and selectivity of the acetylenic coupling reaction. Overall, the development of various catalytic systems and oxidative additives has greatly expanded the scope of the Glaser coupling reaction, allowing for the synthesis of a wide range of conjugated polymers with different properties for various applications.

Monomers based on alkynes have the ability to form polymers with both triple and double bonds (C=C) along the chains. Conductive polymers (CPs) containing double bonds exhibit better conjugation and higher rigidity than those with triple bonds due to the significant delocalization of π-orbitals and steric hindrance caused by vinyl substituents. The polyaddition of triple bonds to nucleophiles are an effective approach to obtain functional vinylene polymers, which is generally atom-economical and tolerant of functional groups [126].

Facile methods such as decarbonylative polyconjugation, polyhydrothiolation, and others can be used to construct conjugated chain with heteroatoms (Scheme 44). Linear poly(arylene chlorovinylene) can be synthesized through the rhodium-catalyzed decarbonylative polyaddition of aromatic diynes, with the catalyst playing a crucial role in determining the structure of the resulting polymer. This method exhibits excellent regio- and stereoselectivity, leading to high molecular weight and thermal stability of the resulting polymers [127].

Thiol-yne click polymerization is a valuable tool for constructing regio- and stereoselective sulfur-enriched polymers, and has gained significant attention in recent years. Poly(vinylene sulfides) (PVS) can be synthesized in a facile and atom-economical manner by starting with aromatic dienes and dithiols under mild conditions. The construction of PVSs involves dienes and 4,4`-thiodibenzenethiol in the presence of a catalytic amount of Rh(PPh$_3$)Cl at room temperature [128] [129]. In addition to using transition metals as catalysts, the thiol-yne click reaction can also be induced by heat, UV irradiation, and organic substances. Moreover, thiol-ene polymerization without a catalyst is also possible. PVS can be obtained in high yield (78-97%) under mild reaction conditions in tetrahydrofuran at 30 °C for 2 hours [130].

I.7 Results and discussion

Rubazonic acid is an attractive compound with significant interest for its potential applications in materials. Nevertheless, further in-depth research is essential to fully explore its range of capabilities. In this work, a series of new derivatives and polymers based on rubazonic acid were synthesized to further explore for their potential applications. The cross-coupling, polycondensation, click reaction, and nucleophilic substitution methods were used to promote this material in future applications.

The primary focus was on the synthesis of new conjugated polymers that could result in novel, processable polymeric materials with unique electrical, electrochemical, and optical properties. Different coupling methods, including Suzuki, Stille, Yamamoto, Sonagashira, and Glaser, were employed, along with decarbonylative polyconjugation, polyhydrothiolation, and nucleophilic substitution, for the polymerization of rubazonic acid copolymers. Initially, the study focused on developing a new polymer based on polyfluorene linked with rubazonic acid. The retrosynthetic scheme for synthesizing polyfluorene derivatives was presented in Scheme 51. Synthesizing the rubazonic acid monomer **I-150** required obtaining the pyrazolone **I-157** from the ketoester **I-152** and hydrazine **I-153**. In addition to the rubazonic acid monomer for cross-coupling, fluorene monomers **I-154** were also used.
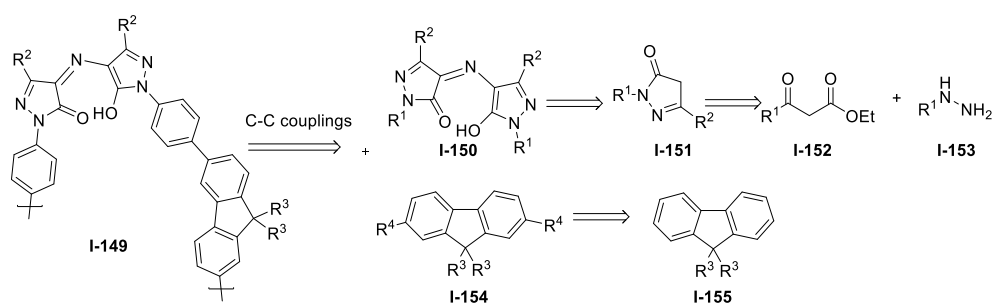
Scheme 51: Retrosynthetic scheme of polyfluorene derivatives synthesis.

The study of rubazonic acids and their reactivity start from the synthesis of rubazonic acids and monomers based on them, followed by the polymerization of these monomers to form novel polymeric materials. This research has the potential to contribute significantly to the field of materials science and engineering, particularly in the development of new materials with unique properties and potential applications.

I.7.1.1 Synthesis of new rubazonic acid derivatives

Rubazonic acid has low solubility, that limit practical using. To solve this problem, β-ketoesters with long alkyl chains such as methyl 3-oxononanoate **I-157** and ethyl 3-oxoundecanoate **I-160** were synthesizedThese compounds have been shown to increase the solubility of rubazonic acid.

Methyl-3-oxononanoate was synthesized via a reaction between methyl 3-oxobutanoate **I-156** and 1-bromopentane, as shown on Scheme 52. Instead of using an LDA solution, the mixture of NaH and n-BuLi in THF were used. The sodium hydride acted as a base, removing a proton from the alpha position of the carbonyl compound to generate the enolate, which was stabilized by THF. The addition of butyllithium converted the enolate to a more nucleophilic lithium enolate. This intermediate then underwent nucleophilic attack on the electrophilic center of the alkyl halide, yielding the final product with a 40% of yield.
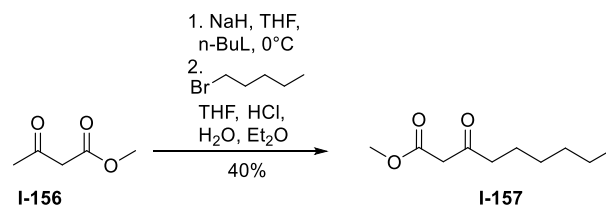
Scheme 52: Synthesis of ethyl-3-oxononanoate **I-157.**

The ethyl-3-oxoundecanoate was synthesized via reaction with ethyl potassium malonate (**I-158)** with the corresponding acid chloride in the presence of magnesium chloride ($MgCl_2$), triethylamine (Et_3N), and acetonitrile (CH_3CN) as the solvent (as shown in Scheme 53). This method give possibility to obtain product high purity.
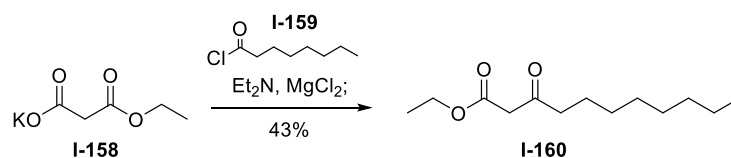
Scheme 53: Synthesis of ethyl-3-oxoundecanoate.

Furthermore, one hydrazine compound was synthesized. The hydrazine compound with four fluorine substituents, **I-162**, was synthesized in the meta and ortho positions of the benzyl ring to enhance its solubility. The hydrazine was prepared by substituting the aromatic halides with nitrogen nucleophiles derived from 1,2,3,4,5-pentafluorobenzene (**I-161**), as shown on Scheme 54.
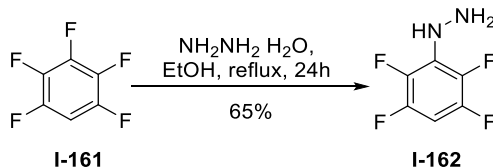
Scheme 54: Synthesis of 2,3,5,6-tetrafluorophenylhydrazine **I-162**.

Pyrazolones **I-165** were synthesized by two different methods, reflux and microwave synthesis. The keto form of pyrazolone was synthesized through the reflux method, as confirmed by NMR and IR analysis, while the enol form was obtained through

microwave synthesis. The cyclization of hydrazine **I-164** with β-ketoesters **I-163** was used to form pyrazolones, and a method involving the reaction of hydrazine with β-ketoesters in an ethanol-water solution in the presence of NaOAc under reflux was proposed. During this study, nine different derivatives **I-166 - I-171** were synthesized with yield in the range 33%-82%, as shown on Scheme 55.

R^1= CH_3, C_2H_6
R^2= CH_3 (a), C_4H_9 (b), C_6H_{13} (c), C_8H_{17} (d)
R^3= H, F; R^4=H,F
R^5= H, Cl, Br, OH, CN

I-166b
51%

I-167b
59%

I-168a,c,d
a:42%; c:41%; d:40%.

I-169b
82%

I-170b,d
b:33%; d:12%

I-171b
60%
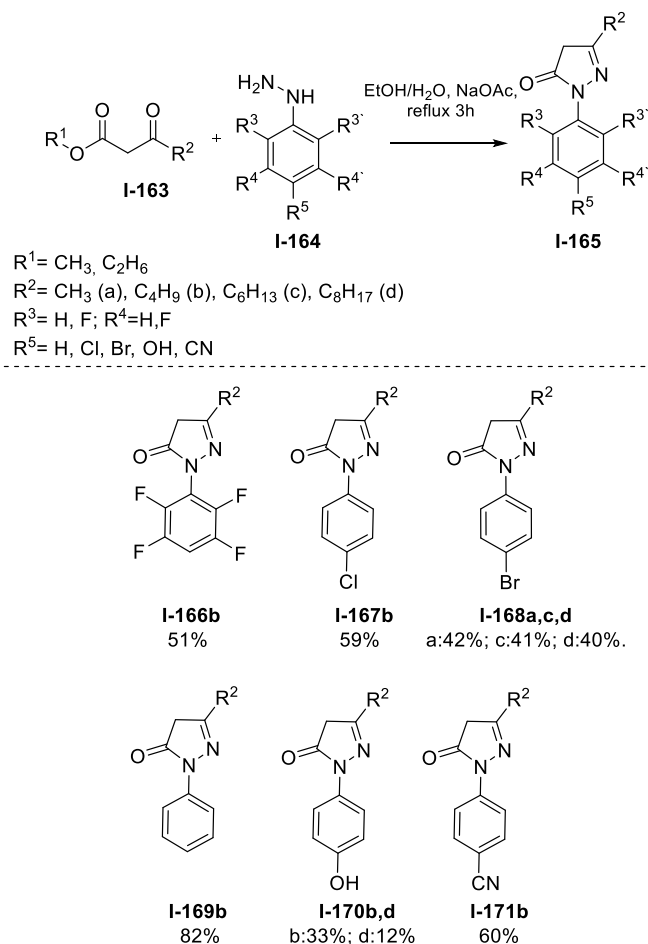
Scheme 55: The cyclization of hydrazine with β-ketoesters.

The second method for synthesizing pyrazolone **I-173** is a solvent-free microwave approach. Hydrazine **I-111** and β-ketoesters **I-172** were transferred into a flask with a magnetic stirrer for the microwave (MW) reaction under N_2 due to the air instability of phenylhydrazine. The reaction is carried out at a temperature of 50 °C for 5 minutes (Scheme 56). This method is easy to execute and cost-effective, but a drawback is the formation of pyrazolone in the enol form, as confirmed by NMR and IR analysis. While this method can be an excellent alternative for future synthesis. It was determined that the keto form of pyrazolone would be preferable over the enol

form, as it addresses solubility issues and minimizes the potential for competitive reactions.
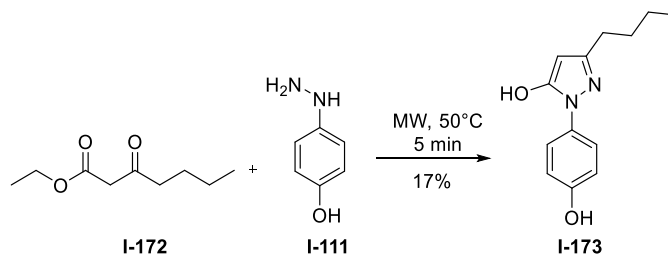
Scheme 56: The cyclization of hydrazine with β-ketoesters by MW activation.

All pyrazolone derivatives were tested for the synthesis of rubazonic acid **I-174**. My Linh Tong and Stefan F. Kirsch reported [101] a convenient and effective method for synthesizing rubazonic acids, this condition was used to synthesis rubazonic acid in this work. For the reaction, portions of iodine (2.2 eq.) and sodium azide (6 eq.) were added to a solution of pyrazolone in DMSO and stirred at room temperature. After 90 minutes, a saturated aqueous sodium thiosulfate solution was added to the mixture and stirred for an additional 60 minutes. The rubazonic acid derivatives were obtained as red solids with yield range 41%-62%, as shown in Scheme 57. As expected, rubazonic acids with extended alkyl chains showed better solubility compared to rubazonic acids with methyl or butyl groups. Furthermore, the presence of fluorine in the benzene ring considerably increased the solubility of rubazonic acid.

R^1= CH$_3$, C$_2$H$_6$
R^2= CH$_3$ (a), C$_4$H$_9$ (b), C$_6$H$_{13}$ (c), C$_8$H$_{17}$ (d)
R^3= H, F; R^4=H,F
R^5= H, Cl, Br, OH, CN

I-175b
41%

I-176b
51%

I-177a,c,d
a: 56%; c:40%; d: 63%

I-178b
43%

I-179b
53%

I-180b,d
b:62%; d:17%
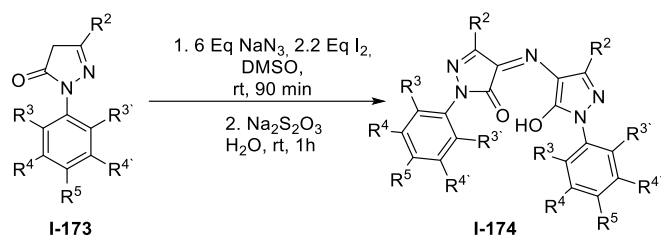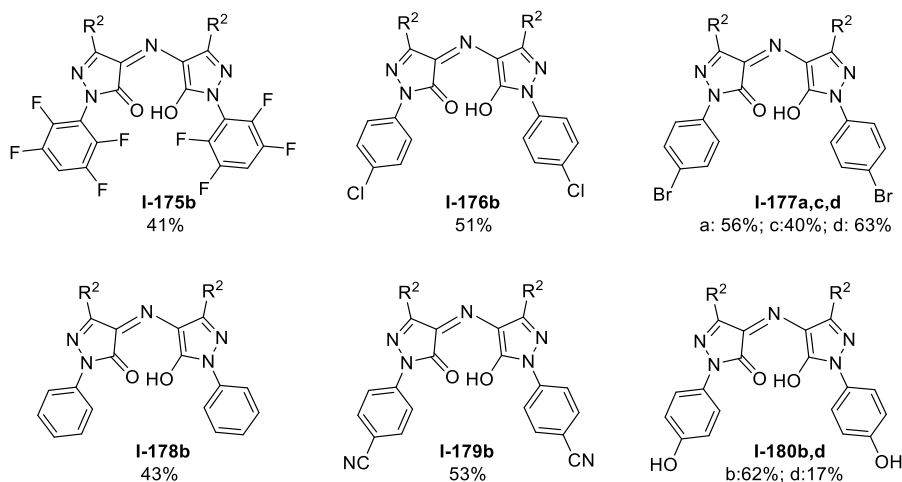
Scheme 57: The synthesis of rubazonic acid derivatives.

Rubazonic acid can also be synthesized from hydrazone pyrazolone derivatives **I-106a-b**, which were previously synthesized and can be found on page 23, Scheme 32(c). The synthesis of rubazonic acids **I-181a-b** was carried out using a previously described procedure (Scheme 58).

R^1=Br (a), CN (b)
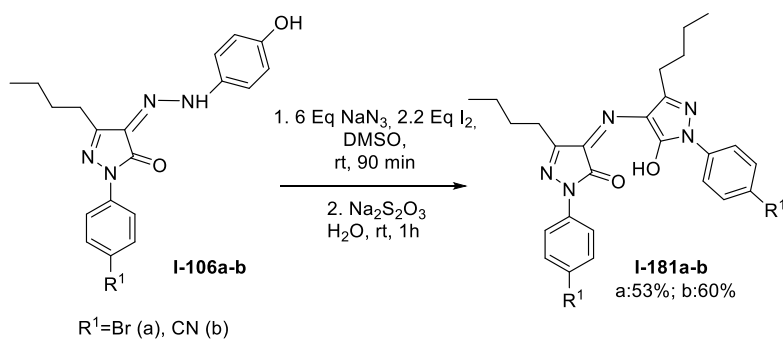
Scheme 58: The synthesis of rubazonic acid from hydrazone pyrazolone derivatives.

61

Rubazonic acid was successfully synthesized from hydrazone-pyrazolone derivatives with of 53% **I-181a** and 60% **I-181b** yields. The use of pyrazolone derivatives for the synthesis of rubazonic acid offers a new and simpler alternative strategy.

The subsequent step involved modifying rubazonic acid to monomers that could be used for polymer synthesis. The initial goal was to reduce the nitrile group in rubazonic acid **I-179b** to an amine using LiAlH$_4$ or by using hydrogen gas in the presence of Raney Ni in dry MeOH, but in both case reduction did not work. In addition, the Pinner reaction was attempted with the nitrile group **I-179b**. The Pinner reaction is a partial solvolysis of a nitrile that forms an iminoether. However, the desired product could not be obtained.

The rubazonic acid **I-180b** was reacted with propargyl bromide **I-182** in the presence of K$_2$CO$_3$ base and ethanol as the solvent. The compound **I-183** was synthesized 87% of yield under argon atmosphere, as shown on Scheme 59.
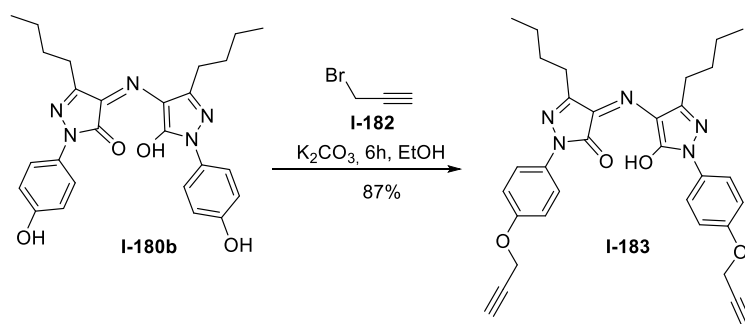
Scheme 59: Synthesis of rubazonic acid monomer **I-183**.

I.7.1.2 Optical and physical study of rubazonic acids

It is well-known that rubazonic acid can exist in three tautomeric forms in solution: imine (**I-125**) lactam (**I-126**) or enol (**I-127**) (Scheme 39a, page 46), depending on the pH value of the solution [131]. During the investigation, the tautomeric properties of rubazonic acid were studied.
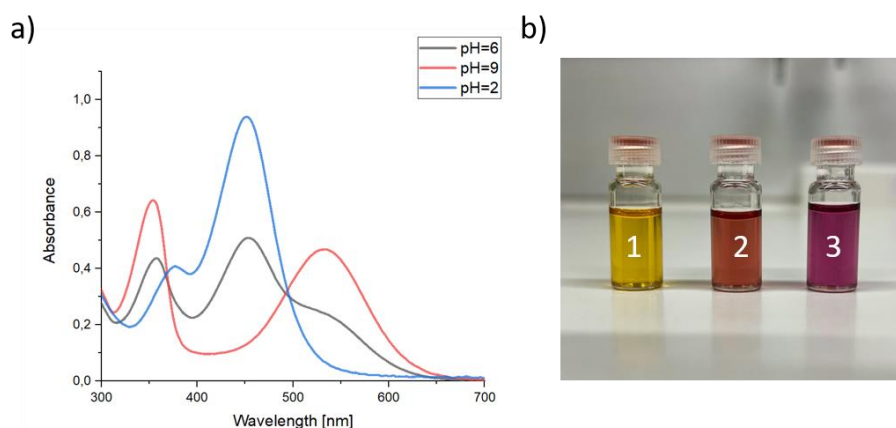
Figure 17: a) changes in the UV-Vis spectra and pH value of **I-183** (1×10^{-5} M) in DMSO solution during adding CsOH·H_2O (pH=9) and HCl solution (pH=2).
b) color changes of **I-183** (1×10^{-5} M) in DMSO solution pH=2 (1), pH=6 (2), pH=9 (3).

The rubazonic acid monomer **I-183** has two absorption maxima at 350 nm and 450 nm and shoulder at 540 nm in DMSO, pH 6. The pH value of rubazonic acid monomer **I-183** in DMSO was increased to 9 by adding a 0.01 M CsOH·H_2O solution. This caused a significant shift in the absorption peak from 355 nm to 376 nm, and a more intense peak at 450 nm was observed. The solution also underwent a color change from dark orange (2) to purple (3), as shown on Figure 17. After completing the titration, two isosbestic points were observed in the UV-Vis spectra at 366 nm and 496 nm (Figure 17a). On the other hand, decreasing the pH value from 9 to 2 by adding HCl solution reversed the absorption peak at 366 nm back to the initial absorption maximum at 376 nm and shifted the absorption maximum from 533 nm to 496 nm (Figure 17a). Two isosbestic points were observed at 368 and 494 nm, and the solution changed color from purple (3) to yellow (2), as shown Figure 17b. These results suggest that **I-183** can switch tautomeric forms (Scheme 39a) in solution depending on the pH value.

Thin film technologies have advanced significantly over the last several decades, becoming one of the major components of electronic, medical, and energy-related industries [132]. Thin films can be used as freestanding structures for applications requiring enhanced surface interactions or coatings to achieve application-specific properties that are unattainable in the substrate material [133].

In this study, the formulation and investigation of thin films containing rubazonic acids were conducted. The glass substrates were carefully cleaned with solvent and ultrasonication. The spin-coating technique was used to make thin films of polymethylmethacrylate (PMMA) and rubazonic acids with controlled thickness.

The solution of 1,2-dichloroethane containing PMMA 100 g/l and rubazonic acids (**I-180b** (OH), **I-175b** (F), **I-179b** (CN), **I-177c** (Br)) 10 % w to PMMA coated on glass slides. The principle of deposition is based on a homogeneous spreading out of the solution on the rotating substrate with an angular speed of 1000 rpm during 60 s. Immediately after the deposition, the thin films were dried in vacuum at 35 °C for 5 h to eliminate any remaining solvent.
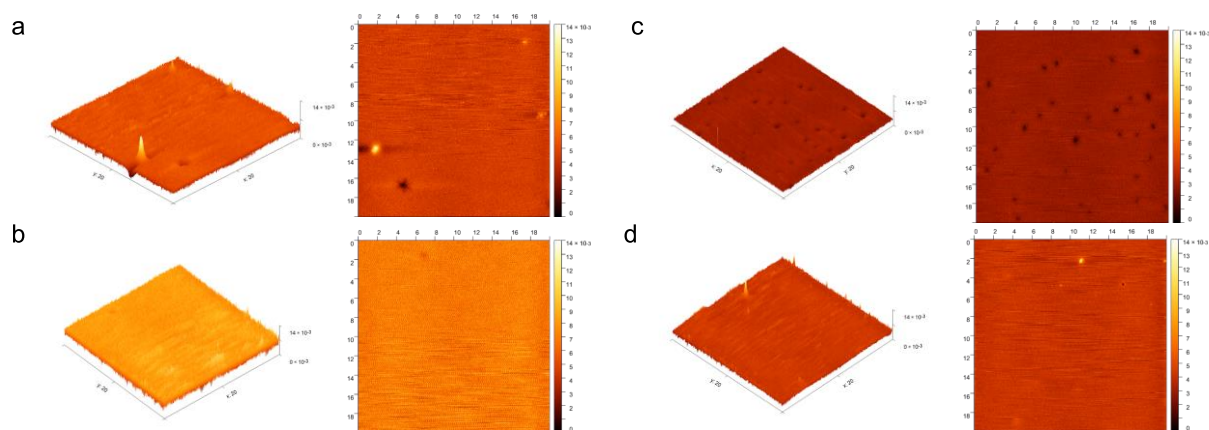
Figure 18: Two-dimensional (2D) and three-dimensional (3D) AFM images of thin films of dyes dispersed in PMMA containing various substituents, such as: a) **I-180b** (OH), b) **I-175b** (F), c) **I-179b** (CN), d) **I-177c** (Br).

Figure 18 presents an AFM image of thin films of rubazonic acid dyes dispersed in PMMA (**I-180b** (OH), **I-175b** (F), **I-179b** (CN), **I-177c** (Br)). The root-mean-square (rms) roughness, which specify the surface quality of the prepared layers, are 0.774 nm, 1.257 nm, 0.411 nm, 0.626 nm. Overall, the AFM measurements suggest that all four rubazonic acid dyes dispersed in PMMA thin films have good smoothness, and the microstructures appear uniform and continuous. The variations in rms roughness values may be attributed to the different physical-chemical properties of the derivatives.

The absorption spectra of thin films of dyes dispersed in PMMA containing various substituents, such as **I-180b** (OH), **I-175b** (F), **I-179b** (CN), and **I-177c** (Br), were measured using UV-vis spectroscopy. The guest-host systems with **I-180b** (OH) and **I-179b** (CN) exhibited significant absorption maxima at 380 and 457 nm, while the absorption maxima for **I-177c** (Br) were slightly shifted to 375 and 450 nm. The most significant difference was observed in the thin films containing rubazonic acid with **I-175b** (F), which exhibited two distinct absorption maxima at 306 and 470 nm (Figure 19a).

Additionally, the UV-vis absorption spectra of rubazonic acids were measured in THF. The **I-180b** (OH) and **I-177c** (Br) exhibited the same absorption maxima at 378 and 459 nm, respectively. The **I-179b** (CN) exhibited a small shift in absorption maxima to 360 and 478 nm. Notably, significant differences were observed in the solution containing rubazonic acid with **I-175b** (F), which exhibited two distinct absorption maxima at 335 and 478 nm (Figure 19b).

The differences in absorption maxima observed in the thin films and solutions of compounds with different substituents can be attributed to the varying electronic and steric effects of the substituents on the molecular structure of the compounds.
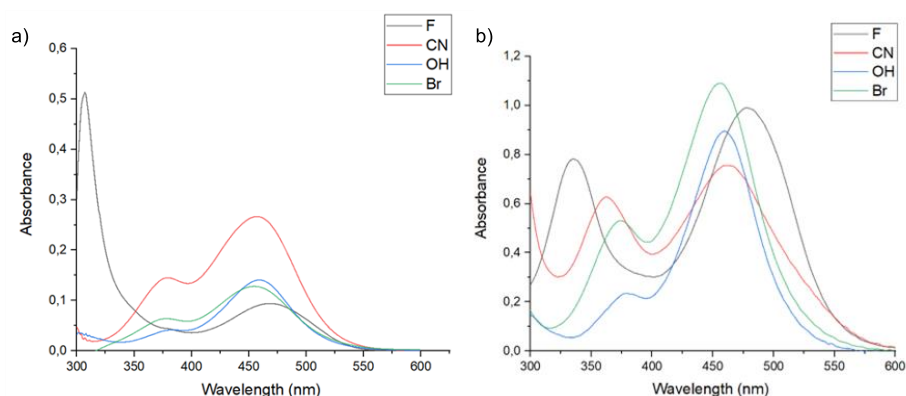
Figure 19: (a) UV-vis spectra of thin film of of rubazonic acid dyes (**I-180b** (OH), **I-175b** (F), **I-179b** (CN), **I-177c** (Br)) dispersed in PMMA; (b) UV-Vis spectra of I-**180b** (OH), **I-175b** (F), **I-179b** (CN), I-**177c** (Br) (1×10^{-5} M) in THF.

I.7.2.1 The synthesis of new rubazonic acid polymers via cross-coupling and polycondensation reactions

Polymers based on the rubazonic acid molecule were synthesized using a lengthy and thorough process that involved several couplings, nucleophilic substitution reactions, carbonylative polyaddition and hydrothiolation.

The initial goal of this study was to develop a new polymer by coupling fluorene with rubazonic acid via C-C bonds. Fluorenes are an important class of electroactive and photoactive materials. They are known for their emission at wavelengths spanning the visible spectrum, high fluorescence efficiency, and good thermal stability. The 9,9-Disubstituted poly(2,7-fluorene)s have been found to exhibit high photoluminescence and electroluminescence quantum efficiencies, as well as high electroluminescence brightness [134] [135].

The study of rubazonic acids reactivity start from the Suzuki coupling reaction (Scheme 60). The direction of research was chosen due to the reaction's theoretical simplicity, which gave us confidence in success. Several experiments were conducted to develop methods for coupling and polycondensation. Two different synthesis methods were used: one using a Schlenk flask and the other using microwave (MW) activation.

Table 6: The conditions of Suzuki coupling/polycondensation of **I-185/I-187** with **I-184** carried out in Schlenk (THF/H_2O) or microwave (dioxan//H_2O) under argon atmosphere (according to Scheme 60).

Method	Fluorene [eq]	Pyrazolone/ Rub. Acid $R^1=C_6H_{13}$ [eq]	Pyrazolone/ Rub. acid $R^1=C_8H_{17}$ [eq]	Pd° [eq]	K_2CO_3 [eq]	H_2O [ml]	Solvent [ml]	Time [h]	T [°C]
Schlenk	2.5		1	0.15	4	1.5	13.5	48	75
Schlenk	2.5		1	0.2	4	1.5	13.5	48	75
Schlenk	2.5		1	0.25	4	1.5	13.5	48	75
MW	0.5	1		0.1	2.5	0.5	4.5	2	110
MW	0.5	1		0.1	2.5	0.5	4.5	3	110
MW	0.5		1	0.2	2.5	0.5	4.5	2	110

The coupling and polycondensation were studied in parallel. For the reactions in Schlenk flasks, it was used commercially available 9,9-dioctylfluorene-2,7-diboronic acid bis(pinacol) ester (**I-184**) and bromo pyrazolones **I-185** or rubazonic acid **I-187** with different alkyl chains, along with $Pd(PPh_3)_4$ and K_2CO_3 as the catalytic system, and a mixture of THF and H_2O as the solvent (see Table 1). The reactions were conducted under an argon atmosphere at 75 °C for 48 hours. Unfortunately, no product formation was observed under different catalyst conditions during the Schlenk flask synthesis. However, it was known that the microwave method of synthesis could be an effective alternative, as it requires a smaller quantity of material and is faster. For this approach, the same catalysts were used, but the solvent mixture was changed to dioxane and H_2O. The reaction conditions were also modified (Two different synthesis methods were used: one using a Schlenk flask and the other using microwave (MW) activation.

Table 6). In the last attempt, no product formation was observed. It should be noted that $Pd(PPh_3)_4$ was commercially available and purified with cold methanol before use. The catalyst had a light-yellow color. Furthermore, the mixture of reactants in the solvent mixture was degassed with argon before adding the catalyst. Therefore, the bad quality of the catalyst can be excluded as a possible hindrance of the reactions.
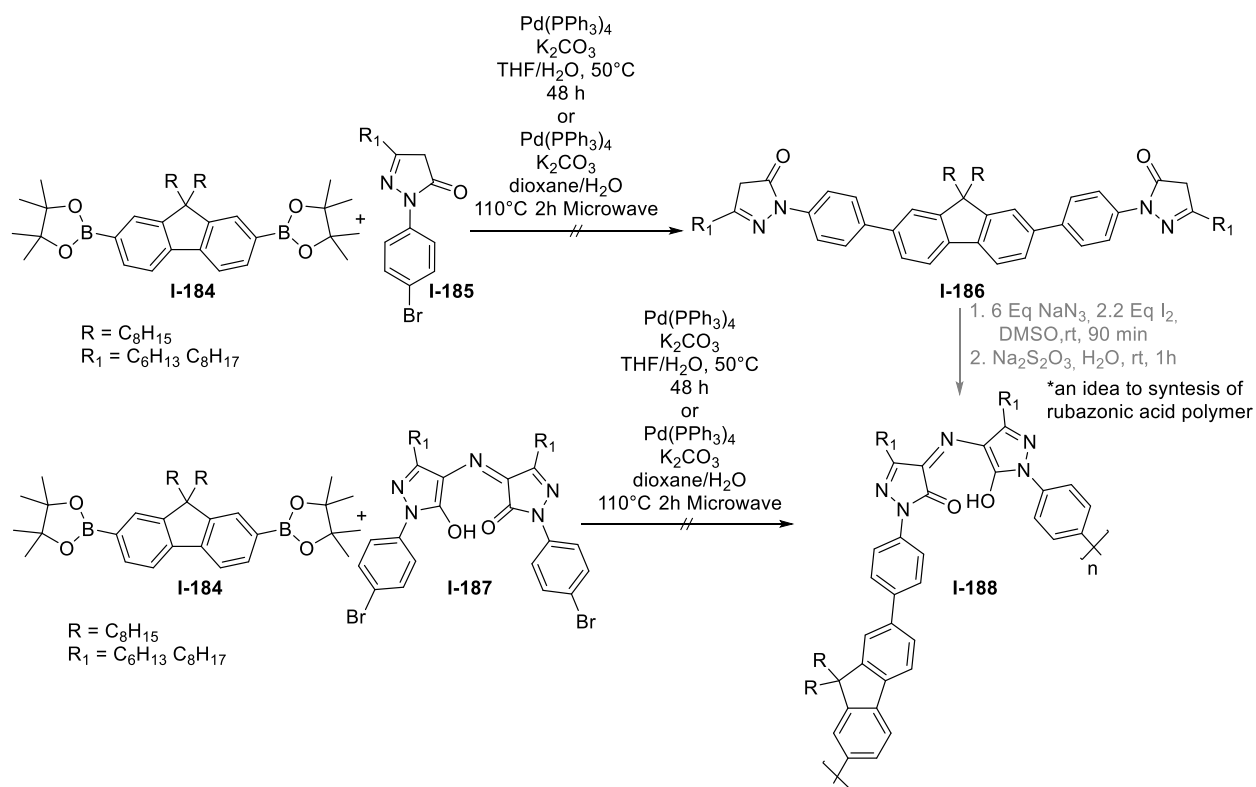
Scheme 60: The Suzuki coupling reaction.

In addition to the Suzuki reaction, the reactivity of rubazonic acid **I-187** was tested in other coupling reactions. The Stille reaction was used as an alternative, utilizing organostannanes as the trans-coupling reagent. (Scheme 61). Therefore, monomers with organostannanes were synthesized. The monomer synthesis involved modifying 2,7-dibromofluorene **I-189** to create a more soluble compound. Initially, the alkylation of fluorene **I-189** via direct C-H alkylation was obtained. Subsequently, monomer **I-191** was synthesized for the Stille coupling and polycondensation.
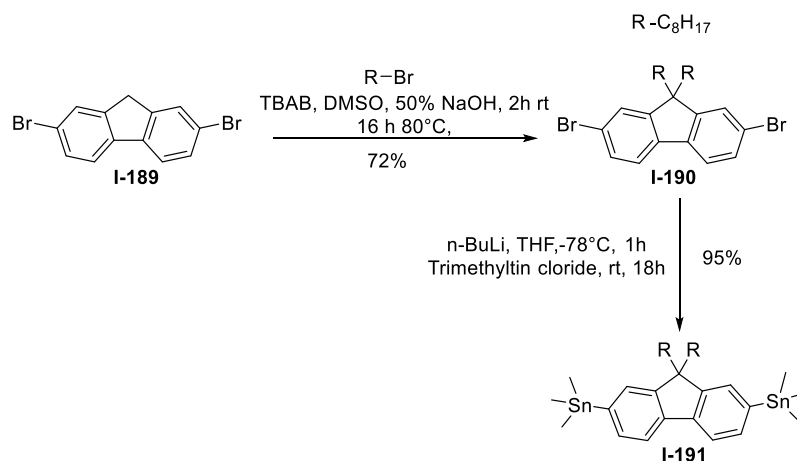
Scheme 61: The synthesis of 2,7-bis(trimethylstannyl)-9,9-dioctylfluorene **I-191**.

Investigating the Stille coupling as an alternative to the Suzuki reaction, a series of experiments were conducted under various conditions. The Stille reaction was investigated using pyrazolone compounds **I-185** or rubazonic acid **I-187** in combination with monomer **I-191** (Scheme 62). The coupling or polycondensation reactions were carried out in a DMF solution under an argon atmosphere, employing monomer **I-191** (1 eq.), Pd(PPh$_3$)$_4$ or PdCl$_2$(PPh$_3$)$_2$, CuI (2 eq), and CsF. The various reaction conditions were explored, with reaction times ranging from 2 to 5 hours (as shown in Table 7), but products not formed.

Table 7: The conditions of Still coupling/polycondensation of **I-186/I-188** with **I-191** (according to Scheme 62).

Pyrazolone/ Rub. acid R^1=C$_6$H$_{13}$ [eq.]	Pyrazolone/ Rub. acid R^1=C$_8$H$_{17}$ [eq.]	Pd(PPh$_3$)$_4$ [eq.]	PdCl$_2$(PPh$_3$)$_2$ [eq.]	CsF [eq.]	Solvent	Time [h]	T [°C]
	2.2	0.2		1.5	DMF	2	40
	2.2	0.2		1.5	DMF	3	40
	3.6	0.4		1.5	DMF	4	40
	6.6	0.6		0.5	DMF	5	60
3.6		0.4		0.5	DMF	5	50
	0.5		2.5	0.5	THF	2	70

The coupling was also attempted with catalyst, PdCl₂(PPh₃)₂, without CsF in THF at 70 °C for 2 hours. However, the Stille coupling did not yield the expected products (Scheme 62).
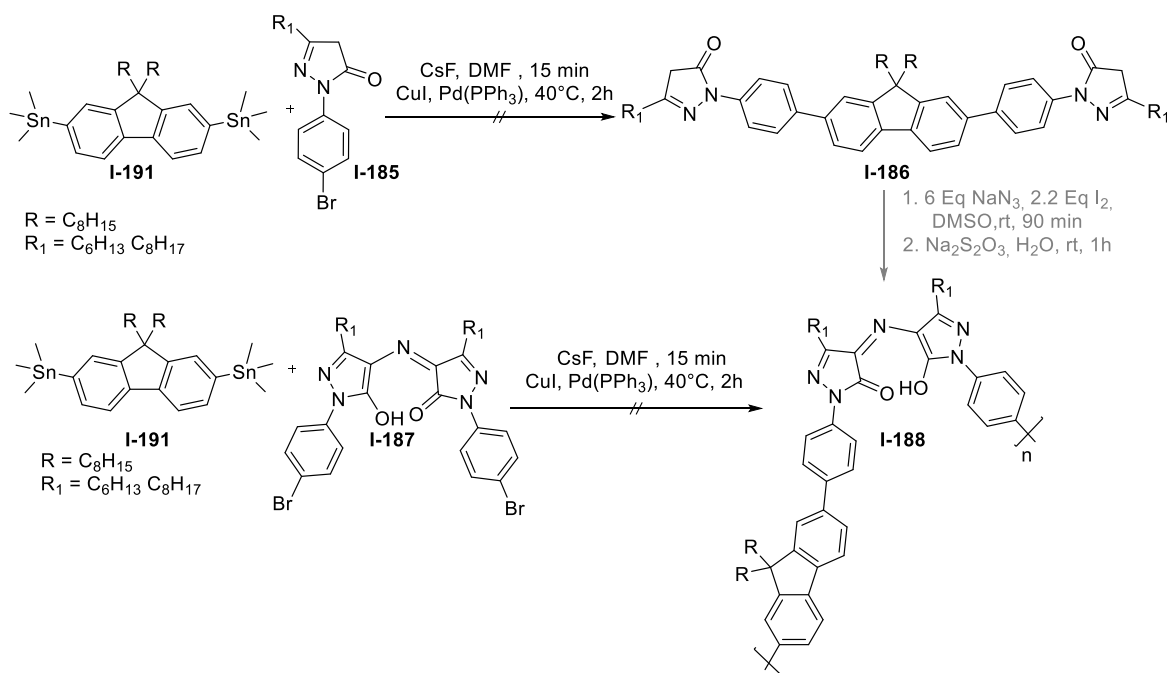
Scheme 62: The Stille coupling reaction.

In addition to exploring Pd catalyst coupling chemistry, the Yamamoto coupling was also investigated using a Ni(0) complex. The method, also known as homocoupling, has found extensive application in the synthesis of copolymers, as mentioned in the literature [136]. In order to investigate the feasibility of using this approach, four experiments were conducted using two different catalytic systems (Scheme 63). All the Yamamoto syntheses were carried out in a microwave using small quantities.

The initial two experiments focused on classical conditioning for coupling and polycondensation. Pyrazolone **I-185** or rubazonic acid **I-187** and bromofluorene **I-190** in a system consisting of bis(1,5-cyclooctadiene)nickel (2.4 eq), 2,2'-bipyridine (2.87 eq), and 1,5-cyclooctadiene (2.55 eq) in a solvent mixture of toluene/DMF (3:1) at 100 °C in a microwave for 30 minutes. Unfortunately, the desired products **I-186** or **I-188** were not formed (Scheme 63).

70
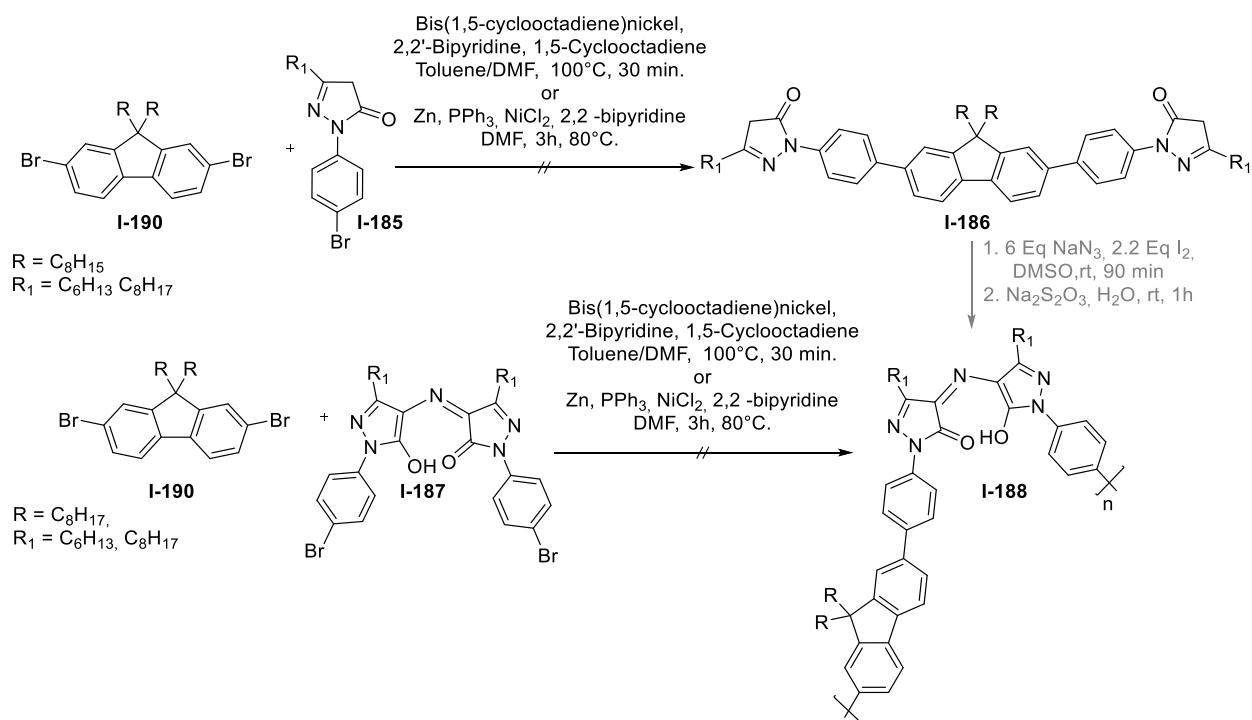
Scheme 63: The Yamamoto coupling/polycondensation reaction.

The coupling and polycondensation of pyrazolone **I-185** or rubazonic acid **I-187** and dibromofluorene using another system. This system included $NiCl_2$ (0.07 eq), zinc powder (3.2 eq), 2,2'-bipyridine (0.05 eq), and triphenylphosphine (0.28 eq) in DMF at 80 °C in a microwave for 3 hours. Unfortunately, the Yamamoto coupling did not yield the expected products as shown on Scheme 63.

After summarizing the results of the reactivity of pyrazolone **I-185** and rubazonic acids **I-188** to cross-coupling reactions, it was decided to discontinue studying this approach. However, other halogens were not tested, and it is possible that changing the halogen could lead to different results. Subsequently, the focus of the study shifted towards rubazonic acid molecules with alkyne group as a substituent and their potential for polycondensation.

I.7.2.2. Glaser as positive side reaction

The Sonogashira polycondensation was used with rubazonic acid **I-183** and 1,4-diiodobenzene (**I-192**) under standard conditions (Scheme 64). The reaction was catalyzed using $Pd(PPh_3)_4$ and CuI, with diisopropylamine as a base and toluene. The reaction was carried out at 40 °C for 24 hours. Although analysis of ^{1}H NMR and GPC indicated that polymerization had occurred, it was observed during the

investigation of the Sonogashira polycondensation approach that the resulting product was not formed. Consequently, additional reactions were conducted to gain insights into the formation of of products.
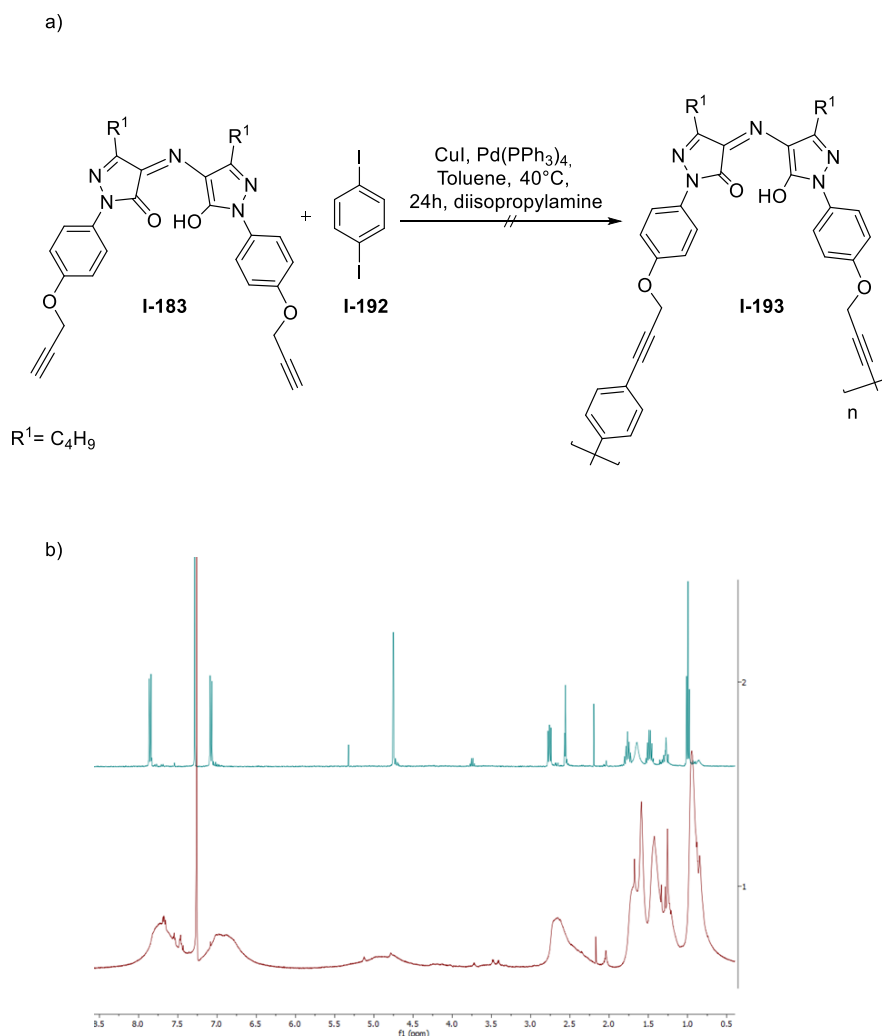
Scheme 64: a) Sonogashira polycondensation of monomers **I-183** and **I-193**, b) ^{1}H NMR of monomer **I-183** (2, green) and polymer product (1, red).

Different monomer systems and reaction conditions were initially tested. The polycondensation of rubazonic acid **I-183** with 2,5-diiodothiophene **I-194** or dibromofluorene **I-190** was conducted with Et$_3$N as a base and carrying out the reaction at 70 °C for 72 hours (Scheme 65). Similar to the previous reaction, polymers were initially formed, leading to the belief that the reactions were successful. However, it became clear over time that the expected polymers **I-195**

and **I-196** had not formed. The polymers were analyzed by ^{1}H NMR and GPC analysis. The fluorescent properties of the polymers were checked, but no fluorescence was observed, which was unexpected, as both thiophene and fluorene derivatives are known to exhibit fluorescence.
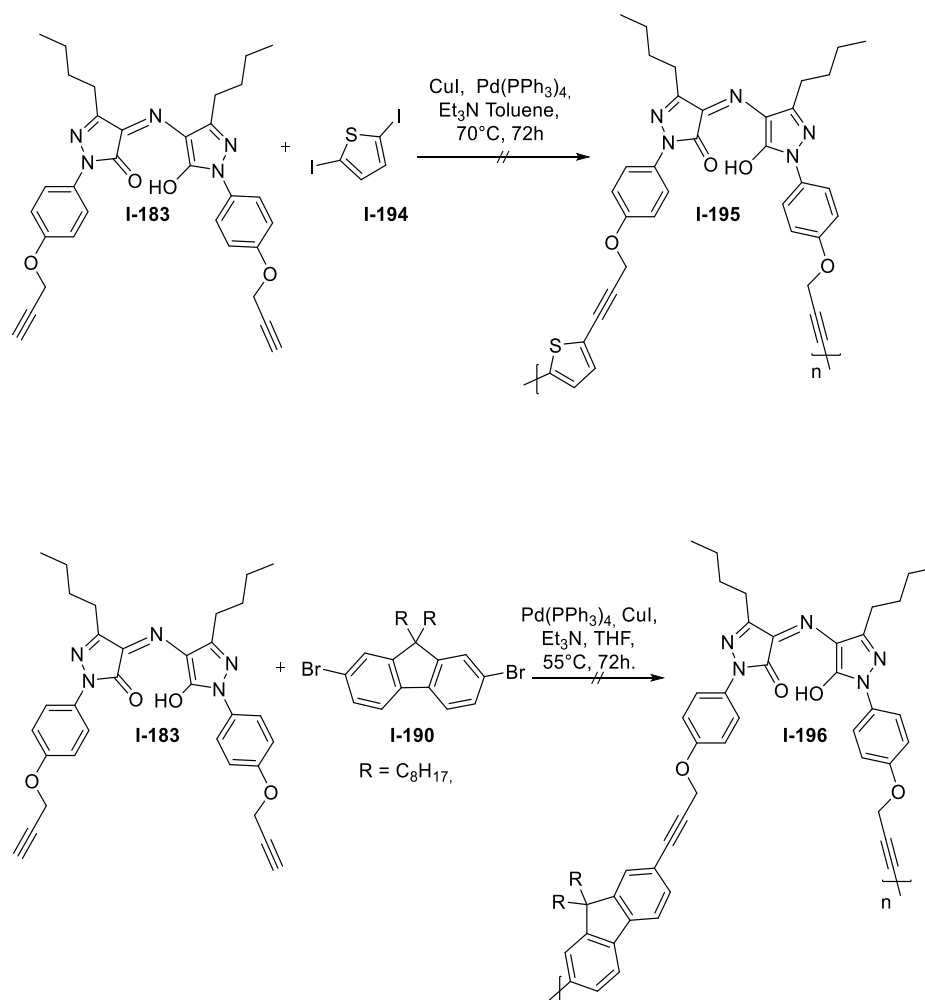
Scheme 65: Sonogashira polycondensation of polymers **I-195** and **I-196**.

The structure of these polymers could not be clearly determined by ^{1}H NMR analysis, as peak integration was difficult and the ^{13}C NMR analysis was incomplete due to the low solubility of the sample. In an effort to overcome this issue, a monomer with an acetyl group in the fluorene moiety was synthesized. This was done because acetyl groups have a distinctive singlet peak at 2.05 ppm in ^{1}H NMR, making it easier to confirm their presence in the molecule.

The monomer **I-199** was synthesized in two steps. In the first step, fluorene **I-189** was alkylated to obtain **I-198**, which contained a symmetrical Br group in its alkyl

chain (as shown on Scheme 66). In the second step, acetic acid was added to **I-198** in a mixture of anhydrous DMF and THF, along with potassium carbonate as a catalyst. The reaction was then heated at 90 °C for 12 hours. The monomer **I-199** was obtained with 87% of yield.
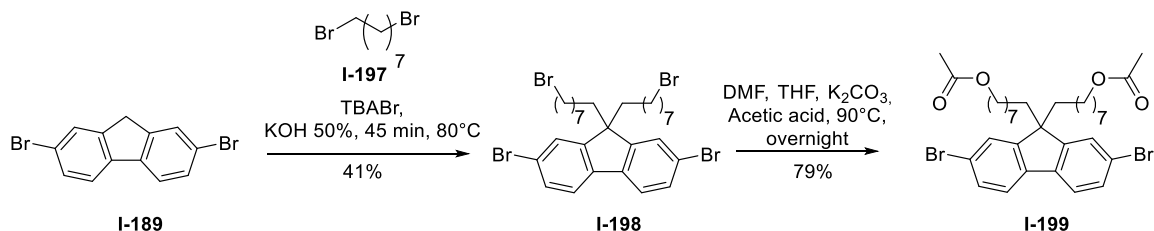
Scheme 66: The synthesis of monomer **I-199**.

The monomer **I-199** was condensed with rubazonic acid under Pd(PPh3)4, CuI conditions and Et3N as a base and toluene, and carrying out at 70 °C for 72 hours. In the ^{1}H NMR spectrum, the absence of the acetyl group was noted, raising suspicions of a Glaser coupling. This suggests the synthesis of a homopolymer, indicating the undesired formation of homocoupling products of acetylene derivatives due to the Glaser reaction in the Sonogashira reaction. In order to confirm this suspicion, the reaction was tested with rubazonic acid **I-183** only, without the presence of the Pd catalyst. However, the expected product did not form. In additional, the classical Glaser polycondensation conditions with monomer **I-183** were tested with CuCl as a catalyst and a mixture of DMF/THF under an O$_2$ atmosphere (with an O$_2$ balloon) at 30 °C for 90 minutes, but the reaction polymer **I-200** was not form (Scheme 67).
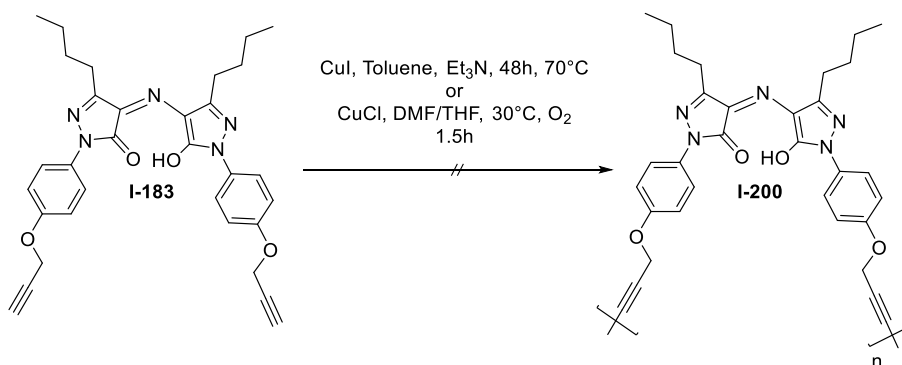
Scheme 67: Glaser condition for polycondensation.

Additionally, the reaction was attempted under the same conditions used for Sonogashira polycondensation, but using only rubazonic acid **I-183** (1 eq.) and Pd(PPh₃)₄ (0.04 eq.) with CuI (0.2 eq.) as the catalyst and Et₃N or DIPA as the base in toluene at 70 °C for 72 hours (Scheme 68). The polymers **I-201** were successfully obtained under these conditions (Table 8).
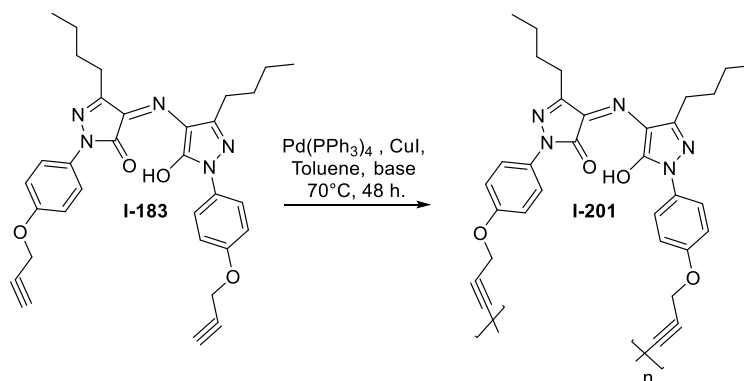
Scheme 68: The Glaser polycondensation of monomer **I-201**.

Table 8: The Glaser polycondensation of **I-201** in different base. (* Measured by GPC and the molar masses were calibrated to polystyrene as an internal standard).

Entry	Base	Mn* [g/mol]	Mw* [g/mol]	Đ*	Yield [%]
1	Et₃N	70 000	122 000	1.7	35
2	DIPA	15 500	33 300	2.1	38

Based on GPC analysis of Entry **1** (Table 8), a symmetrical graph was observed with a sharp peak shape indicating a low molecular weight distribution of the polymer **I-201** (as shown in Figure 4). The SEC result confirm absence of oligomer products.
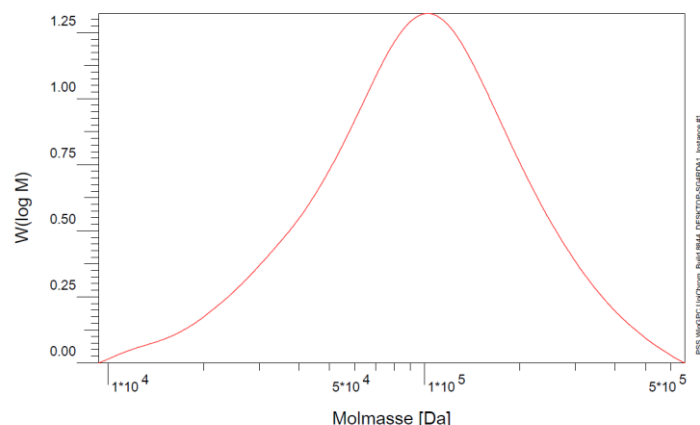
Figure 20: Graph form GPC analysis of homopolymer **I-201** (Entry 1, Table 8).

The use of Et$_3$N as a base in the Glaser polycondensation improved the length of the polymer Entry **1** (Table 8). However, the Glaser reaction conditions required improvements to achieve better yield, solubility in organic solvents, and prevent loss of high Mn for the new polymer.

Two techniques were utilized for the synthesis of the homopolymer: microwave synthesis and Schlenk.

Initially, the microwave synthesis method was used since it required less material and was faster than in Schlenk flasks. Two reactions were performed using rubazonic acid monomer (1 eq.), Pd(PPh$_3$)$_2$Cl$_2$ or Pd(PPh$_3$)$_4$, (0.2 eq.) and CuI (0.2 eq.) as the catalysts, and Et$_3$N as the base in toluene (Table 9). However, the products formed with low yield and low solubility in THF.

Table 9: The conditions of Glaser polycondensation of **I-183** by microwave activation.

Pd(PPh$_3$)$_2$Cl$_2$ [eq.]	Pd(PPh$_3$)$_4$ [eq.]	I$_2$ [eq.]	T [°C]	Time [h]	Yield [%]
0.2			100	2	3
	0.2		40	1	11
	0.2	0.5	40	1	24

Subsequently, all the syntheses were conducted via the Schlenk technique. The reactions were performed using rubazonic acid monomer **I-183** (1 eq.), Pd(PPh$_3$)$_4$,

and CuI as the catalysts, and Et$_3$N as the base in toluene. In this study, the equivalent of the catalysts was varied. Table 10 shows the obtained results of Glaser polycondensation of **I-183** (Scheme 68). According to GPC analysis, a low molecular weight fraction was measured (Table 10), which was attributed to the fact that the polymer had low solubility in the eluent (THF). As a result, the rest of the polymer fraction remained on the filter as insoluble material.

Table 10: The conditions and results of Glaser polycondensation of **I-183**. (* Measured by GPC and the molar masses were calibrated to polystyrene as an internal standard).

Pd [eq.]	CuI [eq.]	Time [h]	Yield [%]	Mn* [g/mol]	Đ
0.1	0.1	72	5		
0.04	0.04	72	6		
0.04	0.2	72	13	1 700	2.2
0.04	0.2	96	15		
0.04	0.2	48	6		
0.2	0.2	72	28	5 300	2.2

I.7.2.3. Improvement yield of Glaser polycondensation via oxidative agent

The literature suggests that the addition of oxidizing agents, such as I$_2$ or benzoquinoline, could increase the yield. In 1997, Hattori T and co-authors [137] proposed oxidative polycondensation as a method for synthesizing polyacetylene. They used Pd(PPh$_3$)$_4$ and CuI as catalysts, Et$_3$N as a base, I$_2$ as an oxidative agent, and 2 hours of reaction. In the same year, Liu Q and Burton D.J [124] published work on the facile synthesis of diynes. A similar approach to synthesis was used, involving Pd(PPh$_3$)$_2$Cl$_2$ and CuI as catalysts, i-Pr$_2$NH as a base, I$_2$ as an oxidative component, and reaction times ranging from 2 to 12 hours. The yields for the reactions ranged from 64% till 88%. Based on this literature knowledge, the attempt was made to adapting this reaction for rubazonic acid.
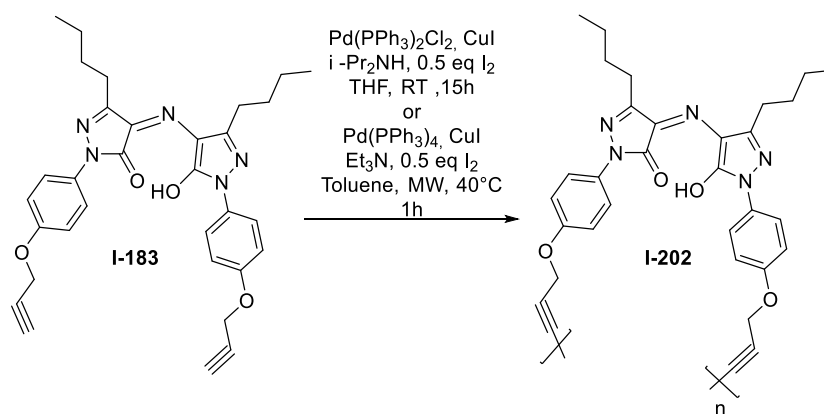
Scheme 69: Oxidative polycondensation of **I-183**.

The oxidative polycondensation of rubazonic acid monomer **I-183** was conducted under the same conditions as proposed by Liu Q (Scheme 69) for the purpose of replicating this reaction. The product **I-202** was obtained, but upon precipitation in methanol, small polymer flakes were observed. At this stage, it was suspected that the polymer **I-202** may have a low molecular weight. This assumption was confirmed after ^{1}H NMR and GPC analysis, which showed Đ = 3 and Mn = 2 300 g/mol and 39% of yield. When comparing the NMR results of the high molecular weight homopolymer **I-201** (70 000 g/mol) (Figure 21a) with homopolymer **I-202** (2 300 g/mol) (Figure 21b), a clear violation of peaks symmetry is visually apparent. Notably, it is observed that homopolymer **I-202** has a shorter length, as evidenced by the continued visibility of the proton at 3.5 ppm from the alkyne group.

Additionally, the reaction was attempted in a microwave with Pd(PPh3)4 and Et3N at 40 °C for 1 hour, with a 24% of yield, but with low solubility in THF for GPC analysis.
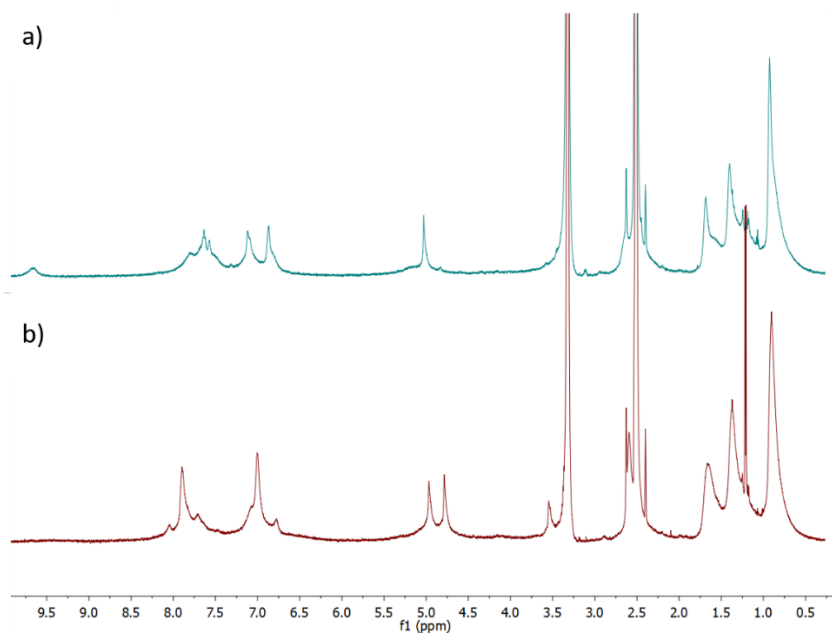
Figure 21: The ^{1}H NMR spectrums of polymers **I-201** (a) and **I-202** (b).

Additionally, a small amount of 4-ethynylanisole **I-203** was added as an end-capping stabilizer (Scheme 70). However, the resulting polymer **I-204** did not show a significant increase in molecular weight. GPC and ^{1}H NMR analysis revealed an oligomeric fragment (n=4) for this sample, with a Đ of 3.4 and Mn of 2 400 g/mol.
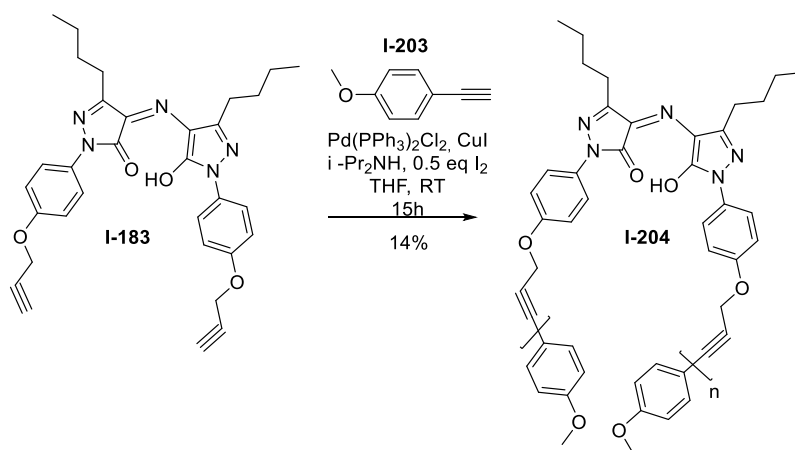
Scheme 70: Oxidative polycondensation conditions for synthesis polymer **I-204**.

It was discovered that p-benzoquinone could also be used as an oxidizing agent in the reaction. In the subsequent reaction, the p-benzoquinone was used as the

oxidizing agent along with Pd(PPh$_3$)$_4$ and CuI as catalysts, i-Pr$_2$NH as the base, and toluene as the solvent (Scheme 71). The reaction was carried out at 70 °C for 72 hours, resulting in two polymers **I-205a-b** with yields of 42% and 56% (Table 11). However, the polymers were not sufficiently soluble in THF for GPC measurements. The polymer was characterized by ^{1}H NMR.
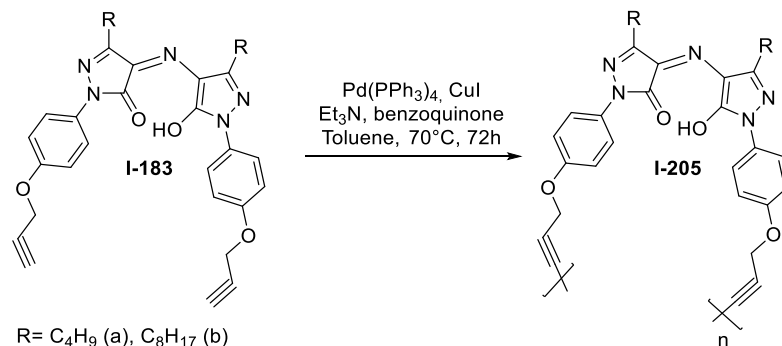
Scheme 71: Oxidative polycondensation conditions with benzoquinone as oxidizer agent.

Table 11: The oxidative conditions and results of Glaser polycondensation of **I-183**.

RA C$_9$H$_{19}$ [eq.]	RA C$_4$H$_9$ [eq.]	Pd° [eq.]	CuI [eq.]	Benzoquinone [eq.]	Yield [%]
1		0.05	0.6	2.5	56
	1	0.05	0.6	2.5	42

I.7.2.4. The studying of rubazonic acid reactivity to different Glaser's reactions

Additionally, well-known Glaser's reactions such as Glaser-Hay and Glaser-Eglinton reactions, as well as some modified Glaser protocols, were tested (Scheme 72).
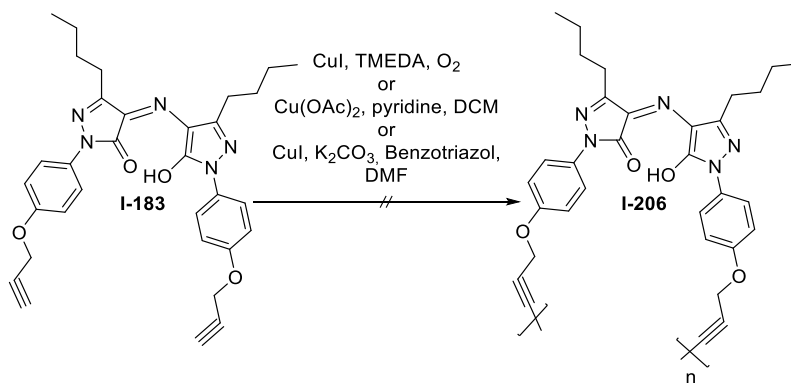
Scheme 72: Different Glaser conditions for synthesis of polymer.

For the Glaser-Hay polycondensation reaction, rubazonic acid was used as the monomer along with CuI as the catalyst, TMEDA as the base, and O_2 as the oxidizer. For the Glaser-Eglinton reaction, $Cu(OAc)_2$ was used as the catalyst, pyridine as the base, and DCM as the solvent. Modified Glaser couplings were also explored, with one study proposing the use of benzotriazole as a ligand, K_2CO_3 as the base, and CuI as the catalyst in DMF at room temperature, resulting in a 99% yield of the product [138]. However, these conditions were unsuccessful for rubazonic acid. Various couplings were attempted, with a mixture of Pd and Cu catalysts ultimately yielding a polymer

As mentioned earlier, the goal of recent experiments was to improve the yield of the reaction, and this was achieved successfully. However, measuring the GPC of the polymers synthesized with a higher yield proved to be difficult.

I.7.2.5. The surface study of thin film formed from rubazonic acid homopolymers

In addition, the possibility of forming thin films was studied for the homopolymer **I-202** and modified polymer **I-204**. Figure 22 displays an atomic force microscope (AFM) image of rubazonic acid homopolymers dispersed in PMMA. The thin films were prepared using the same technique as described on **page 64.**

The root-mean-square (rms) roughness homopolymer **I-202** dispersed in PMMA is 1.105 nm, while that of homopolymer **I-204** dispersed in PMMA is 0.424 nm. Interestingly, the modified homopolymer **I-204** thin film has a lower rms surface

roughness compared to the unmodified homopolymer **I-202** thin film. This indicates that the modification has resulted in a smoother surface.
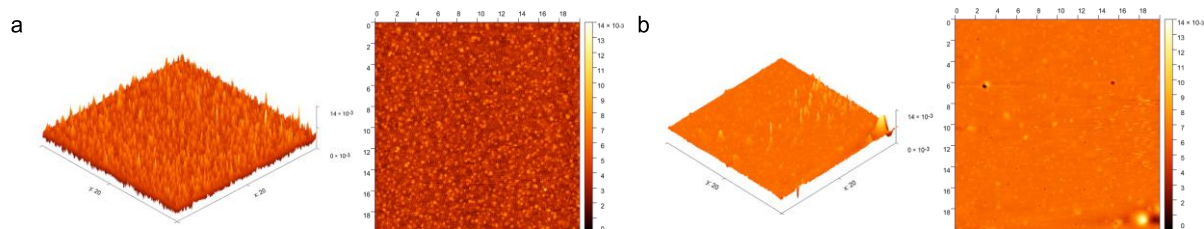
Figure 22: Two-dimensional (2D) and three-dimensional (3D) AFM micrographs of RA homopolymer **I-202** dispersed in PMMA (a) and modified RA homopolymer **I-204** dispersed in PMMA (b).

I.7.3. New double-bonded conjugated rubazonic acid polymers

Double-bonded conjugated rubazonic acid polymers were synthesized through decarbonylative polyaddition and hydrothiolation.

Rhodium complexes have been found to catalyze the regio- and stereoselective decarbonylative reaction of aroyl chlorides with terminal aromatic alkynes, formation only Z-vinyl chlorides. Aroyl chlorides can react with low valence transition-metal species as rhodium and palladium to form aroylchlorometal complexes, which can be further transformed into arylchlorometal complexes through decarbonylation at relatively high temperatures. Chlororhodation of alkynes with arylchlororhodium(III) intermediate and reductive elimination of the final product are possible pathways in the reaction. The effective component in the catalytic cycle is Rh(I) species, which undergoes repeated transitions between Rh(I) and Rh(III) species [127].

The rubazonic acid monomer **I-183** and terephthaloyl dichloride **I-207** were polymerized in toluene with Rh(cod)Cl$_2$ and PPh$_3$ under argon at 110 °C for 12 hours in o-xylene (Scheme 73). The polymerization process proceeded smoothly and resulting in the formation of a rubazonic acid oligomer **I-208** with a yield of 31% and Mn = 1370 g/mol, Đ = 1.4, n = 2.
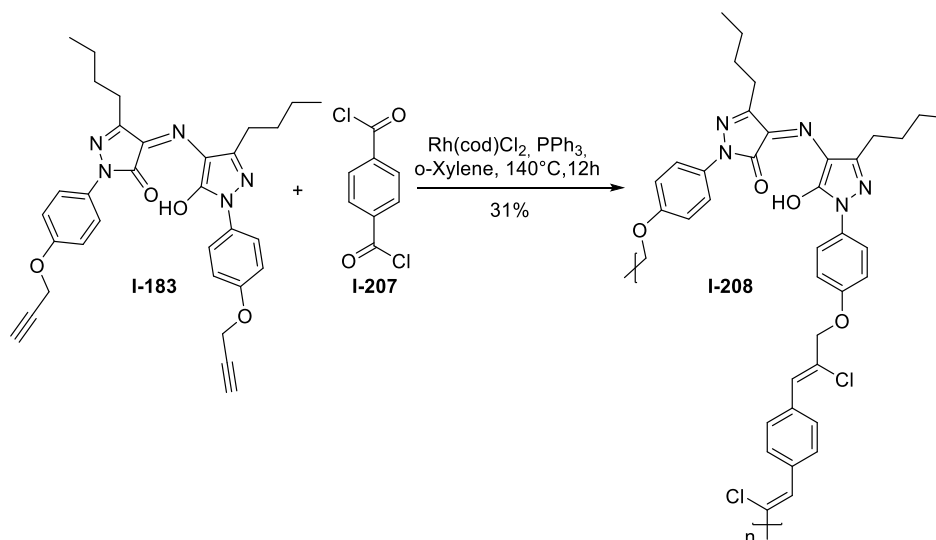
Scheme 73: Synthesis of RA copolymer **I-208** by decarbonylative polyaddition.

Sulfur-containing polymers can be easily prepared through photo- and thermo-initiated, amine-mediated, and transition-metal-catalyzed thiol-yne click polymerizations. These polymers have potential applications as drug-delivery vehicles, high refractive index optical materials, photovoltaic materials, biomaterials, and more [139].
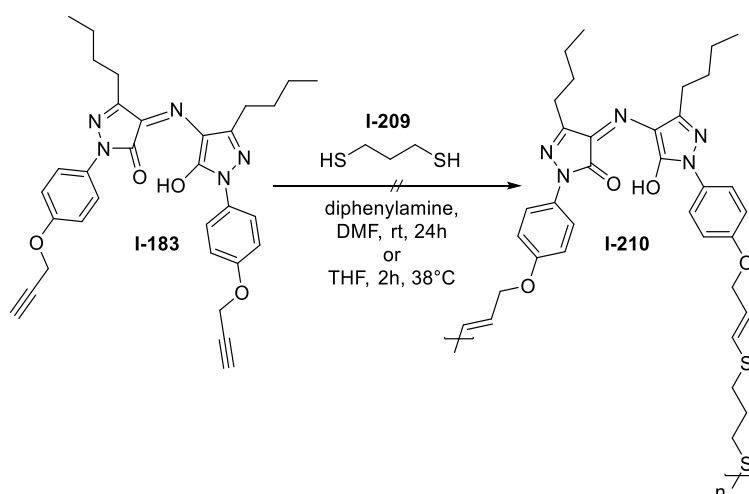
Scheme 74: Synthesis of sulfur-containing rubazonic acid copolymer through organobase-catalyzed regioselective alkyne hydrothiolation or thiol-yne click polymerizations.

Two methods were used to synthesize sulfur-containing rubazonic acid copolymer in this work: organobase-catalyzed regioselective alkyne hydrothiolation and thermo-initiated thiol-yne click polymerization.

Polyhydrothiolation of the rubazonic acid monomer **I-183** with propylpropane-1,3-dithiol **I-209** in DMF with diphenylamine did not result in the expected polymer (Scheme 74). The catalyst-free thermo-initiated thiol-yne click polymerization method was used to synthesize the sulfur-containing rubazonic acid copolymer. The rubazonic acid monomer **I-183** and propylpropane-1,3-dithiol **I-209** were polymerized **I-210** under an argon atmosphere in THF at 38 °C for 2 hours (Scheme 74). Unfortunately, product was not form.

I.7.4.1. The synthesis of rubazonic acid copolymer by nucleophilic aromatic substitution.

A rubazonic acid polymer was synthesized through nucleophilic substitution, with the aim of producing a soluble polyetheretherketone (PEEK) containing rubazonic acid. However, this proved to be a challenging task due to the low solubility of PEEK in many solvents, making it difficult to work with and analyze.

The rubazonic acid **I-180b** or **I-180d** (1 eq.) and 4,4'-difluorobenzophenone **I-211** (1 eq.) were polymerized in DMAc or in the mixture of DMAc and toluene as the solvent, with K_2CO_3 (1 eq.) as the catalyst at 160-180 °C for 6–48 hours (Scheme 75). The polymers **I-212b**, **I-212d** were precipitated in H_2O and purified in a Soxhlet with MeOH. Throughout the experiment, the time, temperature, and solvent were varied to achieve the results (Table 12). The two polymers were obtained and characterized by ^{1}H NMR and GPC (in THF). The Mn for the **I-212b** (R = C_4H_9) is 2 480 g/mol with Đ = 1.2 and n = 4. The Mn for the oligomer **I-212d** (R = C_8H_{18}) is 3 470 g/mol with Đ = 3.8 and n = 4.
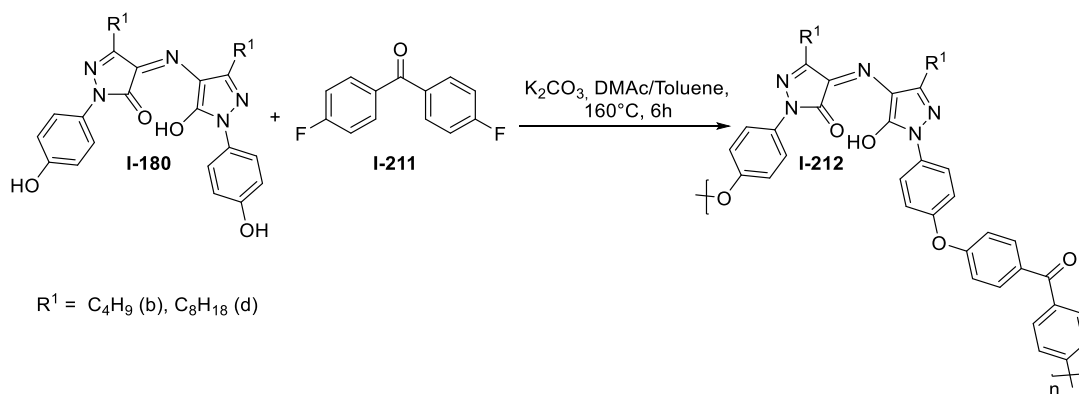
Scheme 75: Synthesis of RA copolymer **I-212b**, **I-212d** by nucleophilic aromatic substitution reaction.

Table 12: The conditions and results of synthesis of **I-212** by nucleophilic aromatic substitution reaction. (* Measured by GPC and the molar masses were calibrated to polystyrene as an internal standard).

I-212	Solvent	T [°C]	Time [h]	Yield [%]	Mn* [g/mol]	Mw* [g/mol]	Đ*	n
b	DMAc/Toluene	170	10	38	1 860	2 730	1.4	2
b	DMAc/Toluene	180	12	82				
b	DMAc/Toluene	160	48	87				
b	DMAc	160	16	80				
b	DMAc/Toluene	160	6	84	2 600	3 270	1.2	4
d	DMAc/Toluene	160	6	41	3 470	9 610	2.7	4

Then, the **I-212d** (R = C_8H_{18}) was modified to poly(dithioacetal) by dithioketalization of the carbonyl groups with 1,2-ethanedithiol **I-213** under strong acidic conditions (Scheme 76). This process was free from degradative or cross-linking side reactions, while the resulting rubazonic acid poly(dithioketal) **I-214** were readily soluble in organic solvent.
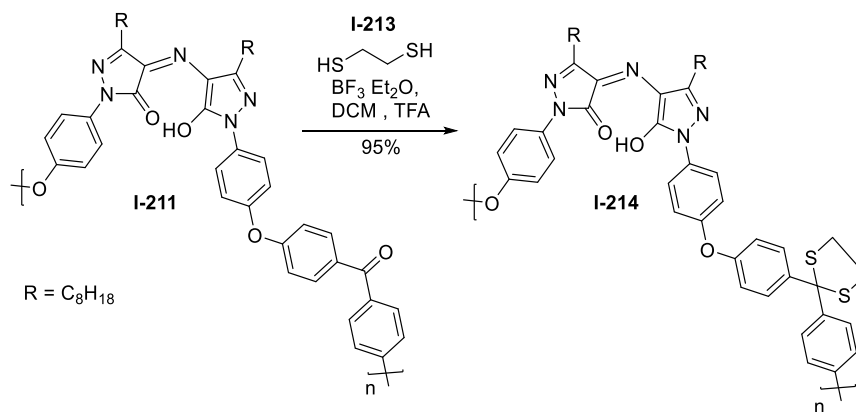
Scheme 76: The dithioketalization of the carbonyl groups of **I-212**.

The polymer was characterized by ^{1}H NMR and GPC. The aliphatic protons of the dithiane ring were resonating at 2.9−2.8 ppm in ^{1}H NMR spectrum. The solubility of this compound increased significantly, and subsequent GPC analysis in THF revealed a relatively broad distribution.
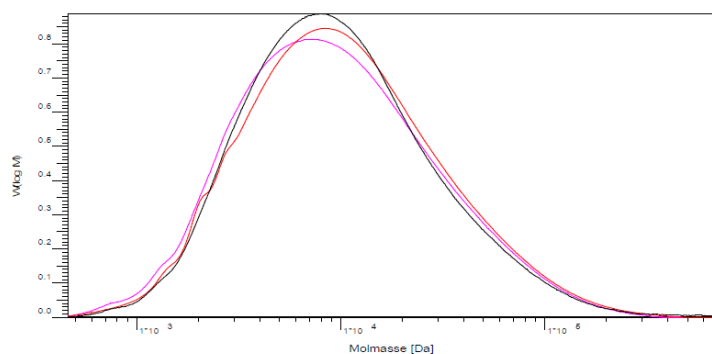
Figure 23:The GPC graph of post functionalize polymer **I-214.**

The GPC measurement was carried out using three detectors, namely diode array detector (DAD) WL1 (204 nm), (DAD) WL2 (222 nm), and refractive index detector (RID), as shown in the Figure 23 and Table 13. All three detectors showed approximately the same result. The number-average molar mass Mn of the post functionalized polymer II-130 significantly increased from 3 470 g/mol to 6 030 g/mol and weight average degree of polymerization n increasing from 4 to 7. The significant increase Mn and n of the post functionalize compound **I-214** can be

explained by the improved solubility of all molecular fraction of the polymer in eluent (THF).

Table 13:The GPC results for polymer **I-214**.

Detector	Mn [g/mol]	Mw [g/mol]	Đ
DAD WL1	5550	17900	3.2
DAD WL 2	6060	19200	3.1
RID	6030	18500	3

I.7.4.2. Tautomerism of rubazonic acid polymer

In addition, an absorption study at different pH values was performed using a solution of the polymer in DMSO. The rubazonic acid in this polymer can exist in two tautomeric forms, depending on the pH value. The absorption maximum at pH 6 is at 458 nm, but upon adding CsOH·H_2O solution, the pH value changes to 10, and the absorption maximum is significantly shifted to 526 nm. This bathochromic shift of 68 nm confirms the formation of the deprotonated form of rubazonic acid. The deprotonated form of rubazonic acid can be reversed to the protonated form of rubazonic acid by adding HCl solution in DMSO, and the absorption maximum at pH 3 is 457 nm.
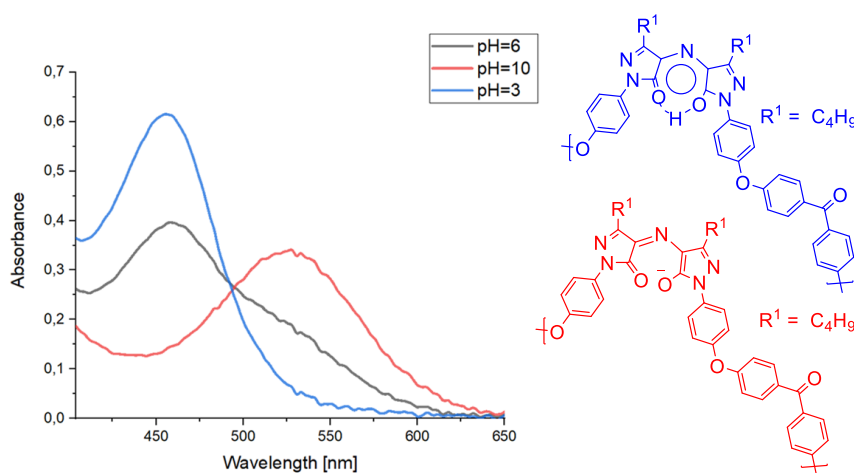
Figure 24: Changes in the UV-Vis spectra and pH value of **I-214** (1×10^{-5} M) a) during titration by CsOH·H_2O and after adding HCl in DMSO.

I.7.5. Introduction of rubazonic acid in polyurethanes polymers family

Firstly, we synthesized rubazonic acid polymer through a reaction with rubazonic acid **I-180b** and 1,6-diisocyanatohexane. Various catalysts can be used for the synthesis of polyurethanes, including organic bases (1,4-diazabicyclo[2.2.2]octane (DABCO), 1,8-diazabicyclo[5.4.0]undec-7-ene, 1,5,7-triazabicyclo(4.4.0)dec-5-en), organic acids (5-(diphenylphosphoryl)pentanoic, methanesulfonic acid, triflic acid), or organotin compounds (dibutyltin dilaurate) [140]. DABCO is a commonly used catalyst for the synthesis of polyurethanes and was utilized in this study with dry THF (Scheme 77). The reaction mixture was refluxed for 7 hours, and the resulting product **I-216** with 53% of yield and Mn of 3 300 g/mol, Đ = 1.5, and weight average degree of polymerization n = 5. For increasing length of polymer, the reaction time should be increase. Also, the using aromatic diisocyanates as monomers can increase the polymer length due to the higher reactivity of aromatic isocyanates compared to aliphatic isocyanates.
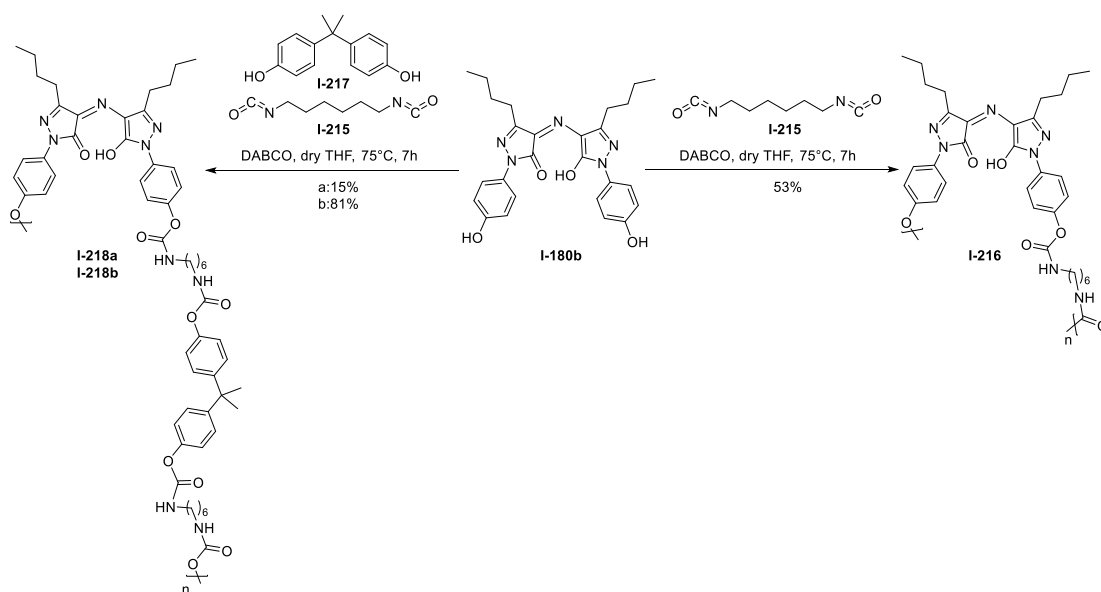
Scheme 77: Condensations of rubazonic acid monomer **I-180b** and 1,6-diisocyanatohexane **I-215.**

Furthermore, was synthesized two polymers with different stereochemical ratios **I-218a** (1 eq.(**I-180b**):1 eq. (**I-217**):1 eq. (**I-215**)) and **I-218b** (0.5 eq.(**I-180b**):1 eq. (**I-217**):0.5 eq. (**215**)). The polymer, **I-218a**, was successfully isolated with a 15% of

yield and Mn= 3 370 g/mol, Đ = 1.4, n = 4. The changes of stereochemistry ratio increase yield of **I-218b** to 81%.
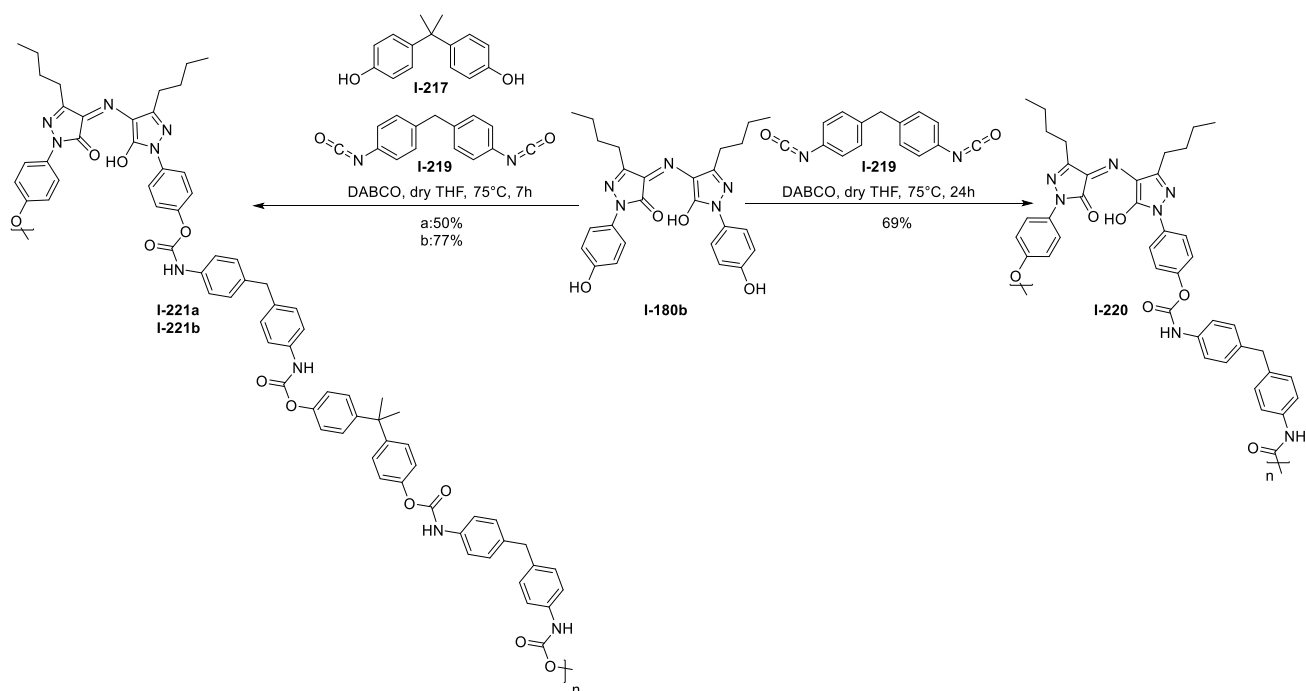
Scheme 78: Condensations of rubazonic acid monomer **I-180b** with aromatic diisocyanates **I-219**.

Exploiting analogous conditions as aforementioned, the synthesis of rubazonic acid polyurethanes employing aromatic diisocyanates **I-219** was carried out. Consequently, polymer **I-220** was obtained with 69% of yield. However, the analysis of this polymer was limited due to its low solubility, allowing only for ^{1}H NMR and IR analyses.

In order to enhance both the solubility and length of the polymer, Bisphenol A (BPA) was introduced into the polymer structure. This modification resulted in the isolation of two polymers **I-221a** (1 eq.(**I-180b**):1 eq. (**I-217**):1 eq. (**I-219**)) with 50% of yield and Mn= 4 220 g/mol, Đ = 1.7, n = 4; **I-221b** (0.5 eq.(**I-180b**):1 eq. (**I-217**):0.5 eq. (**219**)) with 77% of yield and Mn= 7 260 g/mol, Đ = 2.1, n = 8.

Furthermore, synthetic polymers have been tested by incorporating specific end groups (Scheme 79). In this study, methoxy polyethylene glycol 350 was used as an end group. The resulting polymers, **I-222** and **I-223**, were isolated with yields of 55% (Mn = 2 860 g/mol, Đ = 1.4, n = 3, m = 5) and 72% (Mn = 4 150 g/mol, Đ = 1.4, n = 5, m = 5) respectively. Including the end groups, there is a possibility to calculate the molecular weight of a polymer using ^{1}H NMR. This was successfully achieved

for the polymer **I-223**, as the integration of signals indicated a minimum molecular weight of 2 500 g/mol, which is two times less compared to the GPC measurements (4 150 g/mol). It could be explained to difficulty of correct integration a singlet at 3.5 ppm that comes from CH$_3$ from PEG.
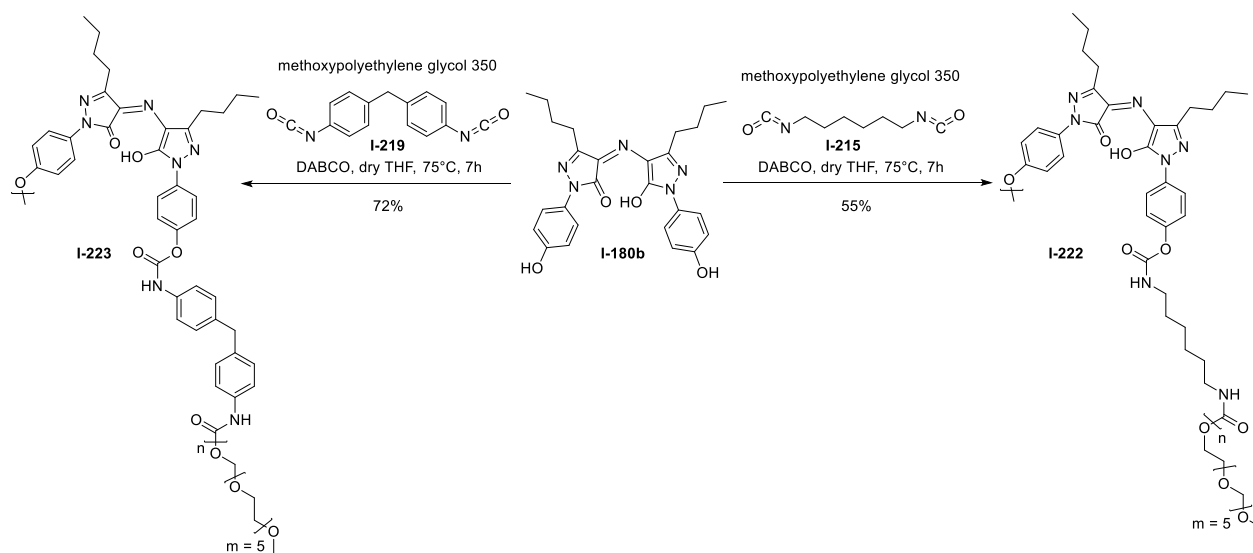
Scheme 79: Condensations of rubazonic acid monomer **I-180b** to polyurethanes **I-222** and **I-223**.
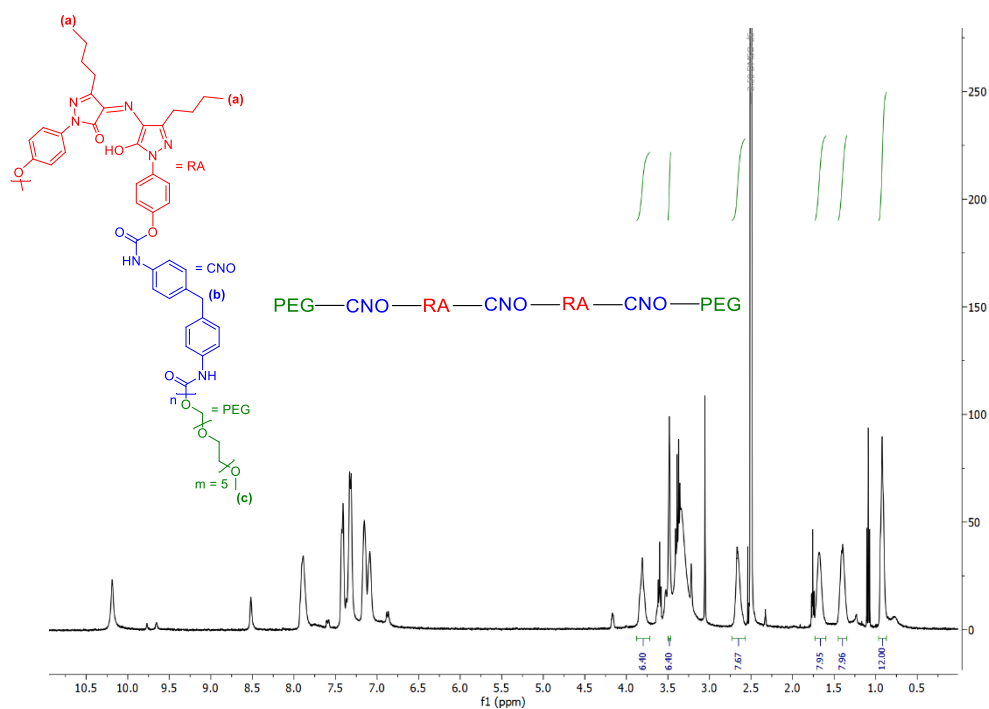
Scheme 80: ^{1}H NMR of polymer **I-223**.

I.8. Conclusion

In summary of this chapter, nine new pyrazolone derivatives were synthesized with yields ranging from 33% till 82%. New rubazonic acid derivatives were synthesized from these pyrazolones, and yield ranged is 40%-62%. The influence of pH on the tautomerism of rubazonic acid were confirmed. The thin films of rubazonic acids dispersed in PMMA were successful forming by spin coating technique. The optical and surface properties of rubazonic acid thin film were investigated.

Various rubazonic acid monomers were tested for differences in reactivity (Scheme 81). The Suzuki, Stille, Yamamoto, and Sonogashira polycondensation gave unsuccessful results. However, it was discovered that rubazonic acid monomer **I-183** could form a homopolymer under Glaser conditions but only in the presence of [Pd] and [Cu] catalysts. The homopolymers were synthesized with yields of 35% and Mn 70 000 g/mol and Đ 1.7, and 38% yield and Mn 15 500 g/mol and Đ 2.1. The oxidative conditions of Glaser coupling with benzoquinone as the oxidizing agent increased the yield of the reaction to 56%.
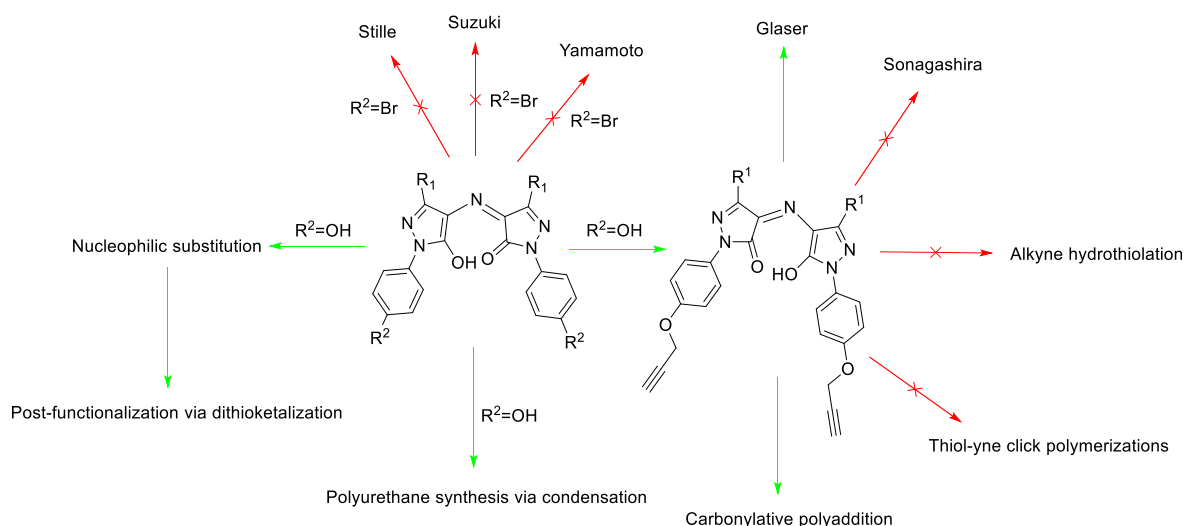
Scheme 81: Reactivity of rubazonic acids monomer

In addition to the successful synthesis of homopolymers, three different copolymers of rubazonic acid were synthesized. Double-bonded conjugated polymers were synthesized through carbonylative polyaddition. A mixture of catalyst Rh(cod)Cl$_2$

and PPh$_3$ was successfully used for the carbonylative polyaddition, and **I-208** was formed with a yield of 31% and Mn = 1 370 g/mol, Đ = 1.4, weight average degree of polymerization n = 2. Nucleophilic aromatic substitution was also used to synthesize PEEK oligomers of rubazonic acid with yields ranging from 41% till 84%, Mn values ranging from 1 860 (n = 2) to 3 470 g/mol (n = 4), and Đ values ranging from 1.2 till 3.4. The dithioketalization of the carbonyl groups with a yield of 95% increased the solubility of the polymer, and the Mn value also increased to 6 030 g/mol (n = 7) with Đ = 3. Rubazonic acid was successfully introduced into the polyurethane family. Various polyurethanes based on rubazonic acid were successfully synthesized with different polymer chain lengths.

The successful synthesis of rubazonic acid homo- and copolymers opens up new possibilities for the study of material since.

Part II:

Innovative Polyester Incorporating Highly Energetic Gem-Diazide Units

II.1 Polyesters synthesis and applications

Polyesters (Scheme 82) are an important and widely used type of polymer, with high molecular weight and ester groups in the polymer backbone instead of the side chain, unlike poly(vinyl acetate) and poly(methyl methacrylate) [141]. Polyesters are one of the most economically important classes of polymers, driven especially by polyethylene terephthalate (PET) [142].
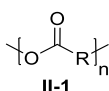
Scheme 82: General structure of polyester.

The discovery of polyester dates back to the late 1930s in the DuPont laboratory, but scientist W.H. Caruthers left the research to work on nylon, which had just been discovered. In 1941, a group of British scientists built upon Caruthers' work and developed the first commercial polyester fiber, known as terylene. DuPont subsequently acquired the legal rights and produced another popular polyester fiber, dacron, in 1946. Another polyester fiber, Kodel, was introduced by Eastman Chemical in 1958 [143].

The polyester family exhibits a wide range of structures and properties, which vary depending on the nature of the R group (Scheme 82). Generally, polyesters can be classified into two groups: natural and synthetic. Natural polyesters include the cutin component of plant cuticles and the cellophane polyester lining produced by bees of the Colletes genus for their underground brood cells [144].
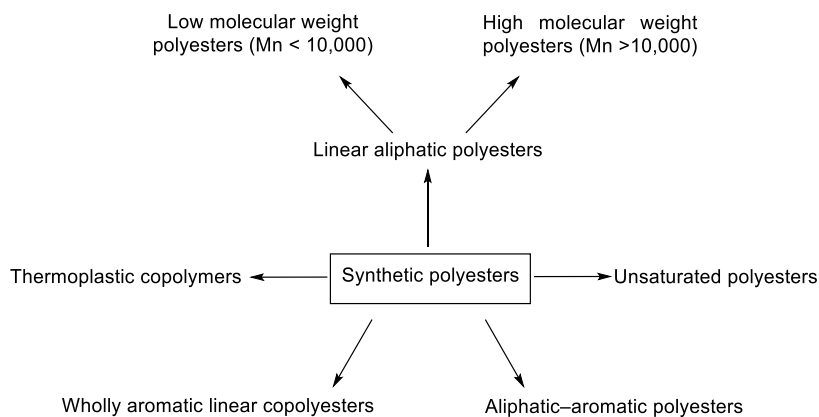
Scheme 83: Classification of synthetic polyester.

Polyesters can be classified into various subgroups, as shown in the Scheme 83, based on their properties and uses. Linear aliphatic polyesters, including polyglycolic acid, polylactic acid, and polyhydroxyalkanoates, are suitable for environmentally-conscious applications [141], such as packaging [145], disposable items, and agricultural mulch films [146], as well as biomedical [147] and pharmaceutical uses [148]. High-molecular-weight linear aliphatic polyesters are semi-crystalline with relatively poor mechanical properties, while low-molecular-weight polyesters are used as macromonomers for polyurethane production [149]. Aromatic polyesters, such as PET [150], polybutylene terephthalate [151], and liquid crystal polyesters [152], are high-performance materials with excellent mechanical and thermal properties. Semi-crystalline aliphatic-aromatic polyesters, such as poly(hexamethylene terephthalate) and poly(propylene terephthalate) (PTT, Sorona), are used as technical thermoplastics, fibers, and films [153]. Unsaturated polyesters are thermosetting polyesters that can be cross-linked and used as matrices in composite materials [154]. Alkyd resins, made from polyfunctional alcohols and fatty acids, are commonly used in the production of coatings and composite materials [155]. Rubbery polyesters called thermoplastic polyester elastomers are also available [156]. In addition, there are thermoplastic copolymers, such as polyethylene terephthalate glycol (PETG) [157], polycarbonate (PC)/polybutylene terephthalat blends [158], and polycarbonate /polyethylene terephthalate (PC/PET) blends [159], which exhibit a range of properties depending on their composition. Overall, the various types of polyesters have different properties and applications, making them a versatile family of materials.

95
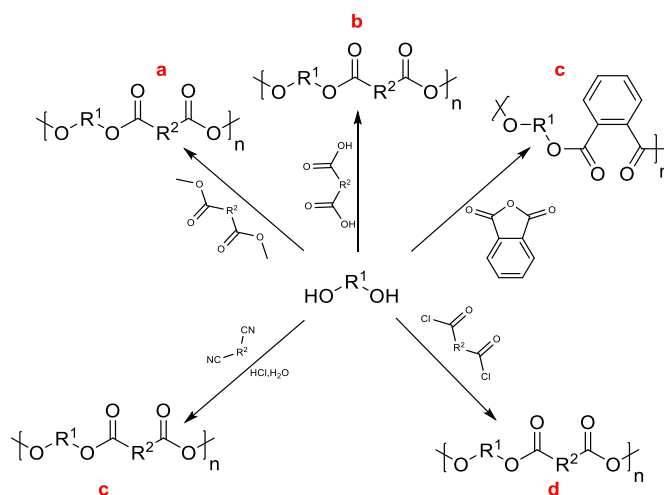
Scheme 84: Synthesis of polyesters.

Polyesters can be synthesized using various methods such as step-growth polymerization, ring-opening polymerization, which are shown in the Scheme 84. The Scheme 84 also demonstrates reactions for polyesterification of polyols with diacids and their derivatives. The transesterification of a dialkyl ether is a common method used for high-melting polymers and low-solubility dicarboxylic acids (Scheme 84a) [160]. Another method is the direct esterification of a dicarboxylic acid with a diol (Scheme 84d), which is typically carried out at boiling temperature for a higher reaction rate than transesterification. Polyesterification is a slow process that requires high reaction temperatures (> 200 °C) and a catalyst such as antimony [161], germanium [162], titanium [163], or aluminum compounds [164] to achieve acceptable reaction rates and high molecular weights. Due to the equilibrium nature of the elementary growth step in polyesterification and polytransesterification, the resulting alcohol or water must be efficiently removed from the reaction vessel to increase the molecular weight [165]. However, this can be difficult during the later stages of polymerization due to the high viscosity of the resulting polymers. To overcome this issue, polycondensation is often carried out in solution and at low pressure, where the evaporating solvent can form an azeotropic mixture with water or alcohol.

Polyesters can also be synthesized from hydroxy acids, which are single reagents. In the presence of a metal catalyst, such as dibutyltin diacetate, p-hydroxyethoxybenzoic acid can self-condense to form a semi-aromatic polyester.

On the other hand, 4-hydroxybenzoic acid and 6-hydroxy-2-naphthoic acid can self-condense to formed fully aromatic esters (Scheme 85) [166]. However, direct self-condensation requires high reaction temperatures (> 300 °C).
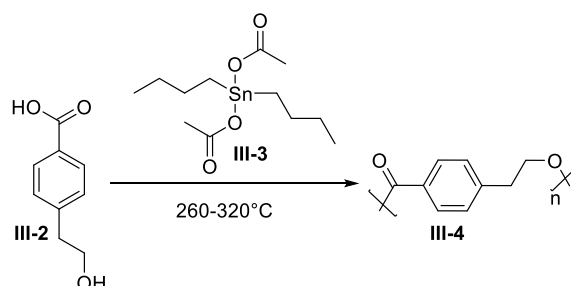
Scheme 85: Synthesis of polyester from hydroxy acids.

Another method for synthesizing polyesters is ester interchange between a dicarboxylic acid and a diester. For example, the reaction between glycol acetate **III-5** and terephthalic acid **III-6** form PET **III-7** (Scheme 86), which is also known as "polyester". This method does not involve glycols, unlike some other polyester synthesis methods [167].
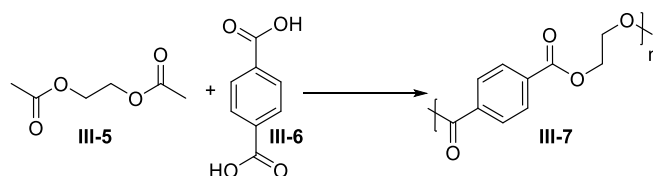
Scheme 86: Synthesis of polyesters by ester interchange between a dicarboxylic acid and a diester.

Ring-opening polymerization (ROP) is one of the methods for synthesizing polyesters using cyclic monomers and oligomers (Scheme 87). This process can form high molecular weight polymers (> 105 kg/mol) without any side products.
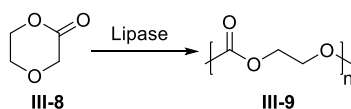
Scheme 87: Ring-opening polymerization to synthesis of polyester.

Aliphatic polyesters can be synthesized from lactones using different catalysis methods [168], such as anionic [169], cationic [169], organometallic [170], or enzyme-based catalysis [171]. These methods allow for very mild reaction conditions. In recent years, several catalytic methods for the copolymerization of epoxides with cyclic anhydrides have also been developed, which can form a wide range of functional polyesters, both saturated and unsaturated. The ring-opening polymerization of lactones and lactides is widely used in industrial production [171].

II.2. Results and discussion

In 2019, Philippe Biallas and his colleagues [172] conducted research on the synthesis and reactivity of small molecules that contain geminal diazido groups. Their study focused on developing a method for synthesizing polyamides that have a gem-diazo block, **II-12**. To achieve this, they proposed a polymerization process that involves direct polyamidation of simple diamines **II-11** and malonate monomers **II-10** with pre-existing diazido functional groups (Scheme 88). This innovative approach eliminated the need for activating reagents and allowed for the process to be carried out at room temperature.
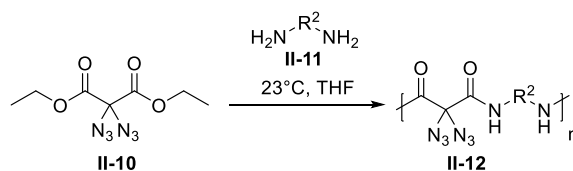
Scheme 88: Synthesis of polyamide with gem-diazo units.

The polyamides synthesized in the study contain highly reactive gem-diazido units, which make them promising materials for use in energetic applications. Furthermore, the stability and sensitivity of these materials can be readily adjusted

to suit different applications, making them even more versatile. These findings hold great potential for researchers in various fields who are focused on developing new materials with potential applications.

Polyamide is a highly functional material with a lot of potential, but the possibilities to synthesize polyester with gem-diazo units should not be overlooked. Polyester is a material with an incredibly wide range of applications, and incorporating gem-diazo units could open up even more possibilities. This research proposes the synthesis of new polyesters that incorporate gem-diazo, with the goal of exploring their future applications.

Incorporating gem-diazo units into these materials has the potential to greatly improve their properties and create new opportunities for their use. These new materials are expected to exhibit unique characteristics that differentiate them from existing polyester materials. The goal of this research is to create materials that not only meet current needs, but also offer new possibilities for innovation and discovery.

The proposed Scheme 89 outlines a method for synthesizing new polyesters. This involves the use of either malonate ether or diazidomalonate as monomers (M_1), which can be incorporated into either polyester. There are two possible routes to synthesizing these polymers. The first method involves synthesizing a polyester **II-14** (a) and then carrying out azidation (b) of the polymer. Alternatively, the second method involves directly carrying out azidation of malonate **II-13** and then synthesizing the polyester (c). This study aims to explore two different methods and compare their effectiveness. By comparing the outcomes of each approach, a better understanding of the advantages and disadvantages of each method can be gained, which can be useful for future research in this field.

II-14

R^1=H; N_3.
R^2= OCH_3; OC_2H_5; OH.
R^3= C_4H_8 ; C_6H_{12} ; $C_6H_{12}O_2$.
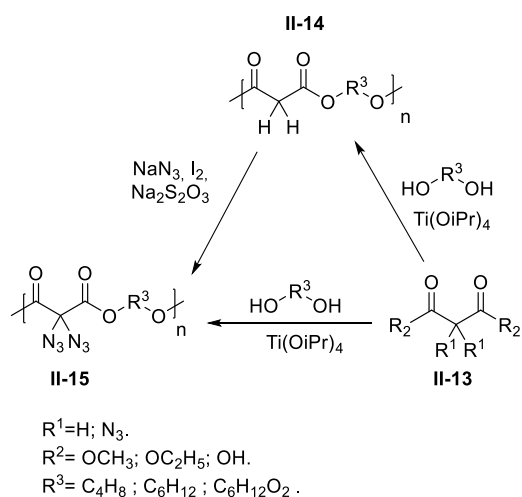
Scheme 89: Synthetic rout for synthesis of polyester/polyurethanes with gem-diazo units.

To begin the process for method (c) (Scheme 89), first was prepared the monomer via conducting an azidation reaction of diethyl malonate **II-16** in the presence of NaN_3 (6 eq.) and I_2 (2.2 eq.) in a mixture of $DMSO/H_2O$ (2:1) at 50 °C for 2 hours with future addition of $Na_2S_2O_3$ solution to form diazide **II-17** (Scheme 90).
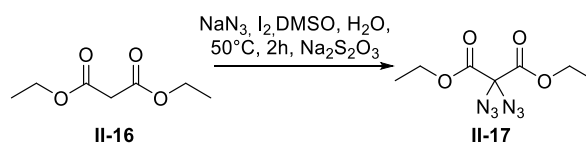
Scheme 90: Synthesis of monomer.

The synthesize polyester **II-20** was performed from the reaction between butane-1,4-diol **II-18** and malonyl chloride **II-19** in the presence of Et_3N in DCM for 24 hours. Unfortunately, the product did not form (as shown on the Scheme 91).
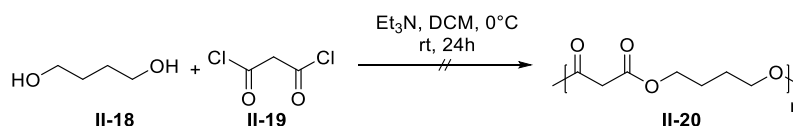
Scheme 91: Synthesis of polyester.

100

The polycondensation under higher temperatures and a high vacuum in the presence of Ti(OiPr)$_4$ was tested, which gave us the desired polymer. However, from the literature, the Ti(OiPr)$_4$ is not the only catalyst that can be used for polycondensation. Sm(OiPr)$_3$, Ti(OEt)$_4$, Zr(OBu)$_4$, Ge(OEt)$_4$, Nb(OEt)$_5$, and Ta(OEt)$_5$ are also suitable options [173]. Despite this, the Ti(OiPr)$_4$ was chosen because it could provide a higher yield and number-average molar mass (Mn) for the polyester according to the literature [173].

To optimize the conditions for polycondensation in the second step, experiments were conducted with varying times and pressures. The results of these experiments are presented in Table 14.

Table 14: Optimal time and pressure to obtained soluble polyester from condensation of **II-21** and **II-22** (Ti(OiPr)$_4$, THF, 120°C).

Entry	Time [h]	Pressure [mbar]	Yield [%]	Solubility in THF
1	6	10	78	no
2	8	10	61	no
3	4 65	190 19	56	yes

R^1=H ; N$_3$.
R^3= C$_4$H$_8$; C$_6$H$_{12}$; C$_6$H$_{12}$O$_2$.
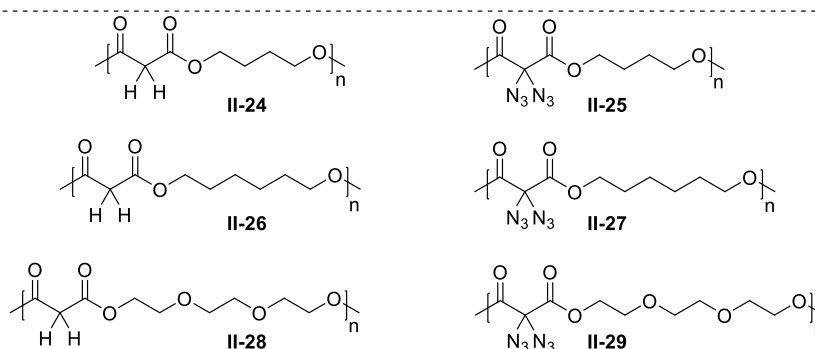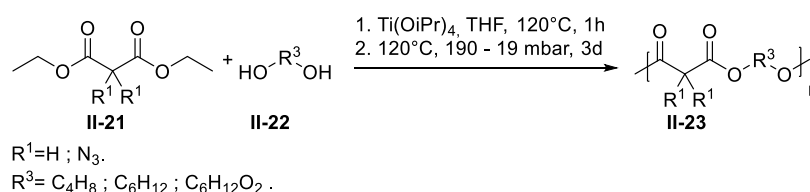
Scheme 92: Synthesis of new polyester by organometallic catalytic method.

Boiling the mixture under an argon atmosphere for one hour was found to be sufficient for the first step. Next, the condenser was switched to a septum and a mobile, non-oily pump was attached to determine the optimal conditions for the next step. The timing of turning on the vacuum was crucial since the reaction was already at a high temperature of 120 °C, which is above the boiling point of THF. The reaction mixture had a high probability of being absorbed by the pump. To prevent this, a small Schlenk flask with a faucet was used, and the pump was connected to the faucet. The faucet was gradually opened to reduce the pressure to around 200 mbar, which significantly reduced the solvent in the reaction mixture. The reaction was then allowed to proceed for 3-4 hours under this pressure. Additionally, it was important to control the mixing of the reaction mixture to prevent splashing in the bottle, which could lead to uneven reactions. The next step involved reducing the pressure to 19-10 mmbar over 65 hours. The resulting yellow product was dissolved in THF and purified in cold MeOH (Scheme 92). This procedure was used for both methods (a) and (c) for synthesis of polyesters (Scheme 89). The six new linear polyester were synthetized with yield from 50% till 74% and n from 5 till 18, as Shown in Table 15.

Table 15: Results of the polycondensations of polyesters in THF with Ti(OiPr)$_4$ at 120 °C. (* Measured by GPC and the molar masses were calibrated to polystyrene as an internal standard).

Polymer	n*	M_n* [g/mol]	Đ*	Yield [%]
II-24	16	2960	2.8	56
II-25	5	1290	2.8	61
II-26	18	3960	3.7	50
II-27	7	2100	3.5	52
II-28	15	3730	1.6	74
II-29	7	2430	2.1	73

Azidation was performed on the polyesters using 6 eq. of NaN$_3$ and 2.2 eq. of I$_2$ in a mixture of DMSO/THF (2:1) at 50 °C for 2 hours, Na$_2$S$_2$O$_3$ solution was added to form a polyester diazide **II-31**. The new three polymers were obtained with yield from 63 to 87% and n from 10 to 12 (Table 16).
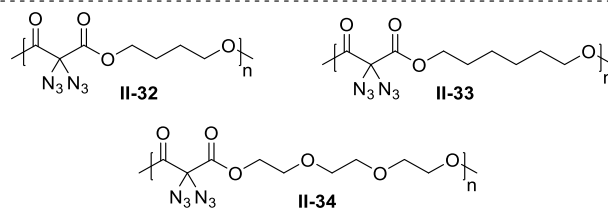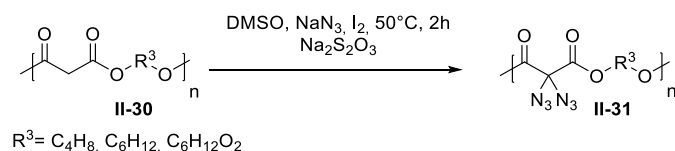
Scheme 93: Azidation of polyesters.

Table 16: Analytical characteristic of Azidation of polyesters. (* [a] Measured by GPC and the molar masses were calibrated to polystyrene as an internal standard, [b] Measured by DSC, [c] Measured by TGA).

Polymer	n	M_n^a [g/mol]	$Đ^a$	Yield [%]	T_g^b [°C]	$T_{decomp.}^c$ [°C]
II-32	10	2660	2.4	63	-	149
II-33	12	3600	2	68	93	147
II-34	11	3730	1.6	87	134	160

All polymers were characterized by ^{1}H NMR, ^{13}C NMR, IR, and GPC (Table 15 and Table 16). In ^{1}H NMR spectra obtained in CDCl$_3$, all polyesters showed a characteristic proton signal at 3.3 ppm, which disappeared after azidation. polyester was further confirmed by IR, where a noticeable shift to 2117.7 cm^{-1} was observed, as shown on Figure 25.
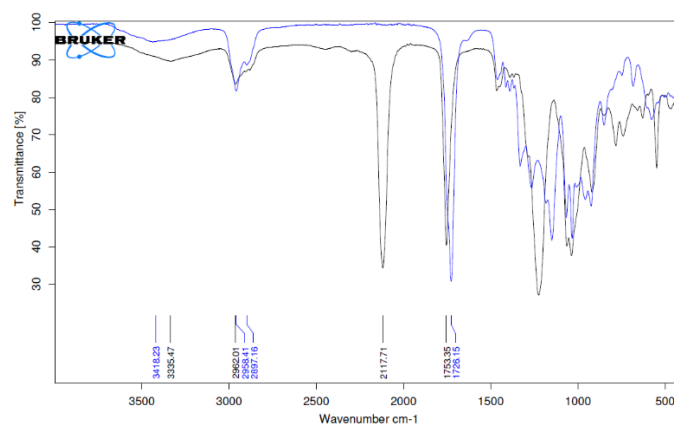
Figure 25: IR measurements of polyester **II-30** (blue) and polyester with gem-diazo units **II-32** (black).

According to Table 15, polyesters synthesized from diazo malonic ester have chains that are two times shorter than those synthesized from malonic ester, despite no change in reaction conditions. This phenomenon is consistently observed across all polyesters with gem-diazo units. However, if polyester with gem-diazo units is synthesized by azidation of the polyester chain, the chain length will only shorter in 1.5 times. Therefore, the synthesis of polyester with gem-diazo units by azidation of polyester is more advantageous.
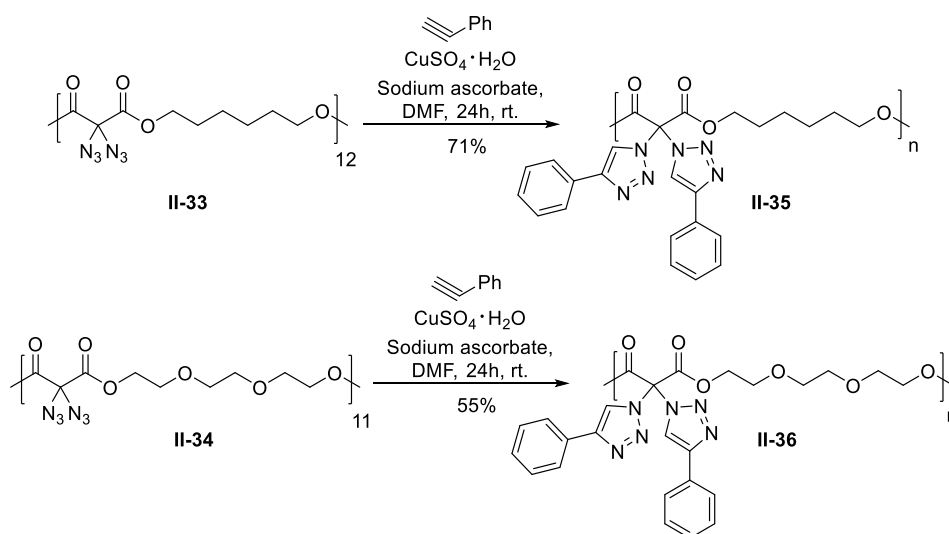
Scheme 94: The click reactions of **II-33** and **II-34**.

The next step involved studying click chemistry with these new polyesters (Scheme 94). Polyester **II-32** was reacted with phenylacetylene, $CuSO_4 \cdot H_2O$, and sodium ascorbate in DMF for 24 hours to synthesize a polyester with two triazole rings. During the reaction, the polymer transformed from a gel to a solid state, and its solubility significantly increased. The triazole polyester was isolated with a yield of 71% and Mn = 3 830 g/mol, Đ = 1.4, n = 8. Additionally, polymer **II-34** was also subjected to click chemistry, resulting in the isolation of a new triazole polyester with a yield of 55% and Mn = 2 550 g/mol, Đ = 1.6, n = 5. However, it remained in the gel form.

Figure 26 show the IR spectra of polyester **II-33** (blue) and the two modified polyesters, **II-35** (red) and **II-36** (black). It is visible that the formation of the triazole ring at 2957 cm^{-1} and 3125 cm^{-1}. Furthermore, the strong azide signal disappears, but **II-36** still retains a small amount of azido groups.
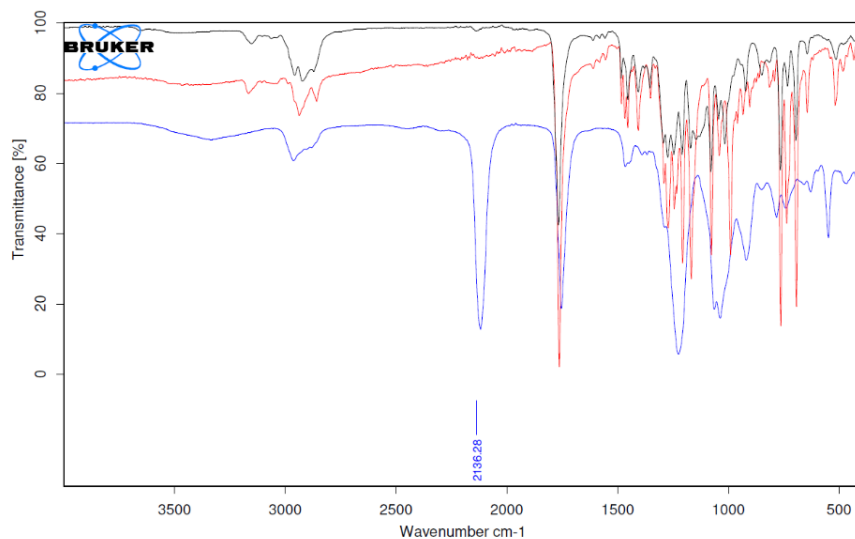
Figure 26: IR measurements of polyester **II-33** (blue) and polyester with triazole ring **II-35** (black) **II-36** (red).

II.3. Conclusions

In summary, two synthetic routes were employed to synthesize polyester with gem-diazo units. The diazo malonate monomer was used to synthesize polyester, which resulted in a shorter polymer chain length of 0.5 time in comparison to the polymer synthesized by direct polyester azidation. The characterization of the polyesters was carried out using NMR, IR, and GPC techniques. The yields of the polyesters ranged from 56% till 87%, with Mn values ranging from 1 290 g/mol till 3 960 g/mol, Đ values ranging from 1.6 till 3.7, and n_w (weight average degree of polymerization) values ranging from 5 till 18. Importantly, our proposed methods of synthesis and these polyesters have not been described in the literature before. Additionally, the newly synthesized polyesters were successfully subjected to click chemistry. The polyesters with triazole rings were isolated with 55%-71% of yield. The highly reactive geminal diazido units present in the new polyester could potentially make them interesting as energetic materials, with easily adjustable stabilities and sensitivities.

III: Experimental part

III.1. General methods. In the general methods section, we used heated glassware under an argon atmosphere and dry solvents for reactions involving substances sensitive to oxygen or moisture. Cryostats were used to regulate temperature for reactions carried out between 0 °C to -90 °C, and oil baths filled with paraffin oil were used for heating, with temperature monitored using a contact thermometer.

III.2. Solvents. Commercially purchased reagents and solvents were used, and for column chromatography, ethyl acetate and cyclohexane were freshly distilled. THF and DCM were obtained using an MB-SPS 800 solvent purification system from MBraun GmbH, while all other dry solvents and deuterated solvents for NMR spectroscopy were commercially purchased.

III.3. Chromatographic methods. Chromatographic methods involved the use of aluminum TLC plates with silica gel 60 F254 from Merck for thin layer chromatography (TLC). The substances were then stained using various methods, including ultraviolet detection at a wavelength of 254 nm or immersion in potassium permanganate solution. To make the substances visible, they were further heated with hot air.

III.4. Apparatus. ^{1}H nuclear magnetic resonance (NMR) and ^{13}C NMR analyses were measured on Bruker 600 MHz FT-NMR, 400 MHz FT-NMR spectrometers using CDCl$_3$ and DMSO-d6 as solvent. Chemical shifts are given in ppm on a scale δ relative to tetramethylsilane (δ = 0 ppm) and the bond constants J in Hz. Before evaluation, the spectra were calibrated to the remaining proton signals of the solvent used.

High-resolution mass spectra (HRMS) were either carried out using ESI on a micrOTOF mass spectrometer from Bruker or FD ionization on a JEOL-TOF.

IR spectra: Bruker FT-IR-Spectrometer ALPHA; attenuated total reflection (ATR) technique in the range of 400–4000 cm^{-1}.

Ultraviolet/visible (UV-vis) absorption spectra: Mettler Toledo spectrophotometer at wavelength of maximum absorption (λ_{max}, nm).

The molecular weights of polymers (**I-108a-e**, **I-109a**, **I-122a-d**, **I-123a**, **I-201**) were obtained by Gel Permeation Chromatography PSS/Agilent SECurity²-GPC using DMAc + LiBr (0.28 g/L) at 50°C as eluent. The system comprised an autoinjector, a precolumn (7 um), PFG columns (100 A, 1000 A and 4000 A), and a refractive-index detector (RID). The GPC system was calibrated with linear poly(methyl methacrylate) standards (M_n 800–2 200 000 Da) and the samples were injected with a maximum concentration of 2 g L^{-1}.

The molecular weights of polymers (**I-204**, **I-205**, **I-208**, **I-212**, **I-214**, **I-216**, **I-218a**, **I-221a-b**, **I-222**, **I-223**, **II-24 – II-29**, **II-32 – II-34**, **II-35**, **II-36**) were obtained by Gel Permeation Chromatography An Agilent SECcurity GPC system with a diode array detector (ALS G1329A) and a refractive index detector (G1362A) was used to determine the molar mass distributions of the polymers by GPC. A set of columns consisting of 2 PSS SDV Linear M (8 x 300 nm, particle size: 5µm) and one PSS SDV precolumn (8 x 300 nm, particle size: 5 µm) were used at room temperature with THF as eluents. The flow rate used was 1 ml/min and the molar masses were calibrated to polystyrene as an internal standard.

Thermogravimetric analysis (TGA) and Differential scanning calorimetry (DSC) measurements were simultaneously carried out using a Netzsch STA 449 F5 Jupiter instrument. Experiments were conducted in crucibles, which were closed with lids. Samples were heated from 25°C to 400°C with a heating rate of 5 K min^{-1} in a nitrogen atmosphere applying a constant nitrogen flow of 25 ml min^{-1}.

III.5. Experimental methods. Transmission of polymeric dyes with hydrazono-pyrazolones fragment was recorded on spectrophotometer Specord 200 plus (Analytik Jena AG) in the spectral range of 300-700 nm. Whereas, spectroscopic ellipsometry (SE) was used to characterize the optical properties such as refractive index (*n*) and the extinction coefficient (*k*) of the thin films of the methacrylic polymeric dyes incorporating hydrazono-pyrazolones moiety. SE measurements were made using a V-VASE ellipsometer (J.A. Woollam Co., Inc., Lincoln, NE, USA) in the range of 250-800 nm. Three angles of incidence (65°, 70°, 75°) were used.

The complex dielectric functions (i.e. $\tilde{\varepsilon} = \varepsilon_1 + i\varepsilon_2$, where $\varepsilon_1 = n^2 - k^2$ and $\varepsilon_2 = 2nk$ are the real and imaginary parts, respectively, whereas, $k = \frac{\alpha\lambda}{4\pi}$ is the extinction coefficient, α is the absorption coefficient, λ is wavelength) for the investigated thin films were determined directly from the ellipsometric data using the WVASE32 software. The optical constants were parameterized using Gauss-shape dispersion relation in the absorption region

III.6. Methods of synthesis
III.6.1. Part I: Design and Synthesis of Novel Polymeric Dyes Incorporating Pyrazolone Units

4-Hydrazineylphenol

I-111
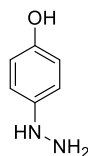
4-hydrazineylphenol
Chemical Formula: $C_6H_8N_2O$
Exact Mass: 124,0637

The concentrated hydrochloric acid (3.7 ml) was added to a suspension of 4-aminophenol **I-110** (3 g, 27.4 mmol) in water (5.5 ml). The mixture cooled to -10°C under nitrogen. The solution of sodium nitrite (1.89 mg, 27.4 mmol) in water (5.5 ml) was added dropwise to the mixture. After completion of the addition, the reaction mixture was stirred 30 minutes at -10 °C. In additional flask was dissolved tin(II)chloride dehydrate (13 g, 68.7 mmol) in 6M hydrochloric acid (16 ml). Then fresh the diazotization mixture was added in the solution of $SnCl_2$ and reaction mixture stirred additional 3.5 h at -10 °C. The formed solid **I-111** was filtered and washed with small portion of water and drying in height vacuum. The product formed with 98% (4.33 g, 26.7 mmol). This hydrazine is sensitive to air.

^{1}H NMR (600 MHz, DMSO-d_6) δ 9.6 (dd, J = 128.7, 89.5 Hz, 2H), 9.1 (s, 1H), 6.9 – 6.8 (m, 2H), 6.7 – 6.6 (m, 2H) [ppm].

^{13}C NMR (101 MHz, DMSO-d_6) δ 153.0, 137.3, 121.0, 117.9, 115.8, 115.4 [ppm].

HRMS: ESI-mass m/z calcd. for $C_6H_9N_2O$: 125.0709 and found: 125.0708
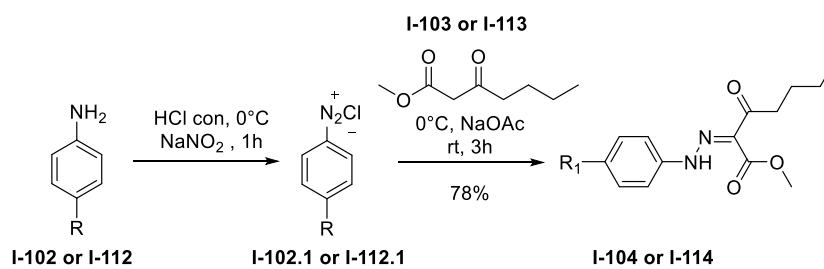
a: R$_1$ = H, b: R$_1$= CN, c: R$_1$ = Br, d: R$_1$ = OCH$_3$, e: R$_1$ = OH

General procedure for synthesis of hydrazono derivatives**(A)**:

Diazotization of substituted anilines

A solution of the **I-102** (1 eq.) in concentrated HCl (12 eq.) was cooled to 0–5 °C then cold sodium nitrite solution (2.2 eq.) in water was added dropwise to the reaction mixture. The reaction mixture was stirred for 1 h. The diazotization process was confirmed by using *β*-naphthol solution as an indicator of diazonium salt.

*The preparation of **I-104**.*

The fresh preparate diazonium salt was added dropwise to an ice-cold mixture of the appropriate active methyl 3-oxoheptanoate **I-103** (1 eq.) and 10% NaOH in ethanol and stirred 1h at 0 °C and then additional 3h at rt. The precipitation was filtered and washed with water, dried under high vacuum. The compound recrystallized from ethanol and gave the product as yellow solid.

Methyl (Z)-2-(2-(4-hydroxyphenyl)hydrazineylidene)-3-oxoheptanoate

I-104
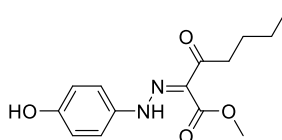
methyl (*Z*)-2-(2-(4-hydroxyphenyl)hydrazineylidene)-3-oxoheptanoate
Chemical Formula: C$_{14}$H$_{18}$N$_2$O$_4$
Molecular Weight: 278,3080

Following procedure, A, the aniline **I-102** (1 g, 9.16 mmol) was solubilized in con. HCl solution (3.3 ml) and solution of NaNO$_2$ (1.4 g, 20.16 mmol) in water (10 ml) was adding. The fresh preparate diazonium salt (9.16 mmol) was added dropwise to an ice-cold mixture of the appropriate active methyl 3-oxoheptanoate **I-103** (1.36

111

ml, 19.6 mmol) and 10% NaOH (5 ml) in ethanol (19 ml). The compound recrystallized from ethanol and gave the product as yellow solid with yield 78% (996 mg, 3.58 mmol).

Rf = 0.53 (Cy/EtOAc = 3/2).

^{1}H NMR (600 MHz, CDCl$_3$) δ 12.9 (s, 1H, NH), 7.3 (m, 1H), 7.2 (m, 1H), 6.9 – 6.8 (m, 2H), 3.8 (s, 2H), 3.8 (s, 1H), 2.9 (dd, *J* = 7.8, 7.1 Hz, 1H), 2.9 – 2.8 (m, 1H), 1.6 (dp, *J* = 20.0, 7.5 Hz, 2H), 1.3 (hd, *J* = 7.4, 5.4 Hz, 2H), 0.9 (td, *J* = 7.4, 0.8 Hz, 3H) [ppm].

HRMS: ESI-mass m/z calcd. for C$_{14}$H$_{18}$N$_2$NaO$_2$: 301.1159 and found: 301.1164.

The analytical data are identical to the literature data [174].

Methyl (Z)-3-oxo-2-(2-phenylhydrazineylidene)heptanoate

I-114a
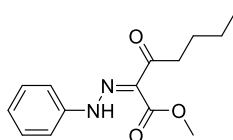
methyl (*Z*)-3-oxo-2-(2-phenylhydrazineylidene)heptanoate
Chemical Formula: C$_{14}$H$_{18}$N$_2$O$_3$
Molecular Weight: 262,3090

Following procedure, A, the aniline **I-112a** (1 ml, 10.95 mmol) was solubilized in con. HCl solution (4 ml) and solution of NaNO$_2$ (1.66 g, 24.1. mmol) in water (0.5 ml) was adding. The fresh preparate diazonium salt (10.95 mmol) was added dropwise to an ice-cold mixture of the appropriate active methyl 3-oxoheptanoate **I-113** (1.59 ml, 10.75 mmol) and 10% NaOH (12.5 ml) in ethanol (50 ml). The compound recrystallized from ethanol and gave the product as yellow solid with yield 45% (1.29 g, 4.93 mmol).

^{1}H NMR (600 MHz, CDCl$_3$) δ 12.7 (s, 1H), 7.4 – 7.3 (m, 3H), 7.3 (d, *J* = 8.0 Hz, 1H), 7.1 (q, *J* = 7.4 Hz, 1H), 3.8 (d, *J* = 15.3 Hz, 3H), 2.9 (t, *J* = 7.4 Hz, 1H), 2.9 (d, *J* = 7.5 Hz, 1H), 1.7 – 1.5 (m, 2H), 1.3 (p, *J* = 8.0 Hz, 2H), 0.9 (td, *J* = 7.4, 3.0 Hz, 3H) [ppm].

^{13}C NMR (151 MHz, CDCl$_3$) δ 200.1, 197.4, 165.7, 164.7, 142.0, 129.9, 125.2, 116.7, 115.8, 52.3, 38.6, 27.2, 22.9, 14.3 [ppm].

HRMS: ESI-mass m/z calcd. for C$_{14}$H$_{18}$N$_2$NaO$_3$: 285.1210 and found: 285.1209.

Methyl (Z)-2-(2-(4-cyanophenyl)hydrazineylidene)-3-oxoheptanoate

I-114b
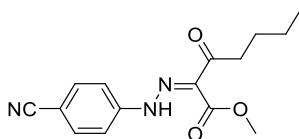
methyl (*Z*)-2-(2-(4-cyanophenyl)hydrazineylidene)-3-oxoheptanoate
Chemical Formula: $C_{15}H_{17}N_3O_3$
Molecular Weight: 287,3190

Following procedure, A, the aniline **I-112b** (1 g, 8.46 mmol) was solubilized in con. HCl solution (3 ml) and solution of $NaNO_2$ (1.28 g, 18.62 mmol) in water (0.4 ml) was adding. The fresh preparate diazonium salt (8.46 mmol) was added dropwise to an ice-cold mixture of the appropriate active methyl 3-oxoheptanoate **I-113** (1.26 ml, 8.46 mmol) and 10% NaOH (4.3 ml) in ethanol (17 ml). The compound recrystallized from ethanol and gave the product as yellow solid with yield 68% (1.64 g, 5.72 mmol).

^{1}H NMR (600 MHz, CDCl$_3$) δ 12.6 (s, 1H), 7.7 – 7.6 (m, 2H), 7.4 – 7.3 (m, 2H), 3.9 (s, 3H), 2.9 (m, 2H), 1.7 – 1.6 (m, 2H), 1.4 (m, 2H), 0.9 (t, *J* = 7.4 Hz, 3H) [ppm].

^{13}C NMR (101 MHz, CDCl$_3$) δ 200.3, 196.7, 163.8, 145.2, 133.9, 129.2, 118.7, 116.3, 115.5, 108.0, 107.4, 52.4, 42.0, 38.4, 26.5, 26.1, 22.4, 22.2, 13.9 [ppm].

HRMS: ESI-mass m/z calcd. for $C_{15}H_{17}N_3NaO_3$: 310.1162 and found 310.1163.

Methyl (Z)-2-(2-(4-bromophenyl)hydrazineylidene)-3-oxoheptanoate

I-114c
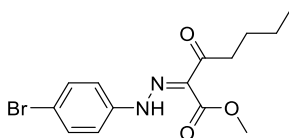
methyl (*Z*)-2-(2-(4-bromophenyl)hydrazineylidene)-3-oxoheptanoate
Chemical Formula: $C_{14}H_{17}BrN_2O_3$
Molecular Weight: 341,2050

Following procedure, A, the aniline **I-112c** (1 g, 5.81 mmol) was solubilized in con. HCl solution (2.1 ml) and solution of $NaNO_2$ (0.882 g, 12.79 mmol) in water (0.3 ml) was adding. The fresh preparate diazonium salt (5.81 mmol) was added dropwise to an ice-cold mixture of the appropriate active methyl 3-oxoheptanoate **I-113** (0.860 ml, 5.81 mmol) and 10% NaOH (3 ml) in ethanol (12 ml). The compound

recrystallized from ethanol and gave the product as yellow solid with yield 52% (1 g, 3.05 mmol).

^{1}H NMR (600 MHz, CDCl$_3$) δ 12.7 (s, 1H), 7.5 (m, 2H), 7.3 (m, 1H), 7.2 (m, 1H), 3.9 (s, 2H), 3.9 (s, 1H), 3.0 (m, 1H), 2.9 (m, 1H), 1.7 – 1.6 (m, 2H), 1.4 (dt, J = 14.5, 7.3 Hz, 2H), 0.9 (td, J = 7.4, 2.0 Hz, 3H) [ppm].

^{13}C NMR (101 MHz, CDCl$_3$) δ 200.5, 197.4, 164.7, 141.3, 133.1, 118.2, 117.4, 52.6, 42.3, 38.7, 27.3, 23.0, 14.4 [ppm].

HRMS: ESI-mass m/z calcd. for C$_{14}$H$_{17}$BrN$_2$NaO$_3$: 363.0315 and found 363.0321.

Methyl (Z)-2-(2-(4-methoxyphenyl)hydrazineylidene)-3-oxoheptanoate

I-114d
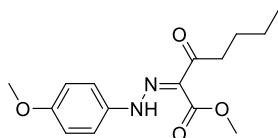
methyl (*Z*)-2-(2-(4-methoxyphenyl)hydrazineylidene)-3-oxoheptanoate
Chemical Formula: C$_{15}$H$_{20}$N$_2$O$_4$
Molecular Weight: 292,3350

Following procedure, A, the aniline **I-112d** (1 g, 8.12 mmol) was solubilized in con. HCl solution (2.9 ml) and solution of NaNO$_2$ (1.23 g, 17.86 mmol) in water (0.2 ml) was adding. The fresh preparate diazonium salt (8.12 mmol) was added dropwise to an ice-cold mixture of the appropriate active methyl 3-oxoheptanoate **I-113** (1.20 ml, 8.12 mmol) and 10% NaOH (17 ml) in ethanol (4 ml). The compound recrystallized from ethanol and gave the product as yellow solid with yield 55% (1.30 g, 4.48 mmol).

^{1}H NMR (400 MHz, CDCl$_3$) δ 12.9 (s, 1H), 7.4 – 7.3 (m, 1H), 7.3 – 7.2 (m, 1H), 6.9 (m, 2H), 3.9 (s, 2H), 3.8 (s, 1H), 3.8 (d, J = 3.6 Hz, 3H), 3.0 – 2.9 (m, 1H), 2.9 – 2.8 (m, 1H), 1.7 – 1.6 (m, 2H), 1.4 – 1.3 (m, 2H), 0.9 (m, 3H) [ppm].

^{13}C NMR (101 MHz, CDCl$_3$) δ 199.5, 197.0, 164.6, 157.9, 135.4, 125.4, 117.8, 116.8, 114.9, 55.5, 41.6, 38.2, 27.0, 22.5, 13.9 [ppm].

HRMS: ESI-mass m/z calcd. for C$_{15}$H$_{20}$N$_2$NaO$_4$: 315.1315 and found 315.1315.

General procedure for cyclisation reactions **(B)**:

The mixture of aromatic hydrazine derivatives **I-104** or **I-114** (1 eq.) and sodium acetate (1 eq.) was dissolved in a solvent mixture of ethanol and water (3:1). The mixture was stirred at room temperature for 5 minutes. Subsequently, hydrazones **I-106** or **I-115** (1 eq.) was added to the mixture. The resulting mixture was stirred under reflux for 3 hours. After completion of the reaction, the reaction mixture was extracted with ethyl acetate (EtOAc) and the organic phase was separated. The organic phase was then washed with water two times, followed by washing with brine. The organic phase was dried over sodium sulfate (Na_2SO_4) and concentrated under reduced pressure to remove the solvent.

(Z)-5-butyl-4-(2-(4-hydroxyphenyl)hydrazineylidene)-2-phenyl-2,4-dihydro-3H-pyrazol-3-one

I-106a
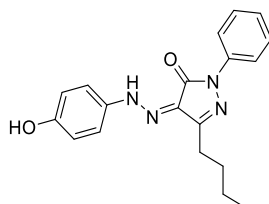
(*Z*)-5-butyl-4-(2-(4-hydroxyphenyl)hydrazineylidene)-2-phenyl-2,4-dihydro-3*H*-pyrazol-3-one
Chemical Formula: $C_{19}H_{20}N_4O_2$
Molecular Weight: 336,3950

Following procedure, B, the sodium acetate (0.470 g, 5.72 mmol), phenyl hydrazine **I-105a** (0.560 ml, 5.72 mmol) was reacted with hydroxyphenyl hydrazone **I-104** (1.59 g, 5.72 mmol) in a mixture of EtOH (7 ml) and H_2O (1.5 ml). After flash chromatography (EtOAc/Cy= 8/2), the product **I-106a** (706 mg, 2.1 mmol, 61 %) was obtained as a red solid.

Rf = 0.8 (Cy/EtOAc = 8/2).

^1H NMR (600 MHz, $CDCl_3$) δ 13.7 (s, 1H), 7.9 (m, 2H), 7.4 (m, 2H), 7.3 (m, 2H), 6.9 – 6.8 (m, 2H), 2.7 (m, 2H), 1.8 – 1.7 (m, 2H), 1.4 (dt, *J* = 14.7, 7.4 Hz, 2H), 0.9 (t, *J* = 7.4 Hz, 3H) [ppm].

^{13}C NMR (101 MHz, $CDCl_3$) δ 154.1, 152.1, 138.3, 135.2, 129.0, 125.2, 118.8, 117.5, 116.6, 29.9, 26.5, 22.7, 14.0 [ppm].

HRMS: ESI-mass m/z calcd. for $C_{19}H_{21}N_4O_2$: 337.1659 and found: 337.1662.

(Z)-4-(3-butyl-4-(2-(4-hydroxyphenyl)hydrazineylidene)-5-oxo-4,5-dihydro-1H-pyrazol-1-yl)benzonitrile

I-106b
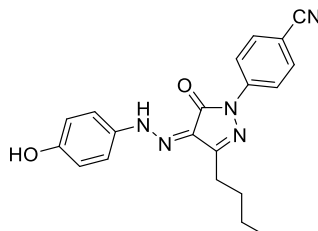
(*Z*)-4-(3-butyl-4-(2-(4-hydroxyphenyl)hydrazineylidene)-5-oxo-4,5-dihydro-1*H*-pyrazol-1-yl)benzonitrile
Chemical Formula: $C_{20}H_{19}N_5O_2$
Molecular Weight: 361,4050

Following procedure, B, the sodium acetate (0.290 g, 3.54 mmol), (4-cyanophenyl)hydrazine hydrochloride **I-105b** (0.600 g, 3.54 mmol) was reacted with hydroxyphenyl hydrazone **I-104** (0.984 g, 3.54 mmol) in a mixture of EtOH (4.5 ml) and H_2O (0.8 ml). The crude product **I-106b** (0.793 g, 2.19 mmol, 62%) was obtained as orange solid. It was directly used for the next step without further purification.

Rf = 0.24 (Cy/EtOAc = 3/2).

^{1}H NMR (600 MHz, CDCl$_3$) δ 13.6 (s, 1H), 8.2 – 8.0 (m, 2H), 7.8 – 7.6 (m, 2H), 7.4 – 7.3 (m, 2H), 7.0 – 6.7 (m, 2H), 2.7 – 2.6 (m, 2H), 1.7 (tt, *J* = 7.6, 6.6 Hz, 2H), 1.4 (h, *J* = 7.4 Hz, 2H), 0.9 (t, *J* = 7.4 Hz, 3H) [ppm].

^{13}C NMR (151 MHz, CDCl$_3$) δ 158.9, 154.7, 142.1, 135.1, 133.4, 118.4, 118.0, 116.9, 29.8, 26.6, 22.9, 14.1 [ppm].

HRMS: ESI-mass m/z calcd. for $C_{20}H_{20}N_5O_2$: 362.1612 and found: 362.1611.

(Z)-2-(4-bromophenyl)-5-butyl-4-(2-(4-hydroxyphenyl)hydrazineylidene)-2,4-dihydro-3H-pyrazol-3-one

I-106c
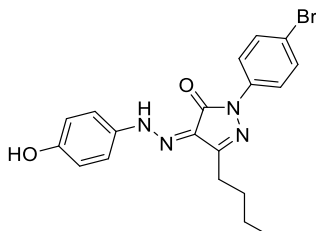
(Z)-2-(4-bromophenyl)-5-butyl-4-(2-(4-hydroxyphenyl)hydrazineylidene)-2,4-dihydro-3*H*-pyrazol-3-one

Chemical Formula: $C_{19}H_{19}BrN_4O_2$

Molecular Weight: 415,2910

Following procedure, B, the sodium acetate (220 mg, 2.68 mmol), 4-bromophenylhydrazine hydrochloride **I-105c** (0.600 g, 2.68 mmol) was reacted with methyl hydroxyphenyl hydrazone **I-104** (0.747 g, 2.68 mmol) in a mixture of EtOH (3.3 ml) and H_2O (0.7 ml). The crude product **I-106c** (0.669 g, 1.16 mmol, 60%) was obtained as red solid. It was directly used for the next step without further purification Rf = 0.34 (Cy/EtOAc = 3/1).

^{1}H NMR (600 MHz, CDCl$_3$) δ 13.6 (s, 1H), 7.9 – 7.8 (m, 2H), 7.5 (m, 2H), 7.3 (m, 2H), 6.9– 6.8 (m, 2H), 2.7 (m, 2H), 1.8 – 1.7 (m, 2H), 1.4 (dt, *J* = 14.8, 7.4 Hz, 2H), 0.9 (t, *J* = 7.4 Hz, 3H) [ppm].

^{13}C NMR (101 MHz, CDCl$_3$) δ 158.1, 154.3, 152.5, 137.3, 134.9, 132.0, 126.9, 120.2, 117.6, 116.7, 29.8, 26.4, 22.7, 13.9 [ppm].

HRMS: ESI-mass m/z calcd. for $C_{19}H_{20}BrN_4O_2$: 415.0764 and found: 415.0766.

(Z)-5-butyl-4-(2-(4-hydroxyphenyl)hydrazineylidene)-2-(4-methoxyphenyl)-2,4-dihydro-3H-pyrazol-3-one

I-106d
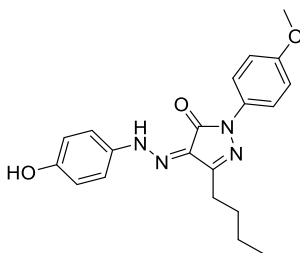
(*Z*)-5-butyl-4-(2-(4-hydroxyphenyl)hydrazineylidene)-2-(4-methoxyphenyl)-2,4-dihydro-3*H*-pyrazol-3-one
Chemical Formula: $C_{20}H_{22}N_4O_3$
Molecular Weight: 366,4210

Following procedure, B, the sodium acetate (0.180 g, 2.29 mmol), (4-methoxyphenyl)hydrazine hydrochloride **I-105d** (0.400 g, 2.29 mmol) was reacted with methyl hydroxyphenyl hydrazone **I-104** (0.637 g, 2.29 mmol) in a mixture of EtOH (2.8 ml) and H_2O (0.5 ml). The crude product **I-106d** (0.546 g, 1.49 mmol, 65%) was obtained as red solid. It was directly used for the next step without further purification.

Rf = 0.26 (Cy/EtOAc = 3/1).

^{1}H NMR (600 MHz, CDCl$_3$) δ 13.7 (s, 1H), 7.8 (m, 2H), 7.3 (m, 2H), 7.0 – 6.9 (m, 2H), 6.9 (m, 2H), 3.8 (s, 3H), 2.7 (m, 2H), 1.8 – 1.7 (m, 2H), 1.5 (dt, *J* = 14.9, 7.4 Hz, 2H), 1.0 (t, *J* = 7.4 Hz, 3H) [ppm].

^{13}C NMR (151 MHz, CDCl$_3$) δ 157.5, 157.1, 154.1, 151.7, 134.8, 131.4, 127.0, 120.6, 117.3, 117.0, 116.5, 114.1, 55.5, 29.8, 26.3, 22.5, 13.8 [ppm].

HRMS: ESI-mass m/z calcd. for $C_{20}H_{23}N_4O_3$: 367.1765 and found: 367.1765.

(Z)-5-butyl-4-(2-(4-hydroxyphenyl)hydrazineylidene)-2-(p-tolyl)-2,4-dihydro-3H-pyrazol-3-one

I-106e
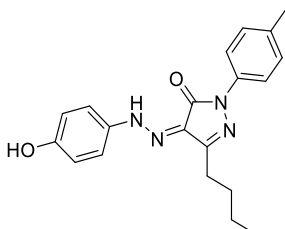
(Z)-5-butyl-4-(2-(4-hydroxyphenyl)hydrazineylidene)-2-(*p*-tolyl)-2,4-dihydro-3*H*-pyrazol-3-one
Chemical Formula: $C_{20}H_{22}N_4O_2$
Molecular Weight: 350,4220

Following procedure, B, the sodium acetate (0.310 g, 3.78 mmol), p-tolylhydrazine hydrochloride **I-105e** (0.600 g, 3.78 mmol) was reacted with methyl hydroxyphenyl hydrazone **I-104** (1.053 g, 3.78 mmol) in a mixture of EtOH (4.7 ml) and H_2O (0.9 ml). The product **I-106e** (0.248 g, 0.71 mmol, 18.7 %) was obtained as a red solid. It was directly used for the next step without further purification.

Rf = 0.75 (Cy/EtOAc = 3/2).

^{1}H NMR (400 MHz, CDCl3) δ 13.7 (s, 1H), 7.8 (m, 2H), 7.3 (m, 2H), 7.2 (m, 2H), 6.9 – 6.8 (m, 2H), 2.7 (m, 2H), 2.3 (s, 3H), 1.8 – 1.7 (m, 2H), 1.5 – 1.4 (m, 2H), 1.0 (t, *J* = 7.4 Hz, 3H) [ppm].

^{13}C NMR (101 MHz, CDCl3) δ 157.8, 154.4, 152.0, 135.7, 135.0, 134.9, 129.5, 127.1, 119.0, 118.1, 117.5, 117.2, 116.7, 116.6, 116.5, 30.0, 26.5, 22.7, 21.1, 14.0 [ppm].

HRMS: ESI-mass m/z calcd. for $C_{20}H_{22}N_4O_3$: 351.1816 and found: 351.1815.

(Z)-5-butyl-2-(4-hydroxyphenyl)-4-(2-phenylhydrazineylidene)-2,4-dihydro-3H-pyrazol-3-one

I-115a
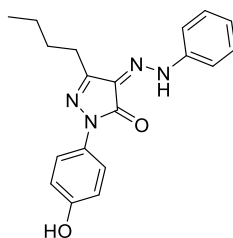
(*Z*)-5-butyl-2-(4-hydroxyphenyl)-4-(2-phenylhydrazineylidene)-2,4-
dihydro-3*H*-pyrazol-3-one
Chemical Formula: $C_{19}H_{20}N_4O_2$
Molecular Weight: 336,3950

Following procedure, B, the sodium acetate (0.204 g, 2.49 mmol), 4-hydrazineylphenol **I-111** (0.400 g, 2.49 mmol) was reacted with hydrazone **I-114a** (0.650 g, 2.49 mmol) in a mixture of EtOH (3 ml) and H_2O (0.6 ml). After flash chromatography (Cy/EtOAc = 3/2), The product (0.275 g, 0.82 mmol, 33%) was obtained as a red solid. It was directly used for the next step without further purification.

Rf = 0.2 (Pe/EtOAc = 3/1).

^{1}H NMR (600 MHz, CDCl₃) δ 13.5 (s, 1H), 7.7 – 7.6 (m, 2H), 7.4 (d, *J* = 4.4 Hz, 4H), 7.1 (hept, *J* = 4.3 Hz, 1H), 6.8 – 6.7 (m, 2H), 2.7 (t, *J* = 7.7 Hz, 2H), 1.8 (p, *J* = 7.6 Hz, 2H), 1.4 (dt, *J* = 14.8, 7.4 Hz, 2H), 0.9 (t, *J* = 7.4 Hz, 3H) [ppm].

^{13}C NMR (151 MHz, CDCl₃) δ 157.4, 154.0, 152.2, 141.2, 130.8, 129.7, 128.08, 125.9, 121.7, 115.9, 29.8, 26.4, 22.6, 13.9 [ppm].

HRMS: ESI-mass m/z calcd. for $C_{19}H_{21}N_4O_2$: 337.1659 and found: 337.1662.

(Z)-4-(2-(3-butyl-1-(4-hydroxyphenyl)-5-oxo-1,5-dihydro-4H-pyrazol-4-ylidene)hydrazineyl)benzonitrile

I-115b
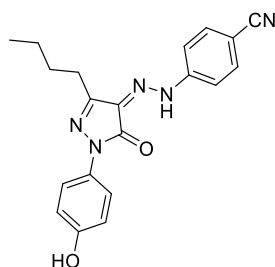
(*Z*)-4-(2-(3-butyl-1-(4-hydroxyphenyl)-5-oxo-1,5-dihydro-4*H*-
pyrazol-4-ylidene)hydrazineyl)benzonitrile
Chemical Formula: $C_{20}H_{19}N_5O_2$
Molecular Weight: 361,4050

Following procedure, B, the sodium acetate (0.255 g, 3.1 mmol), hydrazine hydrochloride **I-111** (0.500 g, 3.1 mmol) was reacted with hydrazone **I-114b** (0.850 g, 3.1 mmol) in a mixture of EtOH (3.7 ml) and H_2O (1.2 ml). After flash chromatography (Cy/EtOAc = 3/2), the product **I-115b** (0.351 g, 0.87 mmol, 28%) was obtained as a red solid. It was directly used for the next step without further purification.

Rf = 0.05 (DCM/MeOH = 9.8/0.2).

^{1}H NMR (600 MHz, CDCl$_3$) δ 13.6 (s, 1H), 8.2 – 8.1 (m, 2H), 7.7 – 7.6 (m, 2H), 7.3 (m, 2H), 6.9 – 6.8 (m, 2H), 2.7 (t, *J* = 7.7 Hz, 2H), 1.7 (p, *J* = 7.5 Hz, 2H), 1.4 (dt, *J* = 14.8, 7.4 Hz, 2H), 0.9 (t, *J* = 7.4 Hz, 3H) [ppm].

^{13}C NMR (151 MHz, CDCl$_3$) δ 158.5, 154.4, 153.1, 141.7, 134.5, 133.0, 126.3, 118.0, 117.1, 116.5, 107.4, 29.4, 26.2, 22.4, 13.7 [ppm].

HRMS: ESI-mass m/z calcd. for $C_{20}H_{19}N_5NaO_2$: 384.1431 and found 384.1433.

(Z)-4-(2-(4-bromophenyl)hydrazineylidene)-5-butyl-2-(4-hydroxyphenyl)-2,4-dihydro-3H-pyrazol-3-one

I-115c
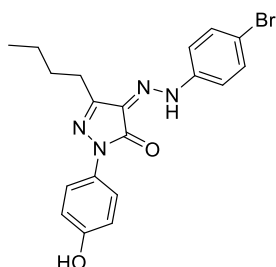
(Z)-4-(2-(4-bromophenyl)hydrazineylidene)-5-butyl-2-(4-hydroxyphenyl)-2,4-dihydro-3*H*-pyrazol-3-one
Chemical Formula: $C_{19}H_{19}BrN_4O_2$
Molecular Weight: 415,2910

Following procedure, B, the sodium acetate (0.255 g, 3.1 mmol), the hydrazine **I-111** (0.500 g, 3.1 mmol) was reacted with hydrazone **I-114c** (1.06 g, 3.1 mmol) in a mixture of EtOH (3.7 ml) and H_2O (1.2 ml). The product **I-115c** (0.248 g, 0.71 mmol, 19%) was obtained as a red solid. It was directly used for the next step without further purification.

Rf = 0.3 (DCM/MeOH = 9.5/0.5).

^{1}H NMR (600 MHz, CDCl$_3$) δ 13.5 (s, 1H), 7.8 – 7.7 (m, 2H), 7.5 (m, 2H), 7.3 – 7.2 (m, 2H), 6.9 – 6.8 (m, 2H), 2.7 – 2.6 (m, 2H), 1.8 – 1.7 (m, 2H), 1.5 – 1.4 (m, 3H), 0.9 (t, *J* = 7.4 Hz, 3H) [ppm].

^{13}C NMR (151 MHz, CDCl$_3$) δ 157.0, 153.8, 151.9, 140.1, 132.6, 130.6, 128.4, 121.3, 118.5, 117.1, 115.7, 29.5, 26.1, 22.4, 13.7 [ppm].

HRMS: ESI-mass m/z calcd. for $C_{19}H_{20}BrN_4O_2$: 415.0764 and found: 415.0763.

(Z)-5-butyl-2-(4-hydroxyphenyl)-4-(2-(4-methoxyphenyl)hydrazineylidene)-2,4-dihydro-3H-pyrazol-3-one

I-115d
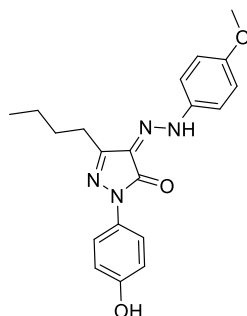
(Z)-5-butyl-2-(4-hydroxyphenyl)-4-(2-(4-methoxyphenyl)hydrazineylidene)-2,4-dihydro-3*H*-pyrazol-3-one
Chemical Formula: $C_{20}H_{22}N_4O_3$
Molecular Weight: 366,4210

Following procedure, B, the sodium acetate (0.255 g, 3.1 mmol), hydrazine **I-111** (0.500 g, 3.1 mmol) was reacted with hydrazone **I-114d** (0.910 g, 3.1 mmol) in a mixture of EtOH (3.7 ml) and H_2O (1.2 ml). The product **I-115d** (0.140 g, 0.38 mmol, 12%) was obtained as a red solid. It was directly used for the next step without further purification.

Rf = 0.25 (Cy/EtOAc = 3/1).

^{1}H NMR (400 MHz, CDCl$_3$) δ 13.7 (s, 1H), 7.8 – 7.7 (m, 2H), 7.4 – 7.3 (m, 2H), 7.0 – 6.9 (m, 2H), 6.9 – 6.8 (m, 2H), 3.8 (s, 3H), 2.7(m, 2H), 1.8 – 1.7 (m, 2H), 1.4 (dt, *J* = 14.6, 7.4 Hz, 2H), 1.0 (t, *J* = 7.4 Hz, 3H) [ppm].

^{13}C NMR (101 MHz, CDCl$_3$) δ 158.0, 157.5, 153.1, 151.7, 134.9, 127.1, 120.9, 117.2, 115.6, 115.0, 55.6, 29.8, 22.5, 13.8 [ppm].

HRMS: ESI-mass m/z calcd. for $C_{20}H_{23}N_4O_3$: 367.1765 and found: 367.1768.

General procedure **(C)** for synthesis of methacrylic monomer:

Methacrylic acid (1.0 eq.), triethylamine (2.0 eq.) and 1- ethyl-3-(3 dimethylaminopropyl)carbodiimide hydrochloride (1.0 eq.) were added to a solution of appropriate hydrazono-pyrazolone derivatives **I-106** (1.0 eq.) in dichloromethane and small amount of DMF. The mixture was stirred at room temperature for 20 h. Then, another portion of methacrylic acid (1.0 eq.), triethylamine (2 eq.) and 1-ethyl-3-(3-dimethylaminopropyl)carbodiimide hydrochloride (1.0 eq.) were added and the mixture was stirred at room temperature for additional 20 h. The precipitate was filtered and the filtrate washed with a solution of 0.1N HCl (2×20 ml), saturated

solution of NaHCO$_3$(2×20 ml), brine (20 ml) and then dried over NaSO$_4$ followed by concentration under vacuo. Column chromatography on silica gel (EtOAc/Cy 1:3) gave compounds **I-107a-e** and **I-116a-d.**

(Z)-4-(2-(3-butyl-5-oxo-1-phenyl-1,5-dihydro-4H-pyrazol-4-ylidene)hydrazineyl) phenyl methacrylate

<div align="center">

I-107a
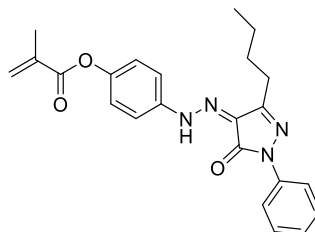
(*Z*)-4-(2-(3-butyl-5-oxo-1-phenyl-1,5-dihydro-4*H*-pyrazol-4-ylidene)hydrazineyl)phenyl methacrylate
Chemical Formula: C$_{23}$H$_{24}$N$_4$O$_3$
Molecular Weight: 404,4700

</div>

Following procedure, C, Methacrylic acid (102,3 µl, 1.21 mmol, 1.0 eq), triethylamine (0.336 ml, 2.43 mmol, 2.0 eq) and 1-ethyl-3-(3 dimethylaminopropyl)carbodiimide hydrochloride (0.232 g, 1.21 mmol, 1.0 eq) were added to a solution of appropriate **I-106a** (0.408 g, 1.21 mmol, 1.0 eq) in DCM (13.6 ml). After flash chromatography (Cy/EtOAc = 3/1), the product **I-107a** (0.253 g, 0.63 mmol, 51.5%) was obtained as orange solid.

Rf = 0.56 (Cy/EtOAc = 3/1).

^{1}H NMR (600 MHz, CDCl$_3$) δ 13.6 (s,1H), 8.0 – 7.9 (m, 2H), 7.5 – 7.4 (m, 4H), 7.2 (m, 3H), 6.4 (s, 1H), 5.8 (p, *J* = 1.5 Hz, 1H), 2.8 – 2.7 (m, 2H), 1.8 (p, *J* = 7.6 Hz, 2H), 1.5 (dt, *J* = 14.9, 7.4 Hz, 2H), 1.0 (t, *J* = 7.4 Hz, 3H) [ppm].

^{13}C NMR (101 MHz, CDCl$_3$) δ 165.7, 157.8, 152.0, 148.5, 138.8, 138.0, 135.7, 128.9, 128.3, 127.4, 125.1, 122.9, 118.6, 116.5, 29.6, 26.3, 22.5, 18.3, 13.8 [ppm].

HRMS: ESI-mass m/z calcd. for C$_{23}$H$_{25}$N$_4$O$_3$: 405.1921 and found: 405.1924.

UV-vis spectrum of monomer in THF solution: absorption shift at 396 nm.

IR(ATR): v [cm^{-1}] 3036, 2957, 2860, 1728, 1652.

(Z)-4-(2-(3-butyl-1-(4-cyanophenyl)-5-oxo-1,5-dihydro-4H-pyrazol-4-ylidene) hydrazineyl)phenyl methacrylate

I-107b
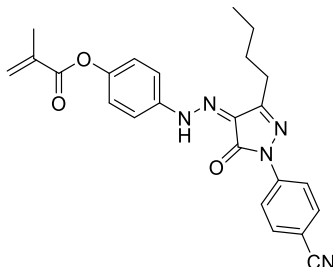
(*Z*)-4-(2-(3-butyl-1-(4-cyanophenyl)-5-oxo-1,5-dihydro-4*H*-pyrazol-4-ylidene)hydrazineyl)phenyl
methacrylate
Chemical Formula: $C_{24}H_{23}N_5O_3$
Molecular Weight: 429,4800

Following procedure, C, Methacrylic acid (116.7 µl, 1.38 mmol, 1.0 eq), triethylamine (0.384 ml, 2.77 mmol, 2.0 eq) and 1-ethyl-3-(3-dimethylaminopropyl)carbodiimide hydrochloride (0.265 g, 1.38 mmol,1.0 eq) were added to a solution of appropriate **I-106b** (0.500 g,1.38 mmol, 1.0 eq) in DCM (15.5 ml). After flash chromatography (Cy/EtOAc = 3/1), the product **I-107b** (0.344 g, 0.8 mmol, 58%) was obtained as orange solid.

Rf = 0.54 (Cy/EtOAc = 3/1).

^{1}H NMR (400 MHz, CDCl$_3$) δ 13.5 (s, 1H), 8.2 – 8.1 (m, 2H), 7.7 – 7.6 (m, 2H), 7.5 – 7.4 (m, 2H), 7.2 (m, 2H), 6.3 (p, *J* = 1.0 Hz, 1H), 5.8 (p, *J* = 1.5 Hz, 1H), 2.8 – 2.7 (m, 2H), 1.3 (p, *J* = 7.5 Hz, 2H), 1.5 – 1.4 (m, 2H), 1.0 (t, *J* = 7.4 Hz, 3H), [ppm].

^{13}C NMR (101 MHz, CDCl$_3$) δ 165.8, 158.5, 153.4, 149.0, 141.7, 138.6, 135.7, 133.2, 127.8, 123.2, 119.0, 118.2, 116.9, 107.9, 29.5, 26.4, 22.6, 18.5, 13.9 [ppm].

HRMS: ESI-mass m/z calcd. for $C_{24}H_{23}N_5NaO_3$: 452.1693 and found: 452.1684.

UV-vis spectrum of monomer in THF solution: absorption shift at 398 nm.

IR(ATR): v [cm^{-1}] 3115, 2954, 2873, 2224, 1730, 1657.

(Z)-4-(2-(1-(4-bromophenyl)-3-butyl-5-oxo-1,5-dihydro-4H-pyrazol-4-ylidene) hydrazineyl)phenyl methacrylate

I-107c
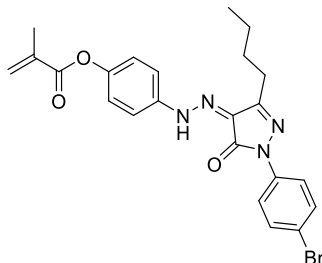
(Z)-4-(2-(1-(4-bromophenyl)-3-butyl-5-oxo-1,5-dihydro-4H-
pyrazol-4-ylidene)hydrazineyl)phenyl methacrylate
Chemical Formula: $C_{23}H_{23}BrN_4O_3$
Molecular Weight: 483,3660

Following procedure, C, Methacrylic acid (101.6 µl, 1.20 mmol, 1.0 eq), triethylamine (0.334 ml, 2.41 mmol 2.0 eq) and 1-ethyl-3-(3-dimethylaminopropyl)carbodiimide hydrochloride (0.230 g, 1.20 mmol, 1.0 eq) were added to a solution of appropriate **I-106c** (0.500 g, 1.2 mmol, 1.0 eq) in DCM (13.5 ml). After flash chromatography (Cy/EtOAc = 3/1), the product **I-107c** (0.227 g, 0.47 mmol, 39 %) was obtained as orange solid.

Rf = 0.7 (Cy/EtOAc = 3/1).

^{1}H NMR (400 MHz, CDCl$_3$) δ 13.6 (s, 1H), 7.9 (m, 2H), 7.5 (m, 2H), 7.5 − 7.4 (m, 2H), 7.2 (m, 2H), 6.3 (q, J = 1.1 Hz, 1H), 5.8 (q, J = 1.5 Hz, 1H), 2.8 − 2.7 (m, 2H), 1.8 (p, J = 7.5 Hz, 2H), 1.4 (dd, J = 15.6, 8.2 Hz, 2H), 1.0 (t, J = 7.4 Hz, 3H) [ppm].

^{13}C NMR (151 MHz, CDCl$_3$) δ 165.7, 157.8, 152.3, 148.6, 138.7, 137.1, 135.6, 131.8, 128.0, 127.5, 122.9, 119.9, 117.9, 116.6, 29.5, 26.3, 22.5, 18.3, 13.8 [ppm].

HRMS: ESI-mass m/z calcd. for $C_{23}H_{24}BrN_4O_3$: 483.1026 and found: 483.1016.

UV-vis spectrum of monomer in THF soluteon: absorption shift at 396 nm.

IR(ATR): v [cm^{-1}] 3105, 2954, 2859, 1727, 1638.

(Z)-4-(2-(3-butyl-1-(4-methoxyphenyl)-5-oxo-1,5-dihydro-4H-pyrazol-4-ylidene) hydrazineyl)phenyl methacrylate

I-107d
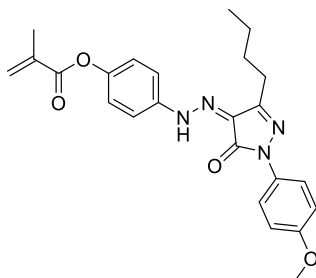
(Z)-4-(2-(3-butyl-1-(4-methoxyphenyl)-5-oxo-1,5-dihydro-
4H-pyrazol-4-ylidene)hydrazineyl)phenyl methacrylate
Chemical Formula: $C_{24}H_{26}N_4O_4$
Molecular Weight: 434,4960

Following procedure, C, Methacrylic acid (120 μl, 1.43 ml, 1.0 eq), triethylamine (0.397 ml, 2.87 mmol, 2.0 eq) and 1-ethyl-3-(3-dimethylaminopropyl)carbodiimide hydrochloride (0.274 g, 1.43 mmol, 1.0 eq) were added to a solution of appropriate **I-106d** (0.525 g, 1,43 mmol, 1.0 eq) in DCM (16 ml). After flash chromatography (Cy/EtOAc = 3/1), the product **I-107d** (0.303 g, 0.7 mmol, 48%) was obtained as orange solid.

Rf = 0.7 (Cy/EtOAc = 3/1).

^{1}H NMR (600 MHz, CDCl$_3$) δ 13.6 (s, 1H), 7.9 – 7.8 (m, 2H), 7.4(m, 2H), 7.2 (m, 2H), 7.0 – 6.9 (m, 2H), 6.4 (t, J = 1.2 Hz, 1H), 3.8 (s, 3H), 2.8 – 2.7 (m, 2H), 1.8 – 1.7 (m, 2H), 1.5 (dt, J = 14.9, 7.4 Hz, 2H), 1.0 (t, J = 7.4 Hz, 3H) [ppm].

^{13}C NMR (151 MHz, CDCl$_3$) δ 165.7, 157.4, 157.1, 151.7, 148.4, 138.9, 135.7, 131.4, 128.4, 127.5, 122.9, 120.5, 116.5, 114.1, 55.5, 29.7, 26.9, 26.3, 22.5, 18.3, 14.1, 13.8 [ppm].

HRMS: ESI-mass m/z calcd. for $C_{24}H_{27}N_4O_4$: 435.2027 and found: 435.2028.

UV-vis spectrum of monomer in THF solution: absorption shift at 397 nm.

IR(ATR): v [cm^{-1}] 2953, 2868, 1720, 1650.

(Z)-4-(2-(3-butyl-5-oxo-1-(p-tolyl)-1,5-dihydro-4H-pyrazol-4-ylidene)hydrazineyl) phenyl methacrylate
I-107e
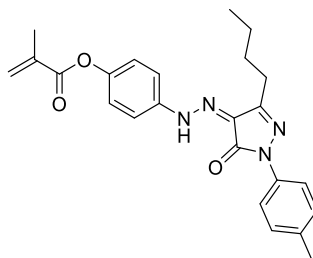
(Z)-4-(2-(3-butyl-5-oxo-1-(p-tolyl)-1,5-dihydro-4H-pyrazol-
4-ylidene)hydrazineyl)phenyl methacrylate
Chemical Formula: $C_{24}H_{26}N_4O_3$
Molecular Weight: 418,4970

Following procedure, C, Methacrylic acid (48.1 µl, 0.57 mmol, 1.0 eq), triethylamine (0.158 ml, 1.14 mmol, 2.0 eq) and 1-ethyl-3-(3-dimethylaminopropyl)carbodiimide hydrochloride (0.109 g, 0.57 mmol 1.0 eq) were added to a solution of appropriate **I-106e** (0.200 g, 0.57 mmol, 1.0 eq) in DCM (6.4 ml). After flash chromatography (Cy/EtOAc = 3/1), the product **I-107e** (0.100 g, 0.24 mmol, 42 %) was obtained as orange solid.

Rf = 0.71 (Cy/EtOAc = 3/1).

^{1}H NMR (600 MHz, CDCl$_3$) δ 13.7 (s, 1H), 7.8 (m, 2H), 7.4 (m, 2H), 7.2 (m, 2H), 7.2 (m, 2H), 6.4 (p, J = 1.0 Hz, 1H), 2.8 – 2.7 (m, 2H), 2.4 (s, 3H) 1.8 (m, 2H), 1.5 – 1.4 (m, 2H), 1.0 (t, J = 7.4 Hz, 3H) [ppm].

^{13}C NMR (101 MHz, CDCl$_3$) δ 165.7, 157.6, 151.7, 148.4, 138.9, 135.7, 134.8, 129.4, 128.4, 127.4, 122.9, 118.7, 116.5, 29.6, 26.9, 26.3, 22.5, 20.9, 18.3, 13.8 [ppm].

HRMS: ESI-mass m/z calcd. for $C_{24}H_{26}N_4NaO_3$: 441.1897 and found: 441.1902.

UV-vis spectrum of monomer in THF solution: absorption shift at 396 nm.

IR(ATR): ν [cm^{-1}] 2954, 2859, 1732, 1653.

(Z)-4-(3-butyl-5-oxo-4-(2-phenylhydrazineylidene)-4,5-dihydro-1H-pyrazol-1-yl) phenyl methacrylate

I-116a
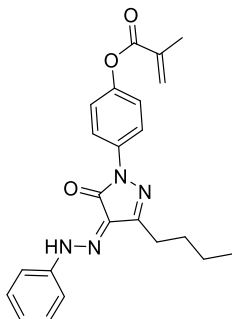
(*Z*)-4-(3-butyl-5-oxo-4-(2-phenylhydrazineylidene)-4,5-dihydro-1*H*-pyrazol-1-yl)phenyl methacrylate
Chemical Formula: $C_{23}H_{24}N_4O_3$
Molecular Weight: 404,4700

Following procedure, C, Methacrylic acid (40.1 µl, 0.48 mmol, 1.0 eq), triethylamine (131.8 ml, 0.95 mmol 2.0 eq) and 1-ethyl-3-(3-dimethylaminopropyl)carbodiimide hydrochloride (91 mg, 0.48 mmol, 1.0 eq) were added to a solution of appropriate **I-115a** (0.160 g, 0.48 mmol, 1.0 eq) in DCM (5.3 ml). After flash chromatography (Cy/EtOAc = 3/1), the product **I-116a** (0.105 g, 0.26 mmol, 55%) was obtained as orange solid.

Rf = 0.7 (Cy/EtOAc = 3/1).

^{1}H NMR (600 MHz, CDCl$_3$) δ 13.5 (s, 1H), 8.0 – 7.9 (m, 2H), 7.4 – 7.3 (m, 4H), 7.2 – 7.1 (m, 3H), 6.3 (s, 1H), 5.7 (t, *J* = 1.7 Hz, 1H), 2.7 (t, *J* = 7.8 Hz, 2H), 2.0 (s, 3H), 1.80 (p, *J* = 7.6 Hz, 2H), 1.4 (h, *J* = 7.4 Hz, 2H), 1.0 (t, *J* = 7.5 Hz, 3H) [ppm].

^{13}C NMR (151 MHz, CDCl$_3$) δ 165.7, 157.6, 152.0, 147.7, 141.1, 135.9, 129.62, 127.1, 125.7, 121.8, 119.1, 115.7, 29.5, 26.2, 22.5, 18.3, 13.8 [ppm].

HRMS: ESI-mass m/z calcd. for $C_{23}H_{24}N_4NaO_3$: 427.1741 and found: 427.1737.

UV-vis spectrum of monomer in THF solution: absorption shift at 398 nm.

IR(ATR): v [cm^{-1}] 2956, 2858, 1732, 1656.

(Z)-4-(3-butyl-4-(2-(4-cyanophenyl)hydrazineylidene)-5-oxo-4,5-dihydro-1H-pyrazol-1-yl)phenyl methacrylate

I-116b
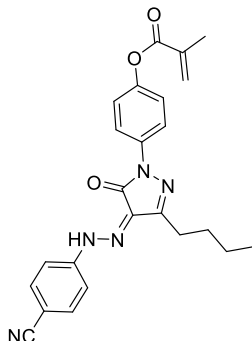
(Z)-4-(3-butyl-4-(2-(4-cyanophenyl)hydrazineylidene)-5-oxo-4,5-dihydro-1H-pyrazol-1-yl)phenyl
methacrylate
Chemical Formula: $C_{24}H_{23}N_5O_3$
Molecular Weight: 429,4800

Following procedure, C Methacrylic acid (46.7 µl, 0.55 mmol, 1.0 eq), triethylamine (153.4 µl, 1.11 mmol 2.0 eq) and 1-ethyl-3-(3-dimethylaminopropyl)carbodiimide hydrochloride (0.106 g, 0.55 mmol, 1.0 eq) were added to a solution of appropriate **I-115b** (0.200 g, 0.55 mmol, 1.0 eq) in DCM (6.2 ml). After flash chromatography (Cy/EtOAc = 3/1), the product **I-116b** (0.182 g, 0.42 mmol, 76%) was obtained as orange solid.

Rf = 0.7 (Cy/EtOAc = 3/1).

^{1}H NMR (600 MHz, CDCl$_3$) δ 13.5 (s, 1H), 8.0 – 7.9 (m, 2H), 7.6 (d, J = 8.3 Hz, 2H), 7.4 (d, J = 8.6 Hz, 2H), 7.2 – 7.1 (m, 2H), 6.3 (s, 1H), 5.7 (t, J = 1.7 Hz, 1H), 2.7 (t, J = 7.7 Hz, 2H), 2.0 (d, J = 18.7 Hz, 3H), 1.7 (p, J = 7.6 Hz, 2H), 1.4 (dt, J = 14.7, 7.3 Hz, 2H), 1.0 (t, J = 7.4 Hz, 3H) [ppm].

^{13}C NMR (151 MHz, CDCl$_3$) δ 165.9, 157.4, 152.3, 148.2, 144.7, 134.0, 130.7, 127.4, 122.2, 119.5, 115.9, 108.3, 29.4, 26.3, 22.6, 18.5, 13.9 [ppm].

HRMS: ESI-mass m/z calcd. for $C_{24}H_{23}N_5NaO_3$: 452.1693 and found: 452.1695.

UV-vis spectrum of monomer in THF solution: absorption shift at 397 nm.

IR(ATR): v [cm^{-1}] 3380, 2960, 2870, 2118, 1727, 1665.

(Z)-4-(4-(2-(4-bromophenyl)hydrazineylidene)-3-butyl-5-oxo-4,5-dihydro-1H-pyrazol-1-yl)phenyl methacrylate

I-116c
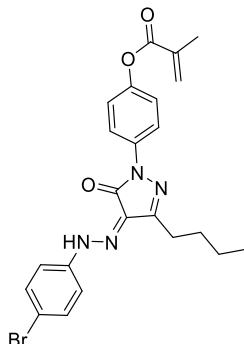
(*Z*)-4-(4-(2-(4-bromophenyl)hydrazineylidene)-3-butyl-5-oxo-4,5-dihydro-1*H*-pyrazol-1-yl)phenyl
methacrylate
Chemical Formula: $C_{23}H_{23}BrN_4O_3$
Molecular Weight: 483,3660

Following procedure, C Methacrylic acid (40.6 µl, 0.48 mmol, 1.0 eq), triethylamine (133.5 µl, 0.96 mmol 2.0 eq) and 1-ethyl-3-(3-dimethylaminopropyl)carbodiimide hydrochloride (92 mg, 0.48 mmol, 1.0 eq) were added to a solution of appropriate **I-115c** (0.200 g, 0.48 mmol, 1.0 eq) in DCM (5.4 ml). After flash chromatography (Cy/EtOAc = 3/1), the product **I-116c** (82 mg, 0.17 mmol, 35%) was obtained as orange solid.

Rf = 0.7 (Cy/EtOAc = 3/1).

^{1}H NMR (600 MHz, CDCl$_3$) δ 13.5 (s, 1H), 7.9 – 7.8 (m, 2H), 7.5 (m, 2H), 7.4 (m, 2H), 7.2 – 7.1 (m, 2H), 6.3 (s, 1H), 5.7 (t, *J* = 1.7 Hz, 1H), 2.7 (t, *J* = 7.7 Hz, 2H), 2.0 (s, 3H), 1.7 (p, *J* = 7.6 Hz, 2H), 1.4 (p, *J* = 7.4 Hz, 2H), 0.9 (t, *J* = 7.4 Hz, 3H) [ppm].

^{13}C NMR (151 MHz, CDCl$_3$) δ 165.8, 158.0, 152.5, 148.8, 138.9, 137.3, 135.8, 132.0, 127.7, 123.1, 120.0, 118.1, 116.7, 29.7, 26.4, 22.6, 18.5, 13.9 [ppm].

HRMS: ESI-mass m/z calcd. for C$_{23}$H$_{23}$BrN$_4$NaO$_3$: 505.0846 and found: 505.0847.

UV-vis spectrum of monomer in THF solution: absorption shift at 399 nm.

IR(ATR): v [cm^{-1}] 2950, 2864, 1728, 1664.

(Z)-4-(3-butyl-4-(2-(4-methoxyphenyl)hydrazineylidene)-5-oxo-4,5-dihydro-1H-pyrazol-1-yl)phenyl methacrylate

I-116d
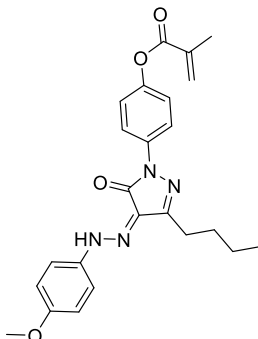
(Z)-4-(3-butyl-4-(2-(4-methoxyphenyl)hydrazineylidene)-5-oxo-4,5-dihydro-1H-pyrazol-1-yl)phenyl
methacrylate
Chemical Formula: $C_{24}H_{26}N_4O_4$
Molecular Weight: 434,4960

Following procedure, C Methacrylic acid (30 µl, 0.35 mmol, 1.0 eq), triethylamine (98 µl, 0.71 mmol 2.0 eq) and 1-ethyl-3-(3-dimethylaminopropyl)carbodiimide hydrochloride (68 mg, 0.35 mmol, 1.0 eq) were added to a solution of appropriate **I-115d** (0.130 g, 0.35 mmol, 1.0 eq) in DCM (4 ml). After flash chromatography (Cy/EtOAc = 3/1), the product **I-116d** (65 mg, 0.15 mmol, 42%) was obtained as orange solid.

R_f = 0.7 (Cy/EtOAc = 3/1).

^{1}H NMR (400 MHz, CDCl₃) δ 13.7 (s, 1H), 8.0 (m, 2H), 7.4 – 7.3 (m, 2H), 7.2 – 7.1 (m, 2H), 7.0 – 6.9 (m, 2H), 6.3 (p, J = 1.0 Hz, 1H), 5.7 (p, J = 1.6 Hz, 1H), 2.8 – 2.7 (m, 2H), 2.1 (t, J = 1.2 Hz, 3H), 1.8 – 1.7 (m, 2H), 1.4 (dt, J = 14.7, 7.4 Hz, 2H), 1.0 (t, J = 7.4 Hz, 3H) [ppm].

^{13}C NMR (151 MHz, CDCl₃) δ 165.7, 157.4, 157.1, 151.7, 148.4, 138.9, 135.7, 131.4, 128.4, 127.5, 122.9, 120.5, 116.5, 114.1, 55.5, 29.7, 26.9, 26.3, 22.5, 18.3, 14.1, 13.8 [ppm].

HRMS: ESI-mass m/z calcd. for $C_{24}H_{23}N_4NaO_4$: 457.1846 and found: 457.1845.

UV-vis spectrum of monomer in THF solution: absorption shift at 398 nm.

IR(ATR): v [cm^{-1}] 2955, 2835, 1733, 1651.

Polymerization

General procedure **(D)** for copolymerization

The methacrylic monomers **I-107 or 115** and methylmethacrylate (MMA) was conducted in anhydrous N,N-dimethylformamide 10% solution with monomers initial mole ratios 1:3 and AIBN (1 wt% of monomer) as radical initiator at 80°C (argon atmosphere) for 48 h. The resulting viscous solution was added into methanol to precipitate polymeric materials.

(Z)-4-(2-(3-butyl-5-oxo-1-phenyl-1,5-dihydro-4H-pyrazol-4-ylidene)hydrazineyl) phenyl poly(methyl methacrylate)

I-108a
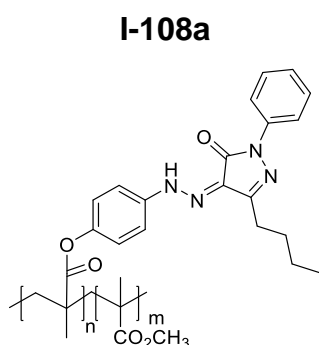
Following procedure, D, monomer **I-107a** (200 mg, 0.49 mmol, 1 eq) and methylmethacrylate (MMA) (157 µl, 1.48 mmol, 3 eq) was conducted in anhydrous N,N-dimethylformamide 10% solution (2 ml) with monomers initial mole ratios 1:3 and AIBN (1 wt% of monomer, 2 mg, 0.01 mmol). The polymer was isolated with 98% of yield (259 mg, 0.48 mmol). n:m = 1:3.

Mn = 47 800 g/mol, Đ = 1.7 (linear poly(methyl methacrylate) standards (M_n 800– 2 200 000 g/mol);).

T_g = 120°C, T_m = 260°C.

^{1}H NMR (400 MHz, CDCl$_3$) δ 13.6, 7.9, 7.4, 7.1, 3.6, 2.7, 1.4, 1.0 [ppm].

IR(ATR): v [cm^{-1}] 2980, 1728, 1659.

(Z)-4-(2-(3-butyl-1-(4-cyanophenyl)-5-oxo-1,5-dihydro-4H-pyrazol-4-ylidene) hydrazineyl)phenyl poly(methyl methacrylate)

I-108b
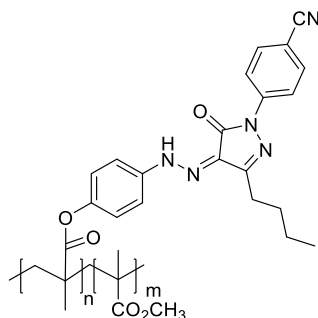
Following procedure, D, monomer **I-107b** (200 mg, 0.47 mmol, 1 eq) and methylmethacrylate (MMA) (148.7 µl, 1.40 mmol, 3 eq) was conducted in anhydrous N,N-dimethylformamide 10% solution (2 ml) with monomers initial moleratios 1:3 and AIBN (1 wt% of monomer, 2 mg, 0.01 mmol). The polymer was isolated with 99% of yield (258 mg, 0.46 mmol). n:m = 1:4,

M_n = 97 100 g/mol, Đ = 1.5 (linear poly(methyl methacrylate) standards (M_n 800–2 200 000 g/mol);).

T_g = 146°C, T_m = 261°C.

^{1}H NMR (600 MHz, CDCl$_3$) δ 13.4, 8.1, 7.6, 7.4, 7.1, 3.5, 2.7, 1.4, 1.2, 0.9 [ppm].

IR(ATR): ν [cm^{-1}] 2957, 2226, 1728, 1666.

(Z)-4-(2-(1-(4-bromophenyl)-3-butyl-5-oxo-1,5-dihydro-4H-pyrazol-4-ylidene) hydrazineyl)phenyl poly(methyl methacrylate)

I-108c
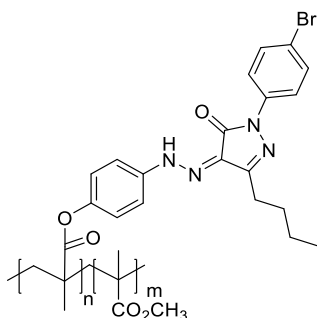
Following procedure, D, monomer **I-107c** (100 mg, 0.21 mmol, 1 eq) and methylmethacrylate (MMA) (66.1 µl, 0.62 mmol, 3 eq) was conducted in anhydrous N,N-dimethylformamide 10% solution (1 ml) with monomers initial moleratios 1:3 and AIBN (1 wt% of monomer, 1 mg, 0.01 mmol). The polymer was isolated with 95% of yield (120 mg, 0.2 mmol). n:m = 1:4.

M_n = 96 900 g/mol, Đ = 1.4 (linear poly(methyl methacrylate) standards (M_n 800–2 200 000 g/mol);).

T_g = 124°C, T_m = 263°C.

^{1}H NMR (600 MHz, CDCl$_3$) δ 13.5, 7.8, 7.4, 7.1, 3.5, 2.7, 1.7, 1.4, 1.2, 1.0, 0.9, 0.8 [ppm].

IR(ATR): v [cm^{-1}] 2950, 1728, 1660.

(Z)-4-(2-(3-butyl-1-(4-methoxyphenyl)-5-oxo-1,5-dihydro-4H-pyrazol-4-ylidene) hydrazineyl)phenyl poly(methyl methacrylate)

I-108d
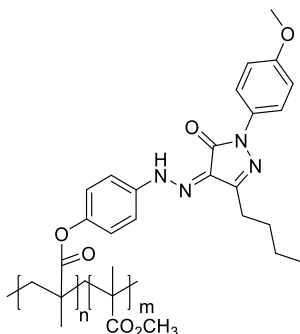
Following procedure, D, monomer **I-107d** (240 mg, 0.55 mmol, 1 eq) and methylmethacrylate (MMA) (176.5 µl, 1.66 mmol, 3 eq) was conducted in anhydrous N,N-dimethylformamide 10% solution (2.4 ml) with monomers initial moleratios 1:3 and AIBN (1 wt% of monomer, 2.5 mg, 0.01 mmol). The polymer was isolated with 98% of yield (306 mg, 0.54 mmol). n:m = 1:4.

M_n = 100 600 g/mol, Đ = 1.6 (linear poly(methyl methacrylate) standards (M_n 800–2 200 000 g/mol);).

T_g = 126°C, T_m = 252°C.

^{1}H NMR (400 MHz, CDCl$_3$) δ 13.6, 7.8, 7.4, 7.1, 6.9, 3.8, 3.5, 2.7, 1.9, 1.7, 1.4, 1.2, 0.9, 0.8 [ppm].

IR(ATR): v [cm^{-1}] 2950, 1728, 1665.

(Z)-4-(2-(3-butyl-5-oxo-1-(p-tolyl)-1,5-dihydro-4H-pyrazol-4-ylidene)hydrazineyl) phenyl poly(methyl methacrylate)

I-108e
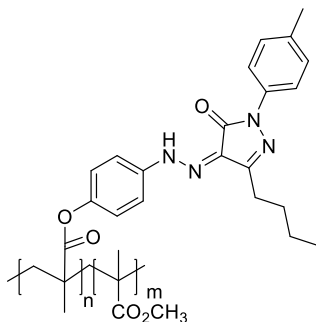
Following procedure, D, monomer **I-107e** (120 mg, 0.29 mmol, 1 eq) and methylmethacrylate (MMA) (91.6 µl, 0.86 mmol, 3 eq) was conducted in anhydrous N,N-dimethylformamide 10% solution (1.2 ml) with monomers initial mole ratios 1:3 and AIBN (1 wt% of monomer, 1.2 mg, 0.01 mmol). The polymer was isolated with 93% of yield (146 mg, 0.27 mmol). n:m = 1:3.

Mn = 97 100 g/mol, Đ = 1.2 (linear poly(methyl methacrylate) standards (M_n 800–2 200 000 g/mol);).

T_g = 131°C, T_m = 249°C.

^{1}H NMR (600 MHz, CDCl$_3$) δ 13.6, 7.8, 7.3, 7.2, 7.1, 3.5, 2.3, 1.7, 1.5, 0.9, 0.8 [ppm].

IR(ATR): ν [cm^{-1}] 2980, 1730,1684.

(Z)-4-(2-(3-butyl-5-oxo-1-phenyl-1,5-dihydro-4H-pyrazol-4-ylidene)hydrazineyl) phenyl polymethacrylate

I-109a
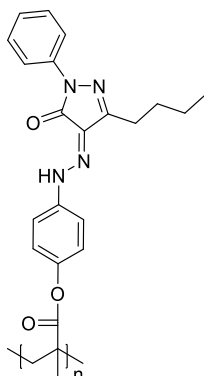
The methacrylic monomer **I-107a** (150 mg, 0.37 mmol) was conducted in anhydrous N,N-dimethylformamide 10% solution (1.5 ml) and AIBN (1 wt% of monomer, 1.3 mg, 0.01 mmol) as radical initiator at 80°C (argon atmosphere)for 48h. The polymer was isolated with 86% of yield (92 mg, 0.21 mmol).

M_n = 83 200 g/mol, Đ = 1.3 (linear poly(methyl methacrylate) standards (M_n 800–2 200 000 g/mol);).

T_g = 142°C, T_m = 262°C.

^{1}H NMR (400 MHz, CDCl$_3$) δ 13.5, 7.8, 7.3, 7.1, 2.5, 1.5, 1.3, 0.8 [ppm].

IR(ATR): v [cm^{-1}] 2980, 2871, 1712,1658.

(Z)-4-(3-butyl-5-oxo-4-(2-phenylhydrazineylidene)-4,5-dihydro-1H-pyrazol-1-yl) phenyl poly(methyl methacrylate)

I-122a
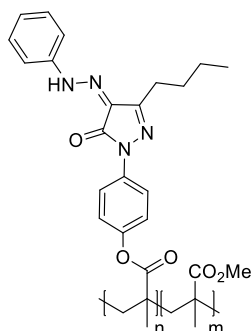
Following procedure, D, monomer **I-116** (0.100 g, 0.25 mmol, 1 eq) and methylmethacrylate (MMA) (78.9 μl, 0.74 mmol, 3 eq) was conducted in anhydrous N,N-dimethylformamide 10% solution (1 ml) with monomers initial moleratios 1:3 and AIBN (1 wt% of monomer, 1 mg, 0.01 mmol). The polymer was isolated with 95% of yield (0.129 g, 0.23 mmol), n:m = 1:2.

M_n = 94 000 g/mol, Đ = 1.4 (linear poly(methyl methacrylate) standards (M_n 800–2 200 000 g/mol);).

T_g = 151°C, T_m = 244°C.

^{1}H NMR (600 MHz, CDCl$_3$) δ 13.5, 7.9, 7.2, 7.1, 3.6, 2.6, 2.0, 1.7, 1.4, 1.2, 1.0, 0.9 [ppm].

IR(ATR): v [cm^{-1}] 2980, 1728, 1659.

(Z)-4-(3-butyl-4-(2-(4-cyanophenyl)hydrazineylidene)-5-oxo-4,5-dihydro-1H-pyrazol-1-yl)phenyl poly(methyl methacrylate)

I-122b
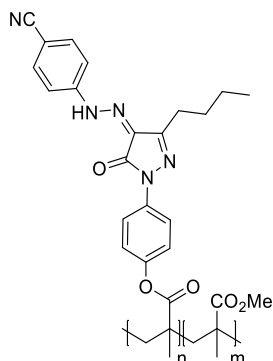
Following procedure, D, monomer **I-116** (150 mg, 0.35 mmol, 1 eq) and methylmethacrylate (MMA) (111.5 µl, 1.05 mmol, 3 eq) was conducted in anhydrous N,N-dimethylformamide 10% solution (1.5 ml) with monomers initial moleratios 1:3 and AIBN (1 wt% of monomer, 1.5 mg, 9.13 µmol). The polymer was isolated with 98% of yield (0.196 g, 0.34 mmol), n:m = 1:4.

Mn = 100 000 g/mol, Đ = 1.3 (linear poly(methyl methacrylate) standards (M_n 800–2 200 000 g/mol);).

T_g = 142°C, T_m = 268°C.

^{1}H NMR (400 MHz, CDCl$_3$) δ 13.4, 7.9, 7.6, 7.4, 7.1, 3.6, 2.7, 1.9, 1.8, 1.5, 1.0, 0.8 [ppm].

IR(ATR): v [cm^{-1}] 2957, 2226, 1728, 1666.

(Z)-4-(4-(2-(4-bromophenyl)hydrazineylidene)-3-butyl-5-oxo-4,5-dihydro-1H-pyrazol-1-yl)phenyl poly(methyl methacrylate)

I-122c
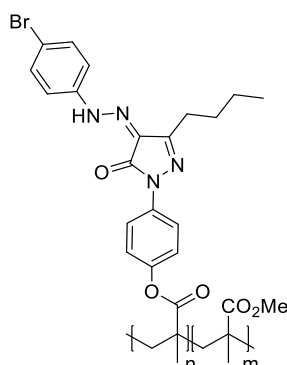
Following procedure, D, monomer **I-116** (65 mg, 0.13 mmol, 1 eq) and methylmethacrylate (MMA) (43 µl, 0.40 mmol, 3 eq) was conducted in anhydrous N,N-dimethylformamide 10% solution (0.6 ml) with monomers initial moleratios 1:3 and AIBN (1 wt% of monomer, 0.6 mg, 3.86 µmol). The polymer was isolated with 98% (83 mg, 0.13 mmol), n:m = 1:4.

M_n = 35 000 g/mol, Đ = 1.7 (linear poly(methyl methacrylate) standards (M_n 800–2 200 000 g/mol);).

T_g = 133°C, T_m = 253°C.

^{1}H NMR (400 MHz, CDCl$_3$) δ 13.4, 7.9, 7.5, 7.2, 7.1, 3.5, 2.7, 2.1, 1.7, 1.4, 1.2, 1.0, 0.8

[ppm].

IR(ATR): v [cm^{-1}] 2950, 1728, 1660.

(Z)-4-(3-butyl-4-(2-(4-methoxyphenyl)hydrazineylidene)-5-oxo-4,5-dihydro-1H-pyrazol-1-yl)phenyl poly(methyl methacrylate)

I-122d
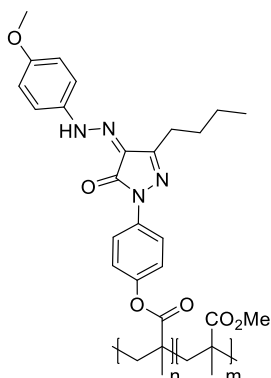
Following procedure, D, monomer **I-116d** (50 mg, 0.12 mmol, 1 eq) and methylmethacrylate (MMA) (37 µl, 3.04 µmol, 3 eq) was conducted in anhydrous N,N-dimethylformamide 10% solution (0.5 ml) with monomers initial moleratios 1:3 and AIBN (1 wt% of monomer, 0.5 mg, 3.04 µmol). The polymer was isolated with 98% of yield (65 mg, 0.11 mmol), n:m = 1:3.

M_n = 120 000 g/mol, Đ = 1.2 (linear poly(methyl methacrylate) standards (M_n 800–2 200 000 g/mol);).

T_g = 154°C, T_m = 238°C.

^{1}H NMR (400 MHz, CDCl3) δ 13.6, 7.9, 7.3, 7.1, 6.9, 3.8, 3.6, 2.6, 1.7, 1.4, 1.2, 1.0, 0.9, 0.8 [ppm].

IR(ATR): ν [cm^{-1}] 2950, 1728, 1665.

(Z)-4-(3-butyl-5-oxo-4-(2-phenylhydrazineylidene)-4,5-dihydro-1H-pyrazol-1-yl) phenyl polymethacrylate

I-123a
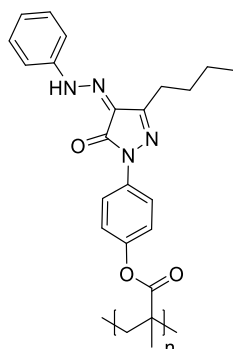
The methacrylic monomers **I-116a** (150 mg, 0.37 mmol) was conducted in anhydrous N,N-dimethylformamide 10% solution (1.5 ml) and AIBN (1 wt% of monomer, 1.3 mg, 0.01 mmol) as radical initiator at 80°C (argon atmosphere) for 48h. The resulting viscous solution was added into methanol to precipitate polymeric materials. The precipitation was filtered and dried. The polymer was isolated with 86% of yield (0.139 g, 0.32 mmol).

M_n = 41 000 g/mol, Đ = 1.7 (linear poly(methyl methacrylate) standards (M_n 800–2 200 000 g/mol);).

T_g = 80°C, T_m = 251°C.

^{1}H NMR (600 MHz, CDCl$_3$) δ 13.5, 7.9, 7.3, 7.1, 2.6, 1.6, 1.6, 1.4, 0.9 [ppm].

IR(ATR): ν [cm^{-1}] 2980, 2871, 1712, 1658.

III.6.2. Part I: Rubazonic acid as a promising material
Methyl 3-oxononanoate

I-157
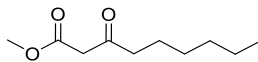
methyl 3-oxononanoate
Chemical Formula: $C_{10}H_{18}O_3$
Molecular Weight: 186,2510

To prepare ethyl 3-oxooctanoate, a suspension of NaH (1.9 g, 81.83 mmol) in THF (100 ml) was first prepared at 0 °C, and then methyl acetoacetate (4.5 ml, 39.53 mmol) was slowly added to the mixture. After stirring for 10 minutes, n-BuLi (2.5 M in hexane) (15.9 ml, 39.92 mmol) was added dropwise over a period of 15 minutes. The mixture was stirred for an additional 20 minutes at 0 °C. Next, 1-bromopentane (5.4 ml, 43.48 mmol) in 6 ml of THF was added dropwise, and the reaction was allowed to proceed for 2 hours. The reaction was then quenched with 8 ml of concentrated HCl in 10 ml of H_2O and 40 ml of Et_2O. The organic layer was washed with brine, dried with anhydrous $MgSO_4$, filtered, and the solvent was removed using a rotary evaporator. Finally, the crude product was purified using column chromatography with silica gel as the stationary phase and 3/1 cyclohexane/Et_2O as the mobile phase. The product was synthetized with 40% of yield as light-yellow oil (2.5 g, 12. 65 mmol).

^{1}H NMR (400 MHz, CDCl3) δ 3.7 (s, 2H), 3.4 (s, 2H), 2.5 (t, J = 7.4 Hz, 2H), 1.5 (t, J = 7.4 Hz, 2H), 1.2 (ddt, J = 7.2, 4.9, 3.0 Hz, 7H), 0.9 – 0.8 (m, 4H) [ppm].

The analytical data are identical to the literature data. [175]

Ethyl 3-oxoundecanoate

I-160
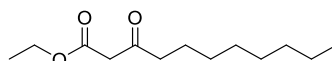
ethyl 3-oxoundecanoate
Chemical Formula: $C_{13}H_{24}O_3$
Molecular Weight: 228,33

In this procedure, ethyl potassium malonate (5.0 g, 29.3 mmol) was added to MeCN (60 ml) at 10-15 °C and under N_2, followed by Et_3N (6.3 ml, 45.2 mmol) and $MgCl_2$ (3.3 g, 35.25 mmol). The mixture was stirred at 20-25 °C for 2.5 hours, then at 0 °C

for 0.5 hours before the corresponding octanoyl chloride (5.0 ml, 29 mmol) was added dropwise over a period of 25 minutes. The mixture was further treated with Et_3N (2.4 ml, 14.10 mmol) and stirred overnight at 20 °C. The resulting mixture was dissolved in toluene, concentrated, and then more toluene was added, stirred, and cooled to 10-15 °C before cautiously adding aq HCl (1 M, 50 ml) while keeping the temperature below 25 °C. The organic layer was washed with 1 M aq HCl (50 ml) and water. The crude oily residue was purified using flash chromatography with $CHCl_3$ as the solvent, resulting in a pale-yellow oil with yield 43% (2.9 g, 12.7 mmol).

^1H NMR (600 MHz, $CDCl_3$) δ 4.1 (q, J = 7.1 Hz, 2H), 3.4 (s, 2H), 2.5 (t, J = 7.4 Hz, 2H), 1.6 (q, J = 7.4 Hz, 2H), 1.2 (td, J = 7.7, 7.2, 4.2 Hz, 13H), 0.8 (t, J = 7.0 Hz, 3H) [ppm].

The analytical data are identical to the literature data. [176]

(2,3,5,6-tetrafluorophenyl)hydrazine

I-162

(2,3,5,6-tetrafluorophenyl)hydrazine
Chemical Formula: $C_6H_4F_4N_2$
Exact Mass: 180,0311

A solution of pentafluorobenzene (1 ml, 9.01 mmol, 1 eq) in EtOH (5.4 ml) was treated with hydrazine monohydrate (0.876 ml, 18.02 mmol, 2 eq). The reaction mixture was refluxed for 20 hours, then cooled to room temperature, poured into water (5 ml), and kept at 5 °C for 3 hours. The resulting precipitate was filtered and recrystallized from hexane. The product **I-162** isolated as white powder with a 68% of yield (550 mg, 3.06 mmol).

^1H NMR (400 MHz, $CDCl_3$) δ 6.5 (tt, J = 9.9, 7.2 Hz, 1H), 5.3 (s, 1H), 4.0 (s, 2H), [ppm].

^{13}C NMR (101 MHz, $CDCl_3$) δ 147.3, 144.9, 138.7, 136.3, 130.8, 96.0, 24.9, 15.5 [ppm].

The analytical data are identical to the literature data . [177].
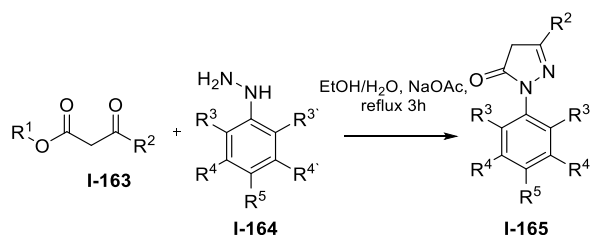
To synthesize pyrazolone derivatives using general procedure (A), first dissolved aromatic hydrazine hydrochloride derivatives (1 eq.) and sodium acetate (1 eq.) in a mixture of ethanol and water (5:1). After stirring the resulting mixture at room temperature for five minutes, then added β-ketoester (1 eq.) and heated the reaction mixture to reflux for three hours. The organic layer was then extracted with a mixture of water and ethyl acetate, followed by washing with brine, drying over Na_2SO_4, and concentration under reduced pressure.

5-butyl-2-(2,3,5,6-tetrafluorophenyl)-2,4-dihydro-3H-pyrazol-3-one

I-166b
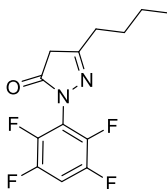
5-butyl-2-(2,3,5,6-tetrafluorophenyl)-2,4-dihydro-3*H*-pyrazol-3-one
Chemical Formula: $C_{13}H_{12}F_4N_2O$
Molecular Weight: 288,2456

In accordance with procedure A, in a mixture of 3 ml of ethanol and 0.6 ml of water were dissolved of 2,3,5,6-tetrafluorophenylhydrazine (0.440 g, 2.43 mmol), methyl 3-oxoheptanoate (0.4 ml, 2.43 mmol), and anhydrous sodium acetate (0.200 g, 2.43 mmol) and refluxed the mixture for 3 hours. The product was obtained as a yellow solid with a yield of 51% (0.356 g, 1.24 mmol).

^{1}H NMR (400 MHz, CDCl₃) δ 7.1 (tt, J = 9.8, 7.1 Hz, 1H), 3.4 (d, J = 0.7 Hz, 2H), 2.5 – 2.4 (m, 2H), 1.6 – 1.5 (m, 2H), 1.4 – 1.3 (m, 2H), 0.9 (t, J = 7.3 Hz, 3H) [ppm].

^{13}C NMR (151 MHz, CDCl₃) δ 171.1, 161.8, 147.0, 145.4, 143.9, 142.3, 117.0, 106.1, 39.3, 31.0, 28.4, 22.3, 13.7 [ppm].

^{19}F NMR (376 MHz, CDCl₃) δ -138.0 (m), -143.6 (m) [ppm].

146

5-butyl-2-(4-chlorophenyl)-2,4-dihydro-3H-pyrazol-3-one

I-167b
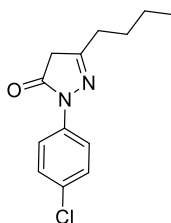
5-butyl-2-(4-chlorophenyl)-2,4-dihydro-3*H*-pyrazol-3-one
Chemical Formula: $C_{13}H_{15}ClN_2O$
Molecular Weight: 250,7260

In accordance with procedure A, in a mixture of 4 ml of ethanol and 1 ml of water were dissolved of 4-(clorophenyl)hydrazine hydrochloride (0.700 g, 3.91 mmol), methyl 3-oxoheptanoate (0.6 ml, 3.91 mmol), and anhydrous sodium acetate (0.320 g, 3.91 mmol) and refluxed the mixture for 3 hours. The product was obtained as a yellow solid with a yield of 59% (0.578 g, 2.31 mmol).

^{1}H NMR (600 MHz, CDCl3) δ 7.8 (m, 2H), 7.3 (m, 2H), 3.4 (d, J = 0.7 Hz, 2H), 2.5 – 2.4 (m, 2H), 1.6 (ddt, J = 8.8, 7.7, 6.5 Hz, 2H), 1.4 (m, 2H), 0.9 (t, J = 7.4 Hz, 3H) [ppm]

^{13}C NMR (101 MHz, DMSO) δ 170.2, 160.1, 136.5, 129.7, 128.6, 119.6, 41.5, 30.7, 28.4, 22.1, 13.5 [ppm].

HRMS: ESI-mass m/z calcd. for $C_{13}H_{17}ClN_2O$: 251.0946 and found: 251.0946.

2-(4-bromophenyl)-5-methyl-2,4-dihydro-3H-pyrazol-3-one

I-168a
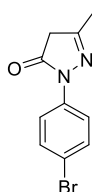
2-(4-bromophenyl)-5-methyl-2,4-dihydro-3*H*-pyrazol-3-one
Chemical Formula: $C_{10}H_9BrN_2O$
Molecular Weight: 253,0990

In accordance with procedure A, In a mixture of 2.8 ml of ethanol and 0.6 ml of water were dissolved of (4-bromophenyl)hydrazine hydrochloride (0.500 g, 2.24 mmol), ethyl acetoacetate (0.3 ml, 2.24 mmol), and anhydrous sodium acetate (0.184 g, 2.24 mmol) and refluxed the mixture for 3 hours. The product was obtained as a yellow solid with a yield of 42% (0.240 g, 0.94 mmol).

^{1}H NMR (400 MHz, DMSO-d_6) δ 7.7 – 7.6 (m, 2H), 7.6 – 7.5 (m, 2H), 2.1 (d, J = 3.2 Hz, 3H) [ppm].

^{13}C NMR (151 MHz, CDCl$_3$) δ 170.4, 160.3, 137.2, 131.7, 120.1, 117.7, 41.7, 14.0 [ppm].

The analytical data are identical to the literature data [178].

2-(4-bromophenyl)-5-hexyl-2,4-dihydro-3H-pyrazol-3-one

I-168c
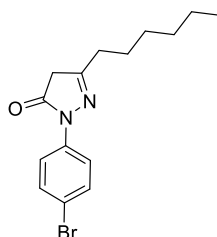
2-(4-bromophenyl)-5-hexyl-2,4-dihydro-3*H*-pyrazol-3-one
Chemical Formula: $C_{15}H_{19}BrN_2O$
Molecular Weight: 323,2340

In accordance with procedure A, In a mixture of 3.3 ml of ethanol and 0.7 ml of water were dissolved of (4-bromophenyl)hydrazine hydrochloride (0.600 g, 2.68 mmol), ethyl 3-oxononanoate (0.56 ml, 2.68 mmol), and anhydrous sodium acetate (0.220 g, 2.68 mmol) and refluxed the mixture for 3 hours. The product was obtained as a yellow solid with a yield of 41% (0.356 g, 1.1 mmol).

^{1}H NMR (600 MHz, CDCl$_3$) δ 7.8 – 7.7 (m, 2H), 7.5 – 7.4 (m, 2H), 3.4 (s, 2H), 2.4 (t, J = 7.7 Hz, 2H), 1.6 (p, J = 7.6 Hz, 2H), 1.4 – 1.3 (m, 2H), 1.3 (tdd, J = 7.2, 4.5, 1.8 Hz, 4H), 0.9 – 0.8 (m, 3H) [ppm].

^{13}C NMR (151 MHz, CDCl$_3$) δ 170.3, 160.3, 137.2, 131.7, 120.1, 117.6, 41.6, 31.1, 28.8, 26.4, 22.4, 13.9 [ppm].

HRMS: ESI-mass m/z calcd. for C$_{15}$H$_{20}$BrN$_2$O: 323.0754 and found: 323.0753.

2-(4-bromophenyl)-5-octyl-2,4-dihydro-3H-pyrazol-3-one

I-168d
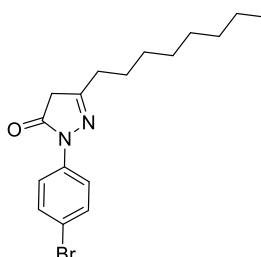
2-(4-bromophenyl)-5-octyl-2,4-dihydro-3*H*-pyrazol-3-one
Chemical Formula: C$_{17}$H$_{23}$BrN$_2$O
Molecular Weight: 351,2880

In accordance with procedure A, In a mixture of 4 ml of ethanol and 0.8 ml of water were dissolved of (4-bromophenyl)hydrazine hydrochloride (0.700 g, 3.13 mmol), ethyl 3-oxoundecanoate (0.75 ml, 3.13 mmol), and anhydrous sodium acetate (0.256 g, 3.13 mmol) and refluxed the mixture for 3 hours. The product was obtained as a yellow solid with a yield of 40% (0.440 g, 1.25 mmol).

^{1}H NMR (400 MHz CDCl$_3$) δ 7.8 – 7.7 (m, 2H), 7.5 – 7.4 (m, 2H), 3.4 (s, 2H), 2.5 – 2.4 (m, 2H), 1.7 – 1.5 (m, 2H), 1.4 – 1.2 (m, 10H), 0.9 – 0.8 (m, 3H) [ppm].

^{13}C NMR (151 MHz, CDCl$_3$) δ 170.8, 160.7, 137.6, 132.1, 120.5, 118.0, 42.1, 32.0, 31.5, 29.5, 29.2, 26.9, 22.9, 14.4 [ppm].

HRMS: no data.

5-butyl-2-phenyl-2,4-dihydro-3H-pyrazol-3-one

I-169b
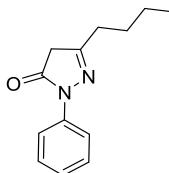
5-butyl-2-phenyl-2,4-dihydro-3*H*-pyrazol-3-one
Chemical Formula: $C_{13}H_{16}N_2O$
Molecular Weight: 216,2840

In accordance with procedure A, in a mixture of 4 ml of ethanol and 0.8 ml of water were dissolved of phenylhydrazine (1 ml, 10.17 mmol), ethyl 3-oxoundecanoate (1.6 ml, 10.17 mmol), and anhydrous sodium acetate (834 mg, 10.17 mmol) and refluxed the mixture for 3 hours. The product was obtained as a yellow solid with a yield of 82% (1.8 g, 8.32 mmol).

^{1}H NMR (600 MHz, CDCl₃) δ 7.8 (m, 2H), 7.4 – 7.3 (m, 2H), 7.1 (tt, J = 7.4, 1.2 Hz, 1H), 3.4 (d, J = 0.7 Hz, 2H), 2.5 (dd, J = 8.3, 7.1 Hz, 2H), 1.6 (m, 2H), 1.4 – 1.3 (m, 3H), 0.9 (t, J = 7.4 Hz, 3H) [ppm].

The analytical data are identical to the literature data [179].

5-butyl-2-(4-hydroxyphenyl)-2,4-dihydro-3H-pyrazol-3-one

I-170b
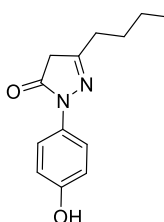
5-butyl-2-(4-hydroxyphenyl)-2,4-dihydro-3*H*-pyrazol-3-one
Chemical Formula: $C_{13}H_{17}N_2O_2$
Molecular Weight: 232,28

In accordance with procedure A, in a mixture of 4 ml of ethanol and 1 ml of water were dissolved of 4-hydrazineylphenol hydrochloride (0.650 g, 4 mmol), methyl 3-oxoheptanoate (0.68 ml, 4 mmol), and anhydrous sodium acetate (0.332 g, 4 mmol) and refluxed the mixture for 3 hours. The rection was under inert atmosphere. After solvent evaporation product lived for overnight to crystallization. The formed solid

wash with DCM and filtrated and dried. The product was obtained as a white solid (0.310 g, 1.37 mmol, 33%).

Microwave method. The 4-hydrazinylphenol hydrochloride (0.500 g, 3.1 mmol) and methyl 3-oxoheptanoate (0.483 ml 3.1 mmol) was transferred to a microwave vial with a magnetic stir bar and maintained an inert atmosphere at 50 °C for 5 minutes. After reaction the EtOAc was added and filtered the resulting precipitation, which was then dried and used for the next step. The product was obtained as white solid without purification (0.122 g, 0.53 mmol, 17%).

^{1}H NMR (400 MHz, DMSO) δ 11.1 (s, 1H), 7.4 – 7.3 (m, 2H), 6.8 – 6.7 (m, 2H), 2.4 – 2.3 (m, 2H), 1.5 – 1.4 (m, 2H), 1.3 (dt, J = 14.8, 7.3 Hz, 2H), 0.8 (t, J = 7.3 Hz, 3H) [ppm].

^{13}C NMR (101 MHz, DMSO) δ 170.5, 161.0, 155.0, 130.1, 122.7, 120.4, 115.1, 30.1, 27.8, 21.9, 13.8 [ppm].

HRMS: ESI-mass m/z calcd. for $C_{13}H_{17}N_2O_2$: 233.1285 and found: 233.1280.

2-(4-hydroxyphenyl)-5-octyl-2,4-dihydro-3H-pyrazol-3-one

I-170d
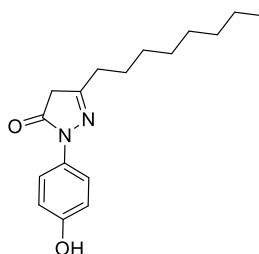
2-(4-hydroxyphenyl)-5-octyl-2,4-dihydro-3*H*-pyrazol-3-one
Chemical Formula: $C_{17}H_{24}N_2O_2$
Molecular Weight: 288,3910

In accordance with procedure A, in a mixture of 48 ml of ethanol and 9.5 ml of water were dissolved of 4-hydrazineylphenol hydrochloride (6 g, 38.36 mmol), ethyl 3-oxoundecanoate (8.7 g, 38.36 mmol), and anhydrous sodium acetate (3.1 g, 38.36 mmol) and refluxed the mixture for 3 hours. The rection was under inert atmosphere. After solvent evaporation product lived for overnight to crystallization. The formed solid wash with DCM and filtrated and dried. The product was obtained as a white solid (1.4 g, 4.85 mmol, 12%).

^{1}H NMR (400 MHz, CDCl$_3$) δ 7.86 – 7.78 (m, 2H), 7.5 – 7.4 (m, 2H), 3.4 (s, 2H), 2.5 – 2.4 (m, 2H), 1.6 (m, 2H), 1.4 – 1.2 (m, 10H), 0.9 – 0.8 (m, 3H) [ppm].

4-(3-butyl-5-oxo-4,5-dihydro-1H-pyrazol-1-yl)benzonitrile

I-171b
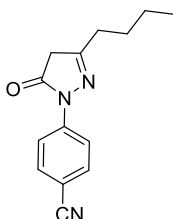
4-(3-butyl-5-oxo-4,5-dihydro-1*H*-pyrazol-1-yl)benzonitrile
Chemical Formula: C₁₄H₁₅N₃O
Molecular Weight: 241,2940

In accordance with procedure A, in a mixture of 2.2 ml of ethanol and 0.4 ml of water were dissolved of 4-cyanophenylhydrazine hydrochloride (300 mg, 1.77 mmol), methyl 3-oxoheptanoate (0.3 ml, 1.77 mmol), and anhydrous sodium acetate (145 mg, 1.77 mmol) and refluxed the mixture for 3 hours. The product was obtained as a yellow solid with a yield of 60% (860 mg, 3.56 mmol).

¹H NMR (600 MHz, CDCl₃) δ 8.1 – 8.0 (m, 2H), 7.6 – 7.6 (m, 2H), 3.4 (s, 2H), 2.5 – 2.4 (m, 2H), 1.7 – 1.5 (m, 2H), 1.4 (h, *J* = 7.4 Hz, 2H), 0.9 (t, *J* = 7.4 Hz, 3H) [ppm].

¹³C NMR (151 MHz, CDCl₃) δ 171.1, 161.4, 141.9, 133.3, 119.2, 118.5, 107.9, 42.1, 31.2, 28.7, 22.6, 14.0 [ppm].

HRMS: ESI-mass m/z calcd. for C₁₄H₁₆N₃O: 242.1288 and found: 242.1283.
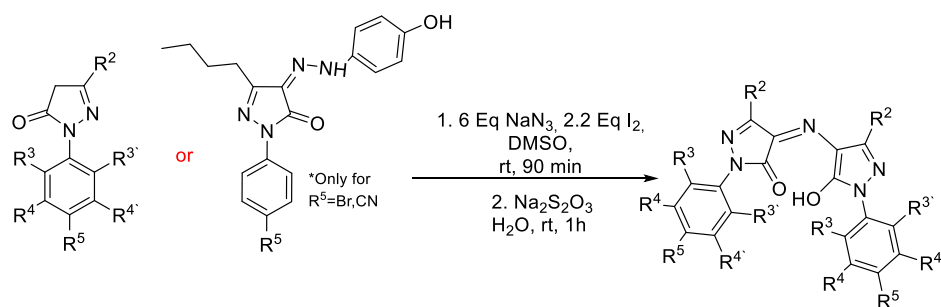
The synthesis of rubazonic acid derivatives was achieved using a general procedure (B). Pyrazolone or HP 2 (1 eq.) was dissolved in DMSO (0.15 M), followed by the addition of sodium azide (6 eq.) and iodine (2.2 eq.). The reaction mixture was stirred at room temperature for 90 minutes. Then, an excess of saturated aqueous sodium thiosulfate solution was added and stirred for an additional 60 minutes. Distilled water was then added and the mixture was extracted twice with dichloromethane. The combined organic phases were extracted with brine, dried over Na_2SO_4, and purified by flash chromatography on silica gel (using DCM/MeOH 9:1).

(Z)-5-butyl-4-((3-butyl-5-hydroxy-1-(2,3,5,6-tetrafluorophenyl)-1H-pyrazol-4-yl) imino)-2-(2,3,5,6-tetrafluorophenyl)-2,4-dihydro-3H-pyrazol-3-one

I-175b
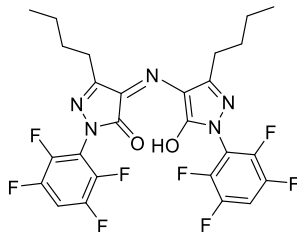
(*Z*)-5-butyl-4-((3-butyl-5-hydroxy-1-(2,3,5,6-tetrafluorophenyl)-1*H*-pyrazol-4-yl)imino)-2-
(2,3,5,6-tetrafluorophenyl)-2,4-dihydro-3*H*-pyrazol-3-one
Chemical Formula: $C_{26}H_{21}F_8N_5O_2$
Molecular Weight: 587,4742

In accordance with procedure B, the pyrazolone **I-166b** (0.300 g, 1.04 mmol) was dissolved in DMSO (7 ml), followed by the addition of sodium azide (0.400 g, 6.24 mmol) and iodine (0. 581 g, 2.29 mmol). The rubazonic acid was obtained as read solid (250 mg, 0.43 mmol, 41%).

^{1}H NMR (400 MHz, CDCl$_3$) δ 7.2 – 7.1 (m, 2H), 2.7 (t, *J* = 7.7 Hz, 2H), 2.6 (q, *J* = 8.0, 7.3 Hz, 2H), 1.7 – 1.6 (m, 4H), 1.4 (h, *J* = 7.4 Hz, 4H), 0.9 (t, *J* = 7.3 Hz, 6H) [ppm].

^{19}F NMR (376 MHz, CDCl$_3$) δ -137.45, -143.53 [ppm].

HRMS: no data.

(Z)-5-butyl-4-((3-butyl-1-(4-chlorophenyl)-5-hydroxy-1H-pyrazol-4-yl)imino)-2-(4-chlorophenyl)-2,4-dihydro-3H-pyrazol-3-one

I-176b
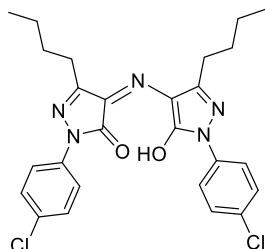
(*Z*)-5-butyl-4-((3-butyl-1-(4-chlorophenyl)-5-hydroxy-1*H*-pyrazol-4-yl)imino)-2-(4-chlorophenyl)-2,4-dihydro-3*H*-pyrazol-3-one
Chemical Formula $C_{26}H_{27}Cl_2N_5O_2$
Molecular Weight: 512,44

In accordance with procedure B, the pyrazolone **I-167b** (0.195 g, 0.78 mmol) was dissolved in DMSO (5 ml), followed by the addition of sodium azide (0.300 g, 4.67 mmol) and iodine (0.434 g, 1.71 mmol). The rubazonic acid was obtained as read solid (0.203 g, 0.4 mmol, 51%).

^{1}H NMR (600 MHz, CDCl$_3$) δ 7.9 – 7.8 (m, 4H), 7.4 (m, 4H), 2.8 – 2.7 (m, 2H), 2.4 (t, *J* = 7.6 Hz, 2H), 1.8 – 1.7 (m, 4H), 1.4 (dq, *J* = 9.1, 7.3 Hz, 5H), 1.0 (t, *J* = 7.4 Hz, 6H) [ppm].

^{13}C NMR (151 MHz, CDCl$_3$) δ 163.8, 158.8, 157.9, 152.3, 135.3, 131.2, 129.1, 125.3, 121.8, 119.8, 118.8, 30.1, 26.9, 22.2, 13.6 [ppm].

HRMS: ESI-mass m/z calcd. for $C_{26}H_{28}N_5O2$: 512.1615 and found: 512.1613.

(Z)-2-(4-bromophenyl)-4-((1-(4-bromophenyl)-5-hydroxy-3-methyl-1H-pyrazol-4-yl)imino)-5-methyl-2,4-dihydro-3H-pyrazol-3-one

II-177a
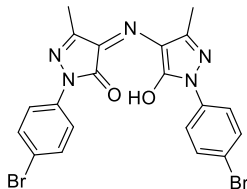
(Z)-2-(4-bromophenyl)-4-((1-(4-bromophenyl)-5-hydroxy-3-methyl-1H-pyrazol-4-yl)imino)-5-methyl-2,4-dihydro-3H-pyrazol-3-one
Chemical Formula: $C_{20}H_{15}Br_2N_5O_2$
Molecular Weight: 517,1810

In accordance with procedure B, the pyrazolone **I-168a** (56 mg, 0.22 mmol was dissolved in DMSO (1.5 ml), followed by the addition of sodium azide (86 mg, 1.33 mmol) and iodine (124 mg, 0.49 mmol). Te product was purified by flash chromatography on silica gel (using DCM/MeOH 9:1). The rubazonic acid was obtained as read solid (64 mg, 0.12 mmol, 56%).

^{1}H NMR (600 MHz, DMSO-d_6) δ 7.9 – 7.4 (m, 8H), 2.1 (s, 6H) [ppm].

^{13}C NMR (151 MHz, DMSO) δ 132.0, 120.5, 12.6 [ppm].

HRMS: no data.

(Z)-2-(4-bromophenyl)-4-((1-(4-bromophenyl)-3-hexyl-5-hydroxy-1H-pyrazol-4-yl)imino)-5-hexyl-2,4-dihydro-3H-pyrazol-3-one

I-177c
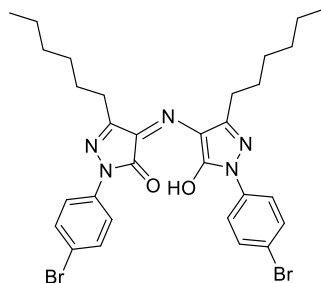
(Z)-2-(4-bromophenyl)-4-((1-(4-bromophenyl)-3-hexyl-5-hydroxy-1H-pyrazol-4-yl)imino)-5-hexyl-2,4-dihydro-3H-pyrazol-3-one
Chemical Formula: $C_{30}H_{35}Br_2N_5O_2$
Molecular Weight: 657,4510

In accordance with procedure B, the pyrazolone **I-168c** (0.200 g, 0.62 mmol was dissolved in DMSO (4 ml), followed by the addition of sodium azide (0.241 g, 3.71 mmol) and iodine (0.346 g, 1.36 mmol). The product was purified by flash chromatography on silica gel (using DCM/MeOH 9:1). The rubazonic acid was obtained as read solid (0.165 g, 0.25 mmol, 40%).

^{1}H NMR (400 MHz, CDCl3) δ 7.8 (m, 2H), 7.8 – 7.7 (m, 2H), 7.6 – 7.5 (m, 4H), 2.7 (m, 2H), 2.4 (d, J = 7.5 Hz, 1H), 1.8 – 1.7 (m, 4H), 1.3 (h, J = 4.0 Hz, 8H), 0.9 (td, J = 7.1, 5.6, 3.8 Hz, 6H) [ppm].

^{13}C NMR (151 MHz, CDCl3) δ 158.1, 152.5, 136.8, 128.7, 127.4, 125.5, 122.2, 120.3, 31.7, 29.4, 28.2, 26.9, 22.7, 14.2 [ppm].

HRMS: no data.

(Z)-2-(4-bromophenyl)-4-((1-(4-bromophenyl)-3-butyl-5-hydroxy-1H-pyrazol-4-yl)imino)-5-butyl-2,4-dihydro-3H-pyrazol-3-one

I-181a
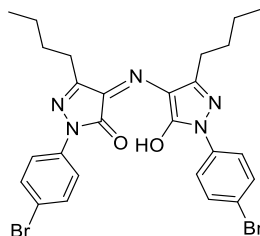
(*Z*)-2-(4-bromophenyl)-4-((1-(4-bromophenyl)-3-butyl-5-hydroxy-1*H*-pyrazol-4-yl)imino)-5-butyl-2,4-dihydro-3*H*-pyrazol-3-one
Chemical Formula: $C_{26}H_{27}Br_2N_5O_2$
Molecular Weight: 601,3430

In accordance with procedure B, the hydrazono-pyrazolone **I-106c** (0.150 g, 0.36 mmol) was dissolved in DMSO (2.5 ml), followed by the addition of sodium azide (0.141 g, 2.17 mmol) and iodine (0.202 g, 0.79 mmol). The rubazonic acid was obtained as read solid (0.137 g, 0.23 mmol, 63%).

^{1}H NMR (400 MHz, CDCl$_3$) δ 7.9 – 7.8 (m, 2H), 7.8 – 7.7 (m, 2H), 7.6 – 7.5 (m, 4H), 2.8 – 2.7 (m, 2H), 2.5 – 2.4 (m, 1H), 1.8 – 1.7 (m, 4H), 1.5 – 1.4 (m, 4H), 1.0 (t, *J* = 7.4 Hz, 6H) [ppm].

^{13}C NMR (101 MHz, CDCl$_3$) δ 158.0, 152.3, 138.4, 132.0, 122.1, 120.1, 30.1, 26.4, 22.7, 13.8 [ppm].

HRMS: ESI-mass m/z calcd. for $C_{26}H_{28}Br_2N_5O_2$: 600.0604 and found: 600.0602.

(Z)-5-butyl-4-((3-butyl-5-hydroxy-1-phenyl-1H-pyrazol-4-yl)imino)-2-phenyl-2,4-dihydro-3H-pyrazol-3-one

I-178b
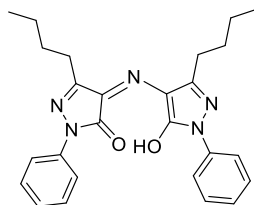
(Z)-5-butyl-4-((3-butyl-5-hydroxy-1-phenyl-1*H*-pyrazol-4-yl)imino)-2-phenyl-2,4-dihydro-3*H*-pyrazol-3-one
Chemical Formula: $C_{26}H_{29}N_5O_2$
Molecular Weight: 443,5510

In accordance with procedure B, the pyrazolone **I-163b** (0.565 g, 2.61 mmol was dissolved in DMSO (18 ml), followed by the addition of sodium azide (1 g, 15.67 mmol) and iodine (1.46 g, 5.75 mmol). The product was purified by flash chromatography on silica gel (using DCM/MeOH 9:1). The rubazonic acid was obtained as read solid (0.498 g, 1.12 mmol, 43%).

^{1}H NMR (400 MHz, CDCl$_3$) δ 7.9 – 7.8 (m, 4H), 7.5 – 7.4 (m, 4H), 7.3 – 7.2 (m, 2H), 2.7 (m, 4H), 1.8 – 1.6 (m, 4H), 1.4 (dt, J = 14.8, 7.4 Hz, 4H), 0.9 (t, J = 7.4 Hz, 6H) [ppm].

^{13}C NMR (101 MHz, CDCl$_3$) δ 157.8, 152.1, 138.2, 131.8, 121.9, 120.0, 29.9, 26.2, 22.5, 13.6 [ppm].

HRMS: ESI-mass m/z calcd. for $C_{26}H_{28}N_5O_2$: 442.2248 and found: 442.2240.

(Z)-4-(3-butyl-4-((3-butyl-1-(4-cyanophenyl)-5-hydroxy-1H-pyrazol-4-yl)imino)-5-oxo-4,5-dihydro-1H-pyrazol-1-yl)benzonitrile

I-179b
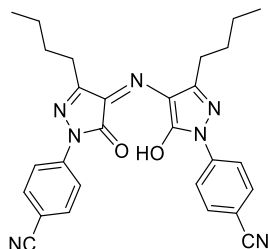
(Z)-4-(3-butyl-4-((3-butyl-1-(4-cyanophenyl)-5-hydroxy-1H-pyrazol-4-yl)imino)-5-oxo-
4,5-dihydro-1H-pyrazol-1-yl)benzonitrile
Chemical Formula: $C_{28}H_{27}N_7O_2$
Molecular Weight: 493,5710

In accordance with procedure B, the pyrazolone **I-171b** (0.800 g, 3.32 mmol was dissolved in DMSO (22 ml), followed by the addition of sodium azide (1.3 g, 19.89 mmol) and iodine (1.851 g, 7.29 mmol). The product was purified by flash chromatography on silica gel (using DCM/MeOH 9:1). The rubazonic acid was obtained as read solid (0.573 g, 1.16 mmol, 35%).

^{1}H NMR (600 MHz, CDCl$_3$) δ 8.1 (d, J = 8.6 Hz, 4H), 7.7 (d, J = 8.6 Hz, 4H), 2.7 (t, J = 7.8 Hz, 4H), 1.7 (p, J = 7.7 Hz, 4H), 1.4 (dt, J = 14.9, 7.5 Hz, 4H), 0.9 (t, J = 7.4 Hz, 6H) [ppm].

^{13}C NMR (151 MHz, CDCl$_3$) δ 158.9, 153.3, 141.2, 133.4, 125.8, 120.7, 118.7, 110.2, 30.2, 26.7, 22.9, 14.1 [ppm].

HRMS: ESI-mass m/z calcd. for $C_{28}H_{28}N_7O_2$: 494.2299 and found: 494.2298.

(Z)-4-(3-butyl-4-((3-butyl-1-(4-cyanophenyl)-5-hydroxy-1H-pyrazol-4-yl)imino)-5-oxo-4,5-dihydro-1H-pyrazol-1-yl)benzonitrile

I-181b
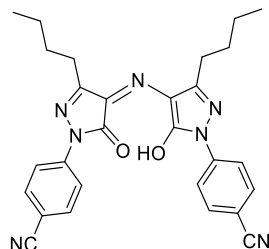
(Z)-4-(3-butyl-4-((3-butyl-1-(4-cyanophenyl)-5-hydroxy-1H-pyrazol-4-yl)imino)-5-oxo-
4,5-dihydro-1H-pyrazol-1-yl)benzonitrile
Chemical Formula: $C_{28}H_{27}N_7O_2$
Molecular Weight: 493,5710

In accordance with procedure B, the hydrazono-pyrazolone I-**106b** (0.100 g, 0.28 mmol was dissolved in DMSO (2 ml), followed by the addition of sodium azide (0.100 g, 1.66 mmol) and iodine (0.155 g, 0.61 mmol). The rubazonic acid was obtained as read solid (72 mg, 0.15 mmol, 53%).

^{1}H NMR (600 MHz, CDCl$_3$) δ 8.1 (d, J = 8.6 Hz, 4H), 7.7 (d, J = 8.6 Hz, 4H), 2.7 (t, J = 7.8 Hz, 4H), 1.7 (p, J = 7.7 Hz, 4H), 1.4 (dt, J = 14.9, 7.5 Hz, 4H), 0.9 (t, J = 7.4 Hz, 6H) [ppm].

^{13}C NMR (151 MHz, CDCl$_3$) δ 158.9, 153.3, 141.2, 133.4, 125.8, 120.7, 118.7, 110.2, 30.2, 26.7, 22.9, 14.1 [ppm].

HRMS: ESI-mass m/z calcd. for $C_{28}H_{28}N_7O_2$: 494.2299 and found: 494.2298.

(Z)-5-butyl-4-((3-butyl-5-hydroxy-1-(4-hydroxyphenyl)-1H-pyrazol-4-yl)imino)-2-(4-hydroxyphenyl)-2,4-dihydro-3H-pyrazol-3-one

I-180b
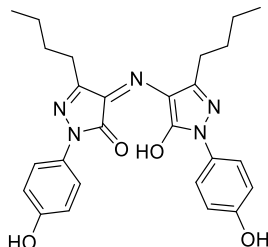
(*Z*)-5-butyl-4-((3-butyl-5-hydroxy-1-(4-hydroxyphenyl)-1*H*-pyrazol-4-yl)imino)-2-(4-hydroxyphenyl)-2,4-dihydro-3*H*-pyrazol-3-one
Chemical Formula: $C_{26}H_{29}N_5O_4$
Molecular Weight: 475,5490

In accordance with procedure B, the pyrazolone **I-170b** (0.166 g, 0.71 mmol) was dissolved in DMSO (5 ml), followed by the addition of sodium azide (0.278 g, 4.29 mmol) and iodine (0.399 g, 1.57 mmol). The rubazonic acid was obtained as read solid (0.210 g, 0.44 mmol, 62%).

^{1}H NMR (400 MHz, DMSO-d_6) δ 9.7 (s, 2H), 7.5 (m, 4H), 6.85 (m, 4H), 2.6 – 2.5 (m, 4H), 1.6 (p, *J* = 7.4 Hz, 4H), 1.4 – 1.3 (m, 4H), 0.8 (t, *J* = 7.3 Hz, 6H) [ppm].

^{13}C NMR (101 MHz, DMSO) δ 156.3, 128.7, 124.5, 122.6, 115.4, 99.4, 29.5, 25.7, 22.0, 13.5 [ppm].

HRMS: ESI-mass m/z calcd. for $C_{26}H_{28}N_5O_4$: 474.2147 and found: 474.2147.

(Z)-4-((5-hydroxy-1-(4-hydroxyphenyl)-3-octyl-1H-pyrazol-4-yl)imino)-2-(4-hydroxyphenyl)-5-octyl-2,4-dihydro-3H-pyrazol-3-one

I-180d
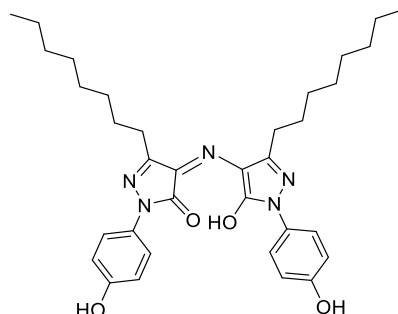
(*Z*)-4-((5-hydroxy-1-(4-hydroxyphenyl)-3-octyl-1*H*-pyrazol-4-yl)imino)-2-(4-hydroxyphenyl)-
5-octyl-2,4-dihydro-3*H*-pyrazol-3-one
Chemical Formula: $C_{34}H_{45}N_5O_4$
Molecular Weight: 587,7650

In accordance with procedure B, the pyrazolone **I-170d** (0.800 g, 2.7 mmol) was dissolved in DMSO (18.5 ml), followed by the addition of sodium azide (1 g, 16.64 mmol) and iodine (1.5 mg, 6.1 mmol). The rubazonic acid was obtained as read solid (0.283 g, 0.48 mmol, 17%).

^{1}H NMR (600 MHz, DMSO-d_6) δ 7.6 – 7.4 (m, 4H), 6.9 – 6.7 (m, 4H), 4.3 (s, 2H), 1.6 (tdd, *J* = 17.0, 13.0, 7.4 Hz, 4H), 1.3 (q, *J* = 7.6 Hz, 4H), 1.2 (m, 20H), 0.8 (dt, *J* = 10.0, 4.1 Hz, 6H) [ppm].

^{13}C NMR (151 MHz, DMSO) δ 120.4, 115.3, 94.4, 57.3, 55.9, 31.2, 28.6, 22.0, 18.5, 13.9 [ppm].

HRMS: no data.

(Z)-5-butyl-4-((3-butyl-5-hydroxy-1-(4-(prop-2-yn-1-yloxy)phenyl)-1H-pyrazol-4-yl)imino)-2-(4-(prop-2-yn-1-yloxy)phenyl)-2,4-dihydro-3H-pyrazol-3-one

I-183
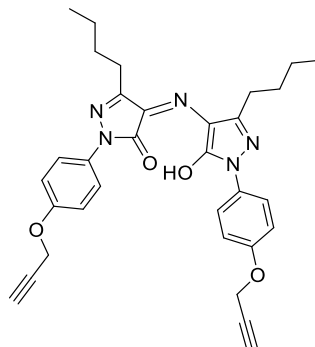
(*Z*)-5-butyl-4-((3-butyl-5-hydroxy-1-(4-(prop-2-yn-1-yloxy)phenyl)-1*H*-pyrazol-4-yl)imino)-2-(4-(prop-2-yn-1-yloxy)phenyl)-2,4-dihydro-3*H*-pyrazol-3-one
Chemical Formula: $C_{32}H_{33}N_5O_4$
Molecular Weight: 551,6470

In accordance with procedure B, the rubazonic acid **I-180b** (95 mg, 0.2 mmol), potassium carbonate (140 mg, 1 mmol) and propargyl bromide solution (80 wt.% in toluene) (89 µl, 0.8 mmol) dissolve in Ethanol (8.5 ml). The mixture refluxing during 6h under inert atmosphere. The product was extracted by CH_2Cl_2 and brine three times and dried with Na_2SO_4. The product was purified by column chromatography (Pe/EtOAc 3:2) Rf = 0.8. the product was obtained as orange solid (96 mg, 0.17 mmol, 87%).

^{1}H NMR (600 MHz, DMSO) δ 7.7 (d, *J* = 8.9 Hz, 4H), 7.1 − 7.0 (m, 4H), 4.8 (d, *J* = 2.4 Hz, 4H), 2.6 (t, *J* = 7.7 Hz, 4H), 1.6 (p, *J* = 7.5 Hz, 4H), 1.4 (dd, *J* = 9.1, 5.7 Hz, 4H), 0.9 (t, *J* = 7.4 Hz, 6H) [ppm].

^{13}C NMR (151 MHz, DMSO) δ 155.7, 130.8, 122.2, 115.2, 78.9, 78.3, 55.6, 29.5, 26.2, 25.7, 22.0, 13.5 [ppm].

HRMS: ESI-mass m/z calcd. for $C_{32}H_{34}N_5O_4$: 552.2605 and found: 552.2616.

2,7-dibromo-9,9-dioctyl-9H-fluorene

I-190
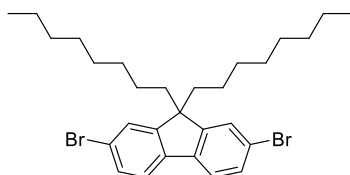
2,7-dibromo-9,9-dioctyl-9*H*-fluorene
Chemical Formula: $C_{29}H_{40}Br_2$
Molecular Weight: 548,4470

The 2,7-Dibromofluorene (1 g, 3.09 mmol) dissolve in DMSO (20 ml) and NaOH aqueous (50 wt%, 1 ml), 1-bromooctane (1.126 ml, 7.41 mmol) was added to the mixture and stirred 2h at rt. After heated the mixture at 80 °C and stirred 24h. MTBE (7 ml) and 2M HCl (60 ml) was added to the mixture and stirred 20 min (mixture should be colorless or light yellow), and after extracted the product with MTBE. Wash the organic phase three times with brine and drayed with sodium sulfate. Solvent was removed under reduced pressure and the crude product was purified via recrystallize product from hexane. (1.219 g, 2.22 mmol, 72%)

^{1}H-NMR (400 MHz, CDCl$_3$): δ 7.5 (d, J = 7.9 Hz, 2H), 7.4 (d, J = 8.0 Hz, 4H), 1.9 - 1.8 (m, 4H), 1.2 - 1.0 (m, 20H), 0.8 (m, 6H), 0.6 - 0.5 (m, 4H) [ppm].

^{13}C NMR (151 MHz, CDCl$_3$) δ 152.9, 139.4, 130.5, 126.5, 121.4, 56.0, 40.5, 32.1, 30.2, 29.5, 27.3, 23.9, 22.9, 14.4 [ppm].

The analytical data are identical to the literature data [180].

(9,9-dioctyl-9H-fluorene-2,7-diyl)bis(trimethylstannane)

I-191
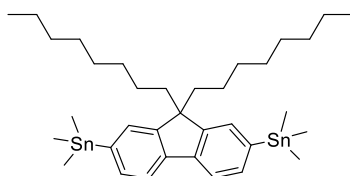
(9,9-dioctyl-9*H*-fluorene-2,7-diyl)bis(trimethylstannane)
Chemical Formula: $C_{35}H_{58}Sn_2$
Molecular Weight: 716,2690

The solution of n-BuLi (1.64 M in hexane, 0,72 ml, 1.81 mmol) was added slowly to a solution of 2,7-dibromo-9,9-didodecylfluorene (0.450 g, 0.82 mmol) in THF (8 ml) at -78. Then was added trimethyltin chloride (0.409 g, 2.05 mmol) in THF (4 ml) at -78 °C after 1 hour. This mixture was stirred for 12 hours at room temperature. The

saturated aqueous NH₄Cl was added to the reaction mixture. The organic layer was extracted with EtOAc. Then the combined organic phase was washed with brine, dried over Na₂SO₄ and concentrated under reduced pressure. The crude product (0.588 g, 0.78 mmol, 95%) was obtained as colorless oil. It was directly used for the next step without further purification

^{1}H NMR (400 MHz, CDCl₃) δ 7.6 (d, J = 7.6 Hz, 2H), 7.4 (m, 3H), 7.3 – 7.2 (m, 1H), 2.00 – 1.91 (m, 4H), 1.26 – 1.03 (m, 24H), 0.87 – 0.82 (m, 6H), 0.69 (s, 6H), 0.34 (d, J = 1.1 Hz, 11H) [ppm].

The analytical data are identical to the literature data [181].

2,7-dibromo-9,9-bis(7-bromoheptyl)-9H-fluorene

I-198
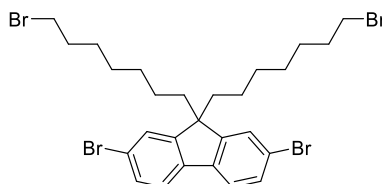
2,7-dibromo-9,9-bis(7-bromoheptyl)-9*H*-fluorene
Chemical Formula: C₂₇H₃₄Br₄
Molecular Weight: 678,1850

The reaction was under inert atmosphere. The potassium hydroxide (15.4 g) dissolve in 30 ml of water and heat to 75-80 °C. The 2,7-dibromofluorene (0.500 g, 1.54 mmol), dibromo octane (4.198 g, 15.43 mmol), and tetrabutylammonium bromide (49.746 mg, 0.15 mmol) adding to hot water base solution. Reaction mixture sire during 1h and then extract with CHCl₃. The organic layer wash with dilute HCl (30 ml), brine (30 ml), and H₂O (30 ml) and drying over Na₂SO₄ and concentrating in vacuo. The yellow oil distils under vacuum to remove excess dibromohexane (about 100 °C). Then product purified by column chloroform/cyclohexane (1:9). The product isolated with 41% of yield (0.450 g, 0.64 mmol).

^{1}H NMR (400 MHz, CDCl₃) δ 7.5 (dd, J = 8.0, 0.6 Hz, 2H), 7.4 (d, J = 1.8 Hz, 1H), 7.4 (m, 3H), 3.3 (t, J = 6.9 Hz, 4H), 1.9 – 1.8 (m, 4H), 1.8 – 1.7 (m, 4H), 1.3 – 1.2 (m, 4H), 1.1 – 1.0 (m, 12H) [ppm].

The analytical data are identical to the literature data [182].

(2,7-dibromo-9H-fluorene-9,9-diyl)bis(heptane-7,1-diyl) diacetate
I-199
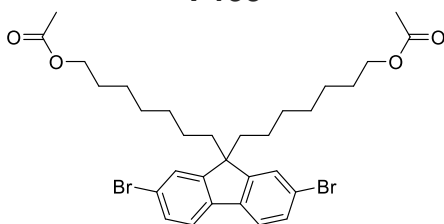
(2,7-dibromo-9*H*-fluorene-9,9-diyl)bis(heptane-7,1-diyl) diacetate
Chemical Formula: $C_{31}H_{40}Br_2O_4$
Molecular Weight: 636,4650

To a 10-ml RBF containing a stir bar and an argon atmosphere was added Reactant **I-198** (0.250 g, 0.35 mmol), anhydrous DMF (2.3 ml), anhydrous THF (1.15 ml), anhydrous potassium carbonate (0.250 g, 1.81 mmol), and Acetic acid (0.145 ml, 1.77 mmol). The reaction was stirred at 90 °C overnight. After cooling to room temperature, the reaction was poured into water (10 ml) and extracted with 2 x 20 ml of Et_2O. After filtering through a pad of silica gel (Cy/EtOAc, 9:1) and concentrating in vacuo, the product was isolated with 79% of yield (0.186 g, 0.28 mmol) as clear oil.

Rf = 0.29 (Cy/EtOAc 9:1).

^{1}H NMR (400 MHz, $CDCl_{3)}$ δ 7.5 – 7.4 (m, 2H), 7.4 – 7.3 (m, 4H), 4.0 (t, *J* = 6.8 Hz, 4H), 2.0 (s, 6H), 1.9 – 1.8 (m, 4H), 1.5 – 1.4 (m, 5H), 1.2 (dq, *J* = 13.6, 7.1, 6.6 Hz, 5H), 1.1 – 1.0 (m, 12H) [ppm].

^{13}C NMR (151 MHz, $CDCl_3$) δ 171.2, 150.7, 141.2, 127.0, 122.9, 119.7, 64.7, 55.1, 40.4, 30.1, 29.2, 28.6, 25.9, 23.8, 21.0 [ppm].

HRMS: no data.

Homopolymers of Rubazonic acid:

I-201
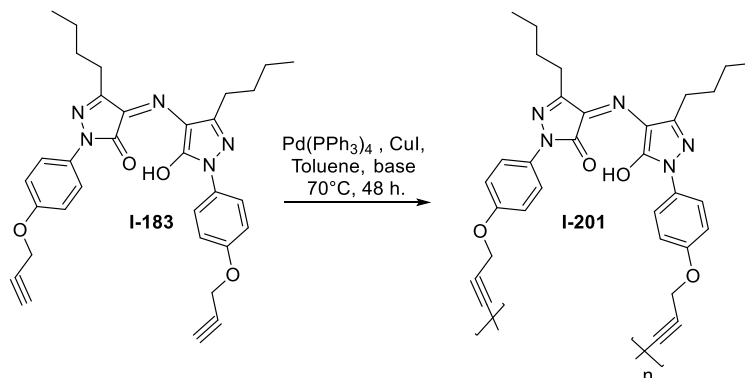
The reaction produces under inert atmosphere in a Schlenk flask in standard Schlenk procedure, the rubazonic acid monomer (240 mg, 0.44 mmol, 1 eq.) were successively introduced to Schlenk round bottom flask. Then, dry toluene (20 ml) and diisopropylamine (DIPA) or triethylamine (Et$_3$N) (5 ml) was added and degassed by bubbling argon under sonications for 20 min. Pd(PPh$_3$)$_4$ (20 mg, 17.55 µmol, 0.04 eq.) and CuI (1.3 mg 6.99 µmol, 0.2 eq.) was quickly added and the reaction mixture was stirred under argon at 70°C for 48 h. The reaction mixture was allowed to cool down at room temperature and concentrating in vacuo. The dark red solid dissolved in THF and filtered through cotton filter. The filtrate was concentrated to 3 ml and precipitated into 150 ml of cold methanol. The precipitation filtrate and dried. The polymer purified by Soxhlet extraction with diethyl ether and then with methanol.

^{1}H NMR (600 MHz, CDCl$_3$) δ 7.6, 7.2, 6.8, 4.9, 2.6, 1.5, 1.4, 1.2, 0.9 [ppm].

Table 17: The Glaser polycondensation of I-183 in different base (* (linear poly(methyl methacrylate) standards (M$_n$ 800–2 200 000 g/mol); in DMAc).

Entry	Base	Mn* [g/mol]	Mw* [g/mol]	Đ*	Yield [%]
1	Et$_3$N	70 000	122 000	1.7	35
2	DIPA	15 500	33 300	2.1	38

MW method

In a 5 ml microwave reactor, rubazonic acid monomer (20 mg, 0.04 mmol, 1 eq.), Pd(PPh$_3$)$_4$ (8 mg, 7.25 µmol, 0.2 eq.), CuI (1.38 mg, 0.01 mmol, 0.2 eq.) were placed. The tube was pumped and filled with Aagon and a mixture of degassed toluene 1.5 ml and Et$_3$N (1.5 ml) was added. To increasing yield, I$_2$ (0.5 eq.) was add as oxidizer agent (

Table **18**). The resulting solution was degassed under argon using ultrasonication for 20 min. The reaction was stirred at 40 °C for 1h under MW irradiation. The reaction mixture was allowed to cool down at room temperature and concentrating in vacuo. The dark red solid dissolved in THF and filtered through cotton filter. The filtrate was concentrated to 0.5 ml and precipitated into 50 ml of cold methanol. The precipitation filtrate and dried. The polymer purified by Soxhlet extraction with methanol.

^{1}H NMR (600 MHz, CDCl$_3$) δ 7.6, 7.2, 6.8, 4.9, 2.6, 1.5, 1.4, 1.2, 0.9 [ppm].

Table 18: The conditions polycondensation of **I-183** by microwave activation.

Pd(PPh$_3$)$_2$Cl$_2$ [eq.]	Pd(PPh$_3$)$_4$ [eq.]	I$_2$ [eq.]	T [°C]	Time [h]	Yield [%]
0.2			100	2	3
	0.2		40	1	11
	0.2	0.5	40	1	24

Polymerization under oxidative conditions:

I-202
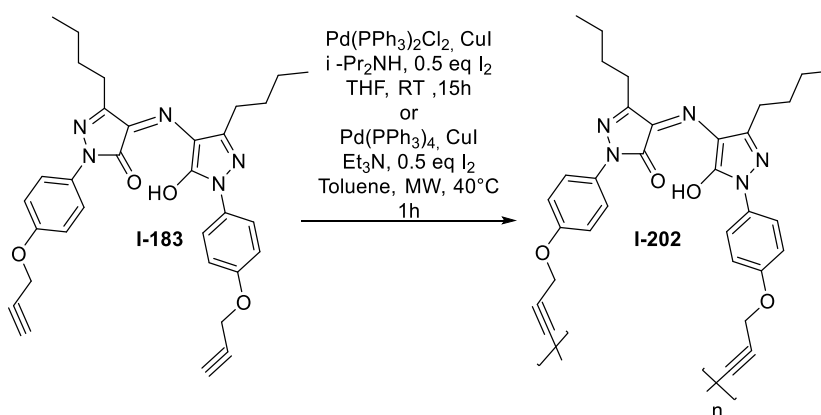
To a mixture of rubazonic acid monomer (105 mg, 0.19 mmol, 1 eq.), Pd(PPh$_3$)$_2$Cl$_2$ (1.8 mg, 2.63 µmol, 0.01 eq.), CuI (1.8 mg, 0.01 mmol, 0.05 eq.), I$_2$ (24 mg, 0.1 mmol, 0.5 eq.) in THF (1 ml) and diisopropyl amine (0.3 ml). The mixture was stirred at room temperature for 15 hours. The solution was filtrate with cotton filter and precipitated in cold MtOH. The product was perfide by Soxhlet. The oligomer was obtained as red solid (43 mg, 0.07 mmol, 39%) with Mn of 2 300 g/mol and Đ of 3 (* measured by GPC in THF and the molar masses were calibrated to polystyrene as an internal standard).

MW method of polymerization under oxidative condition described above.

^{1}H NMR (600 MHz, DMSO) δ 7.8, 6.9, 4.9, 4.7, 2.6, 1.3, 1.3, 1.3, 0.8 [ppm].

I-205

I-205b : R=C_4H_9
I-205c: R=C_8H_{18}
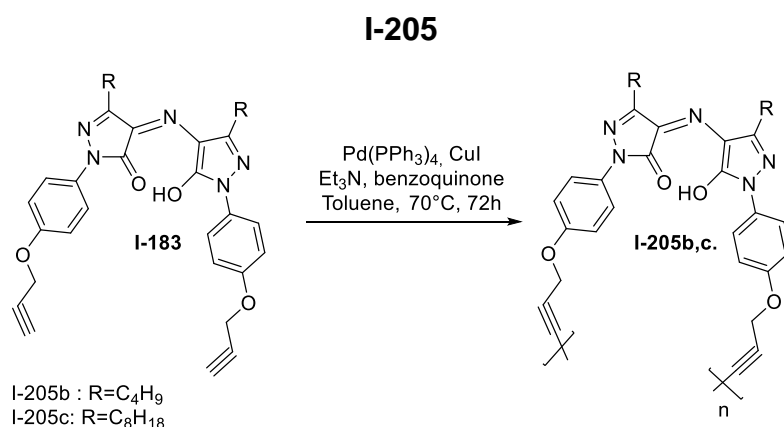
The rubazonic acid monomer (75 mg, 0.11 mmol, 1 eq.), CuI (13 mg, 0.07 mmol, 0.63 eq.), Pd(PPh3)4 (6.3 mg, 5.42 µmol, 0.05 eq.) and benzoquinone (30 mg, 0.27 mmol, 2.5 eq.) were combined under argon in a sealable Schlenk tube fitted with septum. To this were added 4 ml of toluene and 0.7 ml of diisopropylamine. The solution was heated to 60 °C under argon; then, the septum was replaced with a threaded Teflon stopper under a positive pressure of argon. The tube was sealed, and the reaction mixture was stirred at 60 °C for 72 h. The reaction mixture was allowed to cool down at room temperature and concentrating in vacuo. The dark red solid dissolved in THF and filtered through cotton filter. The filtrate was concentrated to 2 ml of THF and precipitated into 200 ml of cold methanol. The precipitation filtrate and dried. The polymer purified by Soxhlet extraction with methanol. After Soxhlet extraction this product was difficult to completely redissolve into THF or other organic solvents after it had been precipitated.

Table 19: The oxidative conditions and results of Glaser polycondensation of **I-183**.

I-205	RA C_8H_{18} Eq.	RA C_4H_9 Eq.	Pd° Eq.	CuI Eq.	Benzoquinone Eq.	Yield %
d	1		0.05	0.6	2.5	56
c		1	0.05	0.6	2.5	42

I-205d: ^{1}H NMR (400 MHz, DMSO) δ 7.6, 7.5, 1.1, 0.8 [ppm].

I-205c: ^{1}H NMR (400 MHz, DMSO) δ 8.1, 7.6, 7.1, 4.9, 1.5, 1.1, 0.8 [ppm].

I-204
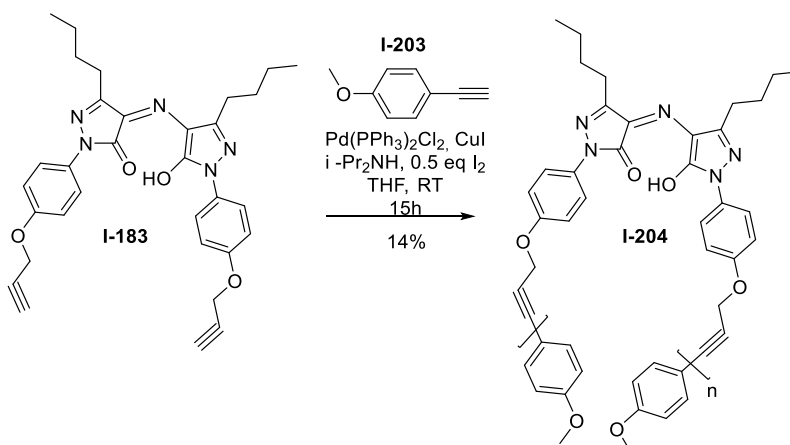
To a mixture of rubazonic acid monomer (70 mg, 0.13 mmol, 1 eq.), 1-ethynyl-4-methoxybenzene (33 mg, 0.25 mmol, 2 eq.) Pd(PPh$_3$)$_2$Cl$_2$ (1.2 mg, 1.75 µmol, 0.01 eq.), CuI (1.2 mg, 0.01 mmol, 0.05 eq.), I$_2$ (15.7 mg, 0.6 mmol, 0.5 eq.) in THF (0.9 ml) and diisopropyl amine (0.2 ml). The mixture was stirred at room temperature for 15 hours. The solution was filtrate with cotton filter and precipitated in cold MtOH. The product was perfide by Soxhlet. The oligomer was obtained as red solid (13 mg, 0.02 mmol, 14%) with Mn of 2 400 g/mol g/mol and Đ of 3.4 and n=4 (measured by GPC in THF and the molar masses were calibrated to polystyrene as an internal standard).

^{1}H NMR (600 MHz, DMSO) δ 9.7, 7.7, 7.5, 7.1, 6.9, 5.0, 4.8, 3.7, 1.6, 1.4, 0.9 [ppm].

Poly rubazonic acid 1,4-bis((Z)-2-chloroprop-1-en-1-yl)benzene

I-208
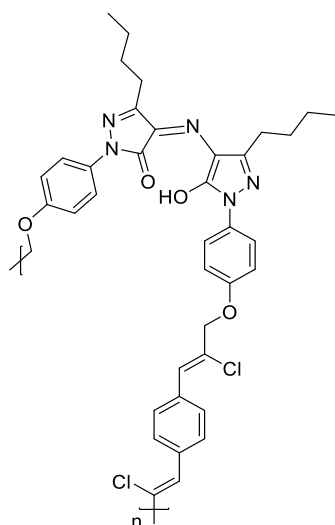
The reaction produces under inert atmosphere in a Schlenk flask in standard Schlenk procedure. To a 5 ml Schlenk tube was placed of Rh(cod)Cl$_2$ (6.1 mg, 0.01 mmol), PPh$_3$ (6.6 mg, 0.03 mmol), rubazonic acid monomer (115 mg, 0.21 mmol) and terephthaloyl dichloride (42.3 mg, 0.21 mmol). Freshly dried *o*-xylene (2 mL) was then injected into the tube using a hypodermic syringe. The resultant mixture was stirred at 140 °C under nitrogen for 12 h. The polymerisation was quenched by the addition of a small amount of methanol. The solution was then added dropwise to 500 mL of hexane via a cotton filter under stirring. The precipitate was allowed to stand overnight and then collected by filtration. The polymer was washed with hexane and dried under vacuum at room temperature to a constant weight. The product was obtained as a red powder with 31% yield (47 mg, 0.06 mmol).

Mn= 1370 g/mol, Đ =1.4, n=2 (measured by GPC in THF and the molar masses were calibrated to polystyrene as an internal standard).

^{1}H NMR (400 MHz, CDCl$_3$) δ 8.1, 8.0, 7.8, 7.7, 7.3, 7.0, 6.9, 6.8, 4.7, 2.7, 1.7, 1.4, 1.2, 0.9 [ppm].

Rubazonic acid polyether ether ketone:

I-128

R = C_4H_9 (a), C_8H_{18} (b)
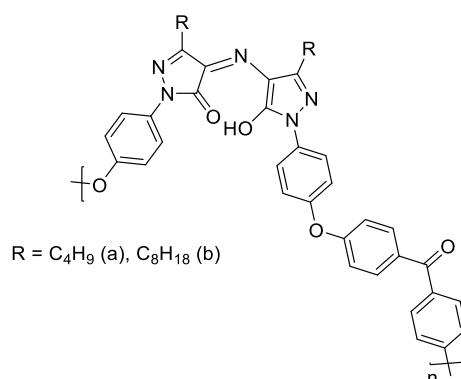
The enol rubazonic acid (120 mg, 0.19 mmol) and 4,4`-difluorobenzophenone (DFBP) (42.5 mg, 0.19 mmol), and K_2CO_3 (40 mg, 0.29 mmol) were added to a three-necked flask equipped with a water separator under nitrogen protection. DMAc (0.5 ml) was used as the reaction solvent, and toluene (0.1 ml) was used as the water-carrying agent. The mixture was stirred at 160 °C for 6 h until the viscosity of the reaction solution no longer increased and stopped heating. After the reaction was complete, it was poured it into the water while it was still hot and the polymer was reversely precipitated. Then precipitation wash with cold MeOH. The polymer purified under Soxhlet extraction with MeOH.

I-212b ^{1}H NMR (600 MHz, DMSO) δ 8.10, 7.76, 7.16, 7.08, 1.70, 1.38, 0.93. [ppm].

I-212d ^{1}H NMR (400 MHz, DMSO) δ 7.7, 7.1, 2.5, 1.1, 0.7 [ppm].

Table 20:The conditions and results of synthesis of I-212 by nucleophilic aromatic substitution reaction(measured by GPC in THF and the molar masses were calibrated to polystyrene as an internal standard).

I-212	Solvent	T [°C]	Time [h]	Yield [%]	Mn [g/mol]	Mw [g/mol]	Đ	n
b	DMAc/Toluene	170	10	38	1 860	2 730	1.4	2
b	DMAc/Toluene	180	12	82				
b	DMAc/Toluene	160	48	87				
b	DMAc	160	16	80				
b	DMAc/Toluene	160	6	84	2 600	3 270	1.2	4
d	DMAc/Toluene	160	6	41	3 470	9 610	2.7	4

I-214

R = C₈H₁₈ (d)

To a stirred solution of rubazonic acid polymer (45 mg, 0.05 mmol) in a dichloromethane (1.3 ml) was added 1,2-ethanedithiol (18.6 µl, 0.22 mmol) followed by boron trifluoride diethyl etherate (7.8 µl, 0.06 mmol) under an atmosphere of nitrogen. After three days at room temperature the deep red solution was poured into methanol (100 ml). The polymer **I-214** was isolated as red solid with 95% of yield (48 mg, 0.05 mmol). Mn is 6 030 g/mol and Đ is 3, n = 7 (measured by GPC in THF and the molar masses were calibrated to polystyrene as an internal standard).

^{1}H NMR (600 MHz, CDCl$_3$) δ 7.8, 7.4, 7.1, 7.0, 2.8, 2.5, 1.5, 1.2, 0.8 [ppm].

Polyurethanes:

The synthesis of rubazonic acid polyurethane was achieved using a general procedure (C). Firstly, rubazonic acid **I-180b** (1 eq.) and DABCO (0.04 eq.) were dissolved in anhydrous THF. Next, diisocyanate (1 eq.) was added to the solution, and the reaction mixture was mixed at 75 °C for 7 hours under a nitrogen atmosphere until the clear solution became significantly viscous, indicating polymerization. The resulting mixture was then cooled to room temperature and precipitated from cold Et_2O. Finally, the product was dried under vacuum at room temperature for 24 hours to obtain the resulting polymer.

Polyurethane RA1.1

I-216
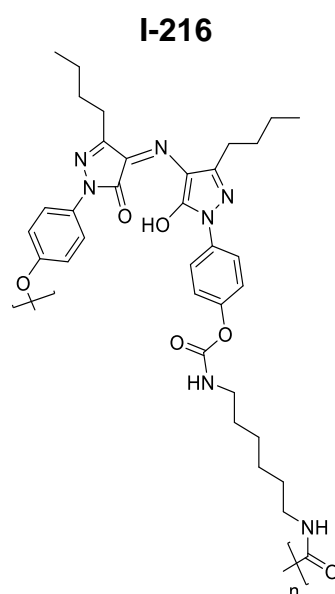
In accordance with procedure C, the rubazonic acid **I-180b** (100 mg, 0.21 mmol) and DABCO (1 mg, 8.91 µmol) were dissolved in 3 ml of anhydrous THF. Next, hexamethylene diisocyanate (48.7 mg, 0.29 mmol) was added to the solution, and the reaction mixture was mixed at 75 °C for 7 hours under a nitrogen atmosphere until. The polymer **I-216** isolated as red solid with 51% of yield (75 mg, 0.11 mmol). Mn= 3 300 g/mol, Đ = 1.5, n = 5 (measured by GPC in THF and the molar masses were calibrated to polystyrene as an internal standard).

^{1}H NMR (400 MHz, DMSO) δ 7.7, 7.2, 7.2, 3.0, 3.0, 2.6, 1.6, 1.5, 1.3, 0.9 [ppm].

Polyurethane RA1.2:

I-218a
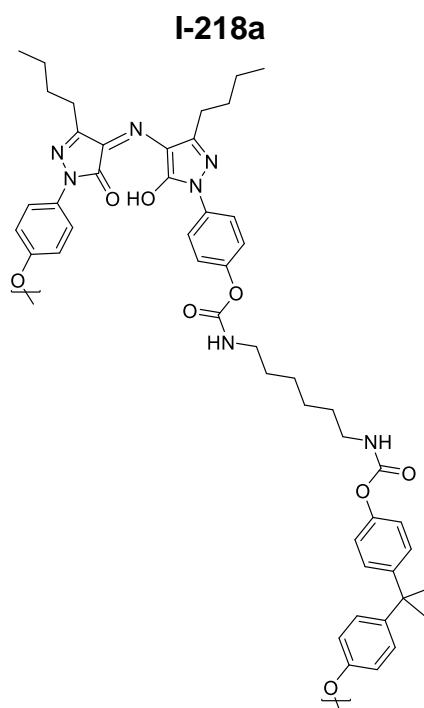
In accordance with procedure C, the rubazonic acid **I-180b** (102 mg, 0.21 mmol) and DABCO (1 mg, 8.91 µmol) were dissolved in 3.2 ml of anhydrous THF. Next, hexamethylene diisocyanate (49.7 mg, 0.3 mmol), bisphenol A (49 mg, 0.21 mmol) was added to the solution, and the reaction mixture was mixed at 75 °C for 7 hours under a nitrogen atmosphere until. The polymer **I-218** isolated as red solid with 17% of yield (33 mg, 0.04 mmol), Mn= 3 370 g/mol, Đ = 1.4, n = 4 (measured by GPC in THF and the molar masses were calibrated to polystyrene as an internal standard).

^{1}H NMR (400 MHz, DMSO) δ 9.7, 7.8, 7.6, 7.1, 6.9, 6.8, 6.6, 2.6, 1.6, 1.5, 1.6, 0.9 [ppm].

I-218b
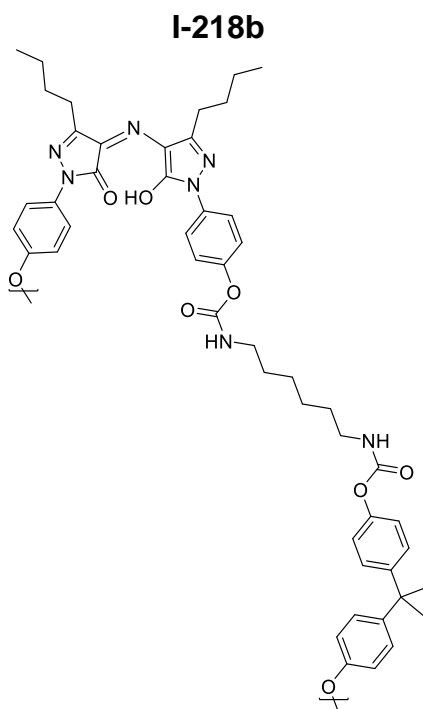
In accordance with procedure C, the rubazonic acid **I-180b** (73 mg, 0.15 mmol) and DABCO (1 mg, 8.91 µmol) were dissolved in 2.2 ml of anhydrous THF. Next, hexamethylene diisocyanate (63.9 µl, 0.4 mmol), bisphenol A (35 mg, 0.15 mmol) was added to the solution, and the reaction mixture was mixed at 75 °C for 7 hours under a nitrogen atmosphere until. The polymer **I-218b** isolated as red solid with 97% of yield (134 mg, 0.15 mmol).

^{1}H NMR (400 MHz, DMSO) δ 7.8, 7.6, 7.2, 7.1, 7.0, 5.8, 5.7, 3.1, 3.0, 2.9, 2.1, 1.6, 1.4, 1.3. 1.2, 0.9 [ppm].

Polyurethane RA2.1:

I-220
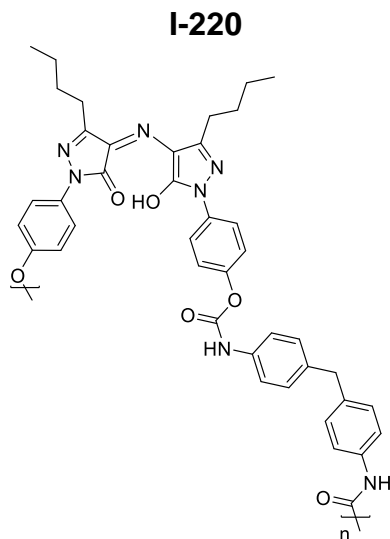
In accordance with procedure C, the rubazonic acid **I-180b** (160 mg, 0.34 mmol) and DABCO (1.6 mg, 14.8 µmol) were dissolved in 5 ml of anhydrous THF. Next, 4,4′-methylenebis(phenyl isocyanate) (116 mg, 0.4 mmol) was added to the solution, and the reaction mixture was mixed at 75 °C for 7 hours under a nitrogen atmosphere until. The polymer **I-220** isolated as red solid with 68% of yield (175 mg, 0.23 mmol).

^{1}H NMR (400 MHz, DMSO) δ 10.2, 8.5, 7.9, 7.4, 7.3, 7.1, 7.0, 3.8, 2.6, 1.6, 1.4, 0.9 [ppm].

Polyurethane RA2.2:

I-221a
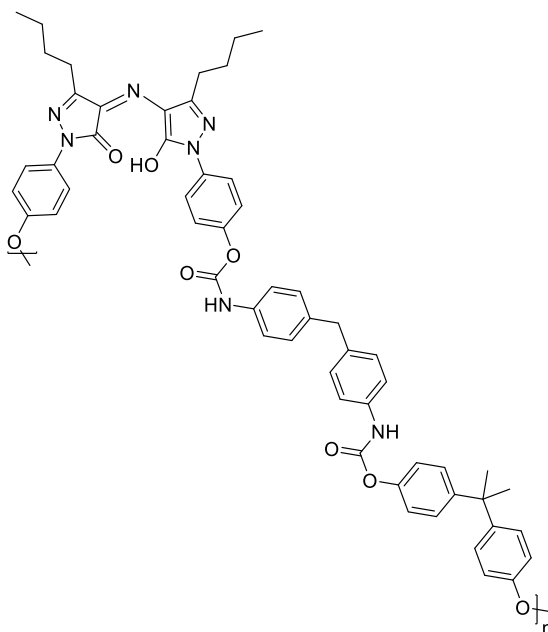
In accordance with procedure C, the rubazonic acid **I-180b** (120 mg, 0.25 mmol) and DABCO (1.2 mg, 11.1 µmol) were dissolved in 3.7 ml of anhydrous THF. Next, 4,4′-methylenebis(phenyl isocyanate) (87 mg, 0.35 mmol), bisphenol A (56 mg, 0.25 mmol) was added to the solution, and the reaction mixture was mixed at 75 °C for 7 hours under a nitrogen atmosphere until. The polymer **I-221** isolated as red solid with 64% of yield (160 mg, 0.16 mmol) Mn= 4 220 g/mol, Đ = 1.7, n = 4 (measured by GPC in THF and the molar masses were calibrated to polystyrene as an internal standard).

^{1}H NMR (400 MHz, DMSO) δ 10.1, 9.7, 7.8, 7.4, 7.3, 7.1, 3.8, 2.6, 1.7, 1.6, 1.3, 0.9 [ppm].

I-221b
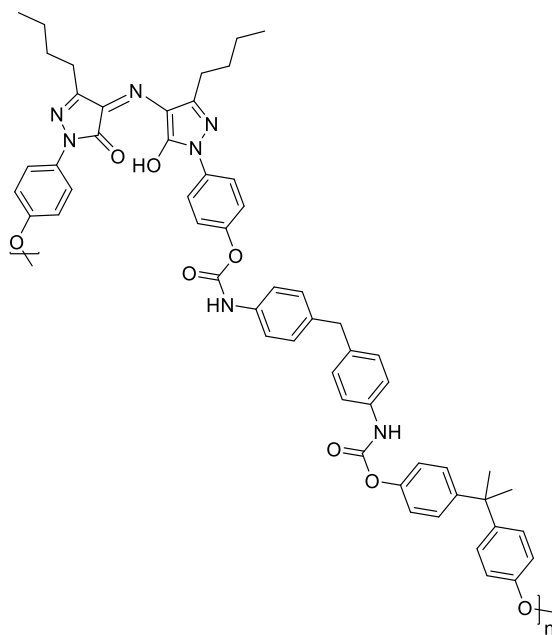
In accordance with procedure C, the rubazonic acid **I-180b** (88 mg, 0.19 mmol) and DABCO (1 mg, 8.17 µmol) were dissolved in 2.7 ml of anhydrous THF. Next, 4,4′-methylenebis(phenyl isocyanate) (120.4 mg, 0.48 mmol), bisphenol A (41.5 mg, 0.19 mmol) was added to the solution, and the reaction mixture was mixed at 75 °C for 7 hours under a nitrogen atmosphere until. The polymer **I-221** isolated as red solid with 98% of yield (178 mg, 0.18 mmol) Mn= 7 260 g/mol, Đ = 2.1, n = 8 (measured by GPC in THF and the molar masses were calibrated to polystyrene as an internal standard).

^{1}H NMR (400 MHz, DMSO) δ 10.1, 8.5, 7.8, 7.4, 7.3, 7.2, 7.1, 7.0, 3.8, 2.6, 1.6, 1.3, 0.9 [ppm].

Polyurethane RA1.3:

I-222

In accordance with procedure C, the rubazonic acid **I-180b** (96 mg, 0.2 mmol) and DABCO (1 mg, 8.17 µmol) were dissolved in 3 ml of anhydrous THF. Next, hexamethylene diisocyanate (45.5 µl, 0.28 mmol), methoxypolyethylene glycol 350 (12.5 mg, 0.16 mmol) was added to the solution, and the reaction mixture was mixed at 75 °C for 7 hours under a nitrogen atmosphere until. The polymer **I-222** isolated as red solid with 45% of yield (70 mg, 0.09 mmol) Mn = 2 860 g/mol, Đ = 1.4, n = 3, m = 5 (measured by GPC in THF and the molar masses were calibrated to polystyrene as an internal standard).

^{1}H NMR (400 MHz, DMSO) δ 7.7, 7.2, 5.7, 3.5, 3.3, 3.0, 2.6, 1.6, 1.5, 1.3, 0.9 [ppm].

Polyurethane RA2.3:

In accordance with procedure C, the rubazonic acid **I-180b** (97 mg, 0.2 mmol) and DABCO (1 mg, 8.17 µmol) were dissolved in 3 ml of anhydrous THF. Next, 4,4′-methylenebis(phenyl isocyanate) (70 mg, 0.28 mmol), methoxypolyethylene glycol 350 (11.7 mg, 0.15 mmol) was added to the solution, and the reaction mixture was mixed at 75 °C for 7 hours under a nitrogen atmosphere until. The polymer **I-223** isolated as red solid with 71% of yield (122 mg, 0.14 mmol) Mn = 4 150 g/mol, Đ = 1.4, n = 5, m = 5 (measured by GPC in THF and the molar masses were calibrated to polystyrene as an internal standard).

^{1}H NMR (400 MHz, DMSO) δ 10.1, 8.5, 7.8, 7.4, 7.3, 7.1, 7.0, 3.8, 3.4, 3.3, 2.6, 1.6, 1.3, 0.9 [ppm].

II.6.3. Part II: Synthesis of new functional linear aliphatic polyester with gem-diazo units
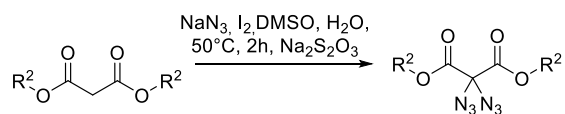
The azidation of malonate derivatives was performed using a general procedure (A). First, malonate derivatives (1 eq.) were dissolved in a mixture of DMSO/H$_2$O or THF (2:1). Sodium azide (6 eq.) was added to the solution, followed by the addition of iodine (2.2 eq.) after cooling the reaction mixture to 0 °C. The reaction mixture was then stirred at 50 °C for 2 hours. Finally, a Na$_2$S$_2$O$_3$ solution was added to the mixture. The water was added and extracted with EtOAc (3 x 200 ml). The combined organic phases were dried over sodium sulfate and the solvent removed under reduced pressure.

Diethyl 2,2-diazidomalonate

II-17
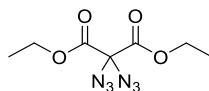
diethyl 2,2-diazidomalonate
Chemical Formula: C$_7$H$_{10}$N$_6$O$_4$
Molecular Weight: 242,20

Following to general procedure A. Diethyl malonate (1 g, 6.24 mmol) was dissolved in DMSO (28 ml) and water (14 ml) or THF (for polymer). Sodium azide (2.43 g, 37.46 mmol), iodine (3.48 g, 13.74 mmol) was added, the reaction mixture reaction was stirred at 50 °C for 2 h. Na$_2$S$_2$O$_3$ solution (200 ml) was added. The crude product is purified by column chromatography (PE:EA 95:5-80:20). The product was obtained as yellow oil (1.25 g, 5.16 mmol, 83%)

^{1}H NMR (600 MHz, CDCl$_3$) δ 4.3 (q, J = 7.1 Hz, 4H), 1.3 (t, J = 7.2 Hz, 6H) [ppm]. The analytical data are identical to the literature data [183].

Poly-4-methoxybutyl 2,2-diazido-3-oxobutanoate

II-32
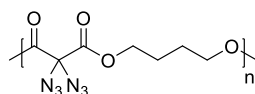
Following to general procedure A. Polyester **II-24** (0.380 g, 2.02 mmol) was dissolved in a mixture of DMSO (8.9 ml) and THF (7.6 ml). Sodium azide (0.787 g, 12.1 mmol) and iodine (1.12 mg, 4.4 mmol). Next, a solution of $Na_2S_2O_3$ (80 ml) was added. The product was obtained as a yellow oil (0.342 g, 1.27 mmol, 63% yield). $Mn = 2\ 660$ g/mol, Đ = 2.4, n = 10 (measured by GPC in THF and the molar masses were calibrated to polystyrene as an internal standard).

$T_{decomp.} = 149$ °C.

^{1}H NMR (600 MHz, CDCl$_3$) δ 4.3 (dt, J = 6.6, 4.0 Hz, 4H), 1.8 – 1.7 (m, 4H) [ppm].

^{13}C NMR (151 MHz, CDCl$_3$) δ 171.2, 163.6, 80.1, 67.2, 24.9 [ppm].

IR(ATR): v [cm^{-1}] 3335, 2962, 2117, 1753.

Poly-6-methoxyhexyl 2,2-diazido-3-oxobutanoate

II-33
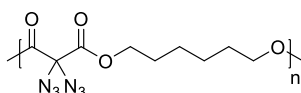
Following to general procedure A. Polyester **II-26** (0.150 g, 0.69 mmol) was dissolved in a mixture of DMSO (3 ml) and THF (2.6 ml). Sodium azide (0.270 g, 4.16 mmol) and iodine (0.390 g, 1.53 mmol). Next, a solution of $Na_2S_2O_3$ (25 ml) was added. The product was obtained as a yellow oil (0.141 g, 0.47 mmol, 68% yield). $Mn = 3\ 600$ g/mol, Đ = 2, n = 12 (measured by GPC in THF and the molar masses were calibrated to polystyrene as an internal standard).

$T_g = 93$ °C, $T_{decomp.} = 147$ °C.

^{1}H NMR (600 MHz, CDCl$_3$) d) δ 4.3 (t, J = 6.6 Hz, 4H), 1.7 (p, J = 7.1 Hz, 4H), 1.4 (ddd, J = 15.4, 7.7, 3.7 Hz, 4H).

^{13}C NMR (101 MHz, CDCl$_3$) δ 171.2, 163.7, 119.1, 80.1, 67.9, 60.5, 28.2, 25.2 [ppm].

IR(ATR): v [cm^{-1}] 3346, 2939, 2104, 1753.

Poly-2-(2-(2-methoxyethoxy)ethoxy)ethyl 2,2-diazido-3-oxobutanoate

II-34
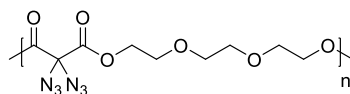
Following to general procedure A. Polyester **II-28** (0.545 g, 2.2 mmol) was dissolved in a mixture of DMSO (10 ml) and THF (8 ml). Sodium azide (0.860 g, 13.22 mmol) and iodine (1.23 mg, 4.85 mmol). Next, a solution of $Na_2S_2O_3$ (110 ml) was added. The product was obtained as a yellow oil (0.632 g, 1.91 mmol, 87% yield). M_n = 3 730 g/mol, Đ = 1.6, n = 11(measured by GPC in THF and the molar masses were calibrated to polystyrene as an internal standard).

T_g = 134 °C, $T_{decomp.}$ = 160 °C.

^{1}H NMR (600 MHz, $CDCl_3$) δ 4.4 (m, 4H), 3.78 (m, 4H), 3.6 (d, J = 13.3 Hz, 4H) [ppm].

^{13}C NMR (151 MHz, $CDCl_3$) δ 163.5, 70.8, 68.6, 66.9, 60.5, 41.1, 29.7, 14.3 [ppm].

IR(ATR): v [cm^{-1}] 3338, 2970, 2119, 1753.
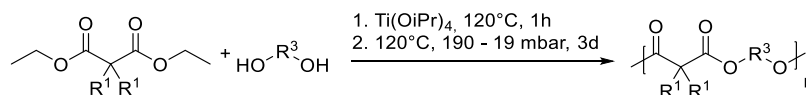
The polymerization of malonate derivatives was carried out using a general procedure (B). First, malonate derivatives (1 eq.) were added to diol derivatives (1 eq.). Titanium (IV) isopropoxide (0.01 eq., 1 mol%) in THF was then added to the reaction mixture, which was stirred under a nitrogen atmosphere at 120 °C for 1 hour, and then at reduced pressure (600 mbar) for 3 hours, followed by further reduction to 19 mbar for 71 hours. The reaction mixture was then cooled and dissolved in THF before addition to cold methanol, then cooled to -20 °C. Methanol is poured off, and the frozen polymer is washed with $CHCl_3$ and dried.

Poly-4-methoxybutyl 3-oxobutanoate

II-24
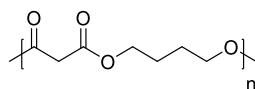
Following to general procedure B. The dimethyl malonate (0.5 ml, 4.37 mmol) was added to 1,4-butandiol (0.4 ml, 4.37 mmol), Titanium (IV) isopropoxide (13 µl, 43.75 µmol) in THF (4.7 ml). The product was obtained as a yellow oil (0.463 g, 2.46 mmol, 56%). M_n = 2 960 g/mol, Đ = 2.8, n = 16 (measured by GPC in THF and the molar masses were calibrated to polystyrene as an internal standard).

^{1}H NMR (600 MHz, CDCl$_3$) δ 4.1 (th, J = 6.6, 3.2 Hz, 4H), 3.3 (s, 2H), 1.7 (hept, J = 3.8 Hz, 4H) [ppm].

^{13}C NMR (101 MHz, CDCl$_3$) δ 166.6, 67.8, 65.0, 29.6, 25.1[ppm].

IR(ATR): v [cm^{-1}] 3418, 2958, 1753.

Poly-4-methoxybutyl 2,2-diazido-3-oxobutanoate

II-25
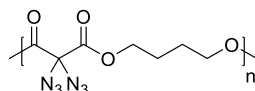
Following to general procedure B. The diethyl 2,2-diazidomalonate (0.180 g, 0.84 mmol) were added to 1,4-butandiol (74.2 µl, 0.84 mmol), Titanium (IV) isopropoxide (2.5 µl, 0.01 mmol) in THF (68 µl). The product was obtained as a yellow oil (0.140 g, 0.51 mmol, 61% yield). M_n = 1 290 g/mol, Đ = 2.8, n = 5 (measured by GPC in THF and the molar masses were calibrated to polystyrene as an internal standard).

^{1}H NMR (600 MHz, CDCl$_3$) δ 4.3 (dt, J = 6.6, 4.0 Hz, 4H), 1.8 – 1.7 (m, 4H) [ppm].

^{13}C NMR (151 MHz, CDCl$_3$) δ 171.2, 163.6, 80.1, 67.2, 24.9 [ppm].

IR(ATR): v [cm^{-1}] 3335, 2962, 2117, 1753.

Poly-6-methoxyhexyl 3-oxobutanoate

II-26
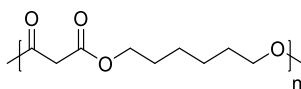
Following to general procedure B. The dimethyl malonate (0.250 g, 1.56 mmol) was added to 1,6-hexandiol (0.185 g, 1.56 mmol), Titanium (IV) isopropoxide (4.6 µl, 0.02 mmol) in THF (127 µl). The product was obtained as a yellow oil (0.170 g, 0.79 mmol, 50% yield). Mn 3 960 g/mol, Đ = 3.7 n = 18 (measured by GPC in THF and the molar masses were calibrated to polystyrene as an internal standard).

^{1}H NMR (600 MHz, CDCl$_3$) δ 4.6 – 3.8 (m, 4H), 3.3 (s, 2H), 2.1 – 1.5 (m, 4H) 1.3 (s, 4H) [ppm].

^{13}C NMR (151 MHz, CDCl$_3$) δ 166.7, 65.5, 41.7, 28.5, 25.5 [ppm].

IR(ATR): v [cm^{-1}] 3379, 2937, 1728.

Poly-6-methoxyhexyl 2,2-diazido-3-oxobutanoate

II-27
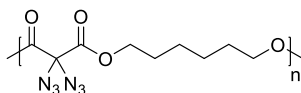
Following to general procedure B. The diethyl 2,2-diazidomalonate (0.200 g, 0.83 mmol) were added to 1,6-hexandiol (97 mg, 0.83 mmol), Titanium (IV) isopropoxide (2.5 µl, 0.01 mmol) in THF (68 µl). The product was obtained as a yellow oil (0.128 g, 0.43 mmol, 52% yield). Mn 2 100 g/mol, Đ = 3.5, n = 7 (measured by GPC in THF and the molar masses were calibrated to polystyrene as an internal standard).

^{1}H NMR (600 MHz, CDCl$_3$) δ 4.3 (t, J = 6.6 Hz, 4H), 1.7 (p, J = 7.1 Hz, 4H), 1.4 (ddd, J = 15.4, 7.7, 3.7 Hz, 4H).

^{13}C NMR (101 MHz, CDCl$_3$) δ 163.5, 71.5, 67.9, 28.1, 25.1 [ppm].

IR(ATR): v [cm^{-1}] 3346, 2939, 2104, 1753.

Poly-2-(2-(2-methoxyethoxy)ethoxy)ethyl 3-oxobutanoate

II-28
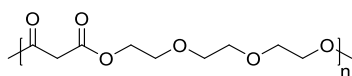
Following to general procedure B. The dimethyl malonate (0.300 g, 1.87 mmol) was added to triethylene glycol (256 µl, 1.87 mmol), Titanium (IV) isopropoxide (5.5 µl, 0.02 mmol) in THF (152 µl). The product was obtained as a yellow oil (0.344 g, 1.39 mmol, 74% yield). M_n = 3 730 g/mol, Đ = 1.6, n = 15 (measured by GPC in THF and the molar masses were calibrated to polystyrene as an internal standard).

^{1}H NMR (600 MHz, CDCl$_3$) δ 4.3 (dt, J = 22.2, 4.5 Hz, 4H), 3.7 – 3.6 (m, 4H), 3.6 (m, 4H), 3.4 (d, J = 7.0 Hz, 2H) [ppm].

^{13}C NMR (151 MHz, CDCl$_3$) δ 166.4, 166.1, 107.9, 70.5, 69.4, 68.8, 64.5, 42.4, 41.2, 29.1, 23.9 [ppm]

IR(ATR): v [cm^{-1}] 3406, 2916, 1726.

Poly-2-(2-(2-methoxyethoxy)ethoxy)ethyl 2,2-diazido-3-oxobutanoate

II-29
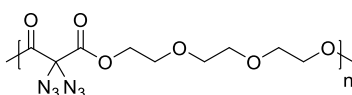
Following to general procedure B. The diethyl 2,2-diazidomalonate (0.200 g, 0.83 mmol) were added to triethylene glycol (114 µg, 0.83 mmol), Titanium (IV) isopropoxide (2.5 µl, 0.01 mmol) in THF (68 µl). The product was obtained as a yellow oil (0.201 g, 0.61 mmol, 73% yield). M_n = 2 430 g/mol, Đ = 2.1, n = 7 (measured by GPC in THF and the molar masses were calibrated to polystyrene as an internal standard).

^{1}H NMR (600 MHz, CDCl$_3$) δ 4.4 (m, 4H), 3.7 (m, 4H), 3.61 (d, J = 13.3 Hz, 4H) [ppm].

^{13}C NMR (101 MHz, CDCl$_3$) δ 163.4, 108.0, 72.7, 69.8, 68.5, 66.6, 61.8, 29.2, 24.0 [ppm].

IR(ATR): v [cm^{-1}] 3338, 2970, 2119, 1753.

The click reaction carried out using a general procedure (C). Phenylacetylene (2.15 eq.) and polyester with diazo units (1 eq.) were dissolved in N,N-dimethylformamide (DMF). To this solution, copper(II) sulfate pentahydrate (0.15 eq.) and sodium ascorbate (0.3 equivalents) were added. The reaction mixture was stirred at room temperature for 24 hours. After the reaction, the crude polymer was dissolved in a 5% ethylenediaminetetraacetic acid (EDTA) aqueous solution to chelate any residual metal ions. The solid precipitate formed was filtered off and washed with water (3 X 100 ml) and diethyl ether (3 x 100 ml portions).

Poly-6-methoxyhexyl 3-oxo-2,2-bis(4-phenyl-1H-1,2,3-triazol-1-yl)butanoate

II-35
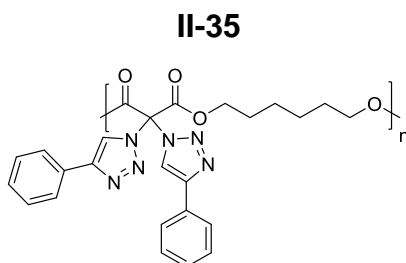
Following to general procedure C. Phenylacetylene (37.5 µl, 0.34 mmol) and polyester with diazo units **II-33** (45 mg, 0.16 mmol) were dissolved in DMF (1.6 ml). To this solution, copper(II) sulfate pentahydrate (5.9 mg , 23.8 µmol) and sodium ascorbate (9.4, 47.6 µmol) were added. The reaction mixture was stirred at room temperature for 24 hours. The polymer was isolated as yellow solid with 71% of yield (55 mg, 0.11 mmol), M_n = 3 830 g/mol, Đ = 1.4, n = 8 (measured by GPC in THF and the molar masses were calibrated to polystyrene as an internal standard).

^{1}H NMR (400 MHz, CDCl$_3$) δ 8.4 (s, 2H), 7.8 (m, 4H), 7.4 – 7.3 (m, 6H), 4.5 (t, J = 6.8 Hz, 4H), 1.7 (s, 4H), 1.4 (s, 4H) [ppm].
IR(ATR): v [cm^{-1}] 3165, 2936, 2857, 1762.

Poly-2-(2-(2-methoxyethoxy)ethoxy)ethyl 3-oxo-2,2-bis(4-phenyl-1H-1,2,3-triazol-1-yl)butanoate

II-36
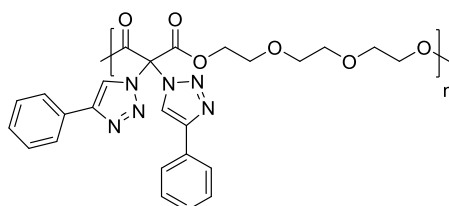
Following to general procedure C. Phenylacetylene (49.4 µl, 0.45 mmol) and polyester with diazo units **II-34** (66 mg, 0.21 mmol) were dissolved in DMF (2 ml). To this solution, copper(II) sulfate pentahydrate (7.8 mg , 31.4 µmol) and sodium ascorbate (12.4, 62.8 µmol) were added. The reaction mixture was stirred at room temperature for 24 hours. The polymer was isolated as yellow solid with 55% of yield (60 mg, 0.12 mmol), Mn = 2 550 g/mol, Đ = 1.6, n = 5 (measured by GPC in THF and the molar masses were calibrated to polystyrene as an internal standard).

^{1}H NMR (400 MHz, CDCl$_3$) δ 8.5 (dd, J = 4.8, 2.4 Hz, 2H), 7.8 – 7.7 (m, 4H), 7.4 – 7.3 (m, 6H), 4.5 (d, J = 18.6 Hz, 5H), 3.7 (s, 6H), 3.6 – 3.4 (m, 7H) [ppm].
IR(ATR): ν [cm^{-1}] 3151, 2957, 2870, 1766.

IV. List of abbreviations and symbols

Å angstrom

AFM atomic force microscopy

AIBN azobisisobutyronitrile

α absorption coefficients

AMP adenosine monophosphateadp

ATP adenosine triphosphate

ATRP atom transfer radical polymerization

CDCl₃ deuterated chloroform

CPs conjugated polymers

°C degree Celsius

DABCO 1,4-diazabicyclo[2.2.2]octane

DAD diode array detector

DCM dichloromethane

DMSO dimethyl sulfoxide

DSC differential scanning calorimetry

Δ Delta

DFBP 4,4'-difluorobenzophenone

DMAc dimethylacetamid

DMF dimethylformamide

Đ index of polydispersity

EDTA ethylenediaminetetraacetic acid

EDC 1-ethyl-3-(3-dimethylaminopropyl)carbodiimide

eq. equivalent

FWHM full width at half maximum

g gram

GPC size-exclusion chromatography/gel permeation chromatography

HQ bisphenol hydroquinone

HRMS high-resolution mass spectrometry

Hz Hertz

IR infrared spectroscopy

LDA lithium diisopropylamide

l liter

λ wavelength

λ_{max} maximum intensity wavelength

MHz megahertz

min minute

mol amount of substance

MMA methyl methacrylate

Mn number-average molar mass

M molarity

Mw weight-average molar mass

MW microwave

mg milligram

NMR nuclear magnetic resonance

n refractive indices

PET polyethylene terephthalate

PEEK poly(ether ether ketone)

PEK poly(ether ketones)

pH potential of hydrogen

PMMA polymethyl methacrylate

Rf retention factor

RA rubazonic acids

RID refractive index detector

RMS root-mean-square

rt room temperature

T temperature

Tg glass transition temperature

THF tetrahydrofuran

Tm melting point

TGA thermogravimetric analysis

μ micro

m/z mass to charge ratio

Mw weight average degree of polymerization

et al. and others

UV-vis ultraviolet–visible spectroscopy

V. References

[1] Fustero, S., Sanchez-Rosello, M., Barrio, P. and Simon-Fuentes, A. From 2000 to mid-2010: A fruitful decade for the synthesis of pyrazoles. *Chem. Rev.*, **2011**, *111*, 6984-7034.

[2] Mustafa, G.; Zia-ur-Rehman, M.; Sumrra, S.H.; Ashfaq, M.; Zafar, W; Ashfaq, M. A critical review on recent trends on pharmacological applications of pyrazolone endowed derivatives. *J. Mol. Struct.*, **2022**, *1262*, 133044.

[3] Görgen, C.; Boden, K.; Reiss, G.J.; Frank, W; Müller, T.J. One-pot activation–alkynylation–cyclization synthesis of 1,5-diacyl-5-hydroxypyrazolines in a consecutive three-component fashion. *Beilstein J. Org. Chem.*, **2019**,*15*, 1360-1370.

[4] Bauer, U.; Egner, B.J.; Nilsson, I.; Berghult, M. Parallel solution phase synthesis of N-substituted 2-pyrazoline libraries. *Tetrahedron Lett.*, **2000**, *41*, 2713-2717.

[5] Boeckman, R.K.; Reed, J.E.; Ge, P. A novel route to 2, 3-pyrazol-1 (5 H)-ones via palladium-catalyzed carbonylation of 1, 2-diaza-1, 3-butadienes. *Org. Lett.,* **2001**, *3*, 3651-3653.

[6] Kato, T.; Sato, M.; Katsumi Tabei; Kawashima, E. Studies on Ketene and Its Derivatives. LXIX. Reaction of Diketene with Hydrazobenzenes. *Chem. Pharm. Bull.,***1975**, *23*, 456–459.

[7] Baciu-Atudosie, L.; Ghinet, A.; Belei, D.; Gautret, P.; Rigo, B.; and Bîcu, E. An efficient one-pot reaction for the synthesis of pyrazolones bearing a phenothiazine unit. *Tetrahedron Lett.*, **2012**, *53*, 6127-6131.

[8] Zhao, Z.; Dai, X.; Li, C.; Wang, X.; Tian, J.; Feng, Y.; Xie, J.; Ma, C.; Nie, Z.; Fan, P.; Qian, M. Pyrazolone structural motif in medicinal chemistry: Retrospect and prospect. *Eur. J. Med. Chem.*, **2020**, *186*, 111893.

[9] Lomax, S.Q.; Learner, T. A review of the classes, structures, and methods of analysis of synthetic organic pigments. *JAIC*, **2006**, *45*, 107-125.

[10] Arai, T.; Nonogawa, M.; Makino, K.; Endo, N.; Mori, H.; Miyoshi, T.; Yamashita, K.; Sasada, M.; Kakuyama, M.; Fukuda, K. The radical scavenger edaravone (3-methyl-1-phenyl-2-pyrazolin-5-one) reacts with a pterin derivative and produces a cytotoxic substance that induces intracellular reactive oxygen species generation and cell death. *JPET*, **2008**, *324*, 529-538.

[11] Shang, H.; Cui, D.; Yang, D.; Liang, S.; Zhang, W.; Zhao, W. The radical scavenger edaravone improves neurologic function and perihematomal glucose

metabolism after acute intracerebral hemorrhage. *J Stroke Cerebrovasc Dis.*, **2015**, *24*, 215-222.

[12] Tripathy, R.; Ghose, A.; Singh, J.; Bacon, E.R.; Angeles, T.S.; Yang, S.X.; Albom, M.S.; Aimone, L.D.; Herman, J.L.; Mallamo, J.P. 1,2,3-Thiadiazole substituted pyrazolones as potent KDR/VEGFR-2 kinase inhibitors. *Bioorganic Med. Chem. Lett.*, **2007**, *17*, 1793-1798.

[13] Piskarev, A.V.; Nesterenko, V.S. Radioprotective effect of some pyrazolone derivatives. EBM, **1975**, *80*, 782-783.

[14] Ziegler, J.H.; Locher, M. Ueber die Tartrazine, eine neue Klasse von Farbstoffen. *Ber. Dtsch. Chem. Ges.*, **1887**, *20*, 834-840.

[15] Kiernan, J.A. Classification and naming of dyes, stains and fluorochromes. *Biotech. Histochem.,* **2001**, *76*, 261-278.

[16] Brown, G.H.; Graham, B.; Vittum, P.W.; Weissberger, A. Azomethine dyes. I. color and constitution of pyrazolone azomethine dyes. *J. Am. Chem. Soc.*, **1951**, *73*, 919-926.

[17] Mykhailiuk, P.K. Fluorinated pyrazoles: From synthesis to applications. *Chem. Rev.*, **2020**, *121*(3), 1670-1715.

[18]Metwally, M.A.; Bondock, S.A.; El-Desouky, S.I.; Abdou, M.M. Pyrazol-5-ones: tautomerism, synthesis and reactions. *Int. J. Modern Org. Chem*, 2012, *1*, 19-54.

[19] Barluenga, J.; Valdés, C. Tosylhydrazones: new uses for classic reagents in palladium-catalyzed cross-coupling and metal-free reactions. *Angew. Chem. Int. Ed.,* **2011**, *50*, 7486-7500.

[20] Anitha, A.G.; Arunagiri, C.; Subashini, A. Synthesis, X-ray crystal structure, Hirshfeld surface analysis and DFT studies of (E)-N′-(2-bromobenzylidene)-4-methylbenzohydrazide. *Acta Crystallogr. E: Crystallogr.*, **2019**, *75*, 109-114.

[21] Sarkar, D.; Choudhury, P.; Dinda, S.; Das, P.K. Vesicle formation by cholesterol-based hydrazone tethered amphiphiles: Stimuli responsive dissipation of self-assembly. *J. Colloid Interface Sci.*, **2018**, *530*, 67-77.

[22] Japp, F.R.; Klingemann, F. Ueber sogenannte» gemischte Azoverbindungen. *Ber. Dtsch. Chem. Ges.*, **1887**, *20*, 3398-3401.

[23] (a) Surry, D.S.; Buchwald, S.L. Biaryl phosphane ligands in palladium-catalyzed amination. Angew. Chem. Int. Ed., **2008**, *47*, 6338-6361. (b) Beccalli, E.M.; Broggini, G.; Martinelli, M.; Sottocornola, S. C−C, C−O, C−N bond formation on sp^2 carbon

by Pd (II)-catalyzed reactions involving oxidant agents. *Chem. Rev.*, **2007**, *107*, 5318-5365.

[24] (a) Monnier, F.; Taillefer, M. Catalytic C-C, C-N, and C-O Ullmann-type coupling reactions. *Angew. Chem., Int. Ed. Engl.,* **2009**, *48*, 6954–6971. (b) Evano, G.; Blanchard, N.; Toumi, M. Copper-mediated coupling reactions and their applications in natural products and designed biomolecules synthesis. *Chem. Rev.,* **2008**, *108* , 3054–3131.

[25] Lefebvre, V.; Cailly, T.; Fabis, F.; Rault, S. Two-step synthesis of substituted 3-aminoindazoles from 2-bromobenzonitriles. *J. Org. Chem. J ORG CHEM,* **2010**, *75*, 2730-2732.

[26] Wagaw, S.; Yang, B.H.; Buchwald, S.L. A palladium-catalyzed strategy for the preparation of indoles: A novel entry into the Fischer indole synthesis. *J. Am. Chem. Soc.*, 1998, *120*, 6621-6622.

[27] Fischer, E. and Fischer, E., Über einige Osazone und Hydrazone der Zuckergruppe. *Untersuchungen Über Kohlenhydrate und Fermente (1884–1908)*, Springer, Berlin, Heidelberg, 1909. pp186-191.

[28] Bayer, E.; Häfelinger, G., Bestimmung der MO-π-Bindungsordnung von Chelatringen mit zwei konjugierten C=N-Doppelbindungen. *Ber. or Chem. Ber.,***1966**, *99*, 1689-1703.

[29] Landge, S.M.; Tkatchouk, E.; Benítez, D.; Lanfranchi, D.A.; Elhabiri, M.; Goddard III, W.A.; Aprahamian, I. Isomerization mechanism in hydrazone-based rotary switches: lateral shift, rotation, or tautomerization? *J. Am. Chem. Soc.*, **2011**, *133*, 9812-9823.

[30] Said, M.A.; Khan, D.J.; Al-Blewi, F.F.; Al-Kaff, N.S.; Ali, A.A.; Rezki, N.; Aouad, M.R.; Hagar, M. New 1,2,3-Triazole scaffold schiff bases as potential anti-COVID-19: Design, synthesis, DFT-molecular docking, and cytotoxicity aspects. *Vaccines*, **2021**, *9*, 1012.

[31] Geng, J.; Xu, D.; Chang, F.F.; Tao, T.; Huang, W. From heterocyclic hydrazone to hydrazone-azomethine dyes: Solvent and pH induced hydrazone and azo-keto transformation for a family of pyrazolone-based heterocyclic dyes. *Dyes Pigm.,* **2017**, *137*, 101-110.

[32] Chen, W.; Liang, H.; Wen, X.; Li, Z.; Xiong, H.; Tian, Q.; Yan, M.; Tan, Y.; Royal, G. Synchronous colorimetric determination of CN^-, F^-, and $H_2PO_4^-$ based on

structural manipulation of hydrazone sensors. *Inorganica Chim. Acta.*, **2022**, *532*, 20760.

[33] Hu, S.; Guo, Y.; Xu, J.; Shao, S. A selective chromogenic molecular sensor for acetate anions in a mixed acetonitrile–water medium. *OBC*, **2008**, *6*, 2071-2075.

[34] Wang, Y.; Lin, H.; Shao, J.; Cai, Z.S.; Lin, H.K. A phenylhydrazone-based indole receptor for sensing acetate. *Talanta*, **2008**, *74*, 1122-1125.

[35] Li, Q.; Guo, Y.; Xu, J.; Shao, S. Novel indole based colorimetric and "turn on" fluorescent sensors for biologically important fluoride anion sensing. *J. Photochem. Photobiol. B, Biol. J PHOTOCH PHOTOBIO B*, **2011**, *103*, 140-144.

[36] Li, Y.; Shao, J.; Yu, X.; Xu, X.; Lin, H.; Cai, Z.; Lin, H. Design of two pyrazole-based Sensors with similar configuration and different fluorescent response to anions. *J. Fluoresc.*, **2010**, *20*, 3-8.

[37] Mukherjee, S.; Chowdhury, S.; Paul, A.K.; Banerjee, R. Selective extraction of palladium (II) using hydrazone ligand: A novel fluorescent sensor. *J. Lumin.*, **2011**, *131*, 2342-2346.

[38] Ganjali, M.R.; Faridbod, F.; Norouzi, P.; Adib, M. A novel Er (III) sensor based on a new hydrazone for the monitoring of Er (III) ions. *Sens. Actuators B: Chem.*, **2006**, *120*, 119-124.

[39] Liao, Z.C.; Yang, Z.Y.; Li, Y.; Wang, B.D.; Zhou, Q.X. A simple structure fluorescent chemosensor for high selectivity and sensitivity of aluminum ions. *Dyes Pigm.,* **2013**, *97*, 124-128.

[40] Goswami, S.; Chakraborty, S.; Paul, S.; Halder, S.; Maity, A.C. A simple quinoxaline-based highly sensitive colorimetric and ratiometric sensor, selective for nickel and effective in very high dilution. *Tetrahedron Lett.*, **2013**, *54*, 5075-5077.

[41] Xiang, Y.; Tong, A.; Jin, P.; Ju, Y. New fluorescent rhodamine hydrazone chemosensor for Cu (II) with high selectivity and sensitivity. Org. Lett., **2006**, *8*, 2863-2866.

[42] Xiang, Y.; Li, Z.; Chen, X.; Tong, A. Highly sensitive and selective optical chemosensor for determination of Cu^{2+} in aqueous solution. *Talanta*, **2008**, *74*, 1148-1153.

[43] Chen, X.; Li, Z.; Xiang, Y.; Tong, A. Salicylaldehyde fluorescein hydrazone: a colorimetric logic chemosensor for pH and Cu (II). *Tetrahedron Lett.*, **2008**, *49*, 4697-4700.

[44] Su, X.; Aprahamian, I. Hydrazone-based switches, metallo-assemblies and sensors. *Chem. Soc. Rev.,* **2014**, *43*, 1963-1981.

[45] Jeong, M.; Park, J.; Seo, Y.; Lee, K.; Pramanik, S.; Ahn, S.; Kwon, S. Hydrazone photoswitches for structural modulation of short peptides. *Chem. Eur. J.,* **2022**, *28*(, e202103972.

[46] Qian, H.; Pramanik, S.; Aprahamian, I. Photochromic hydrazone switches with extremely long thermal half-lives. *J. Am. Chem. Soc.,* **2017**, *139*, 9140-9143.

[47] Moran, M.J.; Magrini, M.; Walba, D.M.; Aprahamian, I. Driving a liquid crystal phase transition using a photochromic hydrazone. *J. Am. Chem. Soc.,* **2018**, *140*, 13623-13627.

[48] Guo, X.; Shao, B.; Zhou, S.; Aprahamian, I.; Chen, Z. Visualizing intracellular particles and precise control of drug release using an emissive hydrazone photochrome. *Chem. Sci.,* **2020**, *11*, 3016-3021.

[49] Yang, S.; Larsen, D.; Pellegrini, M.; Meier, S.; Mierke, D. F.; Beeren, S. R.; Aprahamian, I. Dynamic enzymatic synthesis of γ-cyclodextrin using a photoremovable hydrazone template. *Chem.,* **2021**, *7*, 2190–2200.

[50] Ryabchun, A.; Li, Q.; Lancia, F.; Aprahamian, I.; Katsonis, N. Shape-persistent actuators from hydrazone photoswitches. *J. Am. Chem. Soc.,* **2019**, *141*, 1196-1200.

[51] Yan, L.; Yang, H.; Liu, N.; Meng, F.; Zhang, S. A photochromic salicylaldehyde hydrazone derivative based on CN isomerization and ESIPT mechanisms and its detection of Al^{3+} in aqueous solution. *SAA.,* **2022**, *275*, 121116.

[52] Khattab, T.A.; Tiu, B.D.B.; Adas, S.; Bunge, S.D.; Advincula, R.C.; pH triggered smart organogel from DCDHF-Hydrazone molecular switch *Dyes Pigm.,* **2016**, *130*, 327-336.

[53] Zhao, X.L.; Yan, C.; Qiu, W.S.; Yu, T.; Wang, W.J.; Zhu, W.H. A pH-activated fluorescent probe via transformation of azo and hydrazone forms for lysosomal pH imaging. *Chem comm.,* **2022**, *58*, 10635-10638.

[54] Nagai, K. New developments in the production of methyl methacrylate. *Appl. Aatal. A Gen.,* **2001**, *221*, 367-377.

[55] Ali, U.; Karim, K.J.B.A.; Buang, N.A. A review of the properties and applications of poly (methyl methacrylate)(PMMA). *Polym. Rev.,* **2015**, *55*, 678-705.

[56] Härtner, S.; Kim, H.C.; Hampp, N. Photodimerized 7-hydroxycoumarin with improved solubility in PMMA: Single-photon and two-photon-induced photocleavage

in solution and PMMA films. *J. Photochem. Photobiol. A: Chem.*, **2007**, *187*, 242-246.

[57] Spiridon, M.C.; Iliopoulos, K.; Jerca, F.A.; Jerca, V.V.; Vuluga, D.M.; Vasilescu, D.S.; Gindre, D.; Sahraoui, B. Novel pendant azobenzene/polymer systems for second harmonic generation and optical data storage *Dyes Pigm.*, **2015**, *114*, 24-32.

[58] Matsuyama, K.; Mishima, K.; Kato, T.; Irie, K.; Mishima, K. Transparent polymeric hybrid film of ZnO nanoparticle quantum dots and PMMA with high luminescence and tunable emission color. *J. Colloid Interface Sci.*, **2012**, *367*, 171-177.

[59] Kakuchi, R.; Wongsanoh, K.; Hoven, V.P.; Theato, P. Activation of stable polymeric esters by using organo-activated acyl transfer reactions. *J. Polym. Sci.,* **2014**, *52*, 1353-1358.

[60] Zhang, M.; Ding, X.; Lu, A.; Kang, J.; Gao, Y.; Wang, Z.; Li, H.; Wang, Q.; Generation and precise control of sulfonyl radicals: visible-light-activated redox-neutral formation of sulfonates and sulfonamides. *Org. Chem. Front.*, **2021**, *8*, 961-967.

[61] Bates, C.M.; Seshimo, T.; Maher, M.J.; Durand, W.J.; Cushen, J.D.; Dean, L.M.; Blachut, G.; Ellison, C.J.; Willson, C.G. Polarity-switching top coats enable orientation of sub–10-nm block copolymer domains. *Science*, **2012**, *338*, 775-779.

[62] Ooi, T.; Tayama, E.; Yamada, M.; Maruoka, K. Efficient synthesis of aromatic sec-amides from esters: synthetic utility of bislithium amides. *Synlett*, **1999**, *6*, 729-730.

[63] Khezri, K.; Fazli, Y. ATRP of Methyl methacrylate in the presence of HMDS-modified silica aerogel: ARGET approach. *J. Inorg. Organomet. Polym. Mater.,* **2019**, *29*, 608-616.

[64] Sheng, Y.; Huang, H.; Yu, M.; Zhang, X.; Cheng, L.; Liu, Z.; Liu, W.; Huang, Q.; Yi, J.; Yang, W. Synthesis of 4-arms hydroxy-functionalized PMMA-b-PE through combining free radical polymerization with coordination polymerization. *J. Ind. Eng. Chem.*, **2014**, *20*, 419-425.

[65] Lyoo, W.S.; Noh, S.K.; Yeum, J.H.; Kang, G.C.; Ghim, H.D.; Lee, J.; Ji, B.C. Preparation of high molecular weight poly (methyl methacrylate) with high yield by room temperature suspension polymerization of methyl methacrylate. *Fibers Polym.,* **2004**, *5*, 75-81.

[66] Queffelec, J.; Gaynor, S.G.; Matyjaszewski, K. Optimization of atom transfer radical polymerization using Cu (I)/tris (2-(dimethylamino) ethyl) amine as a catalyst. *Macromolecules*, **2000**, *33*, 8629-8639.

[67] Rzayev, J.; Penelle, J. HP-RAFT: a free-radical polymerization technique for obtaining living polymers of ultrahigh molecular weights. *Angew. Chem.* **2004**, *116*, 1723-1726.

[68] Hsiao, Y.L.; Maury, E.E.; DeSimone, J.M.; Mawson, S.; Johnston, K.P. Dispersion polymerization of methyl methacrylate stabilized with poly (1, 1-dihydroperfluorooctyl acrylate) in supercritical carbon dioxide. *Macromolecules*, **1995**, *28*, 8159-8166.

[69] Lyoo, W.S.; Noh, S.K.; Yeum, J.H.; Kang, G.C.; Ghim, H.D.; Lee, J.; Ji, B.C. Preparation of high molecular weight poly (methyl methacrylate) with high yield by room temperature suspension polymerization of methyl methacrylate. *Fibers and Polym.*, **2004**, *5*, 75-81.

[70] Jiang, W.; Yang, W.; Zeng, X.; Fu, S.; Structure and properties of poly (methyl methacrylate) particles prepared by a modified microemulsion polymerization. *J. Polym. Sci.,* **2004**, *42*, 733-741.

[71] Kato, M.; Kamigaito, M.; Sawamoto, M.; Higashimura, T. Polymerization of methyl methacrylate with the carbon tetrachloride/dichlorotris-(triphenylphosphine) ruthenium (II)/methylaluminum bis (2, 6-di-tert-butylphenoxide) initiating system: possibility of living radical polymerization. *Macromolecules*, **1995**, *28*, 1721-1723.

[72] Lecomte, P.; Drapier, I.; Dubois, P.; Teyssié, P.; Jérôme, R. Controlled radical polymerization of methyl methacrylate in the presence of palladium acetate, triphenylphosphine, and carbon tetrachloride. *Macromolecules*, **1997**, *30*, 7631-7633.

[73] Magenau, A.J.; Kwak, Y.; Matyjaszewski, K. ATRP of methacrylates utilizing Cu^{II}X$_2$/L and copper wire. *Macromolecules*, **2010**, *43*, 9682-9689.

[74] Duquesne, E.; Habimana, J.; Degée, P.; Dubois, P. Nickel-catalyzed supported ATRP of methyl methacrylate using cross-linked polystyrene triphenylphosphine as ligand. *Macromolecules*, 2005, *38*, 9999-10006.

[75] Zhu, G.; Zhang, L.; Zhang, Z.; Zhu, J.; Tu, Y.; Cheng, Z.; Zhu, X. Iron-mediated ICAR ATRP of methyl methacrylate. *Macromolecules*, **2011**, *44*, 3233-3239.

[76] Opstal, T.; Zedník, J.; Sedláček, J.; Svoboda, J.; Vohlídal, J.; Verpoort, F. Atom transfer radical polymerization of styrene and methyl methacrylate induced by Rh^{I}

(cycloocta-1,5-diene) complexes. *Collect. Czech. Chem. Commun.*, **2002,** *67*, 1858-1871.

[77] Matyjaszewski, K.; Xia, J. Atom transfer radical polymerization. *Chem. Rev.*, **2001**, *101*, 2921-2990.

[78] Moad, G.; Rizzardo, E.; Thang, S.H. RAFT polymerization and some of its applications. *Chem. Asian J.,* **2013**, *8*, 1634-1644.

[79] Goto, A.; Sato, K.; Tsujii, Y.; Fukuda, T.; Moad, G.; Rizzardo, E.; Thang, S.H. Mechanism and kinetics of RAFT-based living radical polymerizations of styrene and methyl methacrylate. *Macromolecules*, **2001**, *34*, 402-408.

[80] Moad, G. and Rizzardo, E. eds., *RAFT Polymerization: Methods, Synthesis, and Applications*. John Wiley & Sons. 2021; pp 586.

[81] Koltzenburg, S., Maskos, M. and Nuyken, O., Ionic Polymerization. In *Polymer Chemistry*. Berlin, Heidelberg: Springer Berlin Heidelberg. 2023; pp 247–293.

[82] Schlaad, H. *Polymer self-assembly: adding complexity to mesostructures of diblock copolymers by specific interactions* Ph.D. Dissertation, Universität Potsdam, 2005.

[83] Flory, P.J. *Principles of polymer chemistry*. Cornell university press. 1953; pp 217

[84] M. Pitsikalis, Ionic Polymerization, Reference Module in Chemistry, Molecular Sciences and Chemical Engineering, Elsevier, 2013;

[85] Aoshima, S.; Kanaoka, S. A renaissance in living cationic polymerization. *Chem. Rev.*, **2009**, *109*, 5245-5287.

[86] Beck, S.; Narain, R. Polymer Synthesis. *Polymer Science and Nanotechnology*, **2020**, 21–85.

[87] Carraher Jr, C.E. *Carraher's polymer chemistry*. CRC press. 2016; pp 161.

[88] Tsang, M.W. and Holdcroft, S. Alternative proton exchange membranes by chain-growth polymerization. *Green Energy Environ.,* **2012**, 10, 651.

[89] Kitaura, T.; Kitayama, T. Anionic polymerization of methyl methacrylate with the aid of lithium trimethylsilanolate (Me_3SiOLi)-superior control of isotacticity and molecular weight. *Macromol. Rapid Commun.*, **2007**, *28*, 1889-1893.

[90] Yuan, M.; Huang, D.; Zhao, Y. Development of synthesis and application of high molecular weight poly(methyl methacrylate). *Polymers*, **2022**, *14*, 2632.

[91] Kim, D.; Song, Y.; Kim, S.; Lee, H.J.; Lee, H. N,N′,X-bidentate versus N,N′,X-tridentate N-substituted 2-iminomethylpyridine and 2-iminomethylquinoline coordinated palladium(II) complexes. *J. Coord. Chem.*, **2014**, *67*, 2312-2329.

[92] Le Questel, J.Y.; Berthelot, M.; Laurence, C. Hydrogen-bond acceptor properties of nitriles: a combined crystallographic and ab initio theoretical investigation. *J. Phys. Org. Chem.*, **2000**, *13*, 347-358.

[93] Shojaeiarani, J.; Bajwa, D.S.; Stark, N.M.; Bergholz, T.M.; Kraft, A.L. Spin coating method improved the performance characteristics of films obtained from poly (lactic acid) and cellulose nanocrystals. *SM&T.*, **2020**, *26*, e00212.

[94] Xu, W.; Shao, Z.; Han, Y.; Wang, W.; Song, Y.; Hou, H. Light-adjustable third-order nonlinear absorption properties based on a series of hydrazone compounds. *Dyes Pigm.*, **2018**, *152*, 171-179.

[95] Geng, J.; Xu, D.; Chang, F.F.; Tao, T.; Huang, W. From heterocyclic hydrazone to hydrazone-azomethine dyes: Solvent and pH induced hydrazone and azo-keto transformation for a family of pyrazolone-based heterocyclic dyes. *Dyes Pigm.*, **2017**, *137*, 101-110.

[96] Bagdatli, E.; Ocal, N. Synthesis, spectroscopic, and dyeing properties of new azo and bisazo dyes derived from 5-pyrazolones. *J. Heterocycl. Chem.*, **2012**, *49*, 1179-1186.

[97] Inukai, Y. Syntheses of polymeric azo dyes of pyrazolone series. *Contemporary Topics in Polymer Science:* **1977**, *4,* 183-195.

[98]Jiang, L.; Lu, X.; Zhang, H.; Jiang, Y.; Ma, D. CuI/4-Hydro-l-proline as a more effective catalytic system for coupling of aryl bromides with N-boc hydrazine and aqueous ammonia. J. Org. Chem, **2009**, *74*, 4542-4546.

[99] Solyev, P.N.; Sherman, D.K.; Novikov, R.A.; Levina, E.A.; Kochetkov, S.N. Hydrazo coupling: the efficient transition-metal-free C–H functionalization of 8-hydroxyquinoline and phenol through base catalysis. *Green Chem.*, **2019**, *21*, 6381-6389.

[100] Knorr, L. Synthetische Versuche mit dem Acetessigester. *Ann. oder Liebigs Ann.,* **1887**, *238*, 137-219.

[101] Tong, M.L.; Leusch, L.T.; Holzschneider, K.; Kirsch, S.F. Rubazonic acids and their synthesis. *J. Org. Chem.*, **2020**, *85*, 6008-6016.

[102] Hänsel, W. 4-(5-Hydroxy-4-pyrazolylimino)-2-pyrazolin-5-one und ihre Metallchelate, I Synthese von 4-(5-Hydroxy-4-pyrazolylimino)-2-pyrazolin-5-onen

(Rubazonsäuren) und strukturanalogen Verbindungen. *Ann. oder Liebigs Ann.*, **1976**, 7-8,1380-1394.

[103] Cerchiaro, G.; Ferreira, A.M.D.C.; Teixeira, A.B.; Magalhaes, H.M.; Cunha, A.C.; Ferreira, V.F.; Santos, L.S.; Eberlin, M.N.; Skakle, J.M.; Wardell, S.M.; Wardell, J.L. Synthesis and crystal structure of 2,4-dihydro-4-[(5-hydroxy-3-methyl-1-phenyl-1H-pyrazol-4-yl)imino]-5-methyl-2-phenyl-3H-pyrazol-3-one and its copper(II) complex. *Polyhedron,* **2006**, *25*, 2055-2064.

[104] Erkin, A.V.; Krutikov, V.I. 1-(Pyrimidin-4-yl)pyrazol-5(4H)-one derivatives: I. Synthesis of 3-methyl-1-(6-methyl-2-methylsulfanylpyrimidin-4-yl)-pyrazol-5-ol and specificity of its Knoevenagel reaction. *Russ. J. Gen. Chem.*, **2011**, *81*, 392-396.

[105] Hussain, G.; Khan, S.A.; Ahmad, W.; Athar, M.; Saleem, R. A kinetic study of rubazoic acid formation derived from 4-Amino-1(4-Sulphophenyl)3-Methyl-2-Pyrazolin-5-One. *Int J Advanc Res,* **2017**, *5, 234-241*.

[106] Ballot, A.B.; Steendijk, C. Ammonia determination in a trichloroacetic acid blood filtrate after microdiffusion with the aid of the rubazonic acid reaction. *Clin. Chim. Acta.,* **1965**,*12*, 55-62.

[107] Sheppard, S.E.; Houck, R.C. *Photographic antihalation layer*. U.S. 2,203,659, 1940.

[108] Liu, Y.; Lam, J.W.; Tang, B.Z. Conjugated polymers developed from alkynes. *Natl. Sci. Rev.*, **2015**, *2*, 493-509.

[109] Chinchilla, R.; Nájera, C. The Sonogashira reaction: a booming methodology in synthetic organic chemistry. *Chem. Rev.*, **2007**, *107*, 874-922.

[110] Sonogashira, K.; Tohda, Y.; Hagihara, N. A convenient synthesis of acetylenes: catalytic substitutions of acetylenic hydrogen with bromoalkenes, iodoarenes and bromopyridines. *Tetrahedron lett.,* **1975**, *16*, 4467-4470.

[111] Tohda, Y.; Sonogashira, K.; Hagihara, N. A Convenient synthesis of 1-alkynyl ketones and 2-alkynamides. *Synthesis*, **1977**, 777–778.

[112] Plenio, H. Catalysts for the Sonogashira coupling—the crownless again shall be king. Angew. Chem. Int. Ed., **2008**, *47*, 6954-6956.

[113] Chinchilla, R.; Nájera, C. Recent advances in Sonogashira reactions. *Chem. Soc. Rev.,* **2011**, *40*, 5084-5121.

[114] Tanguy, L.; Hetru, O.; Langlois, A.; Harvey, P.D. Characterization and minimization of glaser competitive homocoupling in sonogashira porphyrin-based polycondensation. *J. Org. Chem.*, **2019**, *84*, 3590-3594.

[115] Glaser, C. Beiträge zur kenntniss des acetenylbenzols. *Ber. Dtsch. Chem. Ges.*, **1869**, *2*, 422-424.

[116] Glaser, C. Untersuchungen über einige Derivate der Zimmtsäure. *liebigs ann. Chem.,* **1870**, *154*, 137-171.

[117] Baeyer, A. Ueber die Verbindungen der Indigogruppe. *Ber. Dtsch. Chem. Ges.*, **1882**.*15*, 775-787.

[118] Siemsen, P.; Livingston, R.C.; Diederich, F. Acetylenic coupling: a powerful tool in molecular construction. *Angew. Chem., Int. Ed. Engl.*, **2000**, *39*, 2632-2657.

[119] Hay, A.S. Oxidative coupling of acetylenes. II[1]. *The J. Org. Chem.*, **1962**, *27*, 3320-3321.

[120] Sonogashira, K.; Tohda, Y.; Hagihara, N. A convenient synthesis of acetylenes: catalytic substitutions of acetylenic hydrogen with bromoalkenes, iodoarenes and bromopyridines. *Tetrahedron lett.*, **1975**,*16*, 4467-4470.

[121] Rossi, R.; Carpita, A.; Bigelli, C. A palladium-promoted route to 3-alkyl-4-(1-alkynyl)-hexa-1,5-dyn-3-enes and/or 1,3-diynes. *Tetrahedron lett.*, **1985**, *26*, 523-526.

[122] Cho, D.H.; Lee, J.H.; and Kim, B.H. An improved synthesis of 1,4-Bis (3,4-dimethyl-5-formyl-2-pyrryl) butadiyne and 1,2-bis(3,4-dimethyl-5-formyl-2-pyrryl)ethyne. *J. Org. Chem.,* **1999**. *64*, 8048-8050.

[123] Kundu, N.G.; Pal, M.; Chowdhury, C., A highly convenient and general method for the synthesis of 1,4-disubstituted 1,3-diynes from terminal alkynes via palladium-copper catalysis. *J. Chem. Res.,* **1993**. 10, 432-433.

[124] Liu, Q.; Burton, D.J. A facile synthesis of diynes. *Tetrahedron lett.*, **1997**, *38*, 4371-4374.

[125] Williams, V.E.; Swager, T.M. An improved synthesis of poly(p-phenylenebutadiynylene)s. *Journal of Polymer Science Part A: Polymer Chemistry*, **2000**, *38*, 4669-4676.

[126] Yu, H.; Chen, C.; Sun, J.; Zhang, H.; Feng, Y.; Qin, M.; Feng, W. Highly thermally conductive polymer/graphene composites with rapid room-temperature self-healing capacity. *Nanomicro Lett.*, **2022**,*14*, 135.

[127] Liu, J.; Deng, C.; Tseng, N.W.; Chan, C.Y.; Yue, Y.; Ng, J.C.; Lam, J.W.; Wang, J.; Hong, Y.; Sung, H.H.; Williams, I.D. A new polymerisation route to conjugated polymers: regio-and stereoselective synthesis of linear and hyperbranched

poly(arylenechlorovinylene)s by decarbonylative polyaddition of aroyl chlorides and alkynes. *Chem. Sci.*, **2011**, *2*,1850-1859.

[128] Tang, W.; Becker, M.L. "Click" reactions: a versatile toolbox for the synthesis of peptide-conjugates. *Chem. Soc. Rev.*, **2014**, *43*, 7013-7039.

[129] Yoshimura, A.; Nomoto, A.; Ogawa, A. Rhodium-catalyzed hydrothiolation of alkynes with thiols for construction of sulfur-containing π-conjugated systems. *Res. Chem. Intermed.*, **2014**, *40*, 2381-2389.

[130] Liu, J.; Lam, J.W.; Jim, C.K.; Ng, J.C.; Shi, J.; Su, H.; Yeung, K.F.; Hong, Y.; Faisal, M.; Yu, Y.; Wong, K.S. Thiol−yne click polymerization: Regio-and stereoselective synthesis of sulfur-rich acetylenic polymers with controllable chain conformations and tunable optical properties. *Macromolecules*, **2011**, *44*, 68-79.

[131] Kovalchukova, O.V.; Strashnova, S.B.; Ilyukhin, A.B.; Sergienko, V.S.; Zaitsev, B.E.; Volyanskii, O.V.; Korolev, O.V.; Dutova, T.Y. Complex compounds of a series of d metals with rubazinic acid (HRub). Crystal and molecular structure of [Co(H$_2$O)$_6$](NO$_3$)$_2$ 2H. RubRuss. J. Coord. Chem., **2010**, *36*, 751-756.

[132] Setter, N.; Damjanovic, D.; Eng, L.; Fox, G.; Gevorgian, S.; Hong, S.; Kingon, A.; Kohlstedt, H.; Park, N.Y.; Stephenson, G.B.; Stolitchnov, I. Ferroelectric thin films: Review of materials, properties, and applications. J. Appl. Phys., **2006**.*100*.

[133] Ozaydin-Ince, G.; Coclite, A.M.; Gleason, K.K. CVD of polymeric thin films: applications in sensors, biotechnology, microelectronics/organic electronics, microfluidics, MEMS, composites and membranes. *Rep. Prog. Phys.*, **2011**, *75*, 016501.

[134] Klaerner, G.; Miller, R.D.; Polyfluorene derivatives: effective conjugation lengths from well-defined oligomers. *Macromolecules*, **1998**, *31*, 2007-2009.

[135] Yu, W.L.; Pei, J.; Huang, W.; Heeger, A.J. Spiro-functionalized polyfluorene derivatives as blue light-emitting materials. *Adv. Mater.*, **2000**, *12*, 828-831.

[136] Chhanda, S.A.; Itsuno, S. Synthesis of cinchona squaramide polymers by Yamamoto coupling polymerization and their application in asymmetric Michael reaction. *React. Funct. Polym.*, **2021**, *164*, 104913.

[137] Hattori, T.; Kijima, M.; Shirakawa, H. Oxidative polycondensation of acetylene by iodine in the presence of a palladium-copper catalyst. *Synth. Met.*, **1997**, *84*, 357-358.

[138] Singh, M.; Singh, A.S.; Mishra, N.; Agrahari, A.K.; Tiwari, V.K. Benzotriazole as an efficient ligand in Cu-catalyzed Glaser reaction. *ACS omega*, **2019**, *4*, 2418-2424.

[139] Jim, C.K.; Qin, A.; Lam, J.W.; Mahtab, F.; Yu, Y.; Tang, B.Z. Metal-Free alkyne polyhydrothiolation: synthesis of functional poly(vinylenesulfide)s with high stereoregularity by regioselective thioclick polymerization. *Adv. Funct. Mater.*, **2010**, *20*, 1319-1328.

[140] Dong, W.; Yoshida, Y.; Endo, T. Synthesis of poly (hydroxyurethane) from 5-membered cyclic carbonate under mild conditions in the presence of bicyclic guanidine and their reaction process. *J. Polym. Sci.*, **2021**, *59*, 502-509.

[141] Gupta, B.; Revagade, N.; Hilborn, J. Poly(lactic acid)fiber: An overview. *Prog. Polym. Sci.*, **2007**, *3*, 455-482.

[142] Rogers, M.E.; Long, T.E.; and Turner, S.R. Introduction to synthetic methods in step-growth polymers. *Synthetic Methods in Step-Growth Polymers*, **2003**,1-16.

[143] Loasby, G. The development of the synthetic fibres. *J. Text. Inst.*, **1951**, *42*, 411-441.

[144] Hefetz, A.; Fales, H.M.; Batra, S.W. Natural polyesters: Dufour's gland macrocyclic lactones form brood cell laminesters in Colletes bees. *Science*, **1979**, *204*, 415-417.

[145] Chiellini, E.; Solaro, R. eds., *Biodegradable polymers and plastics*. Springer Science & Business Media. 2003; pp 36

[146] Kong, X.; Qi, H.; Curtis, J.M. Synthesis and characterization of high-molecular weight aliphatic polyesters from monomers derived from renewable resources. *J. Appl. Polym. Sci.*, **2014**, *131*.

[147] Kim, B.S.; Mooney, D.J. Development of biocompatible synthetic extracellular matrices for tissue engineering. *Trends in biotechnol.*, **1998**,*16*, 224-230.

[148] Park, H.S.; Seo, J.A.; Lee, H.Y.; Kim, H.W.; Wall, I.B.; Gong, M.S.; Knowles, J.C. Synthesis of elastic biodegradable polyesters of ethylene glycol and butylene glycol from sebacic acid. *Acta Biomater*, **2012**, *8*, 2911-2918.

[149] Sonnenschein, M.F., *Polyurethanes: science, technology, markets, and trends*. John Wiley & Sons. 2021; pp 10.

[150] Dumoulin, M.M.; Utracki, L.A. Polypropylene blends with engineering and specialty resins. *Polypropylene: An AZ reference*, **1999**, 627-634.

[151] Holsti-Miettinen, R.M.; Heino, M.T.; Seppälä, J.V. Use of epoxy reactivity for compatibilization of PP/PBT and PP/LCP blends. *J. Appl. Polym. Sci.,* **1995**, *57*, 573-586.

[152] Tjong, S.C. Structure, morphology, mechanical and thermal characteristics of the in-situ composites based on liquid crystalline polymers and thermoplastics. *Mater. Sci. Eng. R Rep.*, **2003**, *41*, 1-60.

[153] Rusu, D.; Boyer, S.; Lacrampe, M.F.; Krawczak, P. Bioplastics for automotive applications. *Handbook Bioplast Biocompos Eng Appl*, **2011**, *81*, 397.

[154] Zhang, M.; Singh, R. P. Mechanical Reinforcement of Unsaturated Polyester by AL_2O_3 Nanoparticles. *Materials Lett.*, **2004**, *58*, 408–412.

[155] Hill, K. Fats and oils as oleochemical raw materials. *Pure Appl. Chem.*, 2000, *72*, 1255-1264.

[156] Petrović, Z.S. Polyurethanes from vegetable oils. *Polym Rev*, **2008**, *48*, 109-155.

[157] Gerschutz, M.J.; Haynes, M.L.; Nixon, D.M.; Colvin, J.M. Tensile strength and impact resistance properties of materials used in prosthetic check sockets, copolymer sockets, and definitive laminated sockets. *J. Rehabil. Res. Dev.*, **2011**, *48*.

[158] Ganguly, A.; Channe, P.; Jha, R.; Mitra, S.; Saha, S. Review on transesterification in polycarbonate–poly (butylene terephthalate) blend. *Polym Eng Sci.*, **2021**, *61*, 650-661.

[159] Licciardello, A.; Auditore, A.; Samperi, F.; Puglisi, C. Surface evolution of polycarbonate/polyethylene terephthalate blends induced by thermal treatments. *Appl. Surf. Sci.*, **2003**, *203*, 556-560.

[160] Billica, H.R.; *Production of polyethylene terephthalate using antimony trioxide as polymerization catalyst*. U.S. 2,647,885. 1953.

[161] Moore, J.A.; Kelly, J.E. Polyesters derived from furan and tetrahydrofuran nuclei. *Macromolecules*, **1978**, *11*, 568-573.

[162] de Jong, E.D.; Dam, M.A.; Sipos, L.; Gruter, G.J. Furandicarboxylic acid (FDCA), a versatile building block for a very interesting class of polyesters. *Biobased monomers, polymers, and materials*. J. Am. Chem. Soc., **2012**, 1-13.

[163] Lewis, C.M.; Mathias, L.J. Preliminary evaluation of polyesters with pendent adamantyl groups synthesized from 5-adamantylisophthalic acid and 1,4-butanediol. *Polymer bulletin*, **1997**, *39*, 15-20.

[164] Andrea, K.A.; Plommer, H.; Kerton, F.M. Ring-opening polymerizations and copolymerizations of epoxides using aluminum-and boron-centered catalysts. *Eur. Polym. J.*, **2019**, *120*, 109202.

[165] Guerrero, P.; Muxika, A.; Zarandona, I.; De La Caba, K. Crosslinking of chitosan films processed by compression molding. *Carbohydr. Polym.*, **2019**, *206*, 820-826.

[166] East, A.J. *Preparation of aromatic polyesters by direct self-condensation of aromatic hydroxy acids.* U.S. 4,393,191. 1983.

[167] Sweeny, W. *Ester interchange polyester preparation with alkali metal fluoride catalyst.* U.S. 4,782,131. 1988.

[168] Kobayashi, S. Enzymatic polymerization: a new method of polymer synthesis. *J. Polym. Sci. Part A Polym. Chem*, 1999, *37*, 3041-3056.

[169] Stridsberg, K.M.; Ryner, M.; Albertsson, A.C. *Controlled ring-opening polymerization: polymers with designed macromolecular architecture*. Springer Berlin Heidelberg. 2002; pp. 41-65

[170] Jérôme, C.; Lecomte, P. Recent advances in the synthesis of aliphatic polyesters by ring-opening polymerization. *Adv. Drug Deliv. Rev.*, **2008**, *60*, 1056-1076.

[171] Hevilla, V.; Sonseca, A.; Echeverría, C.; Muñoz-Bonilla, A.; Fernández-García, M. Enzymatic synthesis of polyesters and their bioapplications: Recent advances and perspectives. *Macromol. Biosci.*, **2021**, *21*, 2100156.

[172] Biallas, P.; Heider, J.; Kirsch, S.F. Functional polyamides with gem-diazido units: synthesis and diversification. *Polym. Chem.*, **2019**, *10*, 60-64.

[173] Shirahama, H.; Kawaguchi, Y.; Aludin, M.S.; Yasuda, H. Synthesis and enzymatic degradation of high molecular weight aliphatic polyesters. J. Appl. Polym. Sci., **2001**, *80*, 340-347.

[174] Singh, U.P.; Bhat, H.R.; Verma, A.; Kumawat, M.K.; Kaur, R.; Gupta, S.K.; Singh, R.K. Phenyl hydrazone bearing pyrazole and pyrimidine scaffolds: design and discovery of a novel class of non-nucleoside reverse transcriptase inhibitors (NNRTIs) against HIV-1 and their antibacterial properties. *RSC advances*, **2013**, *3*, 17335-17348.

[175] Zhang, Y.; Jiao, J.; Flowers, R.A. Mild conversion of β-diketones and β-ketoesters to carboxylic acids. *J. Org. Chem.*, **2006**, *71*, 4516-4520.

[176] Ganeshapillai, D.; Woo, L.L.; Thomas, M.P.; Purohit, A.; Potter, B.V. C-3-and C-4-substituted bicyclic coumarin sulfamates as potent steroid sulfatase inhibitors. *ACS omega*, **2018**, *3*, 10748-10772.

[177] Politanskaya, L.; Bagryanskaya, I.; Tretyakov, E. Synthesis of polyfluorinated arylhydrazines, arylhydrazones and 3-methyl-1-aryl-1H-indazoles. *J. Fluor. Chem.*, **2018**, *214*, 48-57.

[178] Rassu, G.; Zambrano, V.; Pinna, L.; Curti, C.; Battistini, L.; Sartori, A.; Pelosi, G.; Casiraghi, G.; Zanardi, F. Direct and Enantioselective Vinylogous Michael Addition of α-Alkylidenepyrazolinones to Nitroolefins Catalyzed by Dual Cinchona Alkaloid Thioureas. *ASC*, **2014**, *356*, 2330-2336.

[179] Zoss, A.O.; Hennion, G.F. Preparation, Properties and Derivatives of α-Acetylenic Acids1. *J. Am. Chem. Soc.*, **1941**, *63*, 1151-1153.

[180] Lang, C.; Pahnke, K.; Kiefer, C.; Goldmann, A.S.; Roesky, P.W.; Barner-Kowollik, C. Consecutive modular ligation as an access route to palladium containing polymers. *Polym. Chem.*, **2013**, *4*, 5456-5462.

[181] Kayahara, E.; Qu, R.; Kojima, M.; Iwamoto, T.; Suzuki, T.; Yamago, S. Ligand-Controlled Synthesis of [3]-and [4]cyclo-9,9-dimethyl-2,7-fluorenes through Triangle-and Square-Shaped Platinum Intermediates. *Chem. Eur. J.*, **2015**, *21*, 18939-18943.

[182] Stay, D.; Lonergan, M.C. Varying anionic functional group density in sulfonate-functionalized polyfluorenes by a one-phase suzuki polycondensation. *Macromolecules*, **2013**, *46*, 4361-4369.

[183] Bensberg, K.; Kunz, K.A.; Kirsch, S.F. Thermolysis of Geminal Diazido Malonamides: Simple Access to Tetrazoles and Functionalization of In Situ Formed Isocyanates. *European Journal of Organic Chemistry*, **2023**, e202300212.